Terms and Conditions of Use of Digitised Theses from Trinity College Library Dublin

Copyright statement

All material supplied by Trinity College Library is protected by copyright (under the Copyright and Related Rights Act, 2000 as amended) and other relevant Intellectual Property Rights. By accessing and using a Digitised Thesis from Trinity College Library you acknowledge that all Intellectual Property Rights in any Works supplied are the sole and exclusive property of the copyright and/or other IPR holder. Specific copyright holders may not be explicitly identified. Use of materials from other sources within a thesis should not be construed as a claim over them.

A non-exclusive, non-transferable licence is hereby granted to those using or reproducing, in whole or in part, the material for valid purposes, providing the copyright owners are acknowledged using the normal conventions. Where specific permission to use material is required, this is identified and such permission must be sought from the copyright holder or agency cited.

Liability statement

By using a Digitised Thesis, I accept that Trinity College Dublin bears no legal responsibility for the accuracy, legality or comprehensiveness of materials contained within the thesis, and that Trinity College Dublin accepts no liability for indirect, consequential, or incidental, damages or losses arising from use of the thesis for whatever reason. Information located in a thesis may be subject to specific use constraints, details of which may not be explicitly described. It is the responsibility of potential and actual users to be aware of such constraints and to abide by them. By making use of material from a digitised thesis, you accept these copyright and disclaimer provisions. Where it is brought to the attention of Trinity College Library that there may be a breach of copyright or other restraint, it is the policy to withdraw or take down access to a thesis while the issue is being resolved.

Access Agreement

By using a Digitised Thesis from Trinity College Library you are bound by the following Terms & Conditions. Please read them carefully.

I have read and I understand the following statement: All material supplied via a Digitised Thesis from Trinity College Library is protected by copyright and other intellectual property rights, and duplication or sale of all or part of any of a thesis is not permitted, except that material may be duplicated by you for your research use or for educational purposes in electronic or print form providing the copyright owners are acknowledged using the normal conventions. You must obtain permission for any other use. Electronic or print copies may not be offered, whether for sale or otherwise to anyone. This copy has been supplied on the understanding that it is copyright material and that no quotation from the thesis may be published without proper acknowledgement.

Development of Extraction and Analysis of Protocols for RNA in Formalin-Fixed Paraffin-Embedded (FFPE) Materials using TaqMan® real-time PCR

A thesis submitted for the Degree of

Doctor of Philosophy

By

Jinghuan Li

M.Sc., B.Sc.

Trinity College

University of Dublin

April 2009

Supervisors: Prof. Orla Sheils and Prof. John O'Leary

DECLARATION

I declare that this thesis is my own work, and has not been submitted previously for a PhD degree at this or any other university. I agree that the library may lend or copy this thesis on request.

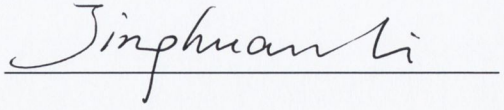

To my parents

CONTENTS

Chapter 2 — Materials and Methods

Chapter 3 — Comparison of RNA extraction protocols

Chapter 5 — Comparison of microRNA expression patterns using total RNA extracted from matched samples of formalin-fixed paraffin-embedded (FFPE) cells and snap frozen cells

Chapter 6 — Analysis of microRNA let-7a and mir-140 expression levels using laser capture microdissection (LCM) on formalin-fixed paraffin-embedded (FFPE) thyroid archive tissues

Chapter 7— General discussion, conclusions and future work

List of Figures

List of Tables

Acknowledgements

I wish to thank all those people who have helped, encouraged and supported me over the last three years of study and research.

First of all, I sincerely thank my supervisor Professor Orla Sheils for her dedication, assistance, guidance and all her kindness throughout the course of this research. I would like to thank her for her comments, advice and patience with my work and the writing of this thesis. As the Chinese saying goes, 'Master and Student are as Father and Son'. I owe you so much that I can never repay. I could only stand on your shoulder and become strong to overcome all the difficulties in my future career and life, but thank you Orla.

I would like to thank Professor John O'Leary for being my co-supervisor and for providing me this opportunity to carry out this PhD course in the Histopathology Department of TCD. Your encouragement for your students, your enthusiasm and talent for your research and your dedication for the department astounds me. Working in your ambitious and impressive research unit has been such a pleasure for which I will always be grateful. I would also like to acknowledge Applied Biosystems for the scholarship and the people in the company, especially Marco Pirotta, Simone Guenther and Astrid Ferlinz who provided technical support.

A big thank you goes to Paul Smyth who has always been there to answer my questions and to advise me theoretically and practically. My work would not have been done without your help. I would like to specially thank Karen Denning and Richard

Flavin for helping me with science and English and for accompanying me for most of the time during these three years. I would like to thank Susanne Cahill for the help in the early stage, Sinead Aherne and Therese Murphy for your great personalities and laugher. I also thank people in the Central Pathology Laboratory for assistance with formalin fixation and paraffin embedding processing, and people in the statistics department for the assistance of data analysis.

I wish to thank my parents for loving me so much. You give me everything you could, show me the best way you know, and are always there to share feelings with me. Thank you to my boyfriend Qiang for going through the difficulties with me and making me so happy now.

List of Abbreviations

A	Adenine
AB-In-House	AB-in-House Protocol
AGPC	Acid guanidinium-phenol-chloroform
Ambion	Ambion RecoverAll™ Total Nucleic Acid Isolation Kit
AR	Antigen retrieval
ATC	Anaplastic thyroid carcinoma
β-ME	β-Mercaptoethanol
C	Cytosine
CDKN1B	Cyclin-Dependent Kinase Inhibitor 1B
cDNA	Complementary DNA
C_T	threshold cycle
DAG	di-acyl-glycerol
DMSO	Dimethyl sulfoxide
DNA	Deoxyribonucleic acid
ERK	Extracellular-signal-regulated kinase
FA	Follicular adenoma
FCS	Foetal Calf Serum
FFPE	Formalin–Fixed Paraffin–Embedded sample
FTC	Follicular thyroid carcinoma
G	Guanine
GAPDH	Glyceraldehyde-3-phosphate dehydrogenase
GEMM	Gene Expression Master Mix

Gentra	Gentra Purescript® RNA Purification Kit
GTP	Guanosine triphosphate
H&E	Haematoxylin and Eosin
HIAR	Heating induced antigen retrieval
HIER	Heat-induced epitope retrieval
HLA	Human leucocyte antigen
HP	Hyperplasia
HT	Hashimoto's thyroiditis
IHC	Immunohistochemistry
IP3	Inositol tri phosphate
ISH	In situ hybridization
J-I	J-I (GTCX)
J-II	J-II (GTCX)
LCM	Laser captured microdissection
LNA	Locked nucleic acid
MAPK	Mitogen-activated protein kinase
MEK	MAPK kinase
MGB	Minor groove binder
miRNA	microRNA
NBF	Neutral buffer formalin
PBS	Phosphate buffered saline
PCR	Polymerase chain reaction
PEG	Plyethylene glycol
PI3K	Phosphatidylinositol 3-kinase
PIER	Protease-induced epitope retrieval

PKA	cAMP-dependent protein kinase
PLCb	Phospholipase C
PreAmp	TaqMan® with pre-amplification method
PTC	Papillary thyroid carcinoma
QRT-PCR	Real-time quantitative TaqMan® reverse transcriptase-polymerase chain reaction
RIN	RNA Integrity Number
RNA	Ribonucleic acid
RQ	Relative quantification
rRNA	Ribosomal RNA
RT	Reverse transcription
SDS	Sodium dodecyl sulphate
siRNA	Short interfering RNA
snRNA	Small nuclear RNA
snoRNAs	Small nucleolar RNAs
Stratagene	Stratagene Absolutely RNA® FFPE Kit,
SV40	Simian Virus 40
T	Thymine
T_3	Triiodothyronine
T_4	Thyroxine
TBG	Thyroxine-binding globulin
TNS	Trypsin Neutralising Solution
Trizol	Invitrogen Trizol® Reagent
tRNAs	Transfer RNAs
TSG	Tumour suppressor genes

TSH	Thyroid stimulating hormone
U	Uracil
UPMM	Universal PCR Master Mix
UTR	Untranslated region

Publications

Flavin R, Jackl G, Finn S, Smyth P, Ring M, O'Regan E, Cahill S, Unger K, Denning K, Li J, Aherne S, Tallini G, Gaffney E, O'Leary J, Zitzelsberger H, Sheils O. RET/PTC Rearrangement Occurring in Primary Peritoneal Carcinoma. *Int J Surg Pathol.* 2009 Jan 14.

Aherne ST, Smyth PC, Flavin RJ, Russell SM, Denning KM, Li JH, Guenther SM, O'Leary JJ, Sheils OM. Geographical mapping of a multifocal thyroid tumour using genetic alteration analysis & miRNA profiling. *Mol Cancer*. 2008 Dec 4;7:89.

Flavin RJ, Smyth PC, Laios A, O'Toole SA, Barrett C, Finn SP, Russell S, Ring M, Denning KM, Li J, Aherne ST, Sammarae DA, Aziz NA, Alhadi A, Sheppard BL, Lao K, Sheils OM, O'Leary JJ. Potentially important microRNA cluster on chromosome 17p13.1 in primary peritoneal carcinoma. *Mod Pathol.* 2009 Feb; 22(2):197-205.

Denning K, Smyth P, Cahill S, Li J, Flavin R, Aherne S, O'Leary JJ, Sheils O. ret/PTC-1 expression alters the immunoprofile of thyroid follicular cells. *Mol Cancer.* 2008 May; 7:44

Flavin RJ, Smyth PC, Finn SP, Laios A, O'Toole SA, Barrett C, Ring M, Denning KM, Li J, Aherne ST, Aziz NA, Alhadi A, Sheppard BL, Loda M, Martin C, Sheils OM, O'Leary JJ. Altered eIF6 and Dicer expression is associated with clinicopathological features in ovarian serous carcinoma patients. *Mod Pathol.*2008 Jun; 21(6):676-84.

Li J, Smyth P, Cahill S, Denning K, Flavin R, Aherne S, Pirotta M, Guenther SM, O'Leary JJ, Sheils O. Improved RNA quality and TaqMan(R) Pre-amplification method (PreAmp) to enhance expression analysis from formalin fixed paraffin embedded (FFPE) materials. *BMC Biotechnol.* 2008 Feb 6;8(1):10

Denning KM, Smyth PC, Cahill SF, Finn SP, Conlon E, Li J, Flavin RJ, Aherne ST, Guenther SM, Ferlinz A, O'Leary JJ, Sheils OM. A molecular expression signature distinguishing follicular lesions in thyroid carcinoma using preamplification RT-PCR in archival samples. *Mod Pathol.* 2007 Oct; 20(10):1095-102.

Li J, Smyth P, Flavin R, Cahill S, Denning K, Aherne S, Guenther SM, O'Leary JJ, Sheils O. Comparison of miRNA expression patterns using total RNA extracted from matched samples of formalin-fixed paraffin-embedded (FFPE) cells and snap frozen cells. *BMC Biotechnol.* 2007 Jun 29; 7:36.

Flavin R, Smyth P, Crotty P, Finn S, Cahill S, Denning K, Jinghuan Li, O'Regan E, O'Leary J, Sheils O.BRAF T1799A mutation occurring in a case of malignant struma ovarii. *Int J Surg Pathol*. 2007 Apr;15(2):116-20.

Cahill S, Smyth P, Denning K, Flavin R, Li J, Potratz A, Guenther SM, Henfrey R, O'Leary JJ, Sheils O. Effect of BRAFV600E mutation on transcription and post-transcriptional regulation in a papillary thyroid carcinoma model. *Mol Cancer*. 2007 Mar 13;6:21.

Cahill S, Smyth P, Finn SP, Denning K, Flavin R, O'Regan EM, Li J, Potratz A, Guenther SM, Henfrey R, O'Leary JJ, Sheils O. Effect of ret/PTC 1 rearrangement on transcription and post-transcriptional regulation in a papillary thyroid carcinoma model. *Mol Cancer*. 2006 Dec 11;5:70.

Summary

Archival Formalin–Fixed, Paraffin–Embedded (FFPE) tissue samples represent an invaluable source of human tissue for gene expression analysis. They are the most abundant and readily available materials and generally well documented with clinical pathological parameter. Data generated can potentially highlight biomarkers useful in disease classification, diagnosis and prognosis, and elucidate novel therapeutic targets. However, they have not been widely used in molecular biology due to the compromised RNA molecules extracted from these tissues which are degraded and chemically modified. Thus, the value of FFPE materials in molecular setting has been shadowed by the technical difficulties limiting extensive analysis of gene expression.

The purpose of this project is to establish a reliable analysis system to study gene expression level using RNA extracted from FFPE materials. The study was carried out using molecular biotechnologies of real-time quantitative TaqMan® reverse transcriptase polymerase chain reaction (QRT-PCR) as the core with the facilitation of Nano-Drop Spectrophotometer and Bioanalyzer, began with the messenger RNA assessment, and progressed towards the analysis of a group of small RNA molecules microRNA.

The results obtained from comparison of extraction showed a variation of RNA quantity and quality generated by different protocols. The Stratagene Absolutely RNA® FFPE Kit and the Ambion RecoverAll™ Total Nucleic Acid Isolation Kit were identified as the best protocols generating superior results among seven examined protocols.

These two identified extraction protocols were further modified by introducing a heating step to improve quantity and quality of RNA extracted from FFPE. TaqMan® technologies and a novel pre-amplification system (PreAmp), designed to enhance expression analysis from tissue samples, were assessed, demonstrating extraction protocol modification in conjunction with TaqMan® PreAmp established a suitable analysis system to analyze messenger RNA expression using FFPE.

The comparison of miRNA expression pattern using paired snap frozen and FFPE cells showed that miRNA extracted from FFPE blocks was successfully amplified using Q-RT-PCR. The levels of miRNA expression detected in total RNA extracted from FFPE were higher than that extracted from snap frozen cells when the quantity of total RNA was identical. Small RNA molecules appear to be less affected by modification and degradation process and are recovered more easily in the extraction process. In general miRNAs demonstrated reliable expression levels in FFPE suggesting these molecules might prove to be robust targets amenable to detection in archival material.

Finally, microRNA detection technique was applied to a cohort of thyroid FFPE blocks. Two microRNA targets let-7a and mir-140 expression levels were examined in total RNA extracted from laser captured microdissected samples representing different thyroid diseases. The results showed that let-7a has a higher expression level in PTC versus Hashmoto thyroiditis or non-autoimmune thyroiditis and mir-140 has a higher expression level in neoplastic and malignant groups compared with non-neoplasm and hyperplastic, suggesting that these microRNAs may regulate related mRNA playing important roles in thyroid diseases.

CHAPTER ONE

GENERAL INTRODUCTION

1.1 Formalin-fixed paraffin-embedded materials

Archival Formalin–Fixed, Paraffin–Embedded (FFPE) tissue samples represent a robust and invaluable source of human tissue for gene expression analysis. This tissue has an inherent advantage in that retrospective patient data, including survival history and treatment response, is the most abundant and readily available material, allowing immediate comparison with clinical pathological parameters. Data generated can potentially highlight biomarkers useful in disease classification, diagnosis and prognosis, and potentially elucidate novel therapeutic targets (Lewis et al., 2001, Srinivasan et al., 2002). However, they have not been widely used in molecular biology due to the compromised RNA molecules extracted from these samples which are degraded and chemically modified. Thus, the value of FFPE materials in molecular setting has been shadowed by the technical difficulties limiting extensive analysis of gene expression. In this project, we used real-time quantitative TaqMan® reverse transcriptase-polymerase chain reaction (QRT-PCR) technology to establish a reliable analysis system to study the gene expression level using RNA extracted from FFPE materials.

1.1.1 History of formalin fixation

Formalin fixation was discovered by Ferdinand Blum in the late 1800's (Puchtler and Meloan, 1985). Blum first tested the bactericidal properties of diluted formalin, which was 4% of formaldehyde aqueous solution, against several bacterial species. He found formaldehyde an effective but slow agent for killing bacteria (Fox et al., 1985). He

later noticed that the skin of his fingers that had come in contact with the diluted solution became hardened, much as with alcohol, then one of the commonest methods for hardening tissues for histological processing. When he examined and prepared the tissues after formaldehyde treatment, excellent staining results were obtained using common staining methods of the time, such as hematoxylin and the analine dyes. His preparations of various organs were examined by a histologist and were found to be entirely suitable for morphology studies. Since then, his fixation method has been used in all areas of biology and medicine and become the most commonly used method to preserve tissue samples (Fox et al., 1985).

FFPE became very commonly used tissue sample in the pathology laboratory not only because of the histology and cytology studies carried out, but also due to some developed techniques that allow the performance of protein detection. Immunohistochemistry (IHC) was started with a publication by Coons et al. in 1941 (Coons et al., 1941) which described an immunofluorescence technique for detecting cellular antigens in tissue sections. FFPE materials were used in detecting some antigens in 1974 by Taylor et al. (Taylor and Burns, 1974) and then were widely used to perform IHC staining in pathology studies since Shi et al. described antigen retrieval technique in FFPE tissues by heating of tissue sections (Shi et al., 1991). The heating induced antigen retrieval (HIAR) helped facilitate the dramatic growth of FFPE in the use of immunohistochemical analysis for surgical pathology. In late 90's, tissue microarray was introduced by Kononen et al., as a subsequent technique which allows simultaneous examination of hundreds of samples on a single microscope slide (Kononen et al., 1998). Hundreds of FFPE tissues can be arrayed at a high density to

form a single paraffin block and efficiently used for simultaneous in situ analysis of DNA, RNA and protein targets.

1.1.2 Theory of formalin fixation

Formalin fixation is one of the chemical fixatives depending on cross-linking mechanism. Formaldehyde is a colourless, toxic, potentially carcinogenic, water-soluble gas, CH_2O. Formalin is a solution containing 35-40% formaldehyde. Most of the formaldehyde in a diluted aqueous solution is present as methylene glycol, which is formed by addition of a molecule of water to one of formaldehyde. The reaction is reversible.

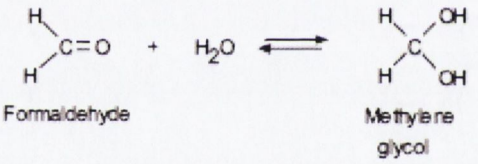

The small molecules of formaldehyde and methylene glycol penetrate quite rapidly through extracellular materials. While the chemical reactions of fixation by formaldehyde are quite slow mainly with proteins. In the fixative solution, free formaldehyde is capable of reacting with the nitrogen atoms to bind the some of the amino acids, such as lysine, tyrosine, asparagines, histidine, arginine, cysteine, and glutamine (Ramos-Vara, 2005). The fixation mechanism has been suggested to involve two steps. The first step is the addition of the methylol groups to the uncharged reactive amino groups (–NH or NH_2) to form N-CH_2OH. The second is the formation of a methylene bridge between two amino groups. Once the addition product (reactive

hydroxy methyl compound) is formed, additional cross-linking will happen. Methylene cross-links are formed between proteins, protein and nucleic acids, and between nucleic acids.

1. Formation of addition products

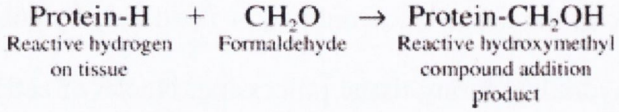

2. Formation of methylene bridges

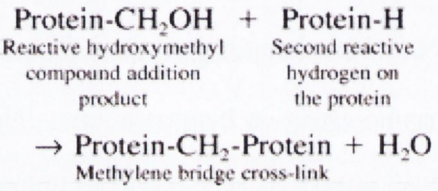

1.1.3 Conditions of formalin fixation

Formalin fixation is a progressive, time- and temperature-dependent process. It depends on the coefficient of diffusibility of the fixative and the rate at which it reacts with the tissue components. Formaldehyde has a molecular weight of only 30 and penetrates tissues rapidly. The coefficient of diffusibility in 1 hour is the distance in millimetres that the fixative has diffused into the tissue and is inversely related to the square root of time (Start et al., 1992, Srinivasan et al., 2002). At room temperature, formaldehyde bound to tissue sections increased with time until equilibrium was reached. At 37°C, the reaction of formaldehyde is considerably faster and equilibrium is reached quicker than that at room temperature.

Adequate fixation in formalin followed by conventional processing produces ethoxylated adducts, crosslinked molecules, and depurination fragments from nucleic acids (Dapson, 2007). Inadequate fixation does not cause sufficient cross-linking to immobilize proteins. Cross-links will happen only in the periphery of the specimen, with the core of the tissue block unfixed or fixed only by coagulation with the alcohol used for dehydration during tissue processing. Nuclei of cells can be greatly damaged during processing through paraffin after inadequate times in formaldehyde (Ramos-Vara, 2005). However, the longer duration of fixation adversely affects the quality of tissue DNA and RNA (Macabeo-Ong et al., 2002) although the relatively broad time range presumably has no effect on histopathology. Thus the tissues are routinely fixed for 24 to 48 hours for normal tissues and several hours for small biopsies.

The pH of a fixative buffer dramatically influences the degree of cross-links. Amino acids are amphoteric substances (contain both acid, –COOH, and basic, $–NH_2$, groups); therefore, they are influenced by pH. Amino acids are charged ($–NH_3^+$) at a lower pH (acid) and uncharged ($–NH_2$) at a higher pH. When neutral buffered formalin is used, the pH is shifted to neutrality, causing dissociation of hydrogen ions from the charged amino groups ($–NH_3^+$) of the side chains of proteins, resulting in uncharged amino groups ($–NH_2$). These uncharged groups contain reactive hydrogen that can react with formalin to form addition groups and cross-links. In other words, the use of 10% buffered formalin will produce more cross-links than non-buffered formalin and therefore will fix tissues efficiently (Ramos-Vara, 2005).

1.1.4 Other fixatives and features of formalin fixation

Fixation methods can be classified into two categories: one is chemical fixation based on cross-linking reagents, the other is physical fixation based on freezing and coagulation or precipitation of the constituents by exposing them to heat, organic solvents, or acids.

Like formaldehyde fixation, glutaraldehyde is another reagent used for chemical fixation. Glutaraldehyde reacts primarily with the e-amino groups of amino acids and nucleic acids. Compared with formaldehyde, glutaraldehyde very slowly penetrates into specimens, and fixes them rapidly and strongly (Yamashita, 2007). The coefficient of diffusibility of 4% glutaraldehyde at 4°C is approximately half that of 4% formaldehyde solution. Although widely used as a fixative for standard electron microscopy, the slow penetration and the need for periodic purification to maintain the functional aldehyde levels have greatly limited its use as a biological fixative. However, it has been shown that 1% glutaraldehyde at pH 7.0 better preserves high-molecular weight DNA as compared to 10% formalin.

Physical fixations include freezing, heat coagulation by microwave irradiation or boiling, precipitation or coagulation with an organic solvent such as ethanol, methanol, or acetone and denaturation or precipitation with an acidic solution, such as acetic acid. Storage of the freezing fixation is expensive and difficult but it is well known that nucleic acids are well preserved in frozen tissue (Farragher et al., 2008). Molecular studies are mainly based on this type of tissue samples to date. Ethanol fixation is the typical coagulation fixative that precipitates proteins by breaking hydrogen bonds in

the absence of protein cross-linking. Most proteins in body fluids have their protein hydrophilic moieties in contact with water and hydrophobic moieties in closer contact with each other, stabilizing hydrophobic bonding. Removing water with ethanol destabilizes protein hydrophobic bonding because the hydrophobic areas are released from the repulsion of water and the protein tertiary structure is unfolded. At the same time, removal of water destabilizes hydrogen bonding in hydrophilic areas, with the final result of protein denaturation. This results in inadequate cellular preservation and a possible shift in the intracellular immunoreactivity (Ramos-Vara, 2005). Ethanol fixation preserves nucleic acids better because they bring about little chemical change, however causes tissue shrinkage and hence not suited for morphological studies.

There are some mixtures of fixatives that have been tried in an attempt to compensate the shortcomings of one by another: Clarke's fixative, a mixture of ethanol and acetic acid; Carnoy's fixative, a mixture of ethanol, chloroform, and glacial acetic acid; Methacarn, a mixture of methanol, chloroform, and glacial acetic acid; Bouin's fixative, formaldehyde and picric acid and acetic acid.

There is no one fixation method ideal for the preservation of all tissue components or all purpose of studies. In most surgical pathology laboratories, tissues are effectively 'double fixed' which includes 10% neutral buffer formalin (NBF) following by periods in 100% ethanol (Taylor et al., 2002). Formalin fixation became the routine fixative of choice in most pathology laboratories for many reasons.

1. Economically, it is cheap readily available.
2. Technically, it is easy to use and stable, works under a broad variety of conditions.

3. Formalin fixation produces good morphological quality with almost any tissue. It is reliable in general histology.

4. Formalin fixation can sterilize tissue specimens, such as inactivate viruses, in a more reliable way than precipitating fixatives.

5. Carbohydrate antigens and immunoreactivity of many proteins is better preserved.

6. It is desirable for routine diagnostics to have paraffin blocks with tissues fixed in the same fixative over the years. Retrospective studies would be possible to be carried out.

1.1.5 Embedding methods

Tissue preparation consists of fixation, subsequent dehydration, and embedding in a support medium to provide a rigid matrix for sectioning. Paraffin is commonly used tissue embedding method for histological studies. After fixation, tissues are dehydrated with alcohol, cleared in xylene, and infiltrated and embedded in paraffin. To conserve more fine tissue structure, fixed specimens are embedded in plastics, such as acrylic and epoxy resins: embedding in plastics is essential for electron microscopy. Plyethylene glycol (PEG) has been used as an embedding medium to prepare sections from tissues without exposing them to organic solvents or high temperature (Yamashita, 2007).

1.2 Protein analysis using FFPE

The chemical modifications of formalin fixation cause the difficulty of analysing protein and nucleic acids in molecular level. The final result of formaldehyde fixation

is a profound change in the conformation of macromolecules, which could make the recognition of proteins (Antigens) by Antibodies difficult. These changes modify the three-dimensional (tertiary and quaternary) structure of proteins, whereas the primary and secondary structures are little affected (Mason and O'Leary, 1991). To date, pathological studies are mainly based on immunohistochemistry technology using FFPE tissues with the facilitation of antigen retrieval.

1.2.1 Immunohistochemistry

Immunohistochemistry is a method for localizing specific antigens in tissues or cells, based on antigen-antibody recognition. An antibody is a molecule that has the property of combining specifically with a second molecule, termed the antigen, based on the three-dimensional structure of protein. Proteins and carbohydrates that are sufficiently complex to possess unique three-dimensional 'charge-shape' profiles, termed an antigenic determinant or epitope, are good antigens (Taylor et al., 2002). The determinant being the exact site on the molecule with witch the antibody combines. Once antigen-antibody binding occurs, it is demonstrated with a coloured histochemical reaction visible by light microscopy or fluorochromes with ultraviolet light (Ramos-Vara, 2005).

Immunohistochemistry was first performed on fresh frozen tissues (Coons et al., 1941) and then became routine in surgical pathology laboratories using FFPE tissues after the antigen retrieval method developed in 1990's. IHC is a valuable tool in diagnosis, prognosis and research of variable diseases.

1.2.2 Antigen retrieval

The protein is modified in the section but not destroyed by fixation. The reaction of side groups of proteins with formaldehyde with the formation of methylene bridges and other bindings among the macromolecules in the tissue, have altered the protein macromolecule in such a way that its reaction with the antibody is now impossible or difficult (Montero, 2003). One of the challenges of IHC is to develop methods that reverse changes produced during fixation. Antigen retrieval (AR) procedure is now so frequently used as a way to increase the final intensity of the colour reaction or, even, to make a reaction that was not occurred without heat positive after its application (Montero, 2003). The two most common AR procedures used in IHC are enzymatic and heat-based retrieval (Ramos-Vara, 2005).

Protease-induced epitope retrieval (PIER) was introduced by Huang et al. (Huang et al., 1976). Many enzymes have been used including trypsin, proteinase K, pronase, ficin, and pepsin. The PIER mechanism is probably digestion of proteins, but this cleavage is non-specific and some Ags might be negatively affected by this treatment. Although the PIER were widely applied, it did not improve IHC staining of the majority of antigens (Leong et al., 1988), and it proved difficult to control the optimal digestion conditions from individual tissue sections when stained with different antibodies.

Heat-induced epitope retrieval (HIER) was introduced by Shi et al. (Shi et al., 1991) as a revolutionized method of the immunohistochemical detection of antigens using FFPE tissue. The HIER is a simple method that involves heating routinely processed FFPE

sections at high temperature (e.g. in a microwave oven or in a pressure wok for 15 to 30 minutes) before IHC staining procedures. The intensity of IHC staining was increased dramatically after HIER treatment. Although the molecular mechanism of HIEP is not fully understood yet, it has been suggested that the loss of immunoreactivity associated with formalin fixation is due to a cross-link at the antibody-binding site (Sompuram et al., 2004). Heating treatment may reverse, at least in part, the chemical reactions that occur between protein and formalin.

1.3 Nucleic acid analysis using FFPE

The feasibility of performing molecular genetic analysis of fixed and embedded biopsies will improve diagnostic procedures and will enable a large number of research studies on various diseases. The chemical reactions of formaldehyde with nucleic acid and protein are quite similar (Chaw et al., 1980). The nucleic acids isolated from FFPE tissues are fragmented and cross-linked (Figure 1.1). Although FFPE tissues still have not been widely used in analysis of nucleic acids, a lot of efforts have been made to extract or analyse nucleic acid using FFPE (Coombs et al., 1999, Shi et al., 2002, Lehmann and Kreipe, 2001).

1.3.1 DNA extracted from FFPE

Compared to the DNA isolated from frozen tissues, FFPE tissues exhibit a frequency of nonreproducible sequence alteration. The formaldehyde initiates DNA denaturation at the AT-rich regions of double-stranded DNA creating sites for chemical interaction

which could subsequently be analyzed as an artificial C-T or G-A mutation (Williams et al., 1999). However, compared to the RNA, DNA isolated from FFPE tissues are less fragmented and have been analysed using comparative genomic hybridization (CGH) (Zielenska et al., 2004), cDNA microarray and RT-PCR techniques (Dedhia et al., 2007).

1.3.2 RNA extracted from FFPE

FFPE tissue has not been commonly used to perform gene expression studies due to the degradation and chemical modification of RNA extracted from FFPE blocks. RNA extracted from FFPE is degraded to fewer than 300 bases (Cronin et al., 2004) in length because archived blocks are often stored at room temperature for long periods of time. The situation is made more complicated by the fact that RNA is modified by methylol groups to form cross-links with protein or nucleic acid during formalin fixation (Haselkorn and Doty, 1961, Chaw et al., 1980, Rait et al., 2006), which results in poor yields (Lewis et al., 2001, Goldsworthy et al., 1999) and compromised extracts.

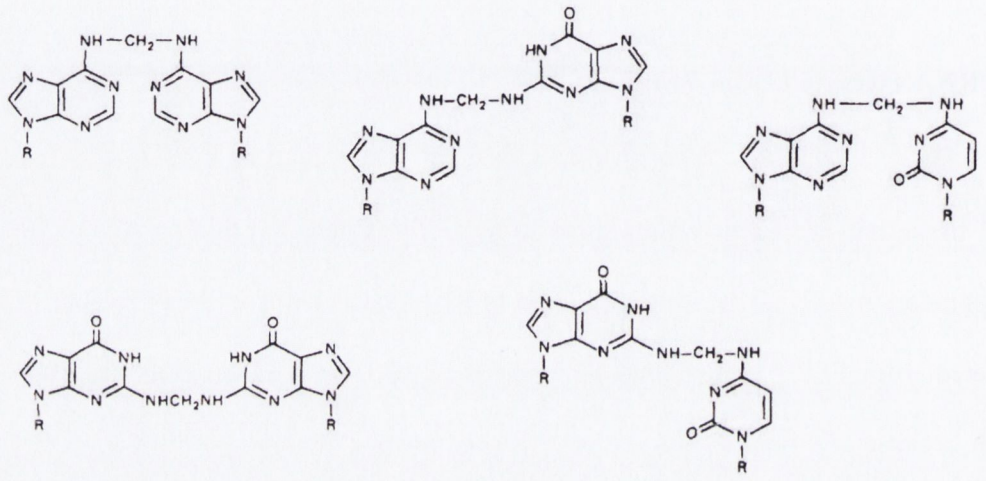

Figure 1.1 Chemical structure of Cross-links among nucleic acids caused by formalin fixation

Chaw et al. isolated cross-linked nucleosides using reverse-phase high-pressure liquid chromatography. They suggested that methylene formed cross-links connect the amino groups of the nucleosides when tissues were fixed in formalin solution (Chaw et al., 1980).

1.4 RNA

Nucleic acids encode genetic information, which include two related types, deoxyribonucleic acid (DNA) and ribonucleic acid (RNA). DNA molecules are long which store master copy of each cell's genome and may each contain many thousands of genes. Each gene is a linear segment of a long DNA molecule. In contrast, RNA molecules are shorter, carrying only one or a few genes, to transmit the genetic information to the cell machinery in human (Clark, 2005).

1.4.1 Chemical structure of RNA

Nucleic acid is linear polymers made of subunits known as nucleotides. The information in each gene is determined by the order of the different nucleotides. There are four different nucleotides in each type of nucleic acid and their order determines the genetic information. Each nucleotide has three components: a phosphate group, a five-carbon sugar, and a nitrogen-containing base (Figure 1.2). The phosphate groups and the sugars form the backbone of each strand of DNA or RNA. In another word, nucleotides are linked by joining the 5'-phosphate of one to the 3'-hydroxyl group of the next. There are five different types of nitrogenous bases associated with nucleotides. DNA contains the bases adenine (A), guanine (G), cytosine (C) and thymine (T). RNA contains A, G, C and uracil (U). The bases are joined to the sugars and stick out sideways. In DNA, the sugar is always deoxyribose; whereas, in RNA, it is ribose. Deoxyribose has one less oxygen than ribose giving the names deoxyribonucleic acid and ribonucleic acid.

RNA is normally found as a single-stranded molecule. While DNA is double helix with antiparallel double strands that the 5'-end of one strand is opposite the 3'-end of the other strand and two separate strands are wound around each other in a helical arrangement. In double stranded DNA, hydrogen bonds are formed to pair the bases on each strand protrude into the centre of the double helix with the bases in the other strand. Adenine (A) in one strand is always paired with thymine (T) in the other, and guanine (G) is always paired with cytosine (C). The A-T base pair has two hydrogen bonds and the G-C base pair has three (Figure 1.3). In RNA, the uracil will base pair with adenine in all the cases when many single-stranded RNA molecules fold up giving double-stranded regions or pair with one of DNA (Lewin, 2000).

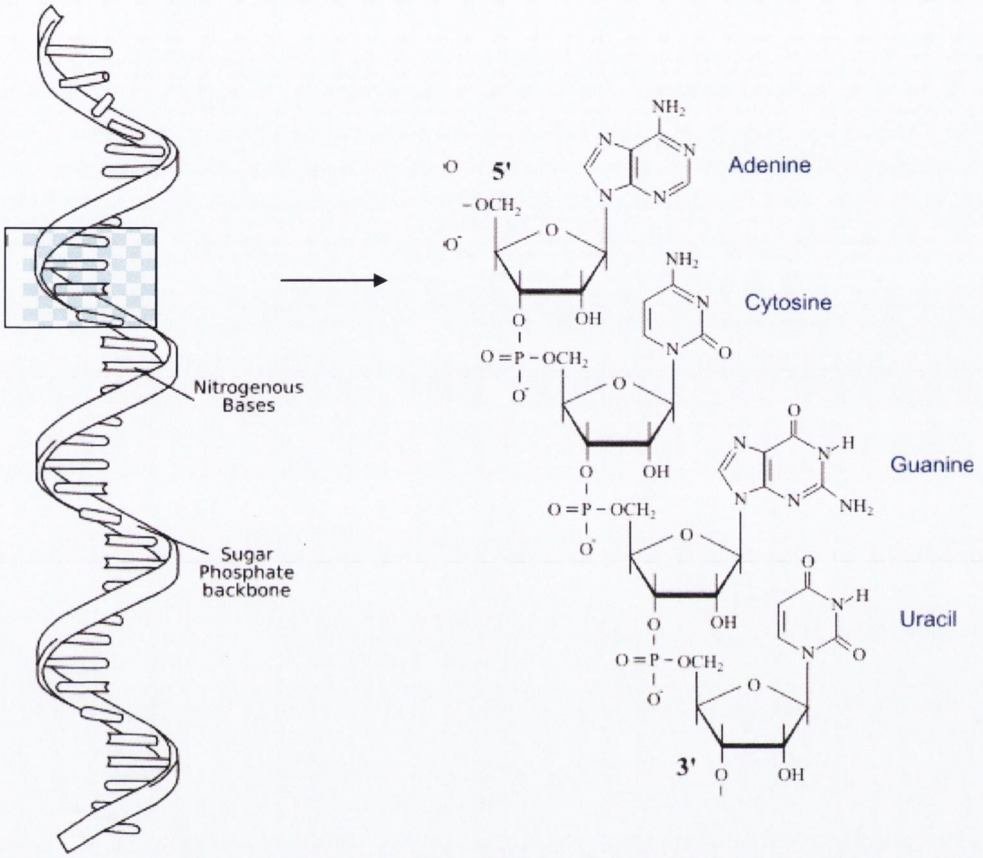

Figure 1.2 Schematic representation of nucleotides forming structure of RNA

The phosphate groups and the sugars form the backbone of each strand of RNA. Nucleotides are linked by joining the 5'-phosphate of one to the 3'-hydroxyl group of the next. RNA contains four types of bases: adenine (A), guanine (G), cytosine (C) and uracil (U). The bases are joined to the sugars and stick out sideways.

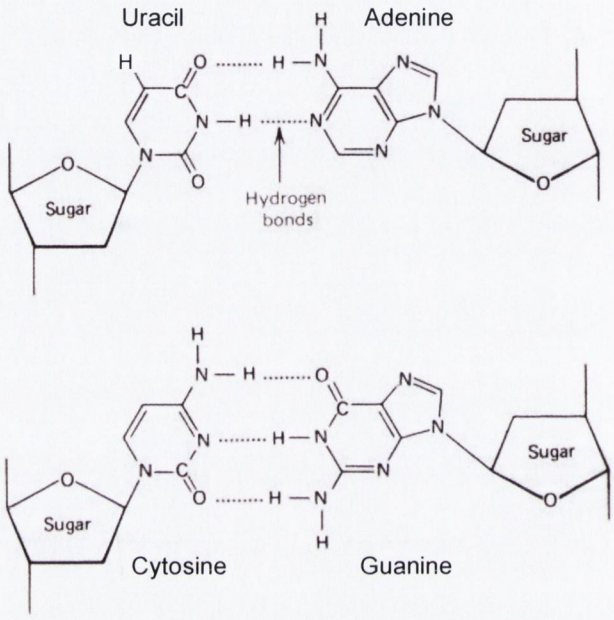

Figure 1.3 Base pairs formed in RNA or in between RNA and DNA

The uracil will base pair with adenine and the cytosine will base pair with guanine in all the cases when many single-stranded RNA molecules fold up giving double-stranded regions or pair with one of DNA. The A-U base pair has two hydrogen bonds and the G-C base pair has three.

1.4.2 RNA classes and functions

Genetic information flows from DNA to RNA to protein during cell growth and metabolism. Messenger RNA molecules are made during transcription process as temporary working copies of the gene, and carry information from the genome to the cytoplasm. In cytoplasm, the information carried by messenger RNA is used by the ribosome to synthesize proteins, which process is called translation. Messenger RNA is then called translated or coding RNA (Clark, 2005).

Non-coding RNA (ncRNA) commonly refers to the RNAs that function directly as RNA but are not translated into protein, which includes a variety of RNA molecules with different functions (Table 1.1). It has been suggested that the majority of the genomes of mammals and other complex organisms are transcribed into ncRNAs (Mattick, 2001, Mattick and Makunin, 2006). rRNA, tRNA and snRNA are the most common ones and have well-established functions among known RNAs. Ribosomal RNA (rRNA) is the central component of the ribosome, by which the protein is synthesized in living cells. By weight, the ribosome consists of about two-thirds rRNA and one-third protein. In eukaryotes, there are four ribosomal RNAs: 18S, 28S, 5.8S and 5S rRNA ranging from hundreds to thousands nucleotides long. The function of the rRNA is to provide a mechanism for decoding mRNA into amino acids and to interact with the tRNAs during translation by providing peptidyl transferase activity. Transfer RNAs (tRNAs) are usually about 74 to 95 nucleotides long that recognize the codon on the mRNA at one end and carry the corresponding amino acid attached to their other end.

Small nuclear RNA (snRNA) is a class of small non-coding RNA molecules, being explosively discovered in the past few years, within the nucleus of eukaryotic cells to regulate a variety of important processes. They largely fall into two classes: snoRNA and miRNA/siRNA. Small nucleolar RNAs (snoRNAs) generally range from 60 to 300 nucleotides in length and guide the site-specific modification of nucleotides in target RNAs, including rRNAs, snRNAs and mRNAs, via short regions of base-pairing (Mattick and Makunin, 2006). microRNA (miRNA) and short interfering RNA (siRNA) are approximately 20 nucleotides long derived either from hairpin or double stranded RNA precursors, and are involved in regulating gene expression and in RNA interference respectively.

Molecular RNA techniques are largely developed and established for messenger RNA analysis. This thesis is focused on messenger RNA discussed in the following sections and in Chapter 3 and 4, and miRNA in Chapter 5 and 6.

Table 1.1 Major classes of non-coding RNA and functions (Clark, 2005)

Name	Function
Ribosomal RNA (rRNA)	Comprising major portion of ribosome and being involved in synthesis of polypeptide chains
Transfer RNA (tRNA)	Carrying amino acids to ribosome and recognizing codons on mRNA
Small nuclear RNA (snRNA)	Being involved in the processing of messenger RNA molecules in the nucleus of eukaryotic cells
Guide RNA	Being involved in processing of RNA or DNA in some organisms
Regulatory RNA	Regulating gene expression by binding to proteins or DNA or to other RNA molecules
Antisense RNA	Regulating gene expression by base pairing to mRNA
Recognition RNA	Being part of a few enzymes and enabling them to recognize certain short DNA sequences
Ribozymes	Enzymatically activating RNA molecules

1.4.3 mRNA features, processing and degradation

In the nucleus, RNA is made by RNA polymerase using a DNA template in the transcription process. The primary transcript is converted to mRNA normally needs some processing steps. In eukaryotes, maturation of mRNA undergoes splicing, capping and tailing (Figure 1.4). The DNA sequence of a gene consists of regions which code for part of the final protein, called the exons, alternating with regions of non-coding DNA, called the introns. The primary transcript RNA contains exons alternating with introns, which is converted to an mRNA by splicing process, involving cutting out the introns and joining the ends of the exons. Before splicing, RNA molecules destined to become messenger RNA have a guanosine triphosphate (GTP), a cap, added to their 5'-ends and a poly (A) tail added to their 3'-ends. Once messenger RNA is capped, tailed and had its introns spliced out, it is free to exit the nucleus through nuclear pore to function in the translation to protein (Clark, 2005).

Messenger RNA is relatively short-lived. It is easily degraded, especially when it is not bound to ribosomes. The degradation progresses after the poly (A) tail and then the cap are removed (Figure 1.4). An exonuclease, Xrn1, degrades the mRNA in the 5' to 3' direction. The stability of mRNA depends on the presence or absence of destabilizing sequences. Short-lived mRNA often contains multiple repeats of a 5 base AU-rich sequence, AUUUA, of about 50 bases known as an ARE (Clark, 2005). An ARE-binding protein recognizes the sequence and promotes degradation.

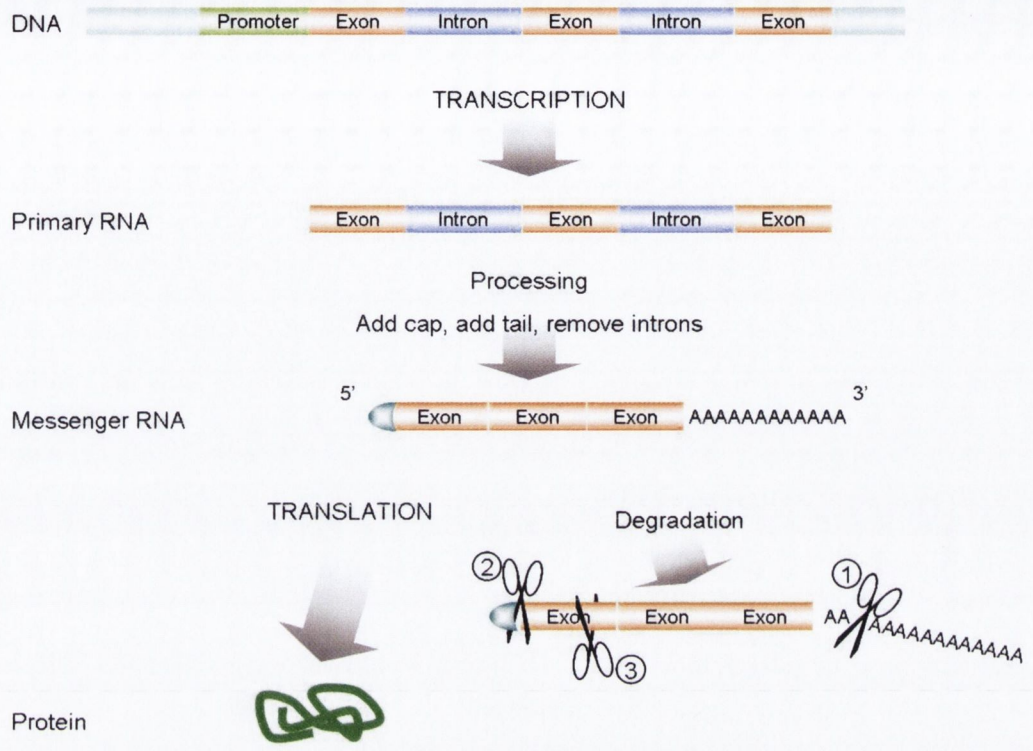

Figure 1.4 Schematic representation of mRNA features, processing and degradation

RNA is made using a DNA template in the transcription process. The primary transcript RNA contains exons alternating with introns, which is converted to an mRNA by processing including splicing, cutting out the introns and joining the ends of the exons, capping added to their 5'-ends and tailing a poly (A) tail to their 3'-ends. Once messenger RNA is capped, tailed and had its introns spliced out, it is free to exit the nucleus through nuclear pore to function in the translation of protein. Messenger RNA is easily degraded. The degradation processes are indicated by numbers from 1 to 3. The poly (A) tail and then the cap are removed. An exonuclease degrades the mRNA in the 5' to 3' direction.

1.5 Gene expression technology

Gene expression is the process by which inheritable information from a gene, the DNA sequence, is made into a functional gene product, such as protein or RNA. Among the tens of thousands of human genes, only a small fraction are expressed in a given cell type at a particular time. Gene expression levels of a cell are dynamic (Roth, 2002) and determine its function, phenotype and response to external stimuli. Thus the profiling can help to elucidate cellular functions, biochemical pathways and regulatory mechanisms (Russo et al., 2003). Gene expression profiles of diseased cells or tissues, compared with normal controls, may promote the understanding of disease pathology and identify new therapeutic points of intervention, improving diagnosis and clarifying prognosis.

The essential components for detecting and quantifying the amount of a specific RNA in a biological sample are a sufficient quantity of total or specific type of RNA, sequence-specific probes, a sensitive detection method, and the proper controls or standards for interpreting the results (Roth, 2002). There are a number of techniques developed for profiling gene expression. The most common ones are microarray, real-time PCR, northern blotting and in situ hybridization, which are generally discussed in the following sections. However, the RNAs in FFPE extracts have led to technical difficulties limiting extensive analysis of gene expression because most of the molecular techniques have been designed to analyze intact messenger RNA molecules which are obtainable from snap frozen samples. To analyze RNA extracted from FFPE, TaqMan® real time PCR as a relatively reliable technique is the focus of this thesis.

1.5.1 Microarray

The microarray is a powerful molecular technology that allows the simultaneous study of the expression of thousands of genes or their RNA products. This technology is based on hybridization between labelled free targets derived from a biological sample and an array of many cDNA or oligonucleotide probes that are immobilized on a matrix (Southern et al., 1999, Stanton, 2001). The hybridization signal produced on each probe is the mRNA expression level of the corresponding gene in the sample, which quantifies the types and amounts of mRNA transcripts present in a collection of cells.

In principle (Figure 1.5), the DNA microarray chip is an ordered collection of microspots, each spot containing one type of polynucleotide probe corresponding to a single species of a nucleic acid and representing the genes of interest. The mRNA is extracted from the specimens, and is reverse transcribed to complementary DNA (cDNA) which is then used to generate biotinylated complementary RNA (cRNA). After fragmentation, this labeled cRNA is placed on a microarray chip, and hybridizes to the probes to which they share sufficient sequence complementarity. The excess sample is washed and stained. The cRNA molecule bound to each polynucleotide probe is quantified by illuminating the solid chip surface with laser light and then measuring the intensity of fluorescence over each probe on the microarray. This intensity of fluorescence should be proportional to the number of molecules of cDNA bound to probe on the chip (Simon, 2008).

The microarray technique has become important because they are easy to use, do not require large-scale DNA sequencing and allow the parallel quantification of thousands of genes from multiple samples. The microarrays have the advantages of producing data for disease diagnosis, screening and prognosis (Russo et al., 2003). It was first used in cancer diagnosis by Khan et al (Golub et al., 1999, Khan et al., 1998) and has been demonstrated on an extensive variety of diseases and cancers, including breast, head and neck, liver, lung, ovary, pancreas, prostate stomach (Russo et al., 2003), and other cancers known to appear similar on routine histology. This technology improved the diagnostic accuracy of current approaches by using immunohistochemical analyses combined with classic histopathological techniques. Moreover, another essential application is the identification of diagnostic markers through the screening of thousands of tested genes and then comparing gene expression profiles from normal, premalignant and malignant tissues from the same organ (Russo et al., 2003). The identified biomarkers may be used to monitor the clinical response to both conventional and targeted therapeutics, and to assist identification of gene sets associated with metastasis or response to treatment.

Although microarray represents a powerful technology for clinical research, it requires high quality and quantity of RNA, which limited its application using the FFPE tissue samples. Processing tissue rapidly to maintain RNA integrity is crucial. False microarray data can be generated from degraded mRNA (Zareparsi et al., 2004, Auer et al., 2003).

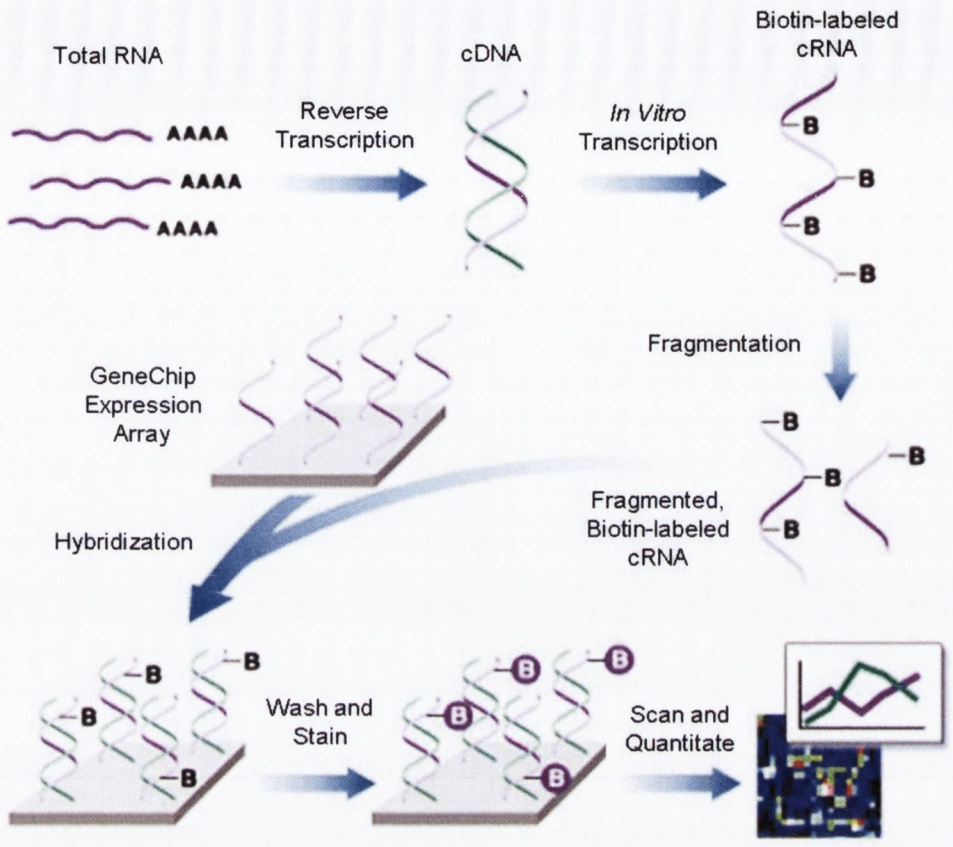

Figure 1.5 Principle of Affymetrix DNA microarray using oligonucleotides

The total mature RNA is isolated from the tissue and is reverse transcribed into a double stranded cDNA. The cDNA is gone through in vitro transcription back to cRNA which is labeled with Biotin. This is done by having all the uracil bases tagged with the Biotin. The labeled cRNA is then randomly fragmented in to pieces from 30 to 400 base pairs in length and is then added to the array. The RNA hybridizes to the probes at anywhere on the array where a RNA fragment and a probe are complimentary. The array is then washed and then stained with the fluorescent molecule that sticks to Biotin (Cy5 conjugated to streptavidin). Lastly, the entire array is scanned with a laser and the information is kept in a computer for quantitative analysis of what genes were expressed and at what approximate level (http://www.dkfz.de/gpcf/affy_technology.html).

1.5.2 Real-time TaqMan® PCR

Real-time quantitative TaqMan® reverse transcriptase-polymerase chain reaction (QRT-PCR) analysis has been introduced as a sensitive, accurate, and highly reproducible method to study gene expression (Mocellin et al., 2003). RNA is reverse transcribed into cDNA and then is amplified by real time TaqMan® RT PCR, during which PCR products are 'real-time' monitored as they accumulate. The benefit of this real-time capability is that it allows the researcher to better determine the amount of starting DNA in the sample before the amplification by PCR, and requires no post-PCR manipulations. The detailed technology is discussed in Chapter 4.

Real-time PCR has distinct advantages over microarray for several reasons. It is extremely sensitive, allowing the detection of less than five copies of a target sequence, making it possible to analyze small samples like clinical biopsies or cells from laser capture microdissection (Valasek and Repa, 2005). It requires only a few nanograms of target DNA or RNA and produces small amplicons, generally less than 200bp. Thus, it has been successfully used to detect gene transcript levels from snap frozen tissue extracts and even from FFPE containing partially fragmented RNA (Sheils and Sweeney, 1999, Sheils et al., 2000, Macabeo-Ong et al., 2002) although the detection rate is lower as indicated for example by invariably higher C_T values in the latter (Godfrey et al., 2000, Van Deerlin et al., 2002, Cohen et al., 2002, Abrahamsen et al., 2003, Koch et al., 2006). As a research tool, a major application of this technology is the rapid and accurate assessment of changes in gene expression as a result of physiology, pathophysiology, or development (Valasek and Repa, 2005).

1.5.3 Northern blotting

The northern blot was developed in 1977 by Alwine et al. (Alwine et al., 1977), which is based on hybridization using RNA as the target molecule and DNA as a probe. It takes its name from its similarity to the Southern blot technique, named after its inventor Edwin Southern (Southern, 1975) and used to study DNA. It serves two main purposes: one is detection of mRNA presence in a cell as evidence for gene transcription, the other is estimation of mRNA size (Dvorak et al., 2003).

The technique uses electrophoresis and detection with a hybridization probe (Figure 1.6) (Scott, 2006, Sambrook et al., 1989). RNA is isolated from various tissues and is separated by size using gel electrophoresis. The gels may be run on either agarose or denaturing polyacrylamide, the latter being preferable for smaller fragments of RNA. For agarose, formaldehyde is added to the gel and acts as a denaturant. For polyacrylamide, urea is the denaturant. The gel is then placed on a paper wick, which absorbs an ionic solution from a trough. A filter that traps RNA is placed above the gel, and blotting paper is placed above the filter. Capillary action can draw the solution through the gel, trapping the RNA on the filter. The filter is incubated with radioactive single-stranded DNA complementary, the hybridization probe, to the mRNA of interest. After any unbound DNA is washed off, autoradiography localizes the mRNA in the samples that contain it.

Northern blots are useful primarily to compare relative abundance of a particular mRNA species present in samples under different physiological or experimental conditions, but not provide absolute quantification (Reue, 1998). Among all the techniques discussed here, Northern blotting is the only one allowing mRNA size

determination, and thus it has been a key method for detecting mutations that result in abnormal mRNA size. However, compared to other quantitative techniques, there are several limitations resulting from the inability to control for the efficiency of RNA transfer and membrane binding, as well as the factors that affect probe hybridization to nucleic acids on a solid support. The most important is the low sensitivity (Dvorak et al., 2003) being suitable for determining relative concentrations of mRNA species that occur only in moderate to high abundance (Reue, 1998). It also requires very high quality RNA evidenced by sharp 28S and 18S bands after denaturing gel electrophoresis. Degraded RNA or incomplete transfer of RNA to the membrane will compromise the value of measurements of mRNA abundance.

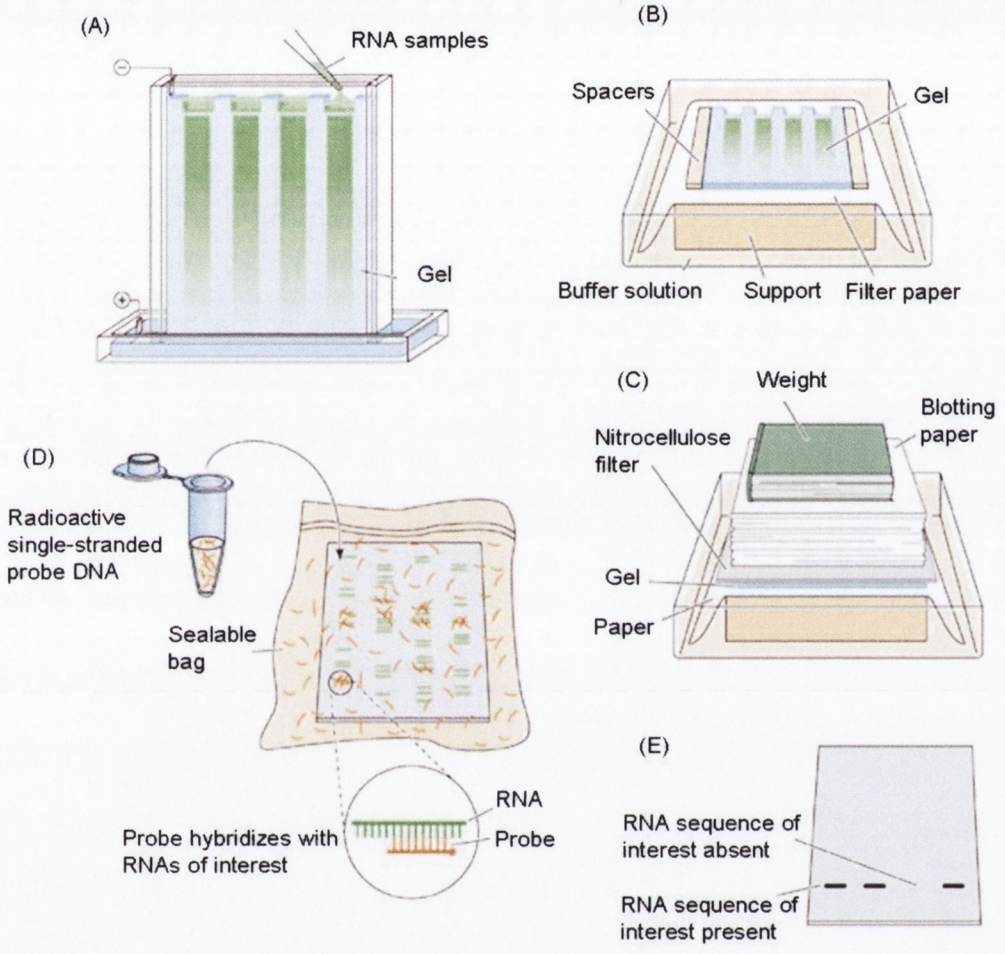

Figure 1.6 Procedure of northern blotting

(A) RNA samples are added to gel and separate according to size by gel electrophoresis. (B) The gel is then placed on a wet filter paper between two spacers. (C) A nitrocellulose filter that traps RNA is placed above the gel, and blotting paper is placed above the filter. RNA moves to filter by capillary action. (D) The filter is incubated with radioactive single-stranded DNA complementary to the mRNA of interest. (E) After any unbound DNA is washed off, autoradiography localizes the mRNA in the samples that contain it (Scott, 2006).

1.5.4 In situ hybridization

In situ hybridization (ISH) was first described in 1969 to analyze nucleic acids (Gall and Pardue, 1969), and was then developed into variations of method. ISH combines molecular biological techniques with histological and cytological analysis of gene expression. It allows direct analysis, through the localization of specific RNA sequences to individual cells within a morphologically preserved tissue (Hicks et al., 2004). In general, two types of probes are established: radioisotope-labelled (^{33}P or ^{35}S) and non-isotopic (e.g., digoxigenin labelled) probes. Detection is carried out using these labelled nucleic acid probes that are complementary to and hybridize with a particular RNA sequence. Those hybrids can be detected either by autoradiographic emulsion for radioactively labelled probes or by histochemical chromogen development for non-isotopically labelled probes (Jin and Lloyd, 1997).

ISH has become an important molecular tool in basic scientific research and clinical diagnosis. It has some unique advantages over other detection method. Because the detection is performed on tissue sections, RNA isolation process is not required. It provides additional morphologic information on the spatial distribution and heterogeneity of gene expression in complex tissues. However, contamination with RNase is a crucial pitfall during preparation of the probe and on day one of the ISH as these steps comprise working with unprotected RNA (Henke et al., 2006). Practically, probe stability and long term probe storage have been problematic (Hicks et al., 2004) and conditions for hybridization and post-hybridization washing should be stringent.

In addition, this technique has been employed on slides made from formalin-fixed paraffin-embedded tissues and was proved to be suitable for hybridization with DNA

or RNA probes (Henke et al., 2006, Mabruk, 2004). Recent development is employing ISH to detect microRNA expression level in FFPE materials (Nuovo, 2008). This application provides a tremendous opportunity to evaluate gene expression results generated using other techniques, and importantly to potentially correlate the histopathological discovery of protein or mRNA biomarker to the microRNA targets detected. FFPE ISH analysis requires patient and careful technical expertise. Proper controls must be used when interpreting final results.

1.6 Aims and objectives

The overall aim of this project was to establish an analysis system to study RNA expression efficiently using FFPE material. Specific objectives were:

i) to determine best extraction protocols among the seven available RNA protocols by comparison of extracts from FFPE tissue blocks, and then by comparison of parallel extracts from FFPE and snap frozen cell preparations using a cell line model.

ii) to improve gene expression analysis by modification of RNA extraction protocols and identifying of the most suitable real-time TaqMan® PCR techniques.

iii) to assess the reliability of miRNA detection in FFPE blocks by interrogation of 160 miRNA assays in paired RNA extracts from fresh and FFPE samples using the cell line model.

iv) to apply the determined microRNA detection method to actual disease settings by analysis of two individual targets across a large number of thyroid FFPE blocks.

1.7 References

ABRAHAMSEN, H. N., STEINICHE, T., NEXO, E., HAMILTON-DUTOIT, S. J. & SORENSEN, B. S. (2003) Towards quantitative mRNA analysis in paraffin-embedded tissues using real-time reverse transcriptase-polymerase chain reaction: a methodological study on lymph nodes from melanoma patients. *J Mol Diagn,* 5, 34-41.

ALWINE, J. C., KEMP, D. J. & STARK, G. R. (1977) Method for detection of specific RNAs in agarose gels by transfer to diazobenzyloxymethyl-paper and hybridization with DNA probes. *Proc Natl Acad Sci U S A,* 74, 5350-4.

AUER, H., LYIANARACHCHI, S., NEWSOM, D., KLISOVIC, M. I., MARCUCCI, G. & KORNACKER, K. (2003) Chipping away at the chip bias: RNA degradation in microarray analysis. *Nat Genet,* 35, 292-3.

CHAW, Y. F., CRANE, L. E., LANGE, P. & SHAPIRO, R. (1980) Isolation and identification of cross-links from formaldehyde-treated nucleic acids. *Biochemistry,* 19, 5525-31.

CLARK, D. (2005) *Molecular Biology: Understanding the genetic revoluation*, Elsevier Academic Press.

COHEN, C. D., GRONE, H. J., GRONE, E. F., NELSON, P. J., SCHLONDORFF, D. & KRETZLER, M. (2002) Laser microdissection and gene expression analysis on formaldehyde-fixed archival tissue. *Kidney Int,* 61, 125-32.

COOMBS, N. J., GOUGH, A. C. & PRIMROSE, J. N. (1999) Optimisation of DNA and RNA extraction from archival formalin-fixed tissue. *Nucleic Acids Res,* 27, e12.

COONS, A. H., CREECH, H. J. & JONES, R. N. (1941) Immunological properties of an antibody containing a fluorescent group. *Proc Soc Exp Biol Med,* 47, 200-202.

CRONIN, M., PHO, M., DUTTA, D., STEPHANS, J. C., SHAK, S., KIEFER, M. C., ESTEBAN, J. M. & BAKER, J. B. (2004) Measurement of gene expression in archival paraffin-embedded tissues: development and performance of a 92-gene reverse transcriptase-polymerase chain reaction assay. *Am J Pathol,* 164, 35-42.

DAPSON, R. (2007) Macromolecular changes caused by formalin fixation and antigen retrieval. *Biotech Histochem,* 82, 133-40.

DEDHIA, P., TARALE, S., DHONGDE, G., KHADAPKAR, R. & DAS, B. (2007) Evaluation of DNA extraction methods and real time PCR optimization on formalin-fixed paraffin-embedded tissues. *Asian Pac J Cancer Prev,* 8, 55-9.

DVORAK, Z., PASCUSSI, J. M. & MODRIANSKY, M. (2003) Approaches to messenger RNA detection - comparison of methods. *Biomed Pap Med Fac Univ Palacky Olomouc Czech Repub,* 147, 131-5.

FARRAGHER, S. M., TANNEY, A., KENNEDY, R. D. & PAUL HARKIN, D. (2008) RNA expression analysis from formalin fixed paraffin embedded tissues. *Histochem Cell Biol,* 130, 435-45.

FOX, C. H., JOHNSON, F. B., WHITING, J. & ROLLER, P. P. (1985) Formaldehyde fixation. *J Histochem Cytochem,* 33, 845-53.

GALL, J. G. & PARDUE, M. L. (1969) Formation and detection of RNA-DNA hybrid molecules in cytological preparations. *Proc Natl Acad Sci U S A,* 63, 378-83.

GODFREY, T. E., KIM, S. H., CHAVIRA, M., RUFF, D. W., WARREN, R. S., GRAY, J. W. & JENSEN, R. H. (2000) Quantitative mRNA expression analysis from formalin-fixed, paraffin-embedded tissues using 5' nuclease quantitative reverse transcription-polymerase chain reaction. *J Mol Diagn,* 2, 84-91.

GOLDSWORTHY, S. M., STOCKTON, P. S., TREMPUS, C. S., FOLEY, J. F. & MARONPOT, R. R. (1999) Effects of fixation on RNA extraction and amplification from laser capture microdissected tissue. *Mol Carcinog,* 25, 86-91.

GOLUB, T. R., SLONIM, D. K., TAMAYO, P., HUARD, C., GAASENBEEK, M., MESIROV, J. P., COLLER, H., LOH, M. L., DOWNING, J. R., CALIGIURI, M. A., BLOOMFIELD, C. D. & LANDER, E. S. (1999) Molecular classification of cancer: class discovery and class prediction by gene expression monitoring. *Science,* 286, 531-7.

HASELKORN, R. & DOTY, P. (1961) The reaction of formaldehyde with polynucleotides. *J Biol Chem,* 236, 2738-45.

HENKE, R. T., EUN KIM, S., MAITRA, A., PAIK, S. & WELLSTEIN, A. (2006) Expression analysis of mRNA in formalin-fixed, paraffin-embedded archival tissues by mRNA in situ hybridization. *Methods,* 38, 253-62.

HICKS, D. G., LONGORIA, G., PETTAY, J., GROGAN, T., TARR, S. & TUBBS, R. (2004) In situ hybridization in the pathology laboratory: general principles, automation, and emerging research applications for tissue-based studies of gene expression. *J Mol Histol,* 35, 595-601.

HUANG, S. N., MINASSIAN, H. & MORE, J. D. (1976) Application of immunofluorescent staining on paraffin sections improved by trypsin digestion. *Lab Invest,* 35, 383-90.

JIN, L. & LLOYD, R. V. (1997) In situ hybridization: methods and applications. *J Clin Lab Anal,* 11, 2-9.

KHAN, J., SIMON, R., BITTNER, M., CHEN, Y., LEIGHTON, S. B., POHIDA, T., SMITH, P. D., JIANG, Y., GOODEN, G. C., TRENT, J. M. & MELTZER, P. S. (1998) Gene expression profiling of alveolar rhabdomyosarcoma with cDNA microarrays. *Cancer Res,* 58, 5009-13.

KOCH, I., SLOTTA-HUSPENINA, J., HOLLWECK, R., ANASTASOV, N., HOFLER, H., QUINTANILLA-MARTINEZ, L. & FEND, F. (2006) Real-time quantitative RT-PCR shows variable, assay-dependent sensitivity to formalin fixation: implications for direct comparison of transcript levels in paraffin-embedded tissues. *Diagn Mol Pathol,* 15, 149-56.

KONONEN, J., BUBENDORF, L., KALLIONIEMI, A., BARLUND, M., SCHRAML, P., LEIGHTON, S., TORHORST, J., MIHATSCH, M. J., SAUTER, G. & KALLIONIEMI, O. P. (1998) Tissue microarrays for high-throughput molecular profiling of tumor specimens. *Nat Med,* 4, 844-7.

LEHMANN, U. & KREIPE, H. (2001) Real-time PCR analysis of DNA and RNA extracted from formalin-fixed and paraffin-embedded biopsies. *Methods,* 25, 409-18.

LEONG, A. S., MILIOS, J. & DUNCIS, C. G. (1988) Antigen preservation in microwave-irradiated tissues: a comparison with formaldehyde fixation. *J Pathol,* 156, 275-82.

LEWIN, B. (2000) *Genes VII,* New York, Oxford University Press Inc.

LEWIS, F., MAUGHAN, N. J., SMITH, V., HILLAN, K. & QUIRKE, P. (2001) Unlocking the archive--gene expression in paraffin-embedded tissue. *J Pathol,* 195, 66-71.

MABRUK, M. J. (2004) In situ hybridization: detecting viral nucleic acid in formalin-fixed, paraffin-embedded tissue samples. *Expert Rev Mol Diagn,* 4, 653-61.

MACABEO-ONG, M., GINZINGER, D. G., DEKKER, N., MCMILLAN, A., REGEZI, J. A., WONG, D. T. & JORDAN, R. C. (2002) Effect of duration of fixation on quantitative reverse transcription polymerase chain reaction analyses. *Mod Pathol,* 15, 979-87.

MASON, J. T. & O'LEARY, T. J. (1991) Effects of formaldehyde fixation on protein secondary structure: a calorimetric and infrared spectroscopic investigation. *J Histochem Cytochem,* 39, 225-9.

MATTICK, J. S. (2001) Non-coding RNAs: the architects of eukaryotic complexity. *EMBO Rep,* 2, 986-91.

MATTICK, J. S. & MAKUNIN, I. V. (2006) Non-coding RNA. *Hum Mol Genet,* 15 Spec No 1, R17-29.

MOCELLIN, S., ROSSI, C. R., PILATI, P., NITTI, D. & MARINCOLA, F. M. (2003) Quantitative real-time PCR: a powerful ally in cancer research. *Trends Mol Med,* 9, 189-95.

MONTERO, C. (2003) The antigen-antibody reaction in immunohistochemistry. *J Histochem Cytochem,* 51, 1-4.

NUOVO, G. J. (2008) In situ detection of precursor and mature microRNAs in paraffin embedded, formalin fixed tissues and cell preparations. *Methods,* 44, 39-46.

PUCHTLER, H. & MELOAN, S. N. (1985) On the chemistry of formaldehyde fixation and its effects on immunohistochemical reactions. *Histochemistry,* 82, 201-4.

RAIT, V. K., ZHANG, Q., FABRIS, D., MASON, J. T. & O'LEARY, T. J. (2006) Conversions of formaldehyde-modified 2'-deoxyadenosine 5'-monophosphate in conditions modeling formalin-fixed tissue dehydration. *J Histochem Cytochem,* 54, 301-10.

RAMOS-VARA, J. A. (2005) Technical aspects of immunohistochemistry. *Vet Pathol,* 42, 405-26.

REUE, K. (1998) mRNA quantitation techniques: considerations for experimental design and application. *J Nutr,* 128, 2038-44.

ROTH, C. M. (2002) Quantifying gene expression. *Curr Issues Mol Biol,* 4, 93-100.

RUSSO, G., ZEGAR, C. & GIORDANO, A. (2003) Advantages and limitations of microarray technology in human cancer. *Oncogene,* 22, 6497-507.

SAMBROOK, J., FRITSCH, E. & MANIATIS, T. (1989) *Molecular Cloning: A Laboratory Manual,* NY, Cold Spring Harbor Laboratory.

SCOTT, F. (2006) *Developmental Biology*, Sunderland, Mass. : Sinauer Associates.

SHEILS, O. M., O'LEARY, J. J. & SWEENEY, E. C. (2000) Assessment of ret/PTC-1 rearrangements in neoplastic thyroid tissue using TaqMan RT-PCR. *J Pathol,* 192, 32-6.

SHEILS, O. M. & SWEENEY, E. C. (1999) TSH receptor status of thyroid neoplasms--TaqMan RT-PCR analysis of archival material. *J Pathol,* 188, 87-92.

SHI, S. R., COTE, R. J., WU, L., LIU, C., DATAR, R., SHI, Y., LIU, D., LIM, H. & TAYLOR, C. R. (2002) DNA extraction from archival formalin-fixed, paraffin-embedded tissue sections based on the antigen retrieval principle: heating under the influence of pH. *J Histochem Cytochem,* 50, 1005-11.

SHI, S. R., KEY, M. E. & KALRA, K. L. (1991) Antigen retrieval in formalin-fixed, paraffin-embedded tissues: an enhancement method for immunohistochemical staining based on microwave oven heating of tissue sections. *J Histochem Cytochem,* 39, 741-8.

SIMON, R. (2008) Challenges of microarray data and the evaluation of gene expression profile signatures. *Cancer Invest,* 26, 327-32.

SOMPURAM, S. R., VANI, K., MESSANA, E. & BOGEN, S. A. (2004) A molecular mechanism of formalin fixation and antigen retrieval. *Am J Clin Pathol,* 121, 190-9.

SOUTHERN, E., MIR, K. & SHCHEPINOV, M. (1999) Molecular interactions on microarrays. *Nat Genet,* 21, 5-9.

SOUTHERN, E. M. (1975) Detection of specific sequences among DNA fragments separated by gel electrophoresis. *J Mol Biol,* 98, 503-17.

SRINIVASAN, M., SEDMAK, D. & JEWELL, S. (2002) Effect of fixatives and tissue processing on the content and integrity of nucleic acids. *Am J Pathol,* 161, 1961-71.

STANTON, L. W. (2001) Methods to profile gene expression. *Trends Cardiovasc Med,* 11, 49-54.

START, R. D., LAYTON, C. M., CROSS, S. S. & SMITH, J. H. (1992) Reassessment of the rate of fixative diffusion. *J Clin Pathol,* 45, 1120-1.

TAYLOR, C., SHI, S.-R., BARR, N. & WU, N. (2002) Techniques of immunohistochemistry: principles, pitfalls, and standardization. *Diagnostic Immunohistochemistry.* ed. Dabbs DJ, ed. New York, Churchill Livingstone.

TAYLOR, C. R. & BURNS, J. (1974) The demonstration of plasma cells and other immunoglobulin-containing cells in formalin-fixed, paraffin-embedded tissues using peroxidase-labelled antibody. *J Clin Pathol,* 27, 14-20.

VALASEK, M. A. & REPA, J. J. (2005) The power of real-time PCR. *Adv Physiol Educ,* 29, 151-9.

VAN DEERLIN, V. M., GILL, L. H. & NELSON, P. T. (2002) Optimizing gene expression analysis in archival brain tissue. *Neurochem Res,* 27, 993-1003.

WILLIAMS, C., PONTEN, F., MOBERG, C., SODERKVIST, P., UHLEN, M., PONTEN, J., SITBON, G. & LUNDEBERG, J. (1999) A high frequency of sequence alterations is due to formalin fixation of archival specimens. *Am J Pathol,* 155, 1467-71.

YAMASHITA, S. (2007) Heat-induced antigen retrieval: mechanisms and application to histochemistry. *Prog Histochem Cytochem,* 41, 141-200.

ZAREPARSI, S., HERO, A., ZACK, D. J., WILLIAMS, R. W. & SWAROOP, A. (2004) Seeing the unseen: Microarray-based gene expression profiling in vision. *Invest Ophthalmol Vis Sci,* 45, 2457-62.

ZIELENSKA, M., MARRANO, P., THORNER, P., PEI, J., BEHESHTI, B., HO, M., BAYANI, J., LIU, Y., SUN, B. C., SQUIRE, J. A. & HAO, X. S. (2004) High-resolution cDNA microarray CGH mapping of genomic imbalances in osteosarcoma using formalin-fixed paraffin-embedded tissue. *Cytogenet Genome Res,* 107, 77-82.

CHAPTER TWO

MATERIALS AND METHODS

2.1 Introduction

This chapter is a comprehensive account of all the methodologies employed in this thesis, accompanied by background information on some of the newer and more complex techniques. Several of the techniques are used in a number of chapters. Where this occurs, the full description of the technique is restricted to this chapter, with specifics (e.g. Gene expression assays) appearing in their relevant chapters only. The descriptions of each technique are broadly listed in the order in which they appear in the text of the thesis.

2.2 Cell culture of thyroid cell lines

Normal thyroid cell line is grown for the purposes of analysis of the formalin fixation impact and comparison of the different extraction protocols. The human thyroid follicular epithelial cell line (Nthy-ori 3-1 ECACC number 90011609) is derived from normal thyroid tissue of an adult. The cells have been immortalized by transfection with a plasmid encoding for the Simian Virus 40 (SV40) large T antigen (Lemoine et al., 1989).

2.2.1 Formulation of cell culture media and other solutions

- Culture media = RPMI + 10% Foetal Calf Serum (FCS) + 2% Penicillin/ Streptomycin (5000U/ml). e.g. Stock solution of 500ml of culture media (450ml RPMI, 40ml FCS and 10ml of Pen Streptomycin). Store at 4°C.
- Trypsin Neutralising Solution (TNS) = RPMI + 20%FCS. Store at -20°C.

- Freezing Solution = RPMI + 20%FCS + 10%Dimethyl sulfoxide (DMSO) (e.g. 35ml/10ml/5ml). Store at -20°C.
- Pre-warm cell culture media for 30 minutes at 37°C before use.

2.2.2 Thawing cells from stocks

- Add 15ml cell culture media into two T75 flasks.
- Remove one cryovial of cells (1ml in each) from liquid nitrogen and bring to room temperature.
- Add the thawed cells drop-wise to 8ml of media in a 15ml tube. Centrifuge for 4 minutes at 1000rpm.
- Resuspend pellets in 1ml media and add 500µl to each T75 flask.
- Change medium initially after 3 days (cells adherent) and at 3 day intervals until confluent.

2.2.3 Splitting confluent flasks

- Remove old medium waste from each flask into a designated waste bottle.
- Wash cells with 5ml phosphate buffered saline (PBS).
- Remove PBS and discard.
- Add 5ml of 1x Trypsin/EDTA to the flask and incubate at 37°C for 2-3 minutes.
- Examine flasks by phase microscopy to assess cell detachment.
- Lightly tap flasks to encourage the release of cells from the plastic surface.
- When >90% of cells detach, add an equal volume 5ml of Trypsin Neutralising Solution (TNS).

- Remove cell suspension to a new 15ml tube.
- Wash the flask with 5ml PBS and remove to the same 15ml tube.
- Pellet the cells (4 minute at 1000rpm) and remove supernatant.
- Resuspend cell pellet in 2ml RPMI (light tapping). Seed new flasks with 25% (500µl, 1:4 split ratios) of the trypsinized cells.

2.2.4 Cryopreservation

- After pelleting by centrifugation resuspend the cells in 2ml freezing solution in cryovials (1ml in each cryovial).
- Place the vials on ice for 10 minutes, then at -20°C for 1 hour and overnight at -80°C. Transfer to a liquid nitrogen storage tank for long-term storage.

2.3 Formalin-Fixed Paraffin-Embedded blocks

Formalin-Fixed Paraffin-Embedded cell pellets and tissue samples are used in this project. When it is needed, the processing of formalin fixation and paraffin embedding is carried out in Central Pathology Laboratory, St James's Hospital.

2.3.1 Formalin fixation of pelleted cells

Tripsinized cell pellets are resuspend in 2ml media and are counted with a hemocytometer. Approximately $1x10^5$ suspended cells are aliquot and are pelleted (a) snap frozen and (b) formalin fixed and paraffin embedded into a cell block. When formalin fixation is required, a cohesive solid cell pellet is constructed using 20% agar. The cells are centrifuged in an eppendorf tube, and the supernatant is removed.

Approximately 30µl of pre-warmed agar (60°C) is added to each tube. The solid cell pellet is formed within a few seconds. Cell blocks are placed in 10% buffered formalin (Sodium phosphate, monobasic 4.0 gm; Sodium phosphate, dibasic 6.5 gm; Formaldehyde, 37% 100.0 ml; and Distilled water 900.0 ml) at room temperature for 5 hours followed by tissue processing on a Tissue-Tek® V.I.P.TM tissue processor for 8 hours comprising: 10% buffered formalin fixation (4 hours at 37°C), 60% ethanol (20 minutes at 37°C), 80% ethanol (20 minutes at 37°C), 100% ethanol (20 minutes at 37°C), xylene (40 minutes at 37°C) and paraffin wax (80 minutes at 60°C). The pellets are subsequently paraffin embedded.

2.3.2 Archival Formalin-Fixed Paraffin-Embedded tissue samples

Total of 182 cases of formalin-fixed paraffin embedded thyroid samples were studied, including malignancy, benign, normal, and hyperplasia. These cases are accessioned from archives dating from 2000 to 2005 at St James Hospital, Dublin. The study has the approval of the St James Hospital and Adelaide and Meath Hospital research ethics committee. Haematoxylin and eosin (H&E) sections are reviewed by a histopathologist and classified according to a recognized system. Corresponding paraffin blocks are then collected from the archives of St James Hospital (Denning et al., 2007).

2.4 Laser capture microdissection

Laser capture microdissection is carried out on formalin fixed paraffin embedded (FFPE) tissue samples using the PixCell®II LCM System (Arcturus Engineering, Inc., CA, USA). The procedures are detailed below:

2.4.1 Prepare

- Cut 7μm FFPE histological sections and stain with a standard haematoxylin and eosin (H&E) stain. Upon drying place on the PixCell®II microscopic stage.
- Enable the laser via the keyswitch located on front of controller.
- Remove the CapSure® cassette module from the PixCell®II platform. It should slide out smoothly over the detents.
- Press down on the flanges of the cassette module. Press the end locking pins in to hold the plate down in the load position.
- Slide a CapSure® cartridge, which holds four film carriers, into the cassette module until it hits a stop. The cassette loads from one end only.
- If more than four caps are required, load a second cartridge in the same manner, making sure there is no space between the two loaded cartridges.
- Press down on the flanges of the loaded cassette. Retract the locking pins and gently raise the cassette to its loaded position.
- The cartridge is now ready to be loaded into the PixCell®II.
- After LCM, when the CapSure® cartridges are empty, press down on the plate and lock into position by pushing the locking pins in. Carefully slide out the spent cartridges and discard.

2.4.2 Locate

- Move the joystick to the vertical position. This centres the translation stage, on the optical axis and ensures proper registration of the sample slide relative to the capture area. This also maximises the transfer area available for microdissection.

- Turn off the vacuum chuck via the switch located on the front of the controller.
- Place the slide on the translation stage, covering the vacuum chuckhole. Manually position it to locate the transfer area in the centre of the field of view.
- Choose the appropriate objective for the desired magnification. Turn on the vacuum chuck.
- Adjust illumination control.
- Adjust focus control.
- Rotate the CapSure® placement arm over the tissue sample.
- Insert the visualiser by pressing the silver plunger button located above the joystick.
- Adjust the microscope light source to obtain a good image on the monitor.
- To perform a microdissection, retract the visualiser by pressing the tab located below the plunger button, and re-adjust the microscope light source.
- Slide the CapSure® cassette module to a detent position, making sure there is a CapSure® cap at the load line.
- Rotate the placement arm to the cap pick-up position. The arm will automatically line up with the cap.
- Raise the placement arm vertically to remove the cap from the cassette module.
- Rotate the placement arm to transfer position over the slide. Release the placement arm. The cap will automatically lower onto the slide. Upon contact with the slide, the placement arm will seat the cap properly on the sample.

2.4.3 Capture

When the laser is enabled, an aiming beam is visible on the monitor.

- Select the laser spot size with the 'Spot Size Adjust' located on the left of the laser tower.
- Use the joystick or the XY controls to aim the laser beam on the capture region.
- Use the front panel digital controls on the controller to adjust laser parameters. Typical values are shown in Table 2.1.

Table 2.1 Typical values of laser parameters

Spot Size	Power	Duration
<7.5μm	40mW	450μs
~15μm	25mW	1.5ms
~30μm	20mW	5ms

- Fire the laser by pressing the remote thumb switch or the 'fire' button on the front of the controller.
- There is an audible beep when the laser fires. The activated portion of the transfer film will be visible as a ring of film fused to the tissue.
- Use the joystick to move to other areas in the tissue and capture other cells of interest.

2.4.4 Microdissect

- To remove the captured tissue, lift the placement arm in a smooth but swift motion.
- With the cap in place, lift and rotate the placement arm to the unload platform.

- Lower the placement arm onto the unload platform – dropping the cap into the extraction slot.
- Rotate the placement arm to the rest position. The cap will be extracted from the arm and suspended in the unload platform.
- Slide the cap insertion tool onto the unload platform. Make sure the open end of the insertion tool faces the suspended cap and the groove fits over the guide rail.
- Slide the insertion tool down the groove until the cap is engaged.
- Remove with cap attached.
- Insert cap into 0.5ml reagent tube.
- Press down firmly to ensure an even seal.

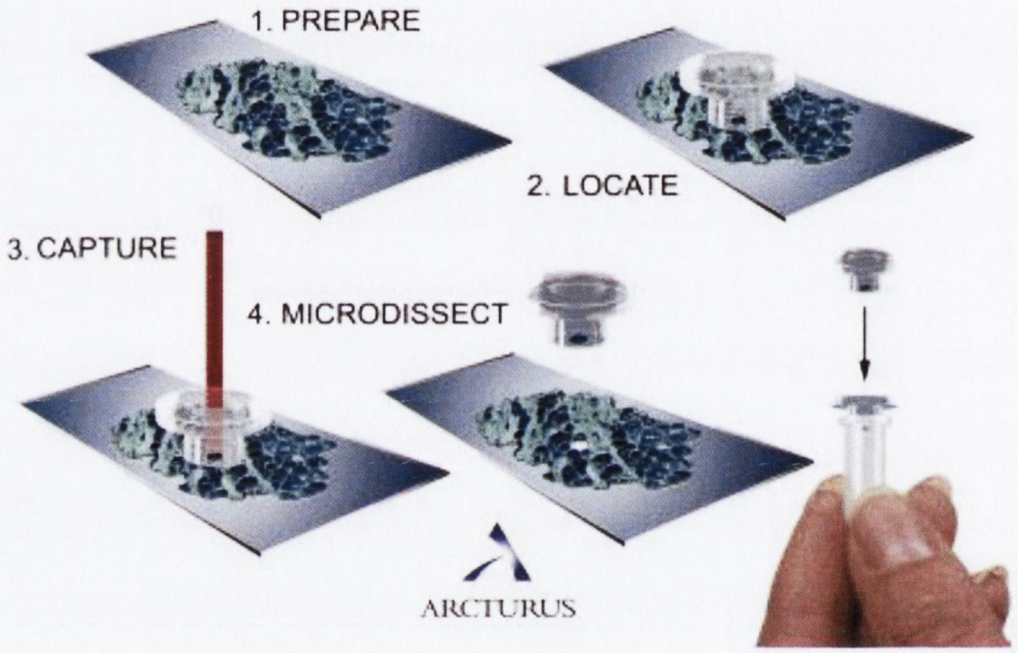

Figure 2.1 The laser capture microdissection process

The procedures include Prepare, Locate, Capture and Microdissect, which were carried out on formalin fixed paraffin embedded (FFPE) tissue samples using the PixCell®II LCM System (Arcturus Engineering, Inc., CA, USA).

2.5 RNA extraction

Throughout this thesis various available extraction protocols are used from thyroid snap frozen cells (10^5 cells), FFPE cells (10^5-10^6 cells) and FFPE tissue samples (5μm thick section or a full cap of LCM). The extraction of RNA with high quantity and quality is important in a variety of molecular biological techniques, and is essential for gene expression analysis. FFPE materials however can cause difficulty of RNA isolation because RNA molecules are chemically modified and degraded (Cronin et al., 2004). It is necessary to compare and optimize the RNA extraction protocols. Isolation procedures were quite different in these protocols. Stratagene, Ambion and 'in-house' system protocols were column based, while Gentra and Invitrogen protocols were RNA precipitation based.

2.5.1 Stratagene Absolutely RNA® FFPE Kit

Materials and reagents provided with the kit

- Prefilter Spin Cups (blue) and 2ml receptacle tubes, RNA-Binding Spin Cups (white) and 2ml receptacle tubes, collection tubes
- Deparaffinization Reagent (d-limonene), Proteinase K Digestion Buffer, Proteinase K (20mg/ml), RNA Binding Buffer, β-Mercaptoethanol (β-ME) (14.2M), High Salt Wash Buffer, Low Salt Wash Buffer, RNase-free DNase I (lyophilized) and DNase Reconstitution Buffer (Reconstitute the lyophilized RNase-free DNase I by adding 290μl of DNase Reconstitution Buffer to the vial. Mix the contents thoroughly to ensure that all the powder goes into solution), DNase Digestion Buffer, Elution Buffer (10mM Tris-HCl, pH 7.5)

Deparaffinization and Rehydration

- Place the cell/tissue sample in a single 1.5ml microcentrifuge tube.
- Add 1ml of Deparaffinization Reagent to the tube. Vortex for 10 seconds and incubate at room temperature for 10 minutes, vortexing for 10 seconds twice during the incubation.
- Spin the tubes for 5 minutes at 14,000g and carefully remove and discard the supernatant.
- Repeat with a fresh 1ml aliquot of Deparaffinization Reagent and spin.
- Wash the pellets by adding 1ml of 100% ethanol. Flick the tubes to dislodge the pellets and then vortex for 10 seconds. Spin the tubes for 5 minutes at 14,000g and carefully remove and discard the supernatant.
- Repeat washing twice using 90% ethanol and 70% ethanol.
- Re-spin for 1 minute at 14,000g and remove any residual fluid. Allow the pellets to air dry for 5 minutes.

Proteinase K Digestion

- Prepare a fresh working solution of Proteinase K by combining 100µl of Proteinase K Digestion Buffer and 10µl of Proteinase K per sample.
- Add 110µl of the Proteinase K working solution to each sample pellet. Incubate at 55°C for 3 hours or until the digestion mixture has clarified (up to 18 hours).

RNA Isolation

- Prepare a fresh working solution of RNA Binding Buffer by combining 125µl of RNA Binding Buffer and 0.875µl of β-ME per sample.
- Add 125µl of the RNA Binding Buffer–β-ME mixture to each sample and vortex or pipet repeatedly until homogenized.

- Transfer each sample to a prefilter spin cup. Place the spin cup in a 2ml receptacle tube (provided) and spin in a microcentrifuge for 1 minute at 14,000g.
- To the filtrate collected in each tube, add 125µl of 100% ethanol. Vortex for 5 seconds.
- Transfer this mixture to a RNA-Binding Spin Cup that has been seated within a 2ml receptacle tube (provided) and snap the cap of the tube onto the top of the spin cup. Spin in a microcentrifuge for 30–60 seconds at 14,000g.
- Remove and retain the spin cup and discard the filtrate. Replace the spin cup in the receptacle tube, and then add 600µl of 1x Low-Salt Wash Buffer and cap the tube. Spin for 30–60 seconds at 14,000g.
- Remove and retain the spin cup and discard the filtrate. Replace the spin cup in the receptacle tube, cap the tube, and spin in a microcentrifuge for 2 minutes at 14,000g to dry the fiber matrix.
- Prepare the DNase treatment solution by gently mixing 5µl of reconstituted RNase-free DNase I with 25µl of DNase Digestion Buffer per sample. Add 30µl of DNase treatment solution directly onto the fiber matrix inside the spin cup and cap the tube. Incubate the samples at 37°C for 15 minutes.
- Add 500µl of 1x High-Salt Wash Buffer and cap the tube. Spin for 30–60 seconds at 14,000g.
- Remove and retain the spin cup and discard the filtrate. Replace the spin cup in the receptacle tube, and then add 600µl of 1x Low-Salt Wash Buffer and cap the tube. Spin for 30–60 seconds at 14,000g.

- Remove and retain the spin cup and discard the filtrate. Replace the spin cup in the receptacle tube, and then add 300µl of 1x Low-Salt Wash Buffer and cap the tube. Spin for 30–60 seconds at 14,000g.
- Remove and retain the spin cup and discard the filtrate. Replace the spin cup in the receptacle tube, cap the tube, and spin for 2 minutes at 14,000g to dry the fiber matrix.

RNA Elution

- Transfer the spin cup to a 1.5ml collection tube (provided). Add 30µl of Elution Buffer (preheated to 75°C) directly onto the fiber matrix inside the spin cup. Cap the spin cup and incubate the sample at room temperature for 2 minutes.
- Spin the sample at 14,000g for 1 minute.
- The purified RNA is in the Elution Buffer in the microcentrifuge tube. Cap the tube and store the RNA at –20°C for up to one month or at –80°C for long-term storage.

2.5.2 Ambion RecoverAll™ Total Nucleic Acid Isolation Kit

Materials and reagents provided with the kit

- Collection tubes, filter cartridges
- Digestion buffer, Protease, 10x DNase Buffer, DNase, Wash 1 concentrate (Add ethanol before use), Wash 2/3 concentrate (Add ethanol before use), Isolation Additive, Elution Solution

Deparaffinization

- Place the equivalent of ≤80µm of tissue slices (i.e., a maximum of four 20µm, eight 10µm, or sixteen 5µm slices) in a 2ml microcentrifuge tube. Add 1ml

100% xylene and incubate for 3 minutes at 50°C. Vortex briefly to mix and incubate for 3 minutes at 50°C to melt the paraffin.

- Centrifuge the sample for 2 minutes at 14,000g to pellet the tissue. Remove the xylene without disturbing the pellet. Discard the xylene. If the pellet is loose, you may need to leave some xylene in the tube to avoid removing any tissue pieces.
- Add 1ml of 100% ethanol at room temperature to the sample and vortex to mix. Centrifuge the sample for 2 minutes at room temperature and 14,000g to pellet tissue. Remove and discard the ethanol without disturbing the pellet. Repeat to wash a second time with 1ml of 100% ethanol. Briefly centrifuge again to collect any remaining drops of ethanol in the bottom of the tube. Remove as much residual ethanol as possible without disturbing the pellet. Air dry the pellet for 10–15 minutes.

Protease Digestion

- Add 400µl of Digestion Buffer to each sample. Add 4µl of Protease to each sample. Swirl the tube gently to mix and to immerse the tissue.
- For RNA isolation, incubate the sample in a heat block for 3 hours at 50°C.
- Most sample mixtures will clarify within 3 hours. If the sample does not clarify, it may be heavily oxidized and therefore somewhat resistant to protease digestion. Samples that do not clarify may have slightly lower yields and smaller RNA fragments.

Nucleic Acid Isolation

- Add 480µl Isolation Additive to each sample. Vortex to mix. The solution should appear white and cloudy after mixing.

- Add 1.1ml 100% ethanol (Pipet in two aliquots of 550µl to accommodate adjustable pipettors). Mix each sample by pipetting up and down carefully. The solution should become clear at this point. Be careful when closing lids as the tubes will be near capacity.
- Place a Filter Cartridge in one of the Collection Tubes supplied. Pipet 700µl of the sample/ethanol mixture onto the Filter Cartridge and close the lid. Do not centrifuge Filter Cartridges at relative centrifugal forces greater than 10,000g; higher forces may damage the filters. Centrifuge at 10,000g (typically 10,000rpm) for 30–60 seconds to pass the mixture through the filter. Discard the flow-through, and re-insert the Filter Cartridge in the same Collection Tube. Repeat until all the sample mixture has passed through the filter (this should take 3 passes).
- Add 700µl of Wash 1 to the Filter Cartridge. Centrifuge for 30 seconds at 10,000g to pass the mixture through the filter. Discard the flow-through, and re-insert the Filter Cartridge in the same Collection Tube.
- Add 500µl of Wash 2/3 to the Filter Cartridge. Centrifuge for 30 seconds at 10,000g to pass the mixture through the filter. Discard the flow-through, and re-insert the Filter Cartridge in the same Collection Tube. Spin the assembly for an additional 30 seconds to remove residual fluid from the filter.

Nuclease Digestion and Final Nucleic Acid Purification

- For RNA isolation, add 60µl DNase mix (containing 6µl 10x DNase Buffer, 4µl DNase and 50µl Nuclease-free Water) to the centre of each Filter Cartridge. Cap the tube and incubate for 30 minutes at room temperature.

- Add 700µl of Wash 1 to the Filter Cartridge. Incubate for 30–60 seconds at room temperature. Centrifuge for 30 seconds at 10,000g. Discard the flow-through, and reinsert the Filter Cartridge in the same Collection Tube.
- Add 500µl of Wash 2/3 to the Filter Cartridge. Centrifuge for 30 seconds at 10,000g. Discard the flow-through, and re-insert the Filter Cartridge in the same Collection Tube. Repeat to wash a second time with 500µl of Wash 2/3. Centrifuge the assembly for 1 minute at 10,000g to remove residual fluid from the filter.
- Transfer the Filter Cartridge to a fresh Collection Tube. Apply 30µl of Elution Solution or nuclease-free water, heated to 95°C, to the centre of the filter, and close the cap. (The Elution Solution contains salts that, if concentrated, may affect downstream applications. If you intend to vacuum dry the sample, elute in nuclease-free water.) Allow the sample to sit at room temp for 1 minute. Centrifuge for 1 minute at maximum speed to pass the mixture through the filter. Repeat with a second 30µl aliquot of eluant, using the same Collection Tube. The volume of collected eluate will be close to 60µl. Store the nucleic acid at –20°C or colder.

2.5.3 J-I (GTCX)

J-I protocol was developed in Professor Jaggi's laboratory, University of Bern, Switzerland. The protocol requires tumour FFPE tissue samples of 10 sections, 10µm thick, 1cm^2 in 2ml eppendorf tubes.

Materials and reagents needed in the protocol

- RecoverAll™ Total Nucleic Acid Isolation Kit (Ambion)

- Guanidine Thiocyanate (Research Grade ICN Biomedical Inc.), Tris (Ultrapure ICN Biomedical Inc.), Triton X-100 (Mol.Biol.Grade Calbiochem), Proteinase K (PCR Grade 14-22mg/ml, 50U/ml Roche) (make 1:20 dilution to 1.0mg/ml before use)

Deparaffinization

- Add 1ml xylene and vortex briefly to mix. Incubate for 20 minutes at 50°C. Repeat once.
- Centrifuge for 2 minutes at 14,000g to pellet the tissue. Remove the xylene without disturbing the pellet. Add 1ml ethanol and centrifuge briefly at room temperature. Air dry for 15 minutes at room temperature.

Digestion:

- Dissolve pellet in 200µl Lysis Buffer (4M Guanidine Thiocyanate/30mM Tris pH 8.0 (GTC)/1% Triton X-100).
- Homogenize on the Mixer Mill for 4 minutes at 20Hz.
- Add ProteinaseK 11.8µl and incubate at 55°C for 60 minutes.
- Dilute sample with Dilution Buffer (1ml 30mM Tris pH 8.0/ 1% Triton X-100). Add Proteinase K 59.3µl and incubate at 55°C for 60 minutes.

Incubation:

- Incubate samples on a hot rack at 70°C for 20 minutes.

Nucleic Acid Isolation

- Centrifuge at 13,000rpm for 3 minutes.
- Transfer 1ml supernatant into a 12ml tube.
- Add 480µl Isolation additive (Ambion) to the sample, vortex to mix.
- Add 500µl ethanol and mix by pipetting.

- Pass the sample mixture through Ambion Filter Cartridge and follow the rest steps in the Nucleic Acid Isolation procedure and in the Nuclease Digestion and Final Nucleic Acid Purification as described in the Ambion RecoverAll™ Total Nucleic Acid Isolation Kit.

Expecting amount of RNA is 10 to 12μg.

2.5.4 J-II (GTCX)

The protocol requires tumour FFPE tissue samples of 10 sections, 10μm thick, 1cm^2 in 2ml eppendorf tubes.

Materials and reagents needed in the protocol

- RecoverAll™ Total Nucleic Acid Isolation Kit (Ambion)
- Guanidine Thiocyanate (Research Grade ICN Biomedical Inc.), Tris (Ultrapure ICN Biomedical Inc.), Triton X-100 (Mol.Biol.Grade Calbiochem), Proteinase K (PCR Grade 14-22mg/ml, 50U/ml Roche)

Deparaffinization

- Add 1ml xylene and vortex briefly to mix. Incubate for 20 minutes at 50°C. Repeat once.
- Centrifuge for 2 minutes at 14,000g to pellet the tissue. Remove the xylene without disturbing the pellet. Add 1ml ethanol and centrifuge briefly at room temperature. Air dry for 15 minutes at room temperature.

Digestion:

- Dissolve pellet in 200μl Lysis Buffer (4M Guanidine Thiocyanate/30mM Tris pH 8.0 (GTC)/1% Triton X-100) (Oberli et al., 2008).
- Homogenize on the Mixer Mill for 4 minutes at 20Hz.
- Add ProteinaseK 12μl and incubate at 55°C for 60 minutes.

- Dilute sample with Dilution Buffer (1ml 30mM Tris pH 8.0/ 1% Triton X-100). Add Proteinase K 60µl and incubate at 55°C for 60 minutes.

Incubation:

- Incubate samples on a hot rack at 94°C for 20 minutes.

Nucleic Acid Isolation

- Centrifuge at 13,000rpm for 3 minutes
- Transfer 1ml supernatant into a 12ml tube.
- Add 1200µl Isolation additive (Ambion) to the sample, vortex to mix.
- Add 2750µl ethanol and mix by pipetting.
- Pass the sample mixture through Ambion Filter Cartridge and follow the rest steps in the Nucleic Acid Isolation procedure and in the Nuclease Digestion and Final Nucleic Acid Purification as described in the Ambion RecoverAll™ Total Nucleic Acid Isolation Kit.

Expecting amount of RNA is 10 to 12µg.

2.5.5 Gentra Purescript® RNA Purification Kit

Reagents provided with the kit

- Cell Lysis Solution, Protein-DNA Precipitation Solution, RNA Hydration Solution

Deparaffinization

- Place sample into a tube and add 300µl Xylene. Incubate 5 minutes at room temperature.
- Centrifuge at 14,000g for 3 minutes to pellet the tissue. Discard the xylene. Repeat xylene wash for a total of 3 times.

- Add 300µl of 100% ethanol and incubate 5 minutes at room temperature. Centrifuge at 14,000g for 3 minutes to pellet the tissue. Discard the ethanol. Repeat ethanol wash once.

Proteinase K digestion

- Add 300µl Cell Lysis Solution and 1.5µl Proteinase K solution (20mg/ml).
- Incubate overnight at 55°C with constant agitation (i.e. a rotary oven).

Protein-DNA precipitation

- Transfer solution to a fresh 1.5ml microcentrifuge tube and add 100µl Protein-DNA Precipitation Solution to the cell lysate.
- Invert tube gently 10 times and place tube into an ice bath for 5 minutes.
- Centrifuge at 14,000g for 3 minutes. The precipitated proteins and DNA will form a tight pellet.
- (optional) Transfer the supernatant to a fresh tube and repeat ice incubation and centrifugation steps.

RNA precipitation

- Pipette the supernatant containing the RNA (leaving behind the precipitated protein-DNA pellet) into a clean 1.5ml microcentrifuge tube containing 300µl 100% isopropanol (2-propanol) and 0.5µl glycogen (20mg/ml).
- Mix the sample by inverting gently 50 times and incubate at -20°C for 1 hour.
- Centrifuge at 14,000g for 3 minutes; the RNA will be visible as a small, translucent pellet.
- Pour off supernatant and drain tube on clean absorbent paper. Add 300µl 70% ethanol. Invert the tube several times to wash the RNA pellet.
- Centrifuge at 14,000g for 1 minute and carefully pour off the ethanol.

- Invert and drain the tube on clean absorbent paper and allow to air dry for 15 minutes.

RNA hydration

- Add 25µl RNA Hydration Solution.
- Pipette sample up and down several times to ensure adequate mixing. Allow RNA to rehydrate at least 30 minutes on ice. Store RNA sample at -70°C to -80°C until use.

2.5.6 Invitrogen Trizol® Reagent

TRIZOL Reagent was provided with the protocol. When it is employed on FFPE materials, deparaffinization is carried out as described in the Ambion RecoverAll™ Total Nucleic Acid Isolation Kit.

Homogenization

- Lyse cells/tissue in 1ml of the TRIZOL Reagent by repetitive pipetting.
- Remove insoluble material from the homogenate by centrifugation at 12,000g for 10 minutes at 2 to 8°C. The resulting pellet contains extracellular membranes, polysaccharides, and high molecular weight DNA, while the supernatant contains RNA.

Phase separation

- Transfer the cleared homogenate solution to a fresh tube and incubate the homogenized samples for 5 minutes at 15 to 30°C to permit the complete dissociation of nucleoprotein complexes.

- Add 0.2ml of chloroform and cap sample tubes securely. Shake tubes vigorously by hand for 15 seconds and incubate them at 15 to 30°C for 2 to 3 minutes.
- Centrifuge the samples at 12,000g for 15 minutes at 2 to 8°C. The mixture separates into a lower red, phenol-chloroform phase, an interphase, and a colourless upper aqueous phase. RNA remains exclusively in the aqueous phase. The volume of the aqueous phase is about 60% of the volume of TRIZOL Reagent used for homogenization.

RNA precipitation

- Transfer the aqueous phase to a fresh tube, and save the organic phase if isolation of DNA or protein is desired.
- Precipitate the RNA from the aqueous phase by mixing with 0.5µl glycogen (20mg/ml) and 0.5ml isopropyl alcohol. The glycogen as carrier is co-precipitated with the RNA. It does not inhibit first-strand synthesis at concentrations up to 4mg/ml and does not inhibit PCR.
- Incubate samples at room temperature for 10 minutes and centrifuge at 12,000g for 10 minutes at 2 to 8°C. The RNA precipitate, often invisible before centrifugation, forms a gel-like pellet on the side and bottom of the tube.
- Remove the supernatant. Wash the RNA pellet once with 1ml of 75% ethanol. Mix the sample by vortexing and centrifuge at 7,500g for 5 minutes at 2 to 8°C.

Redissolving the RNA

- Briefly air-dry the RNA pellet for 5-10 minutes. Do not dry the RNA by centrifugation under vacuum. It is important not to let the RNA pellet dry completely as this will greatly decrease its solubility.

- Dissolve RNA in RNase-free water by passing the solution a few times through a pipette tip, and incubating for 10 minutes at 55 to 60°C. Partially dissolved RNA samples have an A260/280 ratio <1.6.

2.5.7 AB-in-House Protocol

Reagents provided with the kit

- 2x ncRNALysis Buffer

Deparaffinization

- Place sample into a tube and add 1.8ml xylene. Incubate 20 minutes at 37°C.
- Centrifuge at 14,000g for 3 minutes to pellet the tissue. Discard the xylene. Repeat above xylene wash once.
- Add 500µl of 70% ethanol and incubate for 5 minutes at room temperature. Centrifuge at 14,000g for 3 minutes to pellet the tissue. Discard the ethanol. Repeat above ethanol wash three times. Air dry the sample for 5 minutes.

Proteinase K digestion

- Add 300µl of PBS and 500µg of proteinase K (PCR Grade 14-22mg/ml, 50U/ml Roche). Mix well and incubate with shaking at 37°C for a minimum of 2 hours.
- Repeat addition of Proteinase K and further incubation up to overnight treatment appears to improve both the yield and transcript length of RNA isolated.

RNA Isolation

- Add 300µl of 2x ncRNALysis Buffer to generate a final working 1x concentration.

- Following incubation chill the sample on ice for 1 hour. (Important: The sample must be chilled before purification to ensure maximum yield of RNA is obtained).
- Pass the sample mixture through Ambion Filter Cartridge and follow the rest steps in the Nucleic Acid Isolation procedure and in the Nuclease Digestion and Final Nucleic Acid Purification as described in the Ambion RecoverAll™ Total Nucleic Acid Isolation Kit.

2.5.8 Ambion *mir*Vana™ miRNA Isolation Kit

Materials and reagents provided with the kit

- Collection tubes, filter cartridges
- Lysis/Binding Buffer, miRNA Wash Solution 1 concentrate (Add ethanol before use), Wash Solution 2/3 concentrate (Add ethanol before use), Acid-Phenol:Chloroform, miRNA Homogenate Additive, Elution Solution

Cell Lysis and Tissue Disruption

- Collect 10^2–10^7 cells or 0.5–250 mg tissue; wash cells in cold PBS
- Remove the PBS wash and add 300–600µl Lysis/Binding Solution. Cells will lyse immediately upon exposure to the Lysis/Binding Solution. Use the low end of the range (~300µl) for small numbers of cells (hundreds), and use closer to 600µl when isolating RNA from larger numbers of cells (thousands–millions). Vortex or pipet vigorously to completely lyse the cells and to obtain a homogenous lysate. Cell cultures typically do not require mechanical homogenization; however, it will not damage the RNA.

Organic Extraction

- Add 1/10 volume of miRNA Homogenate Additive to the cell lysate (or homogenate) (e.g. add 30µl of miRNA Homogenate Additive to 300µl of the cell lysate), and mix well by vortexing or inverting the tube several times. Leave the mixture on ice for 10 minutes.
- Add a volume of Acid-Phenol:Chloroform that is equal to the lysate volume before addition of the miRNA Homogenate Additive. (Be sure to withdraw from the bottom phase in the bottle of Acid-Phenol:Chloroform, because the upper phase consists of an aqueous buffer.) Vortex for 30–60 seconds to mix. Centrifuge for 5 minutes at maximum speed (10,000g) at room temperature to separate the aqueous and organic phases. After centrifugation, the interphase should be compact; if it is not, repeat the centrifugation.
- Carefully remove the aqueous (upper) phase without disturbing the lower phase, and transfer it to a fresh tube. Note the volume removed.

RNA Isolation – Enrichment Procedure for Small RNAs

This enrichment of small RNAs is accomplished by first immobilizing large RNAs on the filter with a relatively low ethanol concentration and collecting the flow-through containing mostly small RNA species. More ethanol is then added to this flow-through, and the mixture is passed through a second glass filter where the small RNAs are immobilized. This second filter is then washed a few times, and the small-RNA enriched sample is eluted.

- Add 1/3 volume of 100% ethanol to the aqueous phase recovered from the organic extraction (e.g. add 100µl 100% ethanol to 300µl aqueous phase). Mix thoroughly by vortexing or inverting the tube several times.
- Place a Filter Cartridge into one of the Collection Tubes supplied. Pipette the lysate/ethanol mixture (from the previous step) onto the Filter Cartridge. Up to

700µl can be applied to a Filter Cartridge at a time. Collect the filtrate (that is, the liquid flow-through in the Collection Tube); it contains the small RNAs. Centrifuge at 10,000g for ~15 seconds to pass the mixture through the filter. Spinning harder than this may damage the filters. Collect the filtrate. If the lysate/ethanol mixture is >700µl, transfer the flow-through to a fresh tube, and repeat until all of the lysate/ethanol mixture is through the filter. Pool the collected filtrates if multiple passes were done, and measure the total volume of the filtrate.

- Add 2/3 volume room temperature 100% ethanol to filtrate (i.e. flow-through) (e.g. add 266µl 100% ethanol to 400µl of filtrate recovered) and mix thoroughly.
- Place a Filter Cartridge into one of the Collection Tubes supplied. Pipette the filtrate/ethanol mixture (from the previous step) onto a second Filter Cartridge. Up to 700µl can be applied to a Filter Cartridge at a time. For sample volumes greater than 700µl, apply the mixture in successive applications to the same filter. Centrifuge at 10,000g for ~15 seconds to pass the mixture through the filter. Discard the flow-through, and repeat until all of the filtrate/ethanol mixture is through the filter. Reuse the Collection Tube for the washing steps.
- Apply 700µl miRNA Wash Solution 1 (working solution mixed with ethanol) to the Filter Cartridge and centrifuge for ~5–10 seconds to pass the solution through the filter. Discard the flow-through from the Collection Tube, and replace the Filter Cartridge into the same Collection Tube.
- Apply 500µl Wash Solution 2/3 (working solution mixed with ethanol) and draw it through the Filter Cartridge as in the previous step. Repeat with a second 500µl aliquot of Wash Solution 2/3. After discarding the flow-through

from the last wash, replace the Filter Cartridge in the same Collection Tube and spin the assembly for 1 minute to remove residual fluid from the filter.

- Transfer the Filter Cartridge into a fresh Collection Tube provided. Apply 100µl of pre-heated (95°C) Elution Solution or nuclease-free water to the centre of the filter, and close the cap. Spin for ~20–30 seconds at maximum speed to recover the RNA. Collect the eluate (which contains the RNA) and store it at –20°C or colder.

2.6 Nano-Drop® ND-1000 Spectrophotometer

Nucleic acid samples are checked for concentration and quality using the NanoDrop® ND-1000 Spectrophotometer. To measure nucleic acid samples select the 'Nucleic Acid' application module. The NanoDrop® ND-1000 is a full-spectrum (220-750nm) spectrophotometer that measures 1µl samples with high accuracy and reproducibility (Figure 2.2). It utilizes a patented sample retention technology that employs surface tension alone to hold the sample in place. In addition, the ND-1000 has the capability to measure highly concentrated samples without dilution (50x higher concentration than the samples measured by a standard cuvette spectrophotometer).

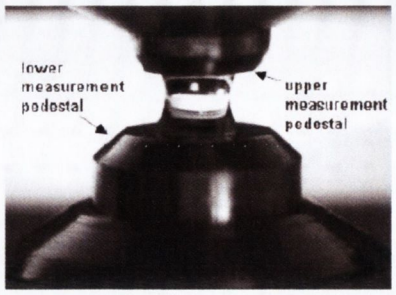

Figure 2.2 Sample pedestal of a NanoDrop® ND-1000 Spectrophotometer

Close the sampling arm and the sample column is automatically drawn between the upper and lower measurement pedestals and the spectral measurement made.

2.6.1 Blank measurement

- Ensure measurement pedestal surfaces are clean. Load 1µl water sample onto the lower measurement pedestal and then click 'OK'. The message "Initializing Spectrometer - please wait" will appear, and the instrument will be ready for use.
- Before making a sample measurement, a blank must be measured and stored. This will assure the user that the instrument is working well and that any non-specific fluorescence is not a concern.
- Load a blank sample (the buffer, solvent, or carrier liquid used with your samples) onto the lower measurement pedestal and lower the sampling arm into the 'down' position. Click on the 'Blank' button.
- Wipe the blanking buffer from both pedestals using a laboratory wipe.
- Analyze an aliquot of the blanking solution as though it were a sample. This is done using the 'Measure' button. The result should be a spectrum with a

relatively flat baseline. Wipe the blank from both measurement pedestal surfaces and repeat the process until the spectrum is flat.

2.6.2 Sample measurements

- 1µl samples are sufficient to ensure accurate and reproducible results when measuring aqueous nucleic acid samples.
- With the sampling arm open, pipette the sample onto the lower measurement pedestal.
- Close the sampling arm and initiate a spectral measurement using the operating software on the PC. The sample column is automatically drawn between the upper and lower measurement pedestals and the spectral measurement made.
- When the measurement is complete, open the sampling arm and wipe the sample from both the upper and lower pedestals using a soft laboratory wipe. Simple wiping prevents sample carryover in successive measurements for samples varying by more than 1000 fold in concentration.

2.6.3 Results illustration

- A260: absorbance of the sample at 260nm represented as if measured with a conventional 10mm path. Note: This is 10x the absorbance actually measured using the 1mm path length and 50x the absorbance actually measured using the 0.2mm path length.
- A280: sample absorbance at 280nm represented as if measured with a conventional 10mm path. Note: This is 10x the absorbance actually measured

using the 1mm path length and 50x the absorbance actually measured using the 0.2mm path length.

- 260/280: ratio of sample absorbance at 260 and 280nm. The ratio of absorbance at 260 and 280nm is used to assess the purity of DNA and RNA. A ratio of ~1.8 is generally accepted as "pure" for DNA; a ratio of ~2.0 is generally accepted as "pure" for RNA. If the ratio is appreciably lower in either case, it may indicate the presence of protein, phenol or other contaminants that absorb strongly at or near 280nm.
- 260/230: ratio of sample absorbance at 260 and 230nm. This is a secondary measure of nucleic acid purity. The 260/230 values for "pure" nucleic acid are often higher than the respective 260/280 values. They are commonly in the range of 1.8-2.2. If the ratio is appreciably lower, this may indicate the presence of co-purified contaminants.
- Concentration (ng/µl): sample concentration in ng/µl based on absorbance at 260nm and the selected analysis constant.

2.7 Agilent 2100 Bioanalyzer

The Agilent 2100 bioanalyzer is the most successful microfluidics-based platform available commercially, offering solutions for the analysis of DNA, RNA, proteins and cells. It is used through this thesis to analyse RNA integrity and generate gel like image and electropherogram digital data.

2.7.1 Setting up the Chip Priming Station

- Place the syringe. Remove the plastic cap of the new syringe and insert it into the clip. Slide it into the hole of the lock adapter and screw it tightly to the chip priming station.
- Adjust the base plate: Open the chip priming station by pulling the latch. Using a screwdriver, open the screw at the underside of the base plate. Lift the base plate and insert it again in position C as below in Figure 2.3. Retighten the screw.
- Adjust the syringe clip: Release the lever of the clip and slide it up to the top position as below in Figure 2.3.

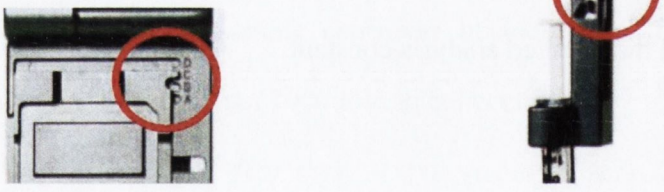

Figure 2.3 Setting up the priming station

The base plate is adjusted to position C as shown on the left. The syringe clip is adjusted by releasing the lever of the clip and sliding it up to the top position as shown on the right.

2.7.2 Decontaminating the Electrodes

To avoid decomposition of the RNA sample, follow this electrode decontamination procedure on a daily basis before running any RNA Nano assays.

- Slowly fill one of the wells of an electrode cleaner with 350µl RNaseZAP.
- Open the lid and place electrode cleaner in the Agilent 2100 bioanalyzer.
- Close the lid and leave it closed for about 1 minute.
- Open the lid and remove the electrode cleaner. Label the electrode cleaner and keep it for future use. You can reuse the electrode cleaner for all 25 chips in the kit.
- Slowly fill one of the wells of another electrode cleaner with 350µl RNase-free water.
- Place electrode cleaner in the Agilent 2100 bioanalyzer.
- Close the lid and leave it closed for about 10 seconds.
- Open the lid and remove the electrode cleaner. Label it and keep it for further use.
- Wait another 10 seconds for the water on the electrodes to evaporate before closing the lid.

2.7.3 Preparing the gel

- Allow all reagents to equilibrate to room temperature for 30 minutes before use.
- Place 550µl of Agilent RNA 6000 Nano gel matrix into the top receptacle of a spin filter.

- Place the spin filter in a microcentrifuge and spin for 10 minutes at 1500g ± 20%.
- Aliquot 65µl filtered gel into 0.5ml RNase-free microfuge tubes that are included in the kit. Store the aliquots at 4°C and use them within one month of preparation.

2.7.4 Preparing the gel dye mix

Kit components contain DMSO. Because the dye binds to nucleic acids, it should be treated as a potential mutagen and used with appropriate care.

- Allow all reagents to equilibrate to room temperature for 30 minutes before use. Protect the dye concentrate from light while bringing it to room temperature.
- Vortex RNA 6000 Nano dye concentrate for 10 seconds and spin down.
- Add 1µl of RNA 6000 Nano dye concentrate to a 65µl aliquot of filtered gel (prepared as described in "Preparing the Gel" above).
- Cap the tube, vortex thoroughly and visually inspect proper mixing of gel and dye.
- Spin tube for 10 minutes at room temperature at 1300g. Use prepared gel-dye mix within one day. A larger volume of gel-dye mix can be prepared in multiples of the 65+1 ratio, if more than one chip will be used within one day. Always re-spin the gel-dye mix at 1300g for 10 minutes before each use.

2.7.5 Loading the gel dye mix, Nano marker, ladder and samples

- Allow the gel-dye mix to equilibrate to room temperature for 30 minutes before use and protect the gel-dye mix from light during this time.
- Place a new RNA Nano chip on the chip priming station.
- Pipette 9.0µl of the gel-dye mix at the bottom of the well marked G and dispense the gel-dye mix:

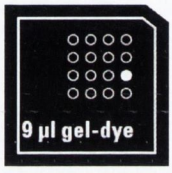

- Set the timer to 30 seconds, make sure that the plunger is positioned at 1ml and then close the chip priming station. The lock of the latch will click when the Priming Station is closed correctly. (Note: When pipetting the gel-dye mix, make sure not to draw up particles that may sit at the bottom of the gel-dye mix vial. Insert the tip of the pipette to the bottom of the chip well when dispensing. This prevents a large air bubble forming under the gel-dye mix. Placing the pipette at the edge of the well may lead to poor results.)
- Press the plunger of the syringe down until it is held by the clip.
- Wait for exactly 30 seconds and then release the plunger with the clip release mechanism.
- Visually inspect that the plunger moves back at least to the 0.3ml mark.
- Wait for 5 seconds then slowly pull back the plunger to the 1ml position.
- Open the chip priming station.

- Pipette 9.0µl of the gel-dye mix in each of the wells marked:

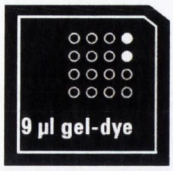

- Pipette 5µl of the RNA 6000 Nano marker into the well marked with the ladder symbol and each of the12 sample wells.
- Do not leave any wells empty or the chip will not run properly. Unused wells must be filled with 5µl of the RNA 6000 Nano marker plus 1µl of the buffer in which the samples are diluted.
- Before use, thaw ladder aliquots and keep them on ice (avoid extensive warming upon thawing process)
- To minimize secondary structure, heat denature (70°C, 2 minutes) the samples before loading on the chip. Pipette 1µl of the RNA ladder into the well marked with the ladder symbol.
- Pipette 1µl of each sample into each of the 12 sample wells.
- Set the timer to 60 seconds.
- Place the chip horizontally in the adapter of the vortex mixer. If there is liquid spill at the top of the chip, carefully remove it with a tissue.
- Vortex for 60 seconds at 2400rpm.
- Open the lid of the Agilent 2100 bioanalyzer and place the chip carefully into the receptacle. The chip fits only one way.
- Carefully close the lid. The electrodes in the cartridge fit into the wells of the chip.

2.7.6 Starting the 2100 expert software and analyzing the samples

- Go to your desktop and double-click the following icon: 
- The screen of the software appears in the *Instrument* context. The icon in the upper part of the screen represents the current instrument/PC communication status. The 2100 expert software screen shows that you have inserted a chip and closed the lid by displaying the chip icon at the top left of the context.
- In the *Instrument* context, select the appropriate assay from the *Assay* menu.
- Click the *Start* button in the upper right of the window to start the chip run. The incoming raw signals are displayed in the *Instrument* context.
- After the chip run is finished, remove the chip from the receptacle of the bioanalyzer and dispose it.
- To check the results of the run, select the Gel or Electropherogram tab in the *Data* context. The electropherogram of the ladder well window should resemble those shown in Figure 2.4.
- To review the results of a specific sample, select the sample name in the tree view and highlight the *Results* sub-tab. The electropherogram of the sample well window for total RNA (eukaryotic) should resemble the one shown here below in Figure 2.4.
- By selecting the *Results* sub-tab, values for the calculated RNA concentration, the ribosomal ratio and the RNA Integrity Number (RIN) are displayed.

A.

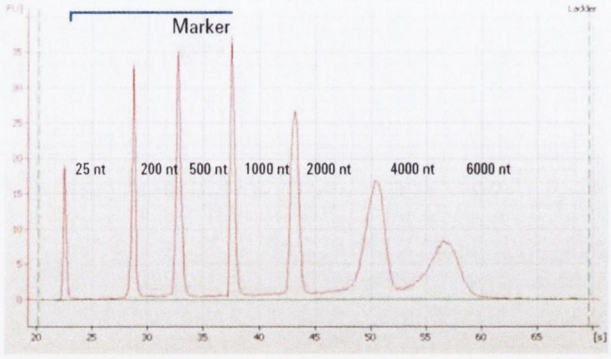

B.

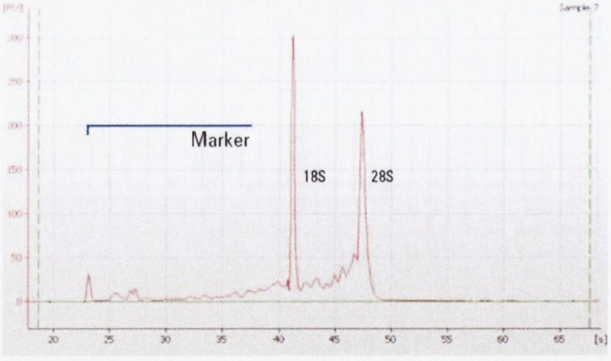

Figure 2.4 Ladder and sample Electropherogram

The RNA quality is shown as the electropherograms: A, the RNA ladder; and B, the sample with intact RNA.

2.8 TaqMan® PCR

Applied Biosystems TaqMan® PCR-based system (Applied Biosystems, CA, USA) was selected for mRNA quantitation and microRNA quantification in this thesis. The instuments, assays, reagents and procedures are descibed as below:

2.8.1 Reverse Transcription cDNA protocol

Applied Biosystems High-Capacity cDNA Archive Kit (P/N: 4322171, Applied Biosystems) was used following manufacturer's protocol for reverse transcription (RT) of total RNA to single-stranded cDNA.

Prepare 2x RT master mix

- Allow the kit components to thaw on ice.
- Calculate the volume of components needed to prepare the cDNA archive reaction plate, using the Table 2.2.

Table 2.2 RT master mix setup for volume of 50µl final reaction

Component	Volume (µl) / Reaction
10x Reverse Transcription Buffer	10
25x dNTPs	4
10x random primers	10
MultiScribe™ Reverse Transcriptase, 50U/µl	5
Nuclease-free H_2O	21
Total per Reaction	**50**

- Place the 2x RT master mix on ice until you prepare the cDNA archive reaction plate.

Preparing the cDNA Archive Reaction Plate

- Pipette 50µl of 2x RT master mix into each well of a 96-well reaction plate.
- Pipette 50µl of RNA sample into wells, pipetting up and down two times to mix.
- Cover the plate with caps.
- Briefly centrifuge the plate to spin down the contents and to eliminate any air bubbles.
- Place the plate on ice until you are ready to load the thermal cycler.

Performing Reverse Transcription

- Program the thermal cycler conditions for RT: Incubation at 25°C for 10 minutes, following by incubation at 37°C for 120 minutes, and then indefinite hold at 4°C.
- Set the reaction volume to 100µl.
- Load the reaction plate into the thermal cycler and start the reverse transcription run.
- The cDNA archive plates prepared can be used in a variety of applications, including short-term and long-term archival storage at –15 to –25°C, quantitative PCR and conversion to cRNA.

2.8.2 TaqMan® Real-Time PCR protocol

Overview target amplification, using cDNA as the template, is the second step in using TaqMan® Gene Expression Assays. In this step, the DNA polymerase, from the TaqMan® Universal PCR Master Mix (2x) or the TaqMan® Fast Universal PCR Master

Mix (2x), No AmpErase UNG, amplifies target cDNA synthesized from the RNA sample, using sequence-specific primers and TaqMan® MGB probe (6-FAM dye-labeled) from the TaqMan® Gene Expression Assay mix. PCR process performing the PCR step for singleplex assays in 384-well or 96-well formats requires the following procedures:

Preparing the reaction plate

- For optimal performance of TaqMan® Gene Expression Assays, use 10 to 100ng of cDNA per 50 or 20µl reaction, when using the TaqMan® Universal PCR Master Mix (2x).
- The recommended reaction sizes vary depending on the PCR master mix used. Prepare the plate so that each PCR reaction contains the components listed in the following Table 2.3.
- Prepare the PCR reaction mix for each sample separately.
- Mix the solutions by gently pipetting up and down then cap the tubes.
- Centrifuge the tubes briefly to spin down the contents and eliminate any air bubbles from the solutions.
- Transfer the appropriate volume of each reaction mixture to wells of an optical plate, as specified in the following table.
- Cover the plate with an optical adhesive cover or with optical flat caps.
- Centrifuge the plate briefly to spin down the contents and eliminate any air bubbles from the solutions.

Table 2.3 TaqMan® real time PCR master mix setup for volume of 20µl final reaction

* Note: If adding UNG to the reaction, the final concentration of UNG should be 0.01U/µl reaction. UNG is shipped at a concentration of 1U/µl. To compensate for additional volume of UNG, decrease the volume of water used to dilute the cDNA template.

Component	Volume (µl) / 20µl Reaction
TaqMan Gene Expression Assay (20x)	1.0
cDNA template + H_2O	9.0
TaqMan Universal PCR Master Mix (2x) (with or without AmpErase UNG)*	10.0
Total	**20.0**

Running the plate

- Place the reaction plate in the instrument.
- Set the thermal cycling conditions as Standard Run: AmpErase UNG Activation UDG (hold) at 50°C for 2 minutes, AmpliTaq Gold Enzyme activation (hold) at 95°C for 10 minutes, following by 40 PCR cycles of 95°C for 15 seconds (Denature) and 60°C for 1 minutes (Anneal/Extend). Note: The 2 minutes, 50°C step is required for optimal AmpErase UNG activity. This step is not needed when AmpErase UNG is not added to the reaction.
- Start the run.

2.8.3 TaqMan® PreAmp

TaqMan® preamplification includes three procedures: pooling the TaqMan® Assays, preparing cDNA from RNA, and running the preamplification reaction (Figure 2.5). TaqMan® pooled assays are employed in this process to amplify specific targets, which product is subsequently analyzed using TaqMan® real time PCR.

Pooling the TaqMan® Assays

- In a microcentrifuge tube, prepare a 0.2x pooled TaqMan® assay mix for running the preamplification reaction by combining equal volumes of each 20x TaqMan® Gene Expression Assay, up to a total of 100 assays. (For example, to pool 50 TaqMan® assays, combine 10µl of each TaqMan® assay.)
- Dilute the pooled TaqMan® assays using 1x TE buffer so that each assay is at a final concentration of 0.2x. (For the above example, add 500µl of 1x TE buffer to the pooled TaqMan® assays for a total volume of 1ml.)

Preparing cDNA from RNA

- Applied Biosystems High Capacity cDNA Reverse Transcription Kit (PN 4368814) was used to synthesize single-stranded cDNA from total RNA samples. The processes are described in section 2.8.1.

Running the Preamplification Reaction

- In this step, you perform multiplex preamplification of up to 100 specific cDNA targets to increase the quantity of the desired cDNA targets for gene expression analysis using TaqMan® Gene Expression Assays.

- Prepare each preamplification reaction in a 0.2ml or 1.5ml microcentrifuge tube, depending on the total volume (Table 2.4)

Table 2.4 TaqMan® PreAmp master mix setup for volume of 50µl final reaction

Component	volume (µl/Reaction)	Final Concentration
TaqMan PreAmp Master Mix (2x)	25.0	1x
Pooled assay mix (0.2x)	12.5	0.05x (each assay)
1–250ng cDNA sample + nuclease-free water	12.5	0.02–5.0ng/µl
Total	**50.0**	—

- Cap the microcentrifuge tube or seal the 96-well plate with a MicroAmp Clear Adhesive Film.
- Mix the reactions by gently inverting the tube or plate, then centrifuge briefly.
- (Optional) If using a 96-well plate, place a MicroAmp Optical Film Compression Pad on top of it.
- Load the plate or tubes into the thermal cycler.
- Set up the thermal cycling conditions for preamplification: Incubation at 95°C for 10 minutes (enzyme activation), following by 10 or 14 cycles of 95°C for 15 seconds (Denature) and 60°C for 4 minutes (Anneal/Extend), and then holding at 4°C.
- Start the run.
- Upon completion, immediately remove the plate from the thermal cycler and place it on ice.

- Perform real time PCR amplification as described in section 2.8.2, or store aliquots of the preamplification product at –20°C. When performing PCR Amplification, the DNA polymerase [from the TaqMan® Gene Expression PCR Master Mix (2x)] amplifies the preamplified target cDNA, using sequence-specific primers and TaqMan® MGB probe (from the TaqMan® Gene Expression Assay Mix).

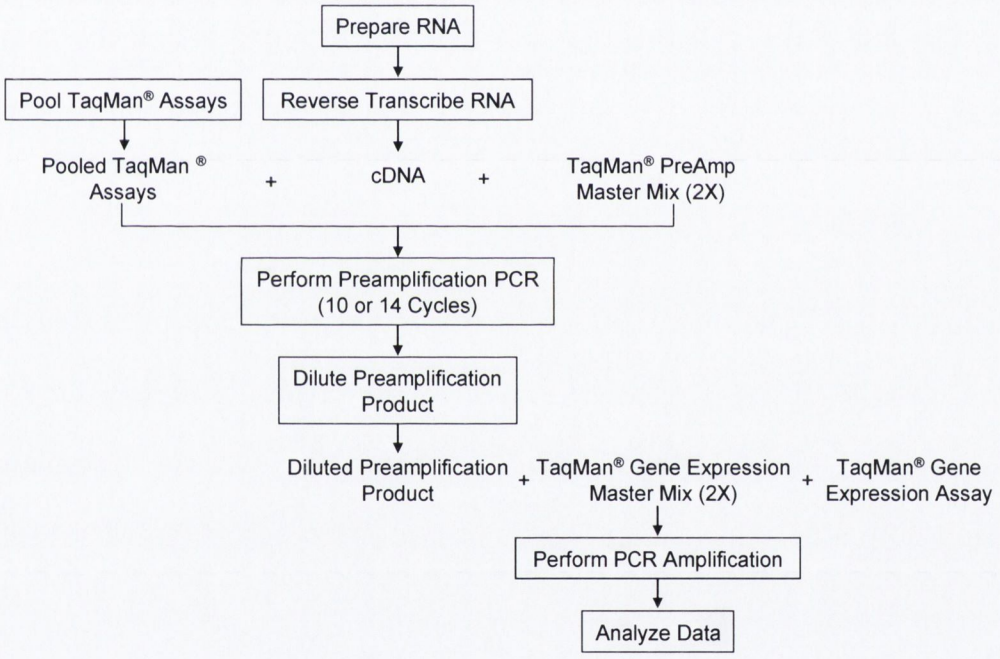

Figure 2.5 A schematic representation of TaqMan® PreAmp workflow

The entire TaqMan® preamplification includes pooling the TaqMan® Assays, preparing cDNA from RNA, and running the preamplification reaction. The PreAmp product then underwent TaqMan® real time PCR analysis.

2.8.4 TaqMan® Gene Expression Cells-to-CT™ Kit

Reverse transcription (RT)-PCR with real-time detection of amplification products is a robust, simple, and quantitative way to measure mRNA levels in biological samples. Traditionally, the first step in gene expression experiments has been to recover pure RNA from experimental samples. Even using the quickest and simplest techniques, however, RNA isolation is fairly time-consuming, often requiring 30 minutes or more of hands-on sample manipulation. Furthermore, with small samples, it can lead to loss of RNA. Cells-to-CT™ technology enables reverse transcription and real-time PCR analysis of lysates from 10–10^5 cultured cells without isolating or purifying RNA. Eliminating the RNA isolation step substantially expedites and simplifies gene expression analysis of cultured cells.

Cells-to-CT lysates exhibit the same sensitivity and specificity as purified RNA in real-time RT-PCR. The lysis procedure simultaneously prepares cell lysates for RT-PCR and removes genomic DNA in under ten minutes. The lysis step is simple to automate with robotic platforms for high-throughput processing of 96- or 384-well plates because it takes place entirely at room temperature. The procedure is also economical; there are only a few pipetting steps and, with cells grown in 96- or 384-well plates, no sample transfers.

Materials provided with the kit

- Stop Solution, DNase I, 20x RT Enzyme Mix, Lysis Solution, 2x RT Buffer, TaqMan® Gene Expression Master Mix

Cell Lysis

- Thaw Stop Solution, invert or flick the tube several times to mix thoroughly (do not vortex), and place on ice. Chill 1x PBS to 4°C. (Important: The maximum number of cells that can be used in this procedure varies somewhat according to cell type, but is generally 10^5 cells. Using too many cells per lysis reaction may result in incomplete lysis and/or inhibition of RT-PCR.)
- Wash cells in cold (4°C) PBS by resuspending them in ~0.5ml PBS per 10^6 cells (or ~50µl PBS for $\leq 10^5$ cells). Gently pellet the cells, then aspirate and discard as much of the PBS as possible without disturbing the cell pellet. Place the cells on ice.
- Resuspend cells in fresh, cold 1x PBS so that 5µl will contain the desired number of cells for a single lysis reaction (10–10^5 cells/lysis).
- Split the cell suspension into individual lysis reactions: distribute 5µl of the suspension to wells of a U-bottom multiwell plate or microcentrifuge tubes. Place the cells on ice.
- To remove genomic DNA during cell lysis, determine the volume of Lysis Solution needed for the experiment, and dilute DNase I into the Lysis Solution at 1:100 for use in the next step by mixing Lysis Solution 49.5µl and DNase I 0.5µl.
- Add 50µl Lysis Solution with DNase I to each cell sample. Mix the lysis reaction by pipetting up and down 5 times. To avoid bubble formation, mix with the pipettor set at 35µl and expel the solution without emptying the pipette tip completely. (Note: Lysis Solution and Cells-to-C_T lysates may appear cloudy at room temperature –this is expected.)
- Incubate the lysis reactions for 5 minutes at room temperature (19–25°C).

- Pipet 5µl of Stop Solution directly into each lysis reaction. Do this by touching the surface of the lysate with the opening of the pipet tip. This helps to ensure that all of the Stop Solution is mixed into the lysate. Mix the lysis reaction by pipetting up and down 5 times. (Important: It is very important to thoroughly mix the Stop Solution into the lysate.)
- Incubate for 2 minutes at room temperature (19–25°C). Do not allow Cells-to-CT lysates to remain at room temperature for longer than 20 minutes after adding the Stop Solution.

Reverse Transcription (RT)

- Program the thermal cycler for the RT: Reverse transcription (hold) at 37°C for 60 minutes, following by RT inactivation (hold) at 95°C for 5 minutes, and then indefinite hold at 4°C.
- Calculate the number of RT reactions in the experiment. Using Table 2.5 below, assemble an RT master mix for all the reactions plus ~10% overage in a nuclease-free microcentrifuge tube on ice. If desired, up to 45% of the RT reaction (22.5µl) can be Cells-to-CT lysate; adjust the volume of Nuclease-free Water accordingly.
- Distribute RT Master Mix to nuclease-free PCR tubes or multiwell plates.
- Add sample lysate to each aliquot of RT master mix for a final 50µl reaction volume. Once assembled, mix reactions gently, then centrifuge briefly to collect the contents at the bottom of the reaction vessel.
- Run a thermal cycler (or real-time PCR instrument). Incubate at 37°C for 60 minutes, then at 95°C for 5 minutes to inactivate the RT enzyme.

Table 2.5 RT master mix setup for volume of 50µl final reaction

* For the minus-RT control, use Nuclease-free Water in place of 20x RT Enzyme Mix.

Component	Each rxn	96rxns	384 rxns
2x RT Buffer	25µl	2.64ml	10.56ml
20x RT Enzyme Mix*	2.5µl	264µl	1.056ml
Nuclease-free Water	12.5µl	1.32ml	5.28ml
Final volume RT master mix	40µl	4.22ml	16.9ml

Real-Time PCR

- Program the real-time PCR instrument for the real-time PCR: UDG Incubation (hold) at 50°C for 2 minutes, Enzyme activation (hold) at 95°C for 10 minutes, following by 40 PCR cycles of 95°C for 15 seconds and 60°C for 1 minute.
- TaqMan® Gene Expression Master Mix contains ROX™ passive reference dye. Specify which fluorescent dye(s) are used in the TaqMan® Gene Expression Assays for the experiment.
- Calculate the number of PCR assays in the experiment. Using Table 2.6 below, assemble a PCR cocktail for all the reactions plus ~10% overage in a nuclease-free microcentrifuge tube at room temperature. If desired, up to 45% of the PCR can be cDNA; adjust the volume of Nuclease-free Water accordingly. (Before use, mix the TaqMan® Gene Expression Master Mix by swirling the bottle. Mix TaqMan® Assays by vortexing briefly or flicking the tube a few times and then centrifuging.)
- Distribute the PCR cocktail into individual PCR tubes or wells of a real-time PCR plate at room temperature.
- Add 4µl of the RT reaction (cDNA sample) to each 16µl of PCR cocktail for a total of 20µl reaction.

- Cover the plate or close the tubes, and mix gently. Then centrifuge briefly to remove bubbles and collect the contents at the bottom of the wells/tubes.
- Place the reactions in a real-time PCR instrument and start the run using the settings programmed. (Important: On Applied Biosystems real-time PCR instruments capable of fast mode thermal cycling, select standard mode.)
- Refer to the real-time PCR instrument guide for information on evaluating the data.

Table 2.6 TaqMan® real time PCR cocktail setup component

Component	20µl PCRs Each rxn	50µl PCRs Each rxn
TaqMan® Gene Expression Master Mix (2x)	10µl	25µl
TaqMan® Gene Expression Assay (20x)	1µl	2.5µl
Nuclease-free Water	5µl	12.5µl
final volume PCR cocktail	16µl	40µl

2.8.5 Early Access Human miRNA Panel

Applied Biosystems TaqMan® microRNA (miRNA) assays (Foster City, CA, USA) are designed to detect and quantify mature miRNAs using a looped-primer real time PCR. The human early access panel used in this study containes 160 individual assays covering many of the identified human miRNAs. Quantification using this panel is done using a two step RT-PCR process: Step one, a Stem-looped RT; and Step two, a Real Time PCR (Figure 2.6).

Step 1: Looped-primer Reverse Transcription

Total RNA samples are used to synthesize single-stranded cDNA using the High capacity cDNA archive kit (Foster City, CA, USA). For each 15µl RT reaction, combine RT master mix and RT microRNA primer with total RNA in the ratio of 7µl: 3µl: 5µl (Table 2.7). 10ng of total RNA is used per 15µg reverse transcription. cDNA is reverse transcribed using specific miRNA primers from the TaqMan® microRNA human assay panel.

Table 2.7 microRNA RT master mix setup for volume of 15µl final reaction

Component	Master Mix Volume µl /15µl reaction
100mM dNTPs	0.15
Multi-scribe Reverse Transcriptase, 50U/µl	1.00
RNase inhibitor	0.188
Nuclease free water	4.162
Total Master Mix	**7.00**
RT microRNA primer	3.00
RNA sample	5.00
Total	**15.00**

Preparing the RT reaction plate

- Combine master mix with RNA. Mix gently and centrifuge briefly.
- Dispense the 12µl into each well on a 96 well plate.
- Transfer 3µl of RT primer from the appropriate wells of the RT primer plates into the wells of the RT reaction plate.
- Seal the plate using microAmp adhesive films.
- Incubate on ice for 5 minutes and load into the thermal cycler.

- Use the following parameters 16°C for 30 minutes, 42°C for 30 minutes, and 85°C for 5 minutes with 4°C hold.

Step 2: Real-time PCR Amplification

During this target amplification step, AmpliTaq® Gold DNA polymerase is used to amplify target cDNA synthesized from the RNA sample. This is preformed using sequence specific primers from the TaqMan® MicroRNA Assays TaqMan® plates. PCR amplification is carried out using sequence specific primers on the Applied Biosystems 7900HT Fast Real-Time PCR system.

Keep all the TaqMan® microRNA assays protected from the light until use. The recommended reaction volume is 20µl. Prepare the plate so that each PCR reaction contains the components as listed in Table 2.8. Each assay was performed in triplicate for each sample. The reactions were incubated in a 96-well optical plate at 95°C for 10 minutes, following by 40 cycles of 95°C for 15 seconds and 60°C for 1 minute.

Table 2.8 microRNA real time PCR master mix setup for volume of 15µl final reaction

Component	Volume µl/ 20µl reaction
TaqMan® microRNA assay mix (10x)	2.00
Product from RT reaction (1:15 dilution)	1.33
TaqMan® 2x Universal master mix (No AmpErase UNG)	10.00
Nuclease free water	6.67
Total	**20.00**

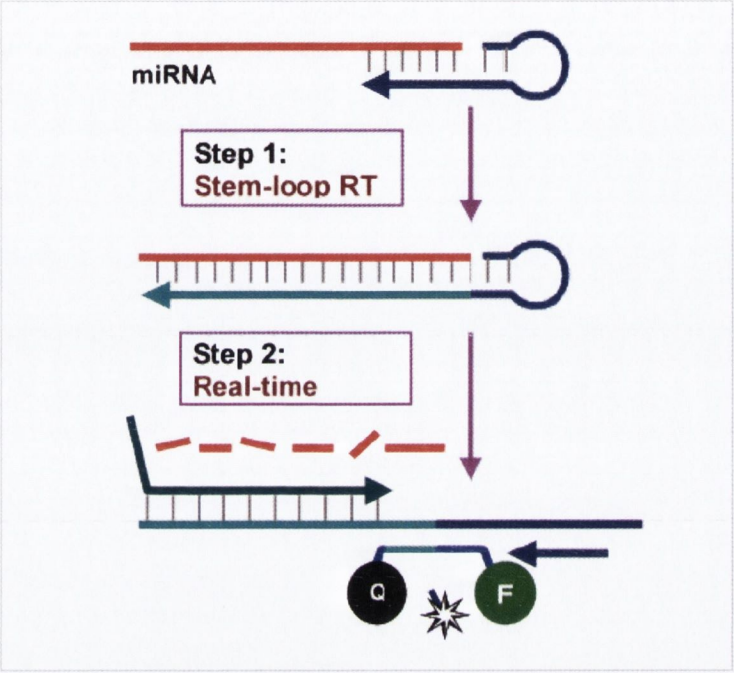

Figure 2.6 A schematic illustration of TaqMan® microRNA assays

There are two steps in this analysis. Step 1, Looped-primer RT: Looped primers are annealed to miRNA targets and extended by reverse transcriptase. Step 2, Real-Time PCR: miRNA-specific forward primer, TaqMan® probe, and universal reverse primer are used for PCR reactions. Quantitation of miRNAs is estimated based on measured C_T values (Chen et al., 2005).

2.9 Reference

CHEN, C., RIDZON, D., BROOMER, A., ZHOU, Z., LEE, D., NGUYEN, J., BARBISIN, M., XU, N., MAHUVAKAR, V., ANDERSEN, M., LAO, K., LIVAK, K. & GUEGLER, K. (2005) Real-time quantification of microRNAs by stem-loop RT-PCR. *Nucleic Acids Res,* 33, e179.

CRONIN, M., PHO, M., DUTTA, D., STEPHANS, J. C., SHAK, S., KIEFER, M. C., ESTEBAN, J. M. & BAKER, J. B. (2004) Measurement of gene expression in archival paraffin-embedded tissues: development and performance of a 92-gene reverse transcriptase-polymerase chain reaction assay. *Am J Pathol,* 164, 35-42.

DENNING, K. M., SMYTH, P. C., CAHILL, S. F., FINN, S. P., CONLON, E., LI, J., FLAVIN, R. J., AHERNE, S. T., GUENTHER, S. M., FERLINZ, A., O'LEARY J, J. & SHEILS, O. M. (2007) A molecular expression signature distinguishing follicular lesions in thyroid carcinoma using preamplification RT-PCR in archival samples. *Mod Pathol,* 20, 1095-102.

LEMOINE, N., MAYALL, E., JONES, T., SHEER, D., MCDERMID, S., KENDALL-TAYLOR, P. & WYNFORD-THOMAS, D. (1989) Characteristics of human thyroid epithelial cells immortalized in vitro by simian virus 40 DNA transfection. *Br J Cancer* 60, 897-903.

OBERLI, A., POPOVICI, V., DELORENZI, M., BALTZER, A., ANTONOV, J., MATTHEY, S., AEBI, S., ALTERMATT, H. J. & JAGGI, R. (2008) Expression profiling with RNA from formalin-fixed, paraffin-embedded material. *BMC Med Genomics,* 1, 9.

CHAPTER THREE

COMPARISON OF RNA EXTRACTION PROTOCOLS

3.1 Summary

RNA extraction is an essential procedure in molecular studies. Several extraction protocols based on different theories are used in the laboratory nowadays. The objective of this chapter was to identify a suitable RNA extraction protocol for FFPE materials. We compared seven available RNA extraction protocols using FFPE tissue samples and a cell line model. Using modern molecular technologies of Nano-Drop Spectrophotometer, Bioanalyzer and TaqMan® RT-PCR, we identified the Stratagene Absolutely RNA® FFPE Kit and the Ambion RecoverAll™ Total Nucleic Acid Isolation Kit as the best protocols generating superior results than others. These two protocols are subsequently used in the following chapters in this thesis.

3.2 Introduction

To isolate good quality of RNA is always crucial for gene studies using molecular technology. It was very challenging in early years to obtain intact RNA molecules from fresh materials due to the labile nature of RNA in conjunction with the limited theoretical understanding of biochemistry. With the effort being made in almost half a century, reliable RNA extraction reagents and methods were developed. These reagents and methods make the foundation of RNA extraction from FFPE materials. Nowadays, many commercial nucleic acid isolation kits, for fresh or snap frozen materials and for FFPE materials, have been developed based on these valuable early findings.

3.2.1 Phenol and chloroform extraction

The earliest literatures describing RNA extraction technique were in midle of 1950's by Gierer and Schramm (Gierer and Schramm, 1956) to extract viral RNA from infected plant tissues. Since then, two extraction methods were employed in early RNA studies. One was phenol based protocol which was modified and developed into different versions (Nakamura and Ueno, 1963) including hot phenol extraction (Wecker, 1959, Feramisco et al., 1982) and sodium dodecyl sulphate (SDS) phenol method (Parish and Kirby, 1966). The other method was described by Reddi in early 60's, called octanol-chloroform extraction method (Reddi, 1963). Both of the methods successfully isolated viral RNA, greatly contributed to the beginning of understanding RNA molecules and became the foundation of RNA extraction technology.

3.2.2 Guanidinium Thiocyanate extraction method

In late 1960's, Guanidine hydrochloride was first used in the isolation of RNA to dissociate the nucleoprotein into its nucleic acid and protein moieties (Cox, 1968). Guanidine hydrochloride is a strong chaotropic agent which denatures and subsequently refolds proteins. It was then replaced by Guanidinium thiocyanate which was found to be more effective on a molar basis than guanidine hydrochloride as equilibrium denaturant (Castellino and Barker, 1968, Von Hippel and Wong, 1964).

Chirgwin et al. (Chirgwin et al., 1979) described the guanidinum thiocyanate technique for RNA isolation. The theory is based on the assumption that guanidinium thiocyanate can rapidly denature RNase to prevent massive degradation of RNA and

permit the isolation of intact rat pancreatic RNA (Chirgwin et al., 1979). In this method, cellular membranes were first broken through homogenization of tissue in a mixture of guanidinium thiocyanate and b-mercaptoethanol, and then RNA was extracted by ethanol or ultracentrifugation in a cesium chloride gradient (Chirgwin et al., 1979). This was a significant advance at that time although the technique was time consuming, inefficient and inconsistent (Gonzalez-Perez et al., 2007).

3.2.3 Acid guanidinium thiocyanate-phenol-chloroform extraction

In 1987, Chomczynski and Sacchi improved extraction method by combining the procedures into a single-step extraction called acid guanidinium-phenol-chloroform (AGPC) method (Chomczynski and Sacchi, 1987 , Chomczynski and Sacchi, 2006). In this method, RNA is separated from DNA after extraction with an acidic solution containing guanidimiun thiocyanate, sodium acetate, phenol and chloroform, followed by centrifugation. Total RNA remains in the upper aqueous phase under acidic conditions, while most of DNA and proteins remain either in the interphase or in the lower organic phase. Total RNA is then recovered by precipitation with isopropanol and can be used for subsequent analysis.

AGPC method significantly improved the yield and quality of RNA giving a sufficient pure preparation of undegraded RNA (Chomczynski and Sacchi, 2006, Gonzalez-Perez et al., 2007). The method reduced the length of the RNA isolation step and can be completed within 4 hours allowing researchers to process large numbers of samples collected at a time. This one-step procedure also reduced RNA loss, enabling scientists to purify RNA from smaller sample sizes. In spite of these advances, the method still

has shortages. For example, AGPC method often yields detectable amounts of genomic DNA contamination by PCR (Siebert and Chenchik, 1993); extraction with harsh organic solvents can lead to the loss and fragmentation of the RNA sample.

With further modifications (Puissant and Houdebine, 1990), AGPC method became one of the most common and consistently successful methods used in molecular biology for isolating intact RNA from fresh materials. The modifications were to reduce DNA contamination to improve the purity of RNA by the addition of a brief RNA selective precipitation step following lysis of the cells (Siebert and Chenchik, 1993), to reduce the time of the isopropanol precipitation from 1 hour to 30 minutes (Siebert and Chenchik, 1993), to improve the RNA recovery by introducing glycerol (Vareli and Frangou-Lazaridis, 1996).

3.2.4 Silica membrane column extraction

Silica column based nucleic acid extraction is a solid phase extraction method which is based on the nucleic acid feature of binding to the solid silica or glass powder under certain pH and buffer conditions, such as in the presence of 6M sodium perchlorate (Marko et al., 1982). Boom et al. (Boom et al., 1990) described a detailed silica binding method for purification of nucleic acids directly and rapidly from clinical specimens such as human serum and urine. In this method (Boom et al., 1990), a small sample was first mixed with size fractionated silica particles, as a solid nucleic acid carrier, in a guanidimiun thiocyanate lysis buffer. The cells were lysed releasing nucleic acid which was bound to the nucleic acid carrier to form complexes. These complexes were then washed twice with a guanidimiun thiocyanate containing

washing buffer, twice with ethanol, once with acetone, and dried. Nucleic acid was subsequently eluted in an aqueous low-salt buffer.

There are several criteria which this silica binding method has fulfilled implying a real change in extraction techniques. First, the method is sensitive and economically inexpensive requiring no specialized equipment, thus allowing for nucleic acid isolation from a large series of clinical specimens routinely. Second, the extracted nucleic acid is sufficiently pure to allow for enzymatic modifications and PCR detection. Third, the method reduced the possibility of cross contamination among samples. Some limitations of this protocol include being not suitable for yeasts (Mutiu and Brandl, 2005) or gram-positive bacteria possibly due to poor lysis, although it is possible from clinical specimens, such as human serum, urine (Boom et al., 1990) and faecal (Hale et al., 1996), and several bacterial species; and restricted processing of larger volumes due to the limited capacity of the silica membranes (Hourfar et al., 2005).

3.2.5 Proteinase K digestion based extraction

Proteinase K digestion was first introduced into extraction in early 1980's (Gopalakrishna et al., 1981, Frazier et al., 1983). It was added to lyze cells procedure prior to phenol phase separation. Digestion conditions include the presence of sodium dodecyl sulphate and incubation at different temperatures from 37°C (Gopalakrishna et al., 1981), 50 °C (Rasool et al., 2002) to 60 °C (Wu et al., 1992) for a variable length for time from 20 minutes to 2 hours according to subsequent modifications.

Proteinase K digestion method was found to be efficient method to degrade other enzymes and proteins (de Paula et al., 2003). It minimizes RNA degradation and importantly improves the total recovery of RNA (Egyhazi et al., 2004, Jackson et al., 1990). In comparison with AGPC method, proteinase K digestion method was found to be more suitable for the longer fragments studies (Akin et al., 1998) possibly by efficiently removing large proteins which formed strong noncovalent association with nucleic acids resulting the release of RNA from protein complexes.

3.2.6 RNA extraction from FFPE

RNA extraction from FFPE is more difficult and complicated than that of fresh or snap frozen materials. Although the materiel was widely available, it was not until 80's that RNA had been extracted from formalin-fixed and paraffin-embedded tissue (Rupp and Locker, 1988). The early technique was based on the success of DNA extraction from archival FFPE samples, while not many DNA extraction methods are suitable for RNA.

Most of methods developed in subsequent years include many procedures such as deparaffinization, digestion and purification. In RNA extraction of FFPE, the first step is to reverse the embedding and dissolve the paraffin. Different deparaffinization techniques have been described including xylene and ethanol (Goelz et al., 1985), non-toxic Histoclear (Mies, 1994), microwave oven melting (Banerjee et al., 1995) and heating in a thermal cycler (Coombs et al., 1999). Proteinase K digestion was then performed in several buffers (Koopmans et al., 1993 , O'Shea et al., 1997, Specht et al., 2001) containing NaCl, Tris EDTA and SDS with different concentrations (Korbler et

al., 2003) under temperature from 45 °C to 60 °C for a few hours or overnight. Finally, purification is carried out using the techniques developed for fresh materials extraction, such as phenol/chloroform extraction and silica membrane column based purification.

Nowadays, some methods have been routinely used in the laboratories, and variable commercial nucleic acid isolation kits for FFPE materials have been developed based on these theories and findings. The development of the extraction technique is aimed to obtain good quality and quantity of RNA, and to become user friendly regarding to optimization of time and processing conditions.

3.2.7 Aims

This study aimed to identify a suitable RNA extraction protocol for FFPE materials. In this chapter, we studied seven available RNA extraction protocols, including Stratagene Absolutely RNA® FFPE Kit, Ambion RecoverAll™ Total Nucleic Acid Isolation Kit, J-I (GTCX), J-II (GTCX), Gentra Purescript® RNA Purification Kit, Invitrogen Trizol® Reagent and AB-in-House Protocol. Using molecular technology of Nano-Drop Spectrophotometer, Bioanalyzer and TaqMan® PCR, we first employed FFPE thyroid tissue blocks and further analysed protocols in a cell line model by comparison of parallel extracts from FFPE and snap frozen cell preparations (Figure 3.1). We finally evaluated extraction results generated in the cell line model, using TaqMan® Gene Expression Cells-to-C_T™ Kit to compare results of with-extraction to that without-extraction.

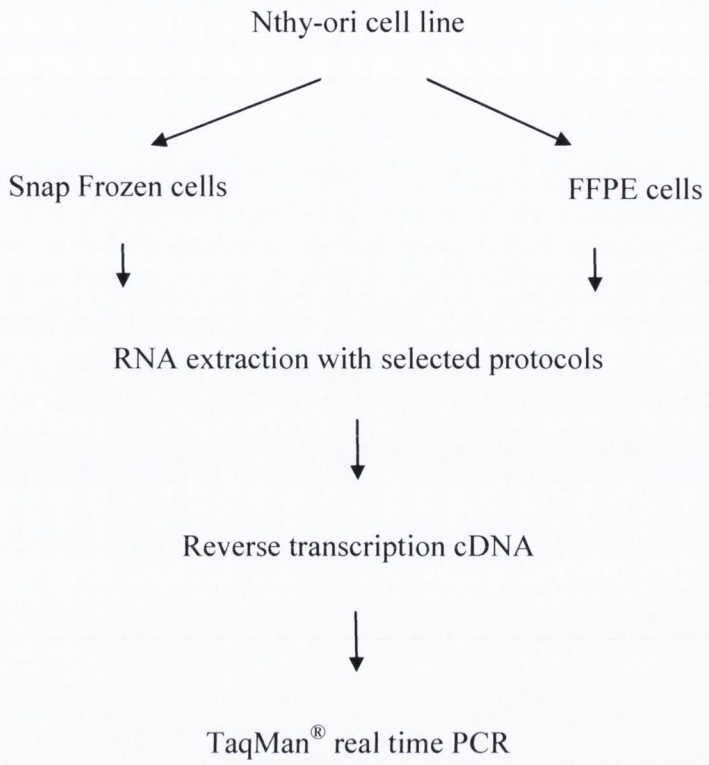

Figure 3.1 A schematic representation of the experimental cell line model

Normal thyroid cell lines were grown into confluence and were split into two aliquots: One was snap frozen, the other formalin fixed and paraffin embedded into a cell block. RNA was extracted using different protocols and was then reverse transcribed into cDNA followed by TaqMan® QRT-PCR analysis.

3.3 Materials and Methods

3.3.1 Archival formalin fixed paraffin embedded (FFPE) tissue samples

A total of nine samples of papillary thyroid carcinoma (PTC) (n=3), anaplastic thyroid carcinoma (ATC) (n=3) and benign/follicular adenoma (FA) (n=3) accessioned between 2000 and 2005 in St. James's Hospital, Dublin were employed in this experiment of extraction protocol comparison. All material was fixed in 10% buffered formalin and embedded in paraffin. Haematoxylin and eosin (H&E) stained sections were reviewed blind by a histopathologist and classified according to a recognised system (Rosai et al., 1992).

3.3.2 Cell Culture and FFPE Cell pellet preparation

Normal thyroid cell lines were grown into confluence and were counted, which procedures have been described in Chapter 2.2. Approximately 10^5 cells were pelleted and were stored using two methods: One was snap frozen, the other formalin fixed and paraffin embedded into a cell block as described in Chapter 2.3.1.

3.3.3 RNA extraction

When RNA extractions were performed using FFPE tissue samples, 5 micrometer thick sections were cut using a microtome (Microm HM 325, Medical Supply Co. Ltd, Ireland) from each FFPE block. Two of these sections were placed into a 2ml

eppendorf tube for RNA extraction. When RNA was extracted from the cells, extraction protocols were performed using one FFPE cell pellet and one snap frozen pellet in parallel.

RNA extraction was performed using the Stratagene Absolutely RNA® FFPE Kit, Ambion RecoverAll™ Total Nucleic Acid Isolation Kit, J-I (GTCX), J-II (GTCX), Gentra Purescript® RNA Purification Kit, Invitrogen Trizol® Reagent and AB-in-House Protocol as previously described in Chapter 2.5. These protocols are briefly outlined in Table 3.1 for the purpose of comparison.

3.3.4 RNA quantity and quality analysis

RNA quantity was assessed using a Nano-Drop 1000 Spectrophotometer (Wilmington, USA) to generate total RNA yields and OD ratio as described in Chapter 2.6. RNA quality was measured using a RNA 6000 Nano LabChip® Kit in conjunction with the Agilent 2100 Bioanalyzer (Agilent technologies, Waldbronn, Germany) following the protocol described in Chapter 2.7.

Applied Biosystems High-Capacity cDNA Archive Kit (P/N: 4322171, Applied Biosystems) was used following manufacturer's protocol for reverse transcription (RT) of total 100ng of RNA to single-stranded cDNA. For the TaqMan® real-time quantitative PCR reaction, amplification was carried out on the Applied Biosystems 7000 Sequence Detection System. The quality of the RNA extracted using the different protocols was analysed by demonstrating amplification of Cyclin-Dependent Kinase Inhibitor 1B (CDKN1B). The 20µl PCR reaction included 10µl of 2x TaqMan®

Universal PCR Master Mix with UNG (P/N 4304437, Applied Biosystems), 5µl of 4x TaqMan® Gene expression Assay (P/N 4331182, Applied Biosystems) and 5µl of cDNA (RT product 2ng/µl).

3.3.5 TaqMan® Gene Expression Cells-to-C_T™ Kit

TaqMan® Gene Expression Cells-to-CT™ is an advanced technology which enables reverse transcription and real-time PCR analysis of lysates from 10–10^5 cultured cells without isolating or purifying RNA. Since cell lysis process can be completed within a few minutes, C_T values can be achieved within a day after cell harvesting. The detailed procedures are described in Chapter 2.8.4 and are briefly compared with the ordinary TaqMan® procedures in Figure 3.2.

One pellet of $4x10^5$ snap frozen cells was suspended in 200µl of PBS, from which 5µl of 10^4 cells was lysed and 1/6 of the lysis was reverse transcribed into cDNA in a 50µl RT reaction. 4µl of cDNA product was analysed using TaqMan® real time PCR.

In comparison of conventional TaqMan® PCR, five of TaqMan® Gene Expression Assays (P/N: 4331182, Applied Biosystems, CA, USA) and one custom designed assay (GAPDH-67) were utilised in this study with a range of amplicon sizes from 67 to 164 (Table 3.2). RNA was extracted using Ambion RecoverAll™ Total Nucleic Acid Isolation Kit and was reverse transcribed into cDNA using High-Capacity cDNA Archive Kit (P/N: 4322171, Applied Biosystems) which was then quantified using TaqMan® real time PCR.

Table 3.1 Comparison of RNA extraction protocols

RNA extraction was performed using available protocols including Stratagene Absolutely RNA® FFPE Kit, Ambion RecoverAll™ Total Nucleic Acid Isolation Kit, J-I (GTCX), J-II (GTCX), Gentra Purescript® RNA Purification Kit, Invitrogen Trizol® Reagent and AB-in-House Protocol. (RM: room temperature; ?: unknown.)

	Gentra	Trizol	Stratagene	Ambion	J-I	J-II	ABinhouse
Step 1 De-paraffinization	0.3ml x3 Xylene RM. 5min 0.3ml 2x 100%Ethanol 1min spin Air dry	1ml x2 Xylene 50°C 3min 1ml 100% Ethanol 1min spin Air dry	1ml x2 **Deparaffin Reagent** RM 10min 1ml 100%, 90%, 70% Ethanol 5min spin Air dry	1ml x2 Xylene 50°C. 3min 1ml 100% Ethanol 1min spin Air dry	1.5ml x2 Xylol 37°C. 20min 1ml 100% Ethanol 15min spin Air dry	1.5ml x2 Xylol 37°C. 20min 1ml 100% Ethanol 15min spin Air dry	1mlx 2 Xylene 37°C.20min 0.5ml 3x70% Ethanol 1min spin Air dry
Step 2 Proteinase K Digestion	1.5µl x20mg/ml proteinaseK 300µl cell lysis solution 55°C overnight **(30µg in 300µl)**	—	10µl x 20mg/ml proteinaseK 100µl digestion buffer 55°C overnight **(200µg in 110µl)**	4µl Protease 400µl digestion buffer 50°C 3 hours **(? µg in 400µl)**	11.8µl x1mg/ml proteinaseK 200µl GTCX 55°C 60min **(11.8µg in 210µl)** 59.3µl x1mg/ml proteinaseK 1ml 30mMTris/ 1% Triton 55°C 60min **(71.1µg in 1270µl)**	12µl x20mg/ml proteinaseK 200µl GTCX 55°C 60min **(240µg in 210µl)** 60µl x20mg/ml proteinaseK 1ml 30mMTris/ 1% Triton 55°C 60min **(1440µg in 1270µl)**	25µl x20mg/ml proteinaseK 300µl PBS 37°C overnight **(500µg in 325µl)**

Table is continued on next page.

Step 3 RNA Isolation	100µl protein-DNA **precipitation** solution Spin 3min Supernatant + 300µl 100% isopropanol + 0.5µl 20mg/ml glycogen -20°C 60min Spin 3min 300µl 70% Ethanol wash Air dry	Homogenize in 1ml Trizol Reagent 200µl Chloroform Spin 15min The aqueous phase + 500µl 100% Isopropanol + 0.5µl 20mg/ml glycogen RM. for 10 min Spin 10min 1ml 75% Ethanol wash Air dry	125µl RNA binding buffer 0.875 b-ME1min Spin in **prefilter spin cup** Filtrate+ 125µl 100% ethanol RNA binding cup Spin 1min Wash with 600µl low salt buffer 5µl DNase +25µl buffer 37°C 15min Wash with 500µl high salt + 600µl + 300µl low salt buffer Spin dry	480µl Isolation Additive 1.1ml 100% Ethanol Filter Cartridge 1min spin Wash with 700µl + 500µl wash solution1+2/3 4µl DNase +56µl buffer RM. 30min Wash with 700µl + 2x 500µl wash solution1+ 2/3 Spin dry	**Incubation 70°C 20min** Spin supernatant 480µl Isolation Additive 500µl 100% Ethanol Filter Cartridge 1min spin Wash with 700µl + 500µl wash solution 1+ 2/3 4µl DNase +56µl buffer RM. 30min Wash with 700µl + 2x 500µl wash solution1+ 2/3 Spin dry	**Incubation 94°C 20min** Spin supernatant 1200µl Isolation Additive 2750µl 100% Ethanol Filter Cartridge 1min spin Wash with 700µl + 500µl wash solution1+2/3 4µl DNase +56µl buffer RM. 30min Wash with 700µl + 2x 500µl wash solution1+ 2/3 Spin dry	325µl 2xncRNAlysis on ice 60min 480µl Isolation Additive 1.1ml 100% Ethanol Filter Cartridge 1min spin Wash with 700µl + 500µl wash solution1+2/3 4µl DNase +56µl buffer RM. 30min Wash with 700µl + 2x 500µl wash solution1+ 2/3 Spin dry
Step 4 RNA Collection	25µl RNA hydration solution 30min on ice	30µl H_2O 10min 55°C	30µl Elution Buffer 75°C RM. 2min spin	30µl x2 Elution solution 95°C RM. 1min	20µl H_2O RM. 3min 10µl elution solution 75°C	20µl + 10µl H_2O 95°C. RM. 1min	20µl + 10µl elution solution 75°C RM. 1min

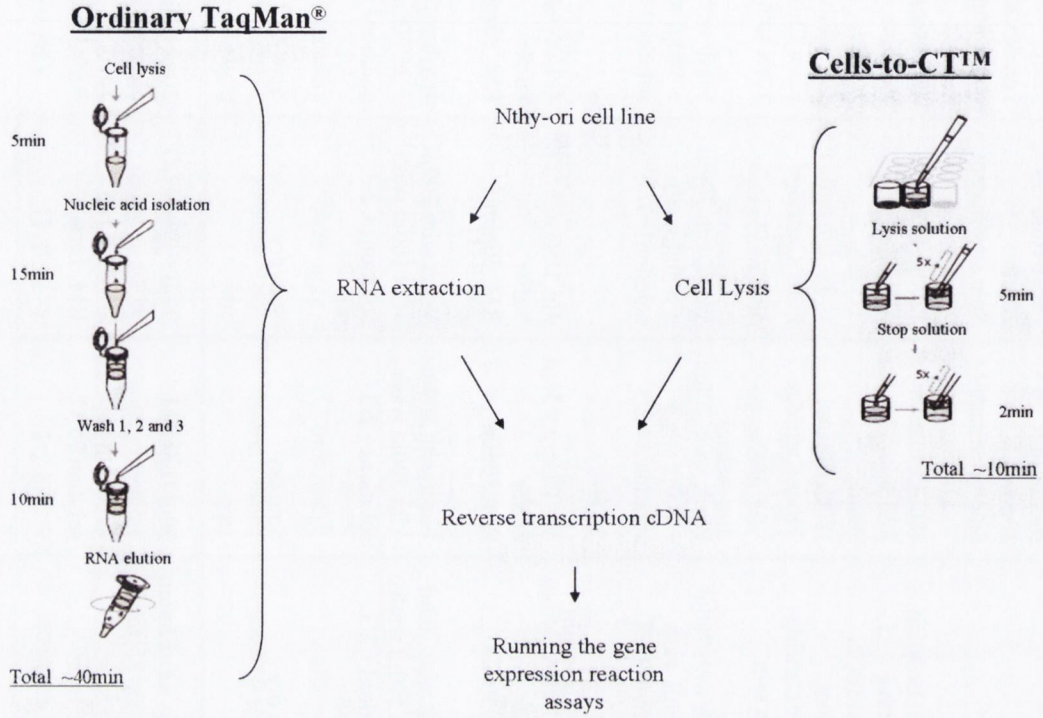

Figure 3.2 A schematic representation of the comparison of ordinary TaqMan® and Cells-to-CT™ procedures

Procedures of RNA extraction from fresh or snap frozen cells include cell lysis, nucleic acid isolation and RNA elution, which take about 40 minutes. Procedure of Cells-to-C_T™ takes only about 10 minutes replacing RNA isolation or purification. Thus, C_T values can be achieved from TaqMan® Gene Expression Cells-to-CT™ in one day after the cells harvesting.

Table 3.2 TaqMan® Gene Expression Assays

Five of these assays were inventoried by Applied Biosystems (P/N: 4331182, Applied Biosystems, CA, USA) and one was a designed assay (GAPDH-67 (Smyth, 2004) Forward primer: CAT CCA TGA CAA CTT TGG TAT CGT; Reverse primer: GGG TGG CAG TGA TGG CAT; Probe: ACT CAT GAC CAC AGT CC).

Gene Symbol – Amplicon Length	Gene Name	Assay ID
GAPDH – 67	glyceraldehyde-3-phosphate dehydrogenase	Designed (Smyth, 2004)
CDKN1B – 71	cyclin-dependent kinase inhibitor 1B (p27, Kip1)	Hs00153277_m1
CD44 – 86	CD44 molecule (Indian blood group)	Hs00153304_m1
SDC2 – 103	syndecan 2 (heparan sulfate proteoglycan 1, cell surface-associated, fibroglycan)	Hs00299807_m1
GAPDH – 122	glyceraldehyde-3-phosphate dehydrogenase	Hs99999905_m1
HLA-A – 164	major histocompatibility complex, class I, A	Hs00740413_g1

3.4 Results

3.4.1 RNA extracted from FFPE tissue samples

RNA was extracted from nine FFPE tissue blocks representing three types of thyroid including ATC, classic type PTC and Benign/Follicular Adenoma. Four extraction protocols were compared in this experiment including Gentra Purescript® RNA Purification Kit, Stratagene Absolutely RNA® FFPE Kit, J-I and AB-in-House protocol.

RNA quantity was assessed spectrophotometrically using NanoDrop® ND-1000 Spectrophotometer, which showed variations in RNA yields depending on the protocols used (Figure 3.3). Gentra, Stratagene and AB-In-House protocols showed good yields across nine FFPE tumour samples. J-I protocol generated the lowest yields compared with all the other extraction protocols with all the samples used.

RNA quality was analysed using TaqMan® real time PCR with six assays including GAPDH, HLA_DMA, HLA_DRA, CTSC, CD44 and CD74 (Figure 3.4). In every assay, different extraction protocols showed different detectable sensitivities when the starting amount of RNA was identical. This variation of TaqMan® sensitivity was observed in all the six assays. Stratagene extracts showed the best detectable RNA with all the six assays. Gentra and J-I protocols showed detectable RNA in some of the assays. However, AB-In-House protocol generated the least amount of detectable RNA for the TaqMan® real time PCR analysis compared with other tested protocols. The variation of RNA quality was also observed across different tissue samples.

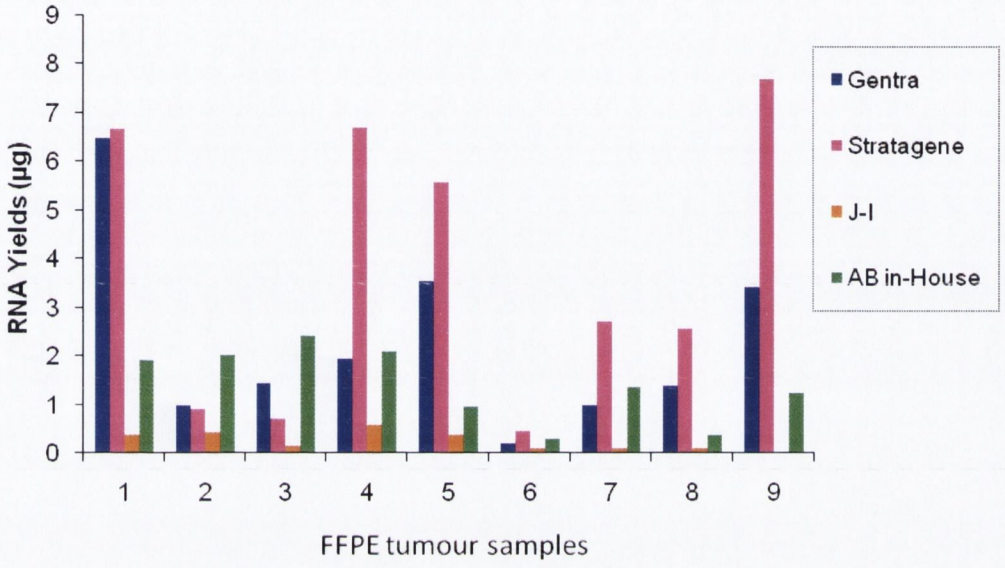

Figure 3.3 RNA yields generated from FFPE thyroid tissue blocks

RNA quantity was assessed spectrophotometrically using NanoDrop® ND-1000 Spectrophotometer. Four selected extraction protocols were compared using nine thyroid tissue blocks. Gentra, Stratagene and AB-In-House protocols showed good yields across nine FFPE tumour samples. J-I protocol generated the lowest yields compared with all the other extraction protocols with all the samples used.

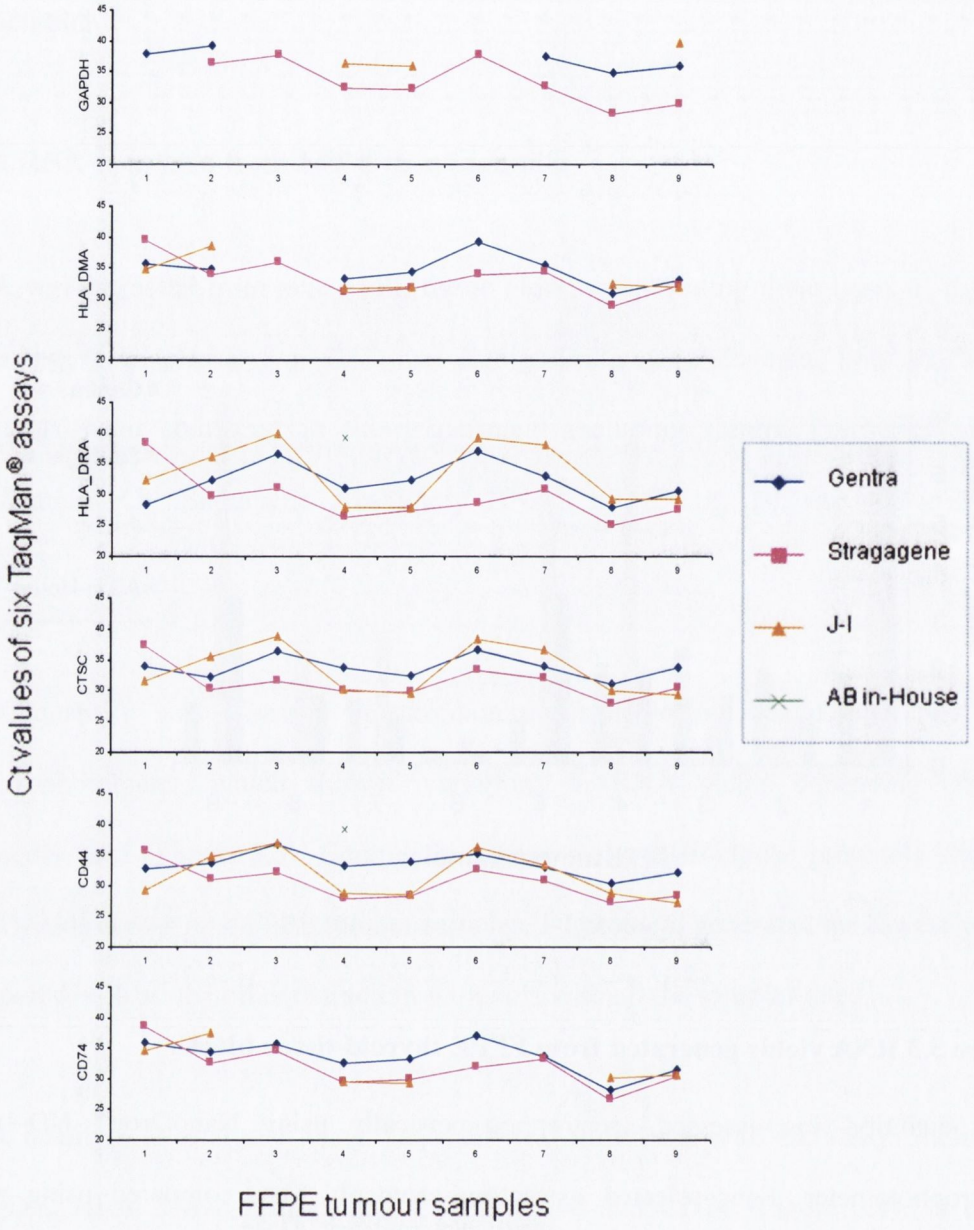

Figure 3.4 TaqMan® analysis of extracts of FFPE thyroid tissue samples

Six TaqMan® assays including GAPDH, HLA_DMA, HLA_DRA, CTSC, CD44 and CD74 were employed to analyse RNA extracted from nine thyroid tissue blocks using four different protocols (Gentra, Stratagene, AB-In-House and J-I). (Dots in the line show Cts of detectable RNA. Dots missing in the line indicate non detection.) Different extraction protocols showed different detectable sensitivities when the starting amount of RNA was identical. This variation of TaqMan® sensitivity was

observed in all the six assays. Stratagene extracts showed the best detectable RNA with all the six assays. Gentra and J-I protocols showed detectable RNA in some of the assays. However, AB-In-House protocol generated the least amount of detectable RNA for the TaqMan® real time PCR analysis compared with other tested protocols.

3.4.2 Extraction protocol comparison using a cell line model

RNA extraction protocols were further compared using a cell line model (Figure 3.1). RNA was extracted in parallel from FFPE cells pellet and snap-frozen with the identical numbers of cells employed in each pellet. Six extraction protocols were compared in this experiment including Stratagene Absolutely RNA® FFPE Kit, Ambion RecoverAll™ kits, J-II, J-I, Gentra Purescript® RNA Purification Kit and Invitrogen Trizol® Reagent protocol.

RNA quantity was assessed spectrophotometrically using NanoDrop® ND-1000 Spectrophotometer, which showed that the yields from snap frozen extracts were greater than those from FFPE when RNA was extracted from identical numbers of cells using all the protocols examined with the exception of J-II protocol (Figure 3.5). In comparison of FFPE extracts (Table 3.3, Figure 3.5), Ambion gave the highest yields, and column based Stratagene and Ambion protocols produced clean RNA with OD 260/280 ratio greater than 1.8.

RNA quality was analysed using Agilent 2100 Bioanalyzer (Figure 3.6) and TaqMan® real time PCR (Figure 3.7), which showed variations in RNA quality. The gel like image showed that all the protocols generated degraded RNA from FFPE cells; while

Stratagene Absolutely RNA® FFPE Kit, Ambion RecoverAll™ kits and Invitrogen Trizol® Reagent protocol generated intact RNA molecules from snap frozen cells. TaqMan® results (Figure 3.7) showed average over 10 higher C_Ts generated from FFPE extracts than that from snap frozen extracts when identical amount of RNA was used in each TaqMan® reaction. For FFPE extracts, Trizol did not generate detectable RNA, while Stratagene, Ambion and J-II generated lower C_Ts compared with other protocol used. To consider all the parameters compared including total RNA yields, OD ratio, quality of snap frozen extracts and TaqMan® C_T values, Stratagene and Ambion RecoverAll™ kits gave superior FFPE RNA results with regard to quality and quantity than the other protocols examined.

Table 3.3 OD ratios of RNA extracted using different protocols

Extraction products were assessed spectrophotometrically using NanoDrop® ND-1000 Spectrophotometer. Three extractions were carried out using each protocol.

OD Ratio (260/280)	FFPE	Snap Frozen
Stratagene	2.1+/-0.1	2.1+/-0.1
Ambion	2.1+/-0.1	2.2+/-0.1
J-II	2.1+/-0.1	2.2+/-0.1
J-I	2.1+/-0.2	2.1+/-0.1
Gentra	1.6+/-0.1	1.6+/-0.1
Trizol	1.6+/-0.1	1.7+/-0.1

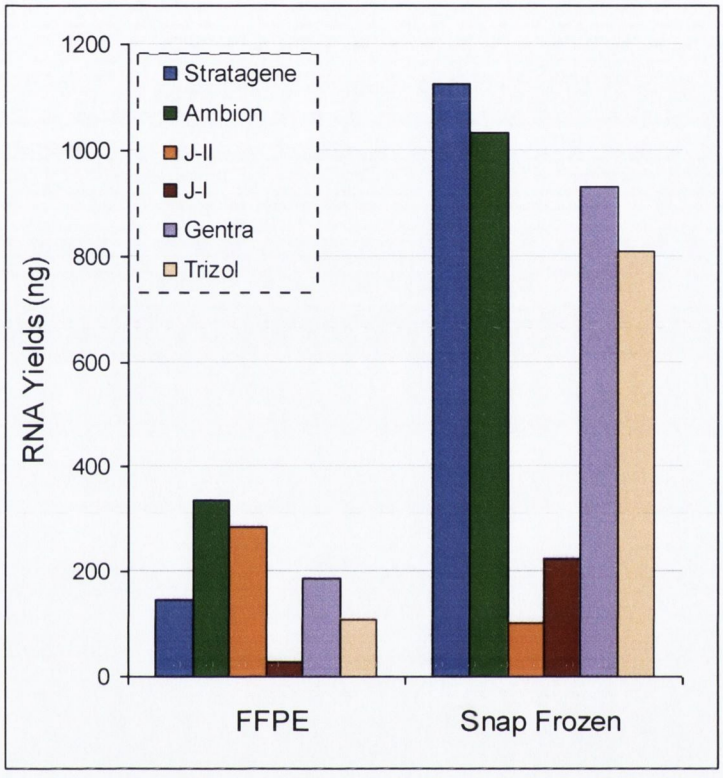

Figure 3.5 Comparison of RNA yields using a cell line model

RNA quantity was assessed spectrophotometrically using NanoDrop® ND-1000 Spectrophotometer. The yields from snap frozen extracts were greater than those from FFPE with the exception of J-II protocol when RNA was extracted from identical numbers of cells using all the protocols examined. In comparison of FFPE extracts, Ambion protocol gave the highest yields.

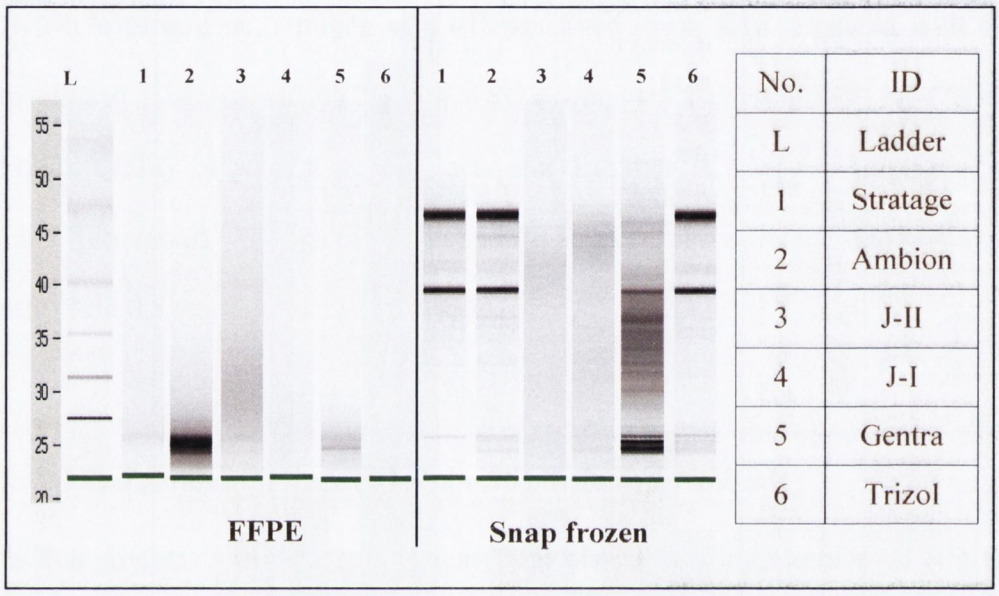

Figure 3.6 Comparison of RNA quality using a cell line model

RNA quality was accessed using Agilent 2100 Bioanalyzer, which showed that all the extracts of FFPE cells produced degraded RNA; while Stratagene Absolutely RNA® FFPE Kit, Ambion RecoverAll™ kits and Invitrogen Trizol® Reagent protocol generated intact RNA molecules from snap frozen cells.

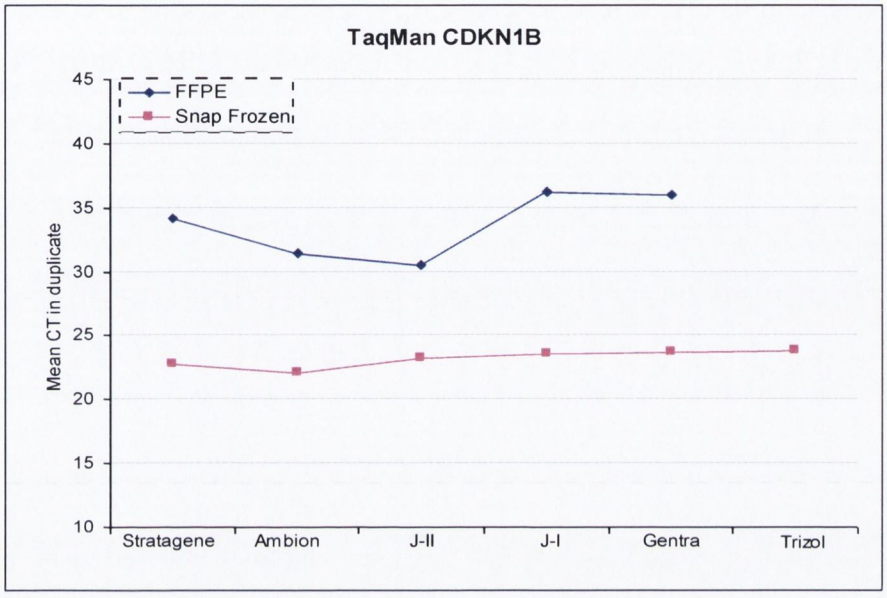

Figure 3.7 TaqMan® analysis of extracts of FFPE and snap frozen cells

TaqMan® analysis with CDKN1B assay showed higher C_Ts generated from FFPE extracts than that from snap frozen extracts when identical amount of RNA was used in each TaqMan® reaction. (Missing dot in FFPE line with Trizol extract indicates non detection.) For FFPE extracts, Stratagene, Ambion and J-II generated lower C_Ts compared with other protocols used.

3.4.3 TaqMan® Cells-to-CT™ data

The starting amount of material needs to be calculated to make a comparison between the C_Ts generated from TaqMan® Cells-to-CT™ and that from the ordinary TaqMan® (Figure 3.8). In TaqMan® Cells-to-CT™ experiment, approximately 67 cells were analysed in each of the TaqMan® real time PCR reaction. In the ordinary TaqMan® experiment, 20ng of total RNA extracted using Ambion RecoverAll™ kit was analysed in each PCR reaction, which is equivalent to approximately 1587 cells according to the yields of this extraction. Thus, the amount of material used in TaqMan® Cells-to-CT™ is only 1/24 times ($=2^{-4.6}$ times) of that used in the ordinary TaqMan® reaction. After calculation based on equilibrating the results for the difference in input cells, we found, for most of the assays, TaqMan® Cells-to-CT™ generated lower C_Ts, regardless of the amplicon length, compared with the C_Ts generated using the ordinary TaqMan® method when the equal amount of starting materials employed (Figure 3.8).

A good correlation is shown between the C_Ts produced from two different methods with $R^2 = 77\%$ and P value = 0.0208 (Figure 3.9). Five out of six assays tested, showed C_Ts close to the linear fit line, while CDKN1B, which can be observed from both figures, generated higher C_T value in TaqMan® Cells-to-CT™ experiment.

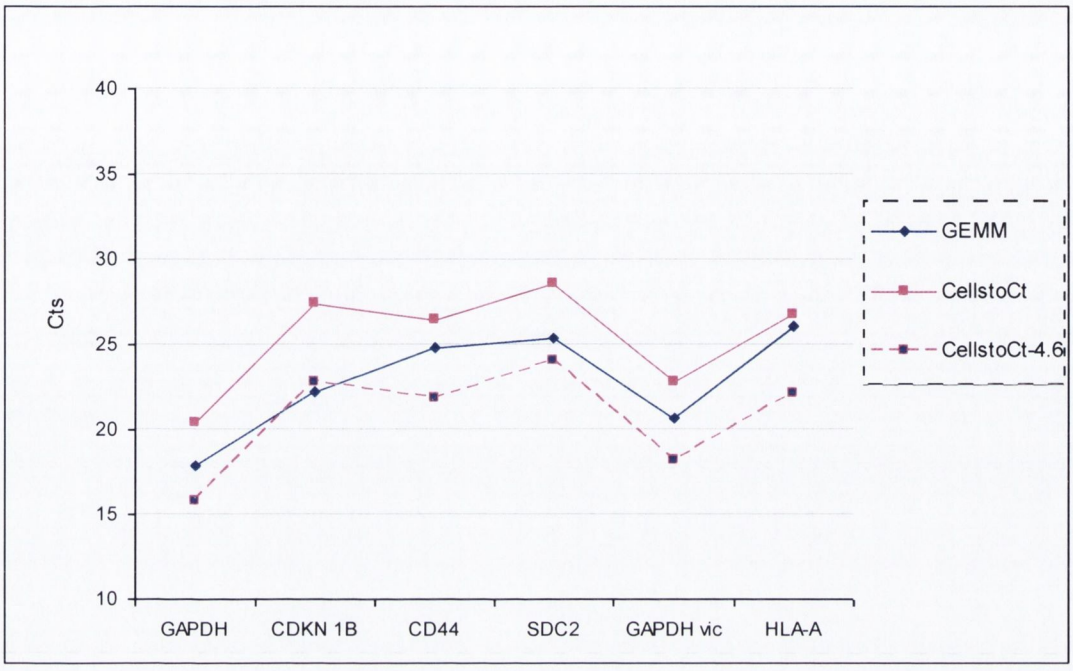

Figure 3.8 Comparison of the C_T values generated from TaqMan® Cells-to-CT™ and that from the ordinary TaqMan®

(The raw C_Ts are indicated by the dark lines; the calculated C_Ts shown using the broken line.) The starting amount of materials needs to be calculated to make the comparison between two methods. The amount of materials used in TaqMan® Cells-to-CT™ is only 1/24 times ($=2^{-4.6}$ times) of that used in the ordinary TaqMan® reaction. For most of the assays, TaqMan® Cells-to-CT™ generated lower C_Ts, regardless of the amplicon length, compared with the C_Ts generated using the ordinary TaqMan® method with the calculation of equal amount of starting materials employed. CDKN1B assay generated higher C_T value in TaqMan® Cells-to-CT™ experiment compared with that in the ordinary TaqMan®.

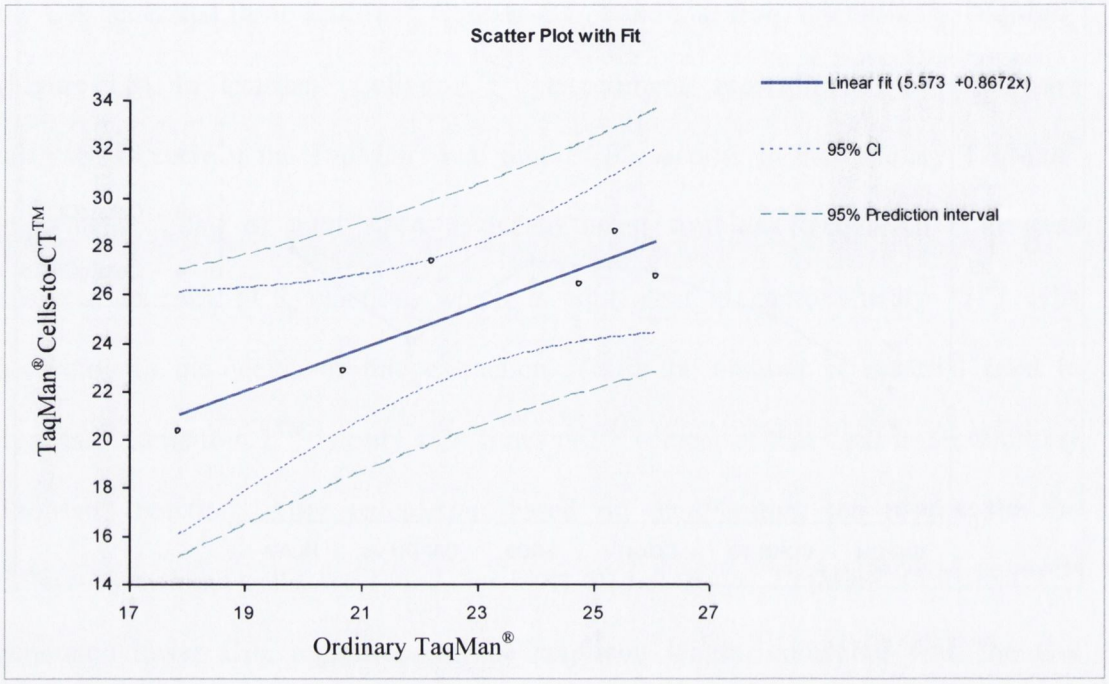

Figure 3.9 Scatter plot showing the correlation of the C_Ts generated using TaqMan® Cells-to-CT™ and the ordinary TaqMan®

A good correlation is shown between the C_Ts produced from two different methods with R^2 = 77% and P value = 0.0208. Five out of six assays tested showed C_Ts close to the linear fit line.

3.5 Discussion

A prerequisite for gene expression studies in formalin-fixed tissue samples is the establishment of a reliable and reproducible extraction method to provide detectable RNAs for subsequent analysis (Lewis et al., 2001). With the use of the extremely sensitive molecular techniques, such as polymerase chain reaction (PCR), for the detection of a few nucleic acid molecules of the extracts, the transmission of nucleic acid might easily lead to false-positive results. There are some laboratory methods and a few commercial nucleic acid isolation kits available for RNA extraction of FFPE. In this study, we first compared the protocols using FFPE tissue blocks. We further designed a cell line model to minimize the sample variation such that equal numbers of cells were processed for FFPE cell block construction and snap freezing for comparative purposes, thus revealing the impact of extractions on gene expression. We found that protocols affected the efficiency of PCR detection rate, identified the most suitable RNA extraction protocols for FFPE materials, and further evaluated extraction results generated in the cell line model, using TaqMan® Gene Expression Cells-to-C_T™ Kit to compare results of with-extraction to that without-extraction.

3.5.1 Extraction protocols of FFPE affected TaqMan® gene expression study

Generally, RNA extracted from FFPE materials is fragmented and chemically modified (Masuda et al., 1999) which causes the difficulty of obtaining good quality and quantity of RNA through extraction processing. Our results showed that different extraction methods generated variable yields and rates of detectable RNA molecules in the extracts. This variety affected the subsequent TaqMan® gene expression study.

Sufficient quantity of RNA is always required in gene expression experiments, which allows the analysis of multi targets to be carried out simultaneously. Good yields of RNA are often obtained from fresh or snap frozen materials, but usually are not obtainable from FFPE (Goldsworthy et al., 1999) (Figure 3.5). Extraction of FFPE tissue blocks (Figure 3.3) showed that protocols Stratagene, Gentra and AB-in-house produced higher yields than protocol J-I. The least yield from FFPE was also produced by J-I in the comparison with other protocols when the identical numbers of cells were used for extractions (Figure 3.5). This data eliminated J-I being a practical protocol for FFPE in gene expression studies.

The quality of RNA is a crucial factor influencing TaqMan® detection efficiency. FFPE extracts have roughly 10 C_Ts reduction (de Lamballerie et al., 1994) in sensitivity of TaqMan® detection compared with snap frozen extracts, which is consistent with our data (Figure 3.7). The extracts of FFPE generated by different extraction protocols have variable detection rates when the starting amount of RNA was identical (Figure 3.4 and 3.7). For example, there were not sufficient amounts of detectable RNA molecules in the FFPE extracts produced by protocols of AB-in-house and Trizol (Figure 3.4 and 3.7), although certain yields were generated (Figure 3.3 and 3.5). Thus, these extracts generated by different extraction protocols result in inconsistent patterns of gene expression (Figure 3.4).

3.5.2 Essential procedures are in the suitable extraction protocols for FFPE

There are several factors, such as the contamination of RNases, proteins and genomic DNA (Fleige and Pfaffl, 2006) and the insufficient lysis of tissue or cells, among different extraction methods which lead the variability of the quality and quantity of extracted RNA. Our results showed that the protocols of Stratagene and Ambion, including procedures: deparaffinization, proteinase K digestion followed by silica column purification, on column DNase digestion and RNA elution, are suitable protocols for FFPE materials producing good yields and detectable RNA in the extracts.

Among these procedures, proteinase K digestion has been demonstrated by many laboratories to be critical in RNA extraction protocol (Lewis et al., 2001, Cronin et al., 2004, Specht et al., 2001, Korbler et al., 2003), which is in agreement with our results. Protocols Stratagene, Ambion, Gentra and J-II include efficient proteinase digestion in specific buffers at optimized temperature 50-55°C (Table 3.1), resulting in certain yields and detectable RNA. On the contrary, other protocols have either no proteinase digestion (Trizol), low concentration of proteinase K (J-I), or in a non specific buffer (AB-in-house), resulting in poor yields (Figure 3.3 and 3.5) or undetectable RNA (Figure 3.4 and 3.7). In the extraction, proteinase K digestion step possibly has two functions. On one hand, it can degrade proteins that are covalently cross-linked with each other and nucleic acid to release RNA from the matrix, thereby allowing efficient RNA extraction from FFPE materials (Specht et al., 2001). On the other, it can inactivate RNases that tend to be stable and do not require cofactors to function. Thus

its activity avoids any potential reactivation of RNase during reversal of fixation in aqueous buffers (Lewis et al., 2001).

Silica column purification followed by on column DNase digestion efficiently purifies RNA and solve DNA contamination problem. Binding RNA to a solid support eliminates the need for organic extraction and alcohol precipitation (Dolter and Braman, 2001), which is sensitive, minimizes RNA handling and shortens the total extraction time. Digestion of RNase-free DNase I has been employed in RNA extraction to greatly reduce DNA contamination (Sanyal et al., 1997, Finke et al., 1993). Our results showed that high OD ratio was produced by protocols containing column purification and DNase digestion procedures (Table 3.3). Among tested protocols, Stratagene, Ambion, J-II and J-I generated purified RNA with OD ratio greater than 2 which is higher than that generated by phase separation and precipitation based protocols, Gentra and Trizol, for both FFPE and snap frozen extracts.

Comparing the extracts of FFPE with snap frozen (Figure 3.6), assessment of Bioanalyzer showed that protocols of J-I and J-II, among silica column based protocols, produced degraded RNA molecules from snap frozen cell pellets. It is most likely affected by the insufficient proteinase K digestion included in J-I and improper heating treatment included in J-II. Heating treatment is further studied in Chapter 4. Therefore, taking all the features discussed above for FFPE extractions, protocols of Stratagene and Ambion are suitable protocols, among all the tested ones, producing comparably good yields, purified detectable RNA but not containing any procedures degrading RNA.

3.5.3 Extraction was evaluated using TaqMan® Gene Expression Cells-to-C_T™

The TaqMan® Gene Expression Cells-to-C_T™ is a newly developed simple and fast technology, which enables reverse transcription and real-time PCR analysis of lysates from cultured cells without isolating or purifying RNA. Using the snap frozen cell pellets, the TaqMan® Gene Expression Cells-to-C_T™ Kit is employed to evaluate identified extraction protocol, Ambion RecoverAll™, to see if these obtained C_Ts using ordinary TaqMan® Gene Expression with-extraction are consistent with that produced by TaqMan® Gene Expression Cells-to-C_T™ without-extraction.

The comparison of the C_T values showed that the TaqMan® Gene Expression Cells-to-C_T™ generated lower C_Ts than the ordinary TaqMan® Gene Expression generated C_Ts (Figure 3.8) for most of the assays with the starting amount of materials identical. This is most likely because that the recovery of RNA, using any extraction techniques from cells or tissues, is not possible to be 100%. A small portion of RNA is always not achievable by extraction from cells or tissue. However, some individual assay, such as CDKN1B, generated higher TaqMan® detection rate using the TaqMan® Gene Expression Cells-to-C_T™ kit, which is possibly due to the RNA secondary structure in the cell lysis solution or any non-covalent association between RNA and protein resulting to a low detection rate of this target.

The ordinary TaqMan® with Ambion RecoverAll™ extraction was found to generate reliable C_T values. A good correlation was obtained (Figure 3.9), with R^2 = 77% and P value = 0.0208, using six mRNA assays with arrange of amplicon lengths, indicating

that the results are comparable between two different techniques. Thus, this extraction protocol is compatible to be employed in the subsequent studies of gene expression.

3.6 Conclusions

Through the comparison of seven available extraction protocols using FFPE tissue blocks and a cell line model, we identified Stratagene Absolutely RNA® FFPE Kit and Ambion RecoverAll™ Total Nucleic Acid Isolation Kit to be suitable protocols for gene expression using FFPE. These two protocols include procedures: deparaffinization, proteinase K digestion followed by silica column purification, on column DNase digestion and RNA elution, which are efficient to extract RNA from FFPE materials, therefore produce good yields and detectable RNA in the extracts. Gene expression results are comparable between techniques of with-extraction and without-extraction, which sufficiently support these two extraction protocols being employed in the subsequent studies of gene expression.

3.7 References

AKIN, A., WU, C. C. & LIN, T. L. (1998) A comparison of two RNA isolation methods for double-stranded RNA of infectious bursal disease virus. *J Virol Methods,* 74, 179-84.

BANERJEE, S. K., MAKDISI, W. F., WESTON, A. P., MITCHELL, S. M. & CAMPBELL, D. R. (1995) Microwave-based DNA extraction from paraffin-embedded tissue for PCR amplification. *Biotechniques,* 18, 768-70, 772-3.

BOOM, R., SOL, C. J., SALIMANS, M. M., JANSEN, C. L., WERTHEIM-VAN DILLEN, P. M. & VAN DER NOORDAA, J. (1990) Rapid and simple method for purification of nucleic acids. *J Clin Microbiol,* 28, 495-503.

CASTELLINO, F. J. & BARKER, R. (1968) The denaturing effectiveness of guanidinium, carbamoylguanidinium, and guanylguanidinium salts. *Biochemistry,* 7, 4135 - 4138.

CHIRGWIN, J. M., PRZYBYLA, A. E., MACDONALD, R. J. & RUTTER, W. J. (1979) Isolation of biologically active ribonucleic acid from sources enriched in ribonuclease. *Biochemistry,* 18, 5294-9.

CHOMCZYNSKI, P. & SACCHI, N. (1987) Single-step method of RNA isolation by acid guanidinium thiocyanate-phenol-chloroform extraction. *Analytical Biochemistry,* 162, 156-159.

CHOMCZYNSKI, P. & SACCHI, N. (2006) The single-step method of RNA isolation by acid guanidinium thiocyanate-phenol-chloroform extraction: twenty-something years on. *Nat Protoc,* 1, 581-5.

COOMBS, N. J., GOUGH, A. C. & PRIMROSE, J. N. (1999) Optimisation of DNA and RNA extraction from archival formalin-fixed tissue. *Nucleic Acids Res,* 27, e12.

COX, R. A. (1968) The Use of Guanidinium Chloride in the Isolation of Nucleic Acids *Methods of Enzymology* 12, 120-129

CRONIN, M., PHO, M., DUTTA, D., STEPHANS, J. C., SHAK, S., KIEFER, M. C., ESTEBAN, J. M. & BAKER, J. B. (2004) Measurement of gene expression in archival paraffin-embedded tissues: development and performance of a 92-gene reverse transcriptase-polymerase chain reaction assay. *Am J Pathol,* 164, 35-42.

DE LAMBALLERIE, X., CHAPEL, F., VIGNOLI, C. & ZANDOTTI, C. (1994) Improved current methods for amplification of DNA from routinely processed liver tissue by PCR. *J Clin Pathol,* 47, 466-7.

DE PAULA, V. S., VILLAR, L. M. & COIMBRA GASPAR, A. M. (2003) Comparison of four extraction methods to detect hepatitis A virus RNA in serum and stool samples. *Braz J Infect Dis,* 7, 135-41.

DOLTER, K. E. & BRAMAN, J. C. (2001) Small-sample total RNA purification: laser capture microdissection and cultured cell applications. *Biotechniques,* 30, 1358-61.

EGYHAZI, S., BJOHLE, J., SKOOG, L., HUANG, F., BORG, A. L., FROSTVIK STOLT, M., HAGERSTROM, T., RINGBORG, U. & BERGH, J. (2004) Proteinase K added to the extraction procedure markedly increases RNA yield from primary breast tumors for use in microarray studies. *Clin Chem,* 50,975-6.

FERAMISCO, J., SMART, J., BURRIDGE, K., HELFMAN, D. & THOMAS, G. (1982) Co-existence of vinculin and a vinculin-like protein of higher molecular weight in smooth muscle. *J Biol Chem.* , 257, 11024-31.

FINKE, J., FRITZEN, R., TERNES, P., LANGE, W. & DOLKEN, G. (1993) An improved strategy and a useful housekeeping gene for RNA analysis from formalin-fixed, paraffin-embedded tissues by PCR. *Biotechniques,* 14, 448-53.

FLEIGE, S. & PFAFFL, M. W. (2006) RNA integrity and the effect on the real-time qRT-PCR performance. *Mol Aspects Med,* 27, 126-39.

FRAZIER, M. L., MARS, W., FLORINE, D. L., MONTAGNA, R. A. & SAUNDERS, G. F. (1983) Efficient extraction of RNA from mammalian tissue. *Mol Cell Biochem,* 56, 113-22.

GIERER, A. & SCHRAMM, G. (1956) Infectivity of ribonucleic acid from tobacco mosaic virus. . *Nature,* 177, 702-703.

GOELZ, S., HAMILTON, S. & VOGELSTEIN, B. (1985) Purification of DNA from formaldehyde fixed and paraffin embedded human tissue. *Biochem Biophys Res Commun.* , 130, 118-26.

GOLDSWORTHY, S. M., STOCKTON, P. S., TREMPUS, C. S., FOLEY, J. F. & MARONPOT, R. R. (1999) Effects of fixation on RNA extraction and amplification from laser capture microdissected tissue. *Mol Carcinog,* 25, 86-91.

GONZALEZ-PEREZ, I., ARMAS CAYARGA, A., GARCIA DE LA ROSA, I. & JOSEFINA GONZALEZ GONZALEZ, Y. (2007) Homemade viral RNA isolation protocol using silica columns: a comparison of four protocols. *Anal Biochem,* 360, 148-50.

GOPALAKRISHNA, Y., LANGLEY, D. & SARKAR, N. (1981) Detection of high levels of polyadenylate-containing RNA in bacteria by the use of a single-step RNA isolation procedure. *Nucleic Acids Res,* 9, 3545-54.

HALE, A. D., GREEN, J. & BROWN, D. W. (1996) Comparison of four RNA extraction methods for the detection of small round structured viruses in faecal specimens. *J Virol Methods,* 57, 195-201.

HOURFAR, M. K., MICHELSEN, U., SCHMIDT, M., BERGER, A., SEIFRIED, E. & ROTH, W. K. (2005) High-throughput purification of viral RNA based on novel aqueous chemistry for nucleic acid isolation. *Clin Chem,* 51, 1217-22.

JACKSON, D. P., LEWIS, F. A., TAYLOR, G. R., BOYLSTON, A. W. & QUIRKE, P. (1990) Tissue extraction of DNA and RNA and analysis by the polymerase chain reaction. *J Clin Pathol,* 43, 499-504.

KOOPMANS, M., MONROE, S., COFFIELD, L. & ZAKI, S. (1993) Optimization of extraction and PCR amplification of RNA extracts from paraffin-embedded tissue in different fixatives. *J Virol Methods,* 43, 189-204.

KORBLER, T., GRSKOVIC, M., DOMINIS, M. & ANTICA, M. (2003) A simple method for RNA isolation from formalin-fixed and paraffin-embedded lymphatic tissues. *Exp Mol Pathol,* 74, 336-40.

LEWIS, F., MAUGHAN, N. J., SMITH, V., HILLAN, K. & QUIRKE, P. (2001) Unlocking the archive--gene expression in paraffin-embedded tissue. *J Pathol,* 195, 66-71.

MARKO, M., CHIPPERFIELD, R. & BIRNBOIM, H. (1982) A procedure for the large-scale isolation of highly purified plasmid DNA using alkaline extraction and binding to glass powder. *Anal Biochem.* , 121, 382-7.

MASUDA, N., OHNISHI, T., KAWAMOTO, S., MONDEN, M. & OKUBO, K. (1999) Analysis of chemical modification of RNA from formalin-fixed samples and optimization of molecular biology applications for such samples. *Nucleic Acids Res,* 27, 4436-43.

MIES, C. (1994) A simple, rapid method for isolating RNA from paraffin-embedded tissues for reverse transcription-polymerase chain reaction (RT-PCR). *J Histochem Cytochem,* 42, 811-3.

MUTIU, A. I. & BRANDL, C. J. (2005) RNA isolation from yeast using silica matrices. *J Biomol Tech,* 16, 316-7.

NAKAMURA, M. & UENO, Y. (1963) Infectious ribonucleic acid of Japanese B encephalitis virus: Optimal conditions for its extraction and for plaque formation in chick embryo cell monolayers, and some biologic properties. *J Immunol,* 91, 136-43.

O'SHEA, U., WYATT, J. & HOWDLE, P. (1997) Analysis of T cell receptor beta chain CDR3 size using RNA extracted from formalin fixed paraffin wax embedded tissue. *J Clin Pathol.,* 50, 811-4.

PARISH, J. H. & KIRBY, K. S. (1966) Reagents which reduce interactions between ribosomal RNA and rapidly labelled RNA from rat liver. . *Biochim. Biophys. Acta,* 129, 554-562.

PUISSANT, C. & HOUDEBINE, L. M. (1990) An Improvement of the Single-Step Method of RNA Isolation by Acid Guanidinium Thiocyanate-Phenol-Chloroform Extraction *BioTechniques,* 8, 148-149.

RASOOL, N., MONROE, S. & GLASS, R. (2002) Determination of a universal nucleic acid extraction procedure for PCR detection of gastroenteritis viruses in faecal specimens. *J Virol Methods.,* 100, 1-16.

REDDI, K. K. (1963) Studies on the formation of tobacco mosaic virus ribonucleic acid, III. Utilization of ribonucleosides of host ribonucleic acid. *Proc Natl Acad Sci U S A,* 50, 419-425.

ROSAI, J., CARCANGIU, M. & DELELLIS, R. (1992) *Atlas of Tumour Pathology – Tumours of the Thyroid Gland,* Washington DC, USA, AFIP.

RUPP, G. & LOCKER, J. (1988) Purification and analysis of RNA from paraffin-embedded tissues. *Biotechniques.* , 6, 56-60.

SANYAL, A., O'DRISCOLL, S. W., BOLANDER, M. E. & SARKAR, G. (1997) An effective method of completely removing contaminating genomic DNA from an RNA sample to be used for PCR. *Mol Biotechnol,* 8, 135-7.

SIEBERT, P. D. & CHENCHIK, A. (1993) Modified acid guanidinium thiocyanate-phenol-chloroform RNA extraction method which greatly reduces DNA contamination. *Nucleic Acids Res,* 21, 2019-20.

SMYTH, P. (2004) Molecular Algorithms in Thyroid Neoplasia. *Histopathology Department.* Dublin, Trinity College Dublin.

SPECHT, K., RICHTER, T., MULLER, U., WALCH, A., WERNER, M. & HOFLER, H. (2001) Quantitative gene expression analysis in microdissected archival formalin-fixed and paraffin-embedded tumor tissue. *Am J Pathol,* 158, 419-29.

VARELI, K. & FRANGOU-LAZARIDIS, M. (1996) Modification of the acid guanidinium thiocyanate-phenol-chloroform method for nuclear RNA isolation. *Biotechniques,* 21, 236-7.

VON HIPPEL, P., H. & WONG, K.-Y. (1964) Neutral Salts: The Generality of Their Effects on the Stability of Macromolecular Conformations. *Science,* 145, 577-580.

WECKER, E. (1959) The extraction of infectious virus nucleic acid with hot phenol. *Virology,* 7, 241-243.

WU, C. C., LIN, T. L., ZHANG, H. G., DAVIS, V. S. & BOYLE, J. A. (1992) Molecular detection of infectious bursal disease virus. *Avian Dis.* , 36 221-226.

CHAPTER FOUR

IMPROVED RNA QUALITY AND TAQMAN® PRE-AMPLIFICATION METHOD (PREAMP) TO ENHANCE EXPRESSION ANALYSIS FROM FORMALIN FIXED PARAFFIN EMBEDDED (FFPE) MATERIAL

4.1 Summary

This study employed the identified best RNA extraction protocols from Chapter 3, the Stratagene Absolutely RNA® FFPE Kit and the Ambion RecoverAll™ Total Nucleic Acid Isolation Kit. It modified these two extraction protocols by introducing a heating step and compared the extracts with and without modification in a cell line model. Further, it assessed TaqMan® technologies and evaluated a novel pre-amplification system (PreAmp) designed to enhance expression analysis from tissue samples using assays with a range of amplicon sizes. This study demonstrated extraction protocol modification, introducing a step of incubation at 70°C for 20 minutes, to improve RNA quality, which in conjunction with TaqMan® PreAmp established a suitable analysis system to analyze messenger RNA expression using FFPE.

4.2 Introduction

Archival Formalin–Fixed, Paraffin–Embedded (FFPE) tissue samples have not been widely used in molecular biology due to the degradation and chemical modification of RNA extracted from FFPE. RNA extracted from FFPE is degraded to fewer than 300 bases (Cronin et al., 2004) in length and is modified by methylol groups to form cross-links with protein or nucleic acid during formalin fixation (Haselkorn and Doty, 1961, Chaw et al., 1980, Rait et al., 2006), which results in poor yields (Lewis et al., 2001, Goldsworthy et al., 1999) and compromised extracts. Heating at high temperature has been introduced, to break up the cross-links formed among protein molecules in FFPE tissue, as an antigen retrieval procedure used in Immunohistochemistry, which has been described in Chapter 1.2. Masuda et al. suggested that a heating step might be

introduced into RNA extraction protocols to reverse chemical modification caused by formalin fixation (Masuda et al., 1999). In this chapter, using modern techniques of Nano-Drop Spectrophotometer and Agilent Bioanalyzer, we assessed the quantity and quality of extracts using extraction protocols of with and without a heating step.

Real-time quantitative TaqMan® reverse transcriptase-polymerase chain reaction (QRT-PCR) analysis was employed for mRNA quantitation in FFPE materials in this study. It is a sensitive, accurate, and highly reproducible method to study gene expression (Mocellin et al., 2003), and only requires a few nanograms of target DNA or RNA. It has been successfully used to detect gene transcript levels from FFPE containing partially fragmented RNA (Sheils and Sweeney, 1999, Sheils et al., 2000, Macabeo-Ong et al., 2002) although the detection rate is lower than that from snap frozen tissue extracts as indicated for example by invariably higher C_T values in the former (Godfrey et al., 2000, Van Deerlin et al., 2002, Cohen et al., 2002, Abrahamsen et al., 2003, Koch et al., 2006). The details of real-time TaqMan® PCR technology are described in the following sections.

4.2.1 Polymerase Chain Reaction (PCR)

The polymerase chain reaction (PCR) was invented in 1983 by Kary Mullis (Saiki et al., 1985, Saiki et al., 1988), for which Kary Mullis was awarded the 1993 Year's Nobel prize in chemistry (Bartlett and Stirling, 2003). By PCR, any nucleic acid sequence present in a complex sample can be amplified in a cyclic process to generate a large number of identical copies that can readily be analyzed (Kubista et al., 2006). PCR has now become a common and often indispensable technique used in medical

and biological research labs for a variety of applications, including DNA cloning for sequencing, DNA-based phylogeny, or functional analysis of genes; the diagnosis of hereditary diseases; the identification of genetic fingerprints; and the detection and diagnosis of infectious diseases.

PCR is performed by temperature cycling on a PCR machine, called thermocycler, with the components present in the reaction: the original DNA molecule as the template, two primers that match the sequences at either end of the target DNA to be amplified, dNTPs as a supply of nucleotides, a heat-stable enzyme DNA polymerase, and magnesium ions in the buffer. There are three major steps in a PCR, which are repeated for 30 or 40 cycles. The PCR cycle starts with denaturation which is at high temperature 95°C to separate the strands of the double helical DNA, then annealing which lowers the temperature to about 60°C letting primers anneal to the template, and finally elongation that sets the temperature to around 72°C to be optimum for the polymerase extending the primers by incorporating the dNTPs (Figure 4.1). There is an exponential increase of the number of the gene copies as the DNA fragments doubled after each PCR cycle.

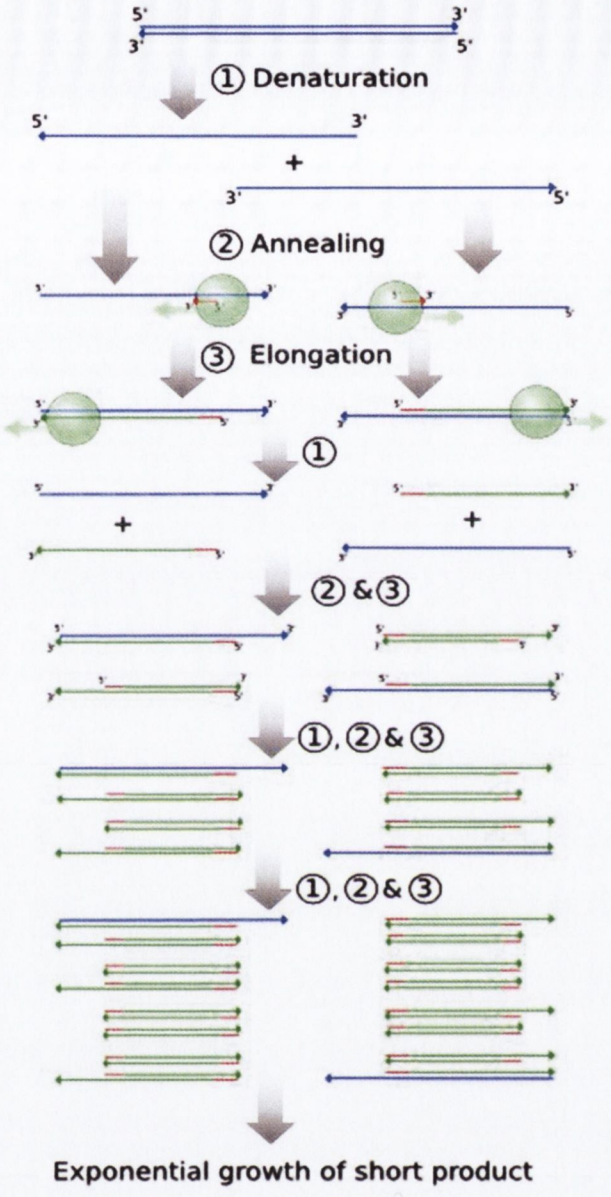

Figure 4.1 Schematic representation of PCR cycles

There are three major steps in a PCR: 1, denaturation at high temperature 95°C to separate the strands of DNA; 2, annealing at about 60°C letting primers anneal to the template; and 3, elongation at 72°C for the polymerase to extend the primers by incorporating the dNTPs. The number of the product grows exponentially as the number of DNA fragments is doubled after each PCR cycle.

4.2.2 Theory of real time TaqMan® PCR

The original PCR had a serious limitation for giving rise to essentially the same amount of product independently of the initial amount of DNA template molecules that were present. A few years later, real time PCR was developed by Higuchi et al. (Higuchi et al., 1992), in which the amount of product formed is monitored during the course of the reaction by monitoring the fluorescence of dyes or probes intruduced into the reaction that is proportional to the amount of product formed. The number of amplification cycles required to obtain a particular amount of DNA molecules is recorded. By real time PCR, it is possible to calculate the number of DNA molecules of the amplified sequence that were initially present in the sample.

With the highly efficient detection systems composed of chemistries, sensitive instruments, and optimized assays, the number of DNA molecules of a particular sequence in a complex sample can be determined with unprecedented accuracy and sensitivity sufficient to detect a single molecule. One of the systems available today is real time TaqMan® PCR. TaqMan® PCR exploits the 5' nuclease activity of AmpliTaq Gold® DNA polymerase to cleave a TaqMan® probe during PCR. The TaqMan® probe contains a reporter dye at the 5' end of the probe and a quencher dye at the 3' end of the probe. During the reaction, cleavage of the probe separates the reporter dye and the quencher dye, resulting in increased fluorescence of the reporter. Accumulation of PCR products is detected directly by monitoring the increase in fluorescence of the reporter dye (Figure 4.2).

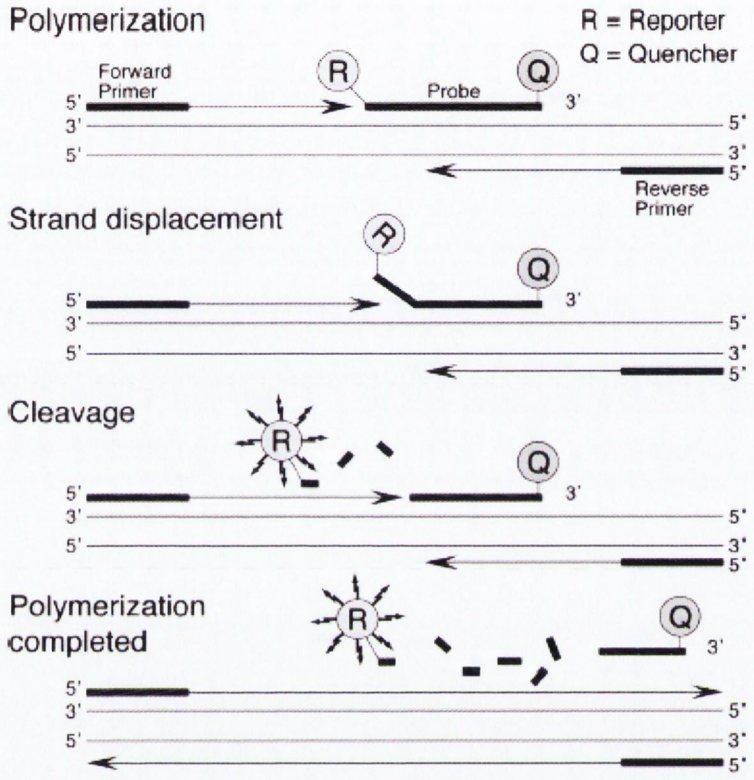

Figure 4.2 Nuclease activity of AmpliTaq® Gold DNA polymerase during PCR

TaqMan® PCR exploits the 5' nuclease activity of AmpliTaq Gold® DNA polymerase to cleave a TaqMan® probe during PCR. The TaqMan® probe contains a reporter dye at the 5' end of the probe and a quencher dye at the 3' end of the probe. During the reaction, cleavage of the probe separates the reporter dye and the quencher dye, resulting in increased fluorescence of the reporter. Accumulation of PCR products is detected directly by monitoring the increase in fluorescence of the reporter dye (Grove, 1999).

4.2.3 TaqMan® Gene Expression Assays

TaqMan® Gene Expression Assays are built on 5' nuclease chemistry. Each assay consists of two unlabeled PCR primers for amplifying the sequence of interest (final concentration of 900nM each) and a FAM™ dye labelled TaqMan® MGB (minor groove binder) probe for detecting the sequence of interest (final concentration of 250nM). The probe consists of an oligonucleotide with a 5'-reporter dye and a 3'-quencher dye. A fluorescent reporter dye, such as FAM, is covalently linked to the 5' end of the oligonucleotide. TET, JOE, and VIC are also used as reporter dyes. Each of the reporters is quenched by a nonfluorescent quencher at the 3' end. In TaqMan® probes, MGBs increase the melting temperature without increasing probe length (Afonina et al., 1997, Kutyavin et al., 1997), and also allow the design of shorter probes.

When the probe is intact, the proximity of the reporter dye to the quencher dye results in suppression of the reporter fluorescence primarily by Förster-type energy transfer (Förster, 1948, Lakowicz, 1983). During PCR, if the target of interest is present, the probe specifically anneals between the forward and reverse primer sites. The 5'-3' nucleolytic activity of the AmpliTaq® Gold DNA Polymerase cleaves the probe between the reporter and the quencher only if the probe hybridises to the target. The probe fragments are then displaced from the target, and polymerisation of the strand continues. The 3' end of the probe is blocked to prevent extension of the probe during PCR. This process occurs in every cycle and does not interfere with the exponential accumulation of product. The increase in fluorescence signal is detected only if the

target sequence is complementary to the probe and is amplified during PCR. Because of these requirements, any nonspecific amplification is not detected.

4.2.4 Detection of real-time quantitative TaqMan® RT-PCR

Real-time quantitative TaqMan® RT-PCR (QRT-PCR) is the ability to monitor the progress of the PCR as it occurs (i.e., in real time). Data is collected throughout the PCR process, rather than at the end of the PCR, which completely revolutionizes the way one approaches PCR-based quantitation of DNA and RNA. In real-time RT-PCR, reactions are characterized by the point in time during cycling when amplification of a target is first detected rather than the amount of target accumulated after a fixed number of cycles. The higher the starting copy number of the nucleic acid target, the sooner a significant increase in fluorescence is observed. In contrast, an endpoint assay (also called a "plate read assay") measures the amount of accumulated PCR product at the end of the PCR cycle.

In the initial cycles of PCR, there is little change in fluorescence signal. This defines the baseline for the amplification plot. An increase in fluorescence above the baseline indicates the detection of accumulated target. A fixed fluorescence threshold can be set above the baseline. The parameter C_T (threshold cycle) is defined as the fractional cycle number at which the fluorescence passes the fixed threshold (Figure 4.3).

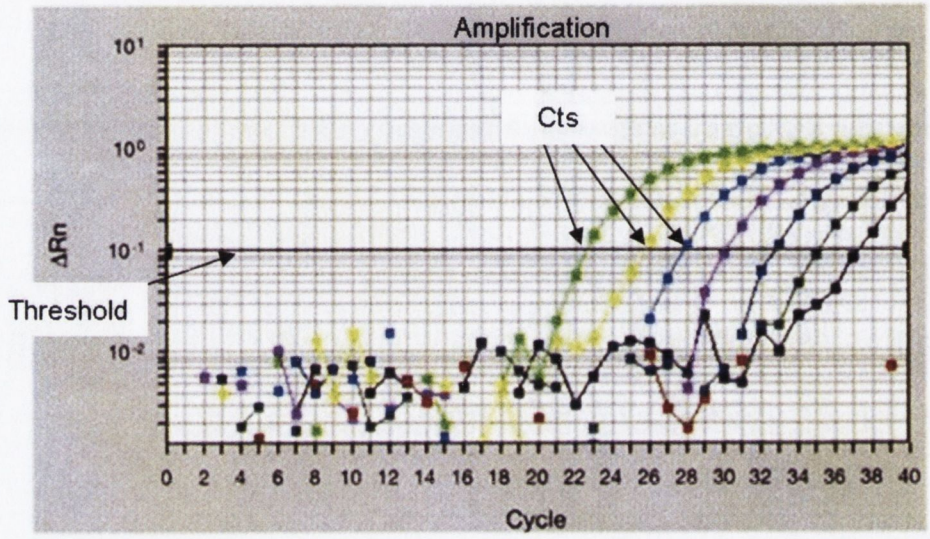

Figure 4.3 Example of an amplification plot of real time TaqMan® PCR

Rn is the measure of reporter signal. Threshold is the point of detection. There is little change in fluorescence signal in the initial cycles of PCR, which defines the baseline for the amplification plot. An increase in fluorescence above the baseline indicates the detection of accumulated target. The parameter C_T (threshold cycle) is defined as the fractional cycle number at which the fluorescence passes the fixed threshold.

4.2.5 TaqMan® PreAmp

TaqMan® PreAmp system was developed by Applied Biosystems (www.appliedbiosystems.com) and the kit was commercially launched in July, 2006. The principle of TaqMan® PreAmp technique is to amplify target cDNA prior to real-time TaqMan® PCR analysis (Figure 4.4). Briefly, cDNA is synthesized from total RNA by use of random priming. The cDNA for the specific target assays is then amplified by pre-amplification reaction using pooled gene-specific primers to increase the number of targeted copies. The pre-amplification product is diluted and finally analyzed by real-time TaqMan® PCR using single assay containing one pair of gene-specific primers and probe.

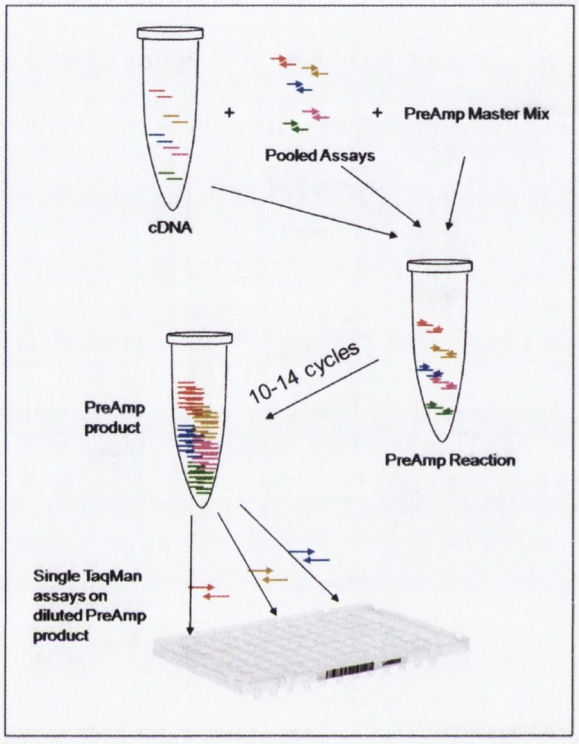

Figure 4.4 A schematic representation of the TaqMan® PreAmp procedures

cDNA is reverse transcribed from prepared RNA using random priming. It is combined with TaqMan® PreAmp Master Mix and pooled assays containing specific primers, and then is amplified by pre-amplification reaction for 10 to 14 cycles to increase the number of targeted copies. The pre-amplification product is diluted and finally analyzed by real-time TaqMan® PCR using single assay containing one pair of gene-specific primers and probe.

4.2.6 Aims

This study aimed to improve the RNA quality and evaluate the feasibility of TaqMan® PreAmp technology for FFPE materials. In this chapter, we introduced a heating step into the identified RNA extraction protocols, Stratagene Absolutely RNA® FFPE Kit and Ambion RecoverAll™ Total Nucleic Acid Isolation Kit. We first examined the extracts by comparison of parallel extracts from FFPE and snap frozen cell preparations using a cell line model (Figure 4.5). We further analyzed these extracts using different TaqMan® protocols, including two types of TaqMan® Master Mix (Universal PCR Master Mix (UPMM) and Gene Expression Master Mix (GEMM)) and newly developed TaqMan® with pre-amplification method (PreAmp), with a panel of assays over a range of amplicon sizes, from 62 to 164bp.

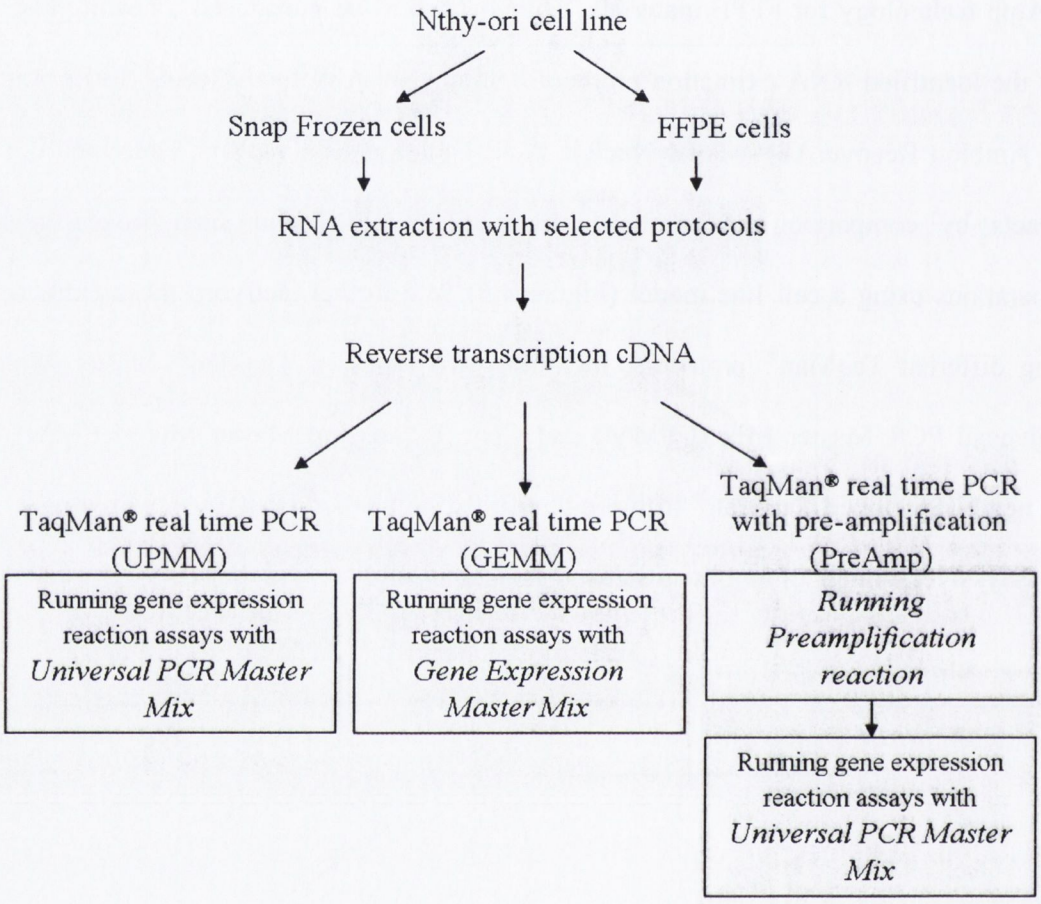

Figure 4.5 A schematic representation of the experimental procedures

Normal thyroid cell lines were split into two aliquots: One was snap frozen, the other formalin fixed and paraffin embedded. RNA was extracted using selected protocols and was then reverse transcribed into cDNA followed by different TaqMan® QRT-PCR analysis, including two types of master mix (UPMM and GEMM) and a PreAmp system.

4.3 Materials and Methods

4.3.1 Cell culture and formalin fixation

Nthy-ori 3-1 (ECACC, Wiltshire, UK) is a normal thyroid follicular epithelial cell line derived from adult thyroid tissue that has been transfected with a plasmid encoding for the SV40 large T gene (Cahill et al., 2006). This cell line was grown to confluence in a humidified atmosphere containing 5% CO_2 at 37°C at described in Chapter 2.2. Approximately $1x10^5$ suspended cells were aliquot and were pelleted (a) snap frozen and (b) formalin fixed and paraffin embedded into a cell block as described in Chapter 2.3.1.

4.3.2 RNA extraction

RNA extraction was performed using Ambion RecoverAll™ Total Nucleic Acid Isolation Kit and Stratagene Absolutely RNA® FFPE Kit as described in Chapter 2.5.1 and 2.5.2, in addition to modified Stratagene and Ambion protocols. Apart from deparaffinazition, RNA was extracted from snap frozen and FFPE cells in parallel according to manufacturer's protocols including proteinase K digestion, RNA isolation and elution or hydration procedures. The modification in Stratagene and Ambion protocols involved incubation at 70°C for 20 minutes after the recommended proteinase K digestion.

RNA quantity was assessed using the NanoDrop® ND-1000 Spectrophotometer (Wilmington, USA), and the quality was measured using the RNA 6000 Pico

LabChip® Kit on an Agilent 2100 Bioanalyser (Agilent technologies, Waldbronn, Germany) as described in Chapter 2.6 and 2.7.

4.3.3 TaqMan® gene expression assays and real-time PCR

Seven TaqMan® Gene Expression Assays (P/N: 4331182, Applied Biosystems, CA, USA) and one custom designed assay (GAPDH-67) were utilised in this study with a range of amplicon sizes from 62 to 164bp (Table 4.1). The extracted RNA was reverse transcribed into cDNA and were then quantified using real time TaqMan® PCR with or without PreAmp procedure.

Applied Biosystems High-Capacity cDNA Archive Kit (P/N: 4322171, Applied Biosystems) was used for reverse transcription (RT) following manufacturer's protocol as described in Chapter 2.8.1. Each RT reaction contained 50µl of 8ng/µl total RNA, 10µl of 10x RT buffer, 4µl of 25x dNTP mixture, 10µl of 10x Random Primers, 5µl of MultiScribe RT (50U/µl) and 21µl of RNase-free water. The 100µl reactions were incubated in an Applied Biosystems Thermocycler for 10 minutes at 25°C, 2 hours at 37°C and then held at 4°C.

For the Real-time TaqMan® PCR step, amplification was carried out on the Applied Biosystems 7000 Sequence Detection System as described in Chapter 2.8.2. Two types of TaqMan® Master Mix were employed in this procedure: TaqMan® Universal PCR Master Mix (UPMM) with UNG (P/N 4304437, Applied Biosystems) or TaqMan® Gene Expression Master Mix (GEMM) (P/N 4370048, Applied Biosystems). The 20µl PCR reaction included 10µl of 2x TaqMan® Master Mix, 5µl of 4x TaqMan® Gene

expression Assay (P/N 4331182, Applied Biosystems) and 5µl of cDNA (RT product 4ng/µl). The reactions were incubated in a 96-well optical plate at 50°C for 2 minutes, at 95°C for 10 minutes, following by 40 cycles of 95°C for 15 seconds and 60°C for 1 minutes. The real-time PCRs for each assay were run in triplicate.

In real time TaqMan® PCR with PreAmp, the preamplification was performed using TaqMan® PreAmp Master Mix Kit protocol (P/N 4366128, Applied Biosystems) as described in Chapter 2.8.3. The pooled assay mix was prepared by combining 8 of 20x TaqMan® Gene Expression Assays into a single tube and using 1x TE buffer to dilute the pooled assays to a final concentration of 0.2x. The 40µl of preamplification reaction included 20µl of 2x TaqMan® PreAmp Master Mix, 10µl of 0.2x pooled assay mix and 10µl of 4ng/µl cDNA sample. The reactions were incubated in an Applied Biosystems Thermocycler for 10 minutes at 95°C following by 10 cycles of 95°C for 15 seconds and 60°C for 4 minutes and then held at 4°C. The concentration of the preamplification product was 2^{10}ng/µl (in theory) which was then 1:5 diluted and analyzed by TaqMan® real time PCR using TaqMan® Universal PCR Master Mix following the procedures described.

4.3.4 Data analysis

Replicates were omitted if C_T standard deviation was greater than 1.5 in the triplicate. All the data were collected in Excel form. The formulas used to generate the figures are as below:

1. ΔC_T (A–B) = C_T X_mean(A) – C_T X_mean(B)

2. Theoretical ΔC_T = Log_2(Amount cDNA in A / Amount of cDNA in B)

Table 4.1 Eight of TaqMan® Gene Expression Assays

Seven of these assays were inventoried by Applied Biosystems (P/N: 4331182, Applied Biosystems, CA, USA) and one was a designed assay (GAPDH-67 Forward primer: CAT CCA TGA CAA CTT TGG TAT CGT; Reverse primer: GGG TGG CAG TGA TGG CAT; Probe: ACT CAT GAC CAC AGT CC).

Gene Symbol – Amplicon Length	Gene Name	Assay ID
MT4 – 62	metallothionein IV	Hs00262914_m1
GAPDH – 67	glyceraldehyde-3-phosphate dehydrogenase	Designed
CDKN1B – 71	cyclin-dependent kinase inhibitor 1B (p27, Kip1)	Hs00153277_m1
MAPK4 – 72	mitogen-activated protein kinase 4	Hs00177074_m1
CD44 – 86	CD44 molecule (Indian blood group)	Hs00153304_m1
SDC2 – 103	syndecan 2 (heparan sulfate proteoglycan 1, cell surface-associated, fibroglycan)	Hs00299807_m1
GAPDH – 122	glyceraldehyde-3-phosphate dehydrogenase	Hs99999905_m1
HLA-A – 164	major histocompatibility complex, class I, A	Hs00740413_g1

4.4 Results

4.4.1 Evaluation of modified protocols

RNA quantity was assessed spectrophotometrically using NanoDrop® ND-1000 Spectrophotometer (Wilmington, USA), which showed that the yields from snap frozen extracts were greater than those from FFPE when RNA was extracted from identical numbers of cells using the selected protocols. Modification to the Stratagene and Ambion protocols generated approximately 25-40% greater yields and larger fragments of RNA (Figure 4.6) than the standard procedure. Adjustment to Stratagene and Ambion protocols produced decreased C_Ts (e.g. with a mean of 2.95 cycles in GEMM experiment and a mean of 3.14 cycles in PreAmp), indicating the improved quality of RNA extracted from FFPE (Figure 4.7).

A separate experiment using Ambion RecoverAll™ kit enabled extraction of large RNA molecules including cross-linked RNAs (Figure 4.8). Incubation of eluted RNA at 70°C for 20 minutes was found to be the best condition to disrupt cross-links while not compromising RNA integrity in comparison with other modifications (70°C for 10 minutes, 95°C for 10 minutes and 95°C for 20 minutes).

4.4.2 Comparison of TaqMan® Universal PCR Master Mix (UPMM), Gene Expression Master Mix (GEMM) and PreAmp

C_T values were also dependent on the type of TaqMan® PCR Master Mix that was used (Figure 4.7 and Figure 4.9). TaqMan® with UPMM generated higher C_Ts for long

amplicons than GEMM. This was observed by a comparison of two GAPDH assays – one 122bp and the other 67bp. There was a mean threshold detection difference of 17 cycles using UPMM and a mean difference of 4 cycles using GEMM with RNA template extracted using Ambion RecoverAll™ kit (Figure 4.7). In addition, HLA_A is the largest amplicon (164bp) which produced no product with UPMM, however, GEMM and PreAmp both allowed the detection of this amplicon size (Figure 4.7). GEMM improved the C_T values for long amplicons (over 100bp) compared with UPMM (Figure 4.9-a). When the ΔC_Ts were compared to Theoretical ΔC_Ts, PreAmp results generally correlated with GEMM for all the 8 assays analyzed (Figure 4.9-c).

4.4.3 Evaluation of TaqMan® PreAmp using CDKN1B

TaqMan® PreAmp analysis consistently achieved decreased C_T values in both snap frozen and FFPE aliquots compared with TaqMan® without pre-amplification step (Figure 4.9-b, c). A good correlation between PreAmp and UPMM was observed using CDKN1B to analyze RNA extracted with different protocols (Figure 4.10), suggesting that PreAmp does not introduce any bias into the reaction.

4.4.4 Comparison of C_T difference between FFPE and snap frozen cells

TaqMan® analysis over all assays showed C_Ts to be 2 to 11 cycles higher when using FFPE extracts compared to snap frozen counterparts when the amounts of input RNA were identical (Figure 4.7). Focussing on an analysis of GAPDH using two assays with different amplicon sizes revealed the smaller amplicon assay (67bp) produced C_Ts from snap frozen and FFPE samples that were closer together (Figure 4.11). We

further measured the amplification efficiencies associated with these two sizes of GAPDH assays using a broad dilution range, five Log_{10}s, which showed efficiencies with 99.98% for GAPDH-67 and 99.92% for GAPDH-122 (Figure 4.12). These relatively close high efficiencies indicate non-bias amplification or detection produced by these two sizes of assays.

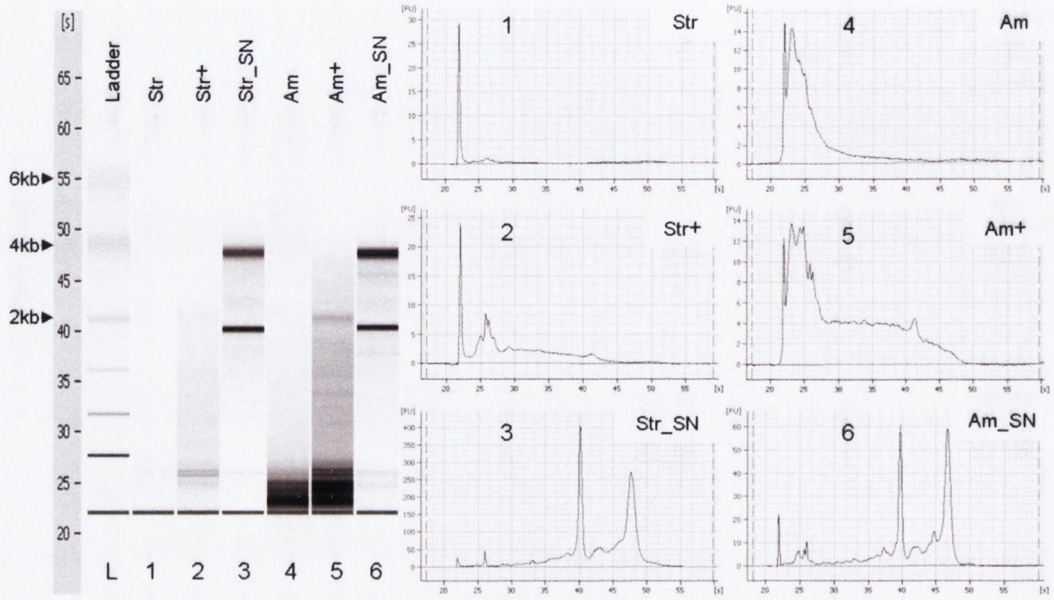

Figure 4.6 Qualities of RNA measured using Agilent 2100 Bioanalyzer

(Str = Stratagene protocol; Am = Ambion protocol; + = modified with incubation in Proteinase K buffer at 70°C for 20 minutes; and SN = snap frozen.) Modification to the Stratagene and Ambion protocols generated larger fragments (lane 2 and 5) compared to the extracts generated using the original protocols (lane 1 and 4). Each well contained 1µl of extracted RNA from equal amount of starting materials of 10^5 cells.

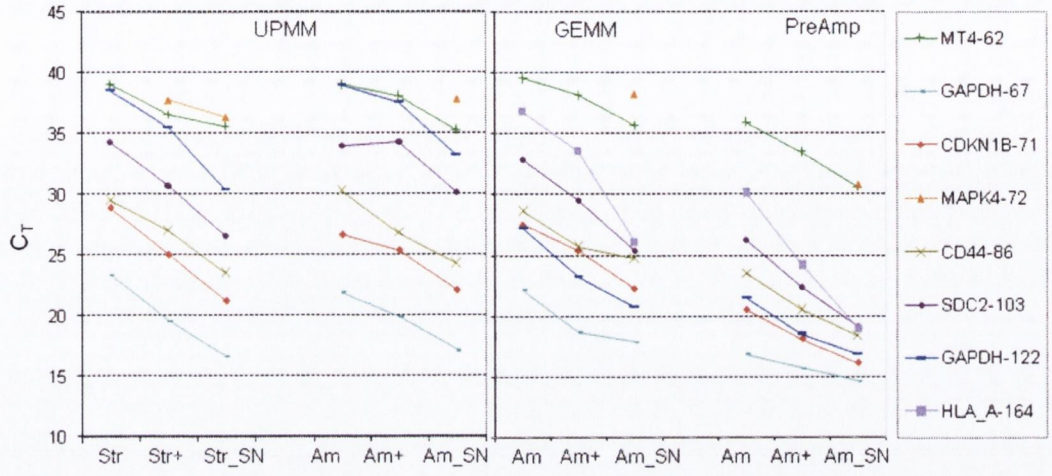

Figure 4.7 TaqMan® gene expression pattern using UPMM, GEMM and PreAmp

(Str = Stratagene protocol; Am = Ambion protocol; + = modified protocols with incubation in Proteinase K buffer at 70°C for 20 minutes; and SN = snap frozen cells. Not all assays produced products, e.g. HLA_A in UPMM.) C_Ts were higher using FFPE extracts compared to snap frozen counterparts when the amount of input RNA was identical. Modification to Stratagene and Ambion protocols produced decreased C_Ts. TaqMan® with UPMM generated higher C_Ts than GEMM and PreAmp when using longer amplicon lengths. This was particularly evident when comparing two GAPDH assays – one 122bp and the other 67bp. A mean difference of 17 cycles between small and large assays using UPMM and a mean difference of 4 cycles between small and large assays using GEMM was observed.

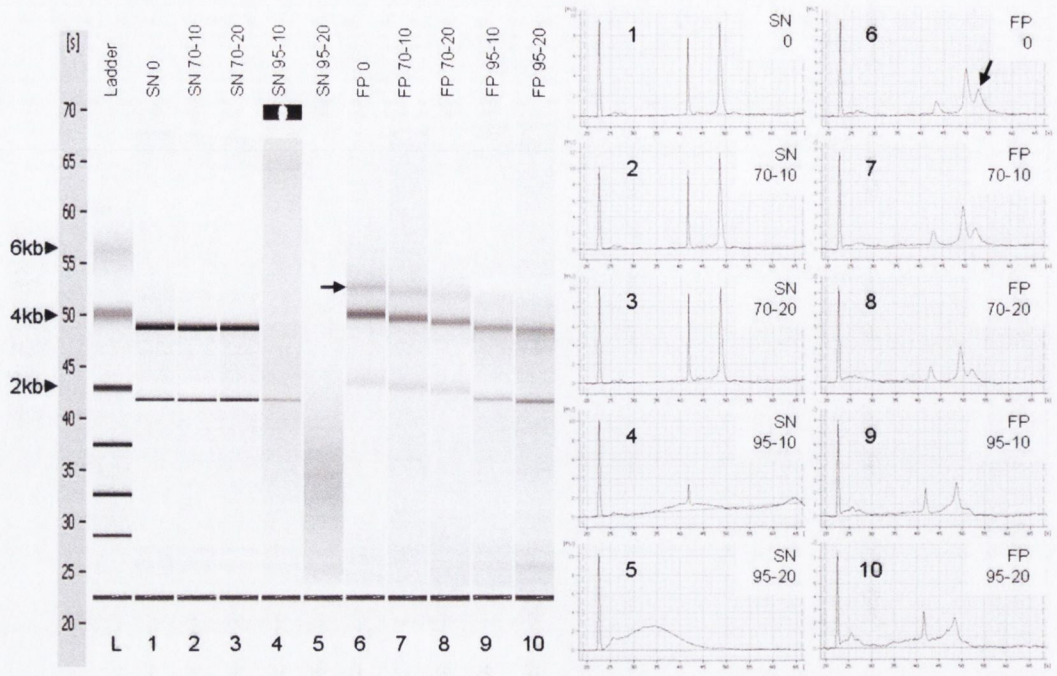

Figure 4.8 The effect of different incubation conditions on RNA

Total RNA was extracted from a large number ($2x10^6$ cells) of formalin fixed paraffin embedded cells using Ambion RecoverAll™ kit. Five eluted RNA aliquots from one extraction were subjected to different incubation conditions on a hot rack (FP, lane 6 to 10). In parallel, five eluted RNA aliquots from one snap frozen extraction were incubated (SN, lane 1 to 5). Each well contained 1µl of 4ng/µl RNA in Ambion Elution Solution. Incubation conditions were as follows: 0= no treatment; 70-10 = 70°C for 10 minutes; 70-20 = 70°C for 20 minutes; 95-10 = 95°C for 10 minutes and 95-20 = 95°C for 20 minutes. RNA from snap frozen preparations was not degraded at 70°C for 20 minutes (lane 3), but was degraded at 95°C (lane 4 and 5). RNA from FFPE showed large fragments and cross-linked RNAs which are approximately 5kb (lane 6 – arrow). It was found that incubation of eluted RNA at 70°C for 20 minutes is the optimal condition, among these tested, to break up cross-links while not compromising RNA integrity.

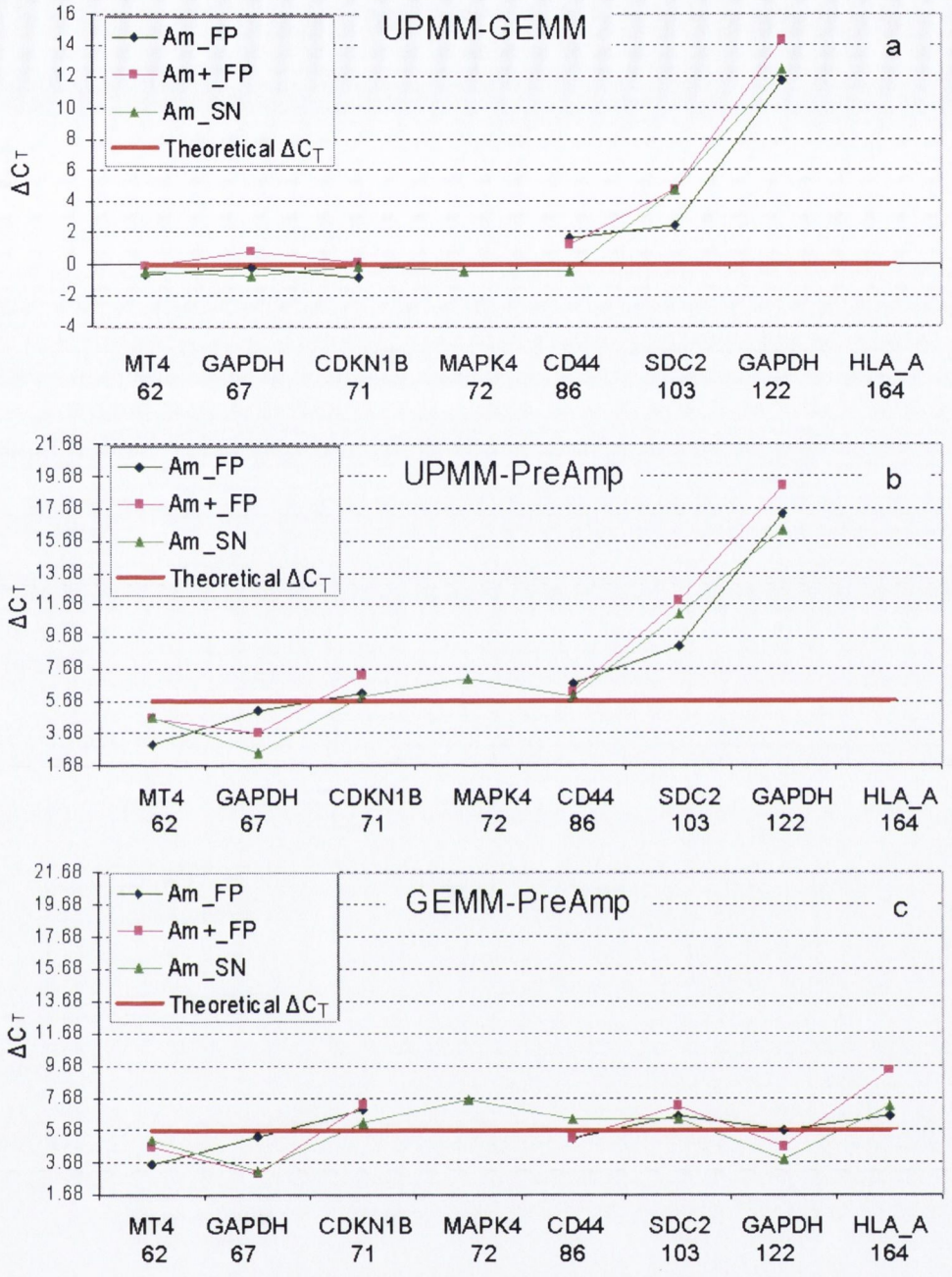

Figure 4.9 Comparison of TaqMan® gene expression pattern using ΔC_T method

(Am = Ambion protocol; FP = FFPE cells; + = modified protocols with incubation in Proteinase K buffer at 70°C for 20 minutes; and SN = snap frozen cells. Not all assays produced products, e.g. HLA_A in UPMM.) These ΔC_T data was generated from the C_Ts shown in Figure 4.7. A Theoretical ΔC_T was calculated for each chart based on

equilibrating the results for any variation in input cDNA. In panel a, $\Delta C_T = C_T\_UPMM - C_T\_GEMM$. The Theoretical ΔC_T of UPMM-GEMM was 0 [$=Log_2(20ng/20ng)$] given identical input quantities (20ng) were used in each system. In panel b, $\Delta C_T = C_T\_UPMM - C_T\_PreAmp$. In panel c, $\Delta C_T = C_T\_GEMM - C_T\_PreAmp$. The Theoretical ΔC_T in panel b and c was 5.68 [$=Log_2(1024ng/20ng)$], which was calculated based on an input of 1024ng of cDNA for the TaqMan® real time PCR component of pre-amplification process. This quantity was generated from an initial 1ng subjected to 10 cycles of pre-amplification with a 100% efficiency and no bias introduced from the PreAmp. The relevant Theoretical ΔC_T is plotted on each chart as a reference point for measuring the actual detected ΔC_T against the theoretically optimal ΔC_T. The benefit of GEMM over UPMM was evident as amplicon size increased (Panel a). A comparison of UPMM and PreAmp showed a similar pattern (Panel b). However, PreAmp results generally correlated with GEMM regardless of amplicon size for the series of 8 assays analysed (Panel c).

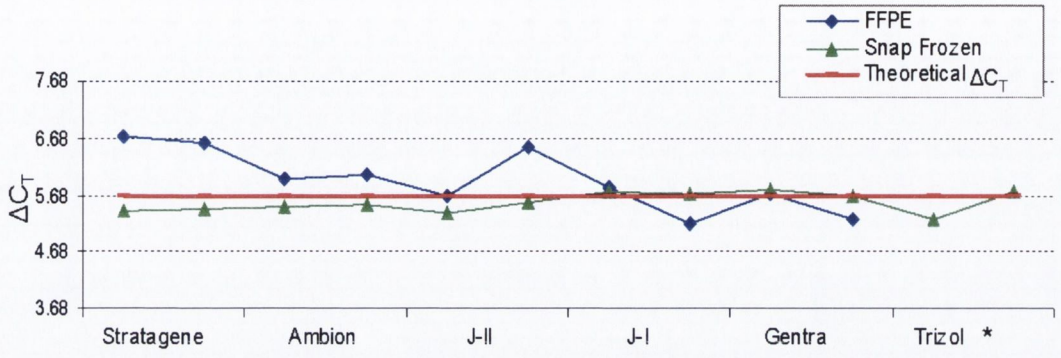

Figure 4.10 Comparison of TaqMan® real time PCR with and without PreAmp using CDKN1B assay on extracts produced by different extraction protocols

(* = No amplification was achieved from FFPE) ΔC_T = C_T (no_PreAmp) – C_T (with_PreAmp). The Theoretical ΔC_T was 5.68 [=Log_2(1024ng/20ng)] which was calculated based on an input of 1024ng of cDNA for the TaqMan® real time PCR component of pre-amplification process and 20ng of cDNA for the TaqMan® without pre-amplification. Ideally, ΔC_T is in a range between Theoretical ΔC_T +/- 1 which was achieved in this experiment indicating there is no bias in the PreAmp.

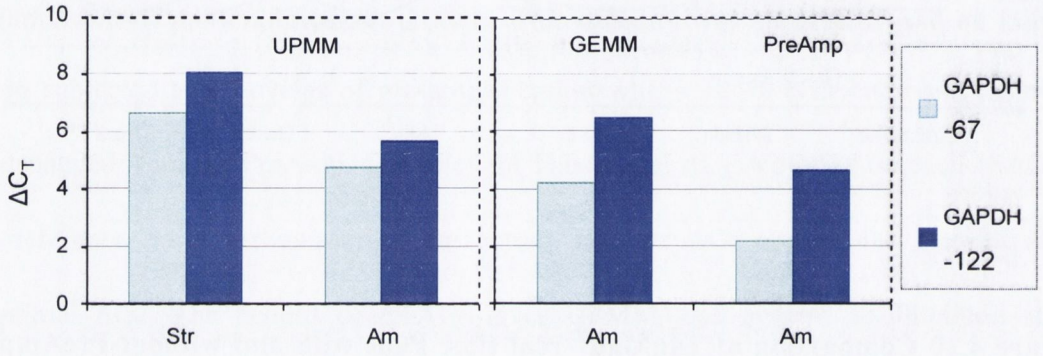

Figure 4.11 Analysis of GAPDH using two sizes of amplicon showing the difference of C_Ts between FFPE and snap frozen counterparts

$\Delta C_T = C_T$ (FFPE) – C_T (Snap-Frozen). The smaller amplicon size of GAPDH (67bp) generated lower ΔC_Ts than the larger amplicon size of 122bp indicating that smaller amplicon sizes produced more comparable C_Ts in snap frozen and FFPE samples.

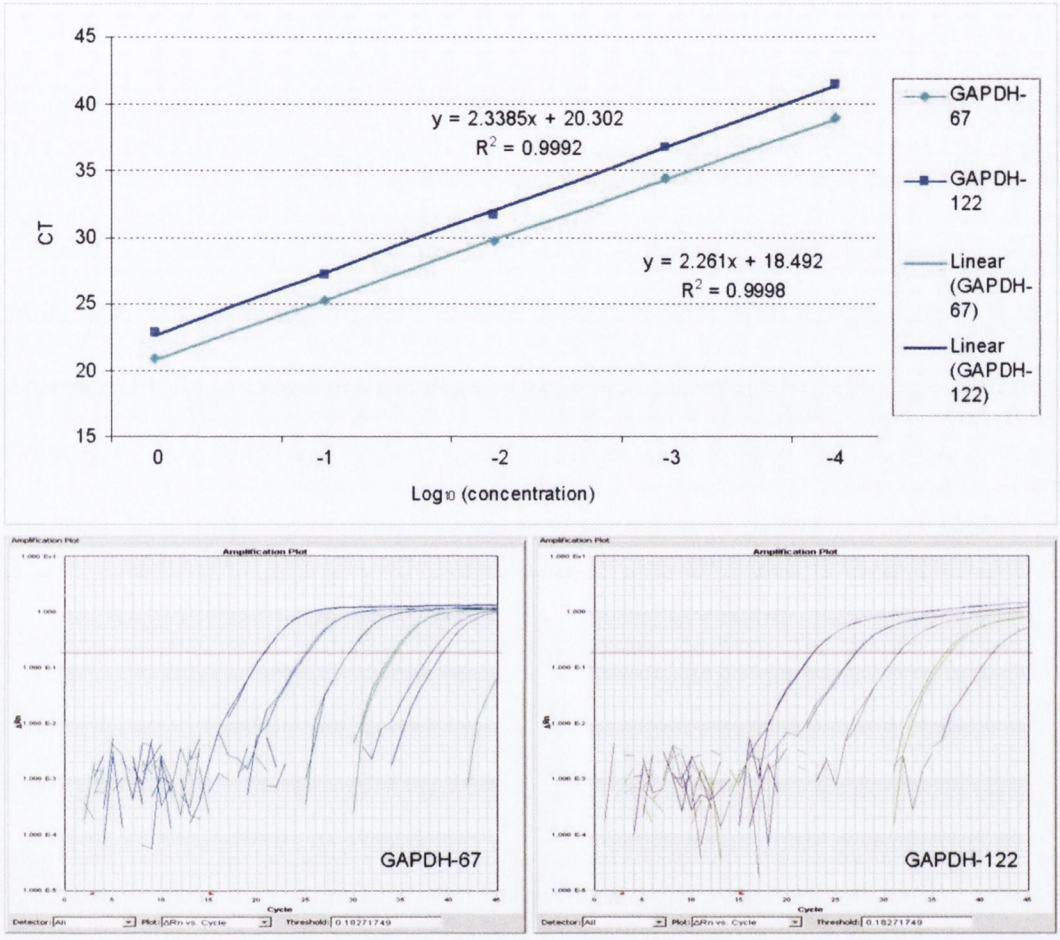

Figure 4.12 Amplification efficiencies of two sizes of assay GAPDH

The analyzed data is shown on the top. The original amplification plots are shown on the bottom. The amplification efficiencies associated with these two sizes of GAPDH assays using a broad dilution range, five Log_{10}s, showed closed efficiencies with 99.98% for GAPDH-67 and 99.92% for GAPDH-122.

4.5 Discussion

RNA analysis has generally been performed on snap-frozen or fresh materials, using variable techniques including microarray, northern blotting and RT-PCR. However, a constant challenge has been robust and reliable analysis of gene expression in archival tissues. This application has been frustrated by poor RNA yields, small sizes of extracted fragments and low levels of detectable RNA in the extracts (Godfrey et al., 2000). In this study we established a cell line model to test modified extraction protocols and quantify differences in performance using a panel of QRT-PCR assays on FFPE compared with parallel snap-frozen cell preparations using TaqMan® methodology. We found that our modified extraction method and TaqMan® PreAmp enhanced expression analysis from FFPE cells optimally.

4.5.1 RNA and FFPE

Generally, RNA extracted from FFPE materials is fragmented and chemically modified. Fragmentation occurs possibly since tissues are surgically removed, and it continuously occurs during fixation and preservation. Experimental design was such that equal numbers of cells were processed for FFPE cell block construction and snap freezing for comparative purposes. By using cells fixed under controlled conditions possible variables due to the effects of storage on RNA degradation were negated, thus revealing the true impact of formalin fixation on RNA quality. We extracted intact RNA fragments in a separate experiment from pellets with a large number of formalin fixed paraffin embedded normal thyroid cells (Figure 4.8), which was consistent with a finding by Scicchitana et al. (Scicchitano et al., 2006). In that study, intact RNA

molecules were extracted from newly formalin fixed paraffin embedded human bone marrow stromal cells suggesting that RNA degradation could be a minor problem for recently fixed FFPE in some types of cells. Our study showed that the differences in RNA quality between the small and large fixed pellets (Figure 4.6 and Figure 4.8) might be due to the fact that the majority of cells in the centre of the large pellet were remained alive during construction of the large solid cell pellet. This could limit the access of RNases to intracellular mRNA because degradation will not fully occur until the fixation process begins resulting to the intact mRNA being maintained. Unfortunately, intact mRNA is not generally obtained in majority of fixed tissues or cell lines, and RNA extracted from FFPE is normally degraded to fewer than 300bp.

Figure 4.8 displays the degree of RNA modification in FFPE cells caused by methylol groups during formalin fixation. Masuda and colleagues (Masuda et al., 1999) suggested that formaldehyde reacts with RNA forming an N-methylol followed by an electrophilic attack to form a methylene bridge between amino groups. Interestingly, our results show a clear large RNA band, approximately 5kb in length (Figure 4.8-lane 6), which is hypothetically the cross-linked RNA. The other two bands visualized were also larger than that extracted from snap frozen cells indicating the modification of RNA in FFPE. Furthermore, with incubation at high temperature, the large RNA band (~5kb) was removed, and the sizes of the other two bands became closer to 18s and 28s of the snap frozen extracts. This is in agreement with the results of a mass spectrometric analysis that was carried out by Masuda group, suggesting methylol modification is reversible by heating (Masuda et al., 1999, Hamatani et al., 2006). However, a balance must be achieved between breaking cross-links while not contributing to degradation of labile RNA. Our results showed that incubation at 70°C

for 20 minutes was the optimal condition, among those tested, to de-modify cross-linked RNA while maintaining RNA integrity (Figure 4.8).

4.5.2 Modification in the extraction protocols

Our results from Chapter 3 have shown that the quality of extracted RNA can be variable among different extraction methods due to several factors, such as the contamination of RNases, proteins and genomic DNA (Fleige and Pfaffl, 2006). Efficient protocols include some essential procedures, such as proteinase K digestion followed by on column DNase digestion and RNA elution produced good detectable RNA of FFPE. In these identified protocols, our data demonstrates that incubation in proteinase K buffer at 70°C for 20 minutes facilitated the disruption of cross-links, resulting in improved quantity and quality of RNA. The RNA extracted using the modified protocols (with the incubation) enhanced detection by a mean of 3 cycles (Figure 4.7), which is equivalent to 8 fold increased sensitivity. It is most likely that the additional incubation step removed the remaining cross-links between RNA and protein leading to the longer RNA molecules being extracted (Chapter 5) (Li et al., 2007). In addition, this incubation denatured proteinase K, thus avoided its further damage to RNA in the following purification procedure, which suggests the necessity of a heating (at 70°C for 20 minutes) application in any proteinase K based extraction of FFPE samples.

4.5.3 Features of TaqMan® PreAmp

TaqMan® QRT-PCR technique is based on the 5' nuclease activity of Taq DNA polymerase and involves cleavage of a specific fluorogenic hybridization probe that is flanked by PCR primers (Heid et al., 1996, Gibson et al., 1996). Because of the small target size, many laboratories have demonstrated that it is possible to measure gene expression levels using FFPE tissues as a source of mRNA (Cronin et al., 2004). Still, it seems to be problematic to perform large scale of analysis on FFPE because of the high C_Ts and limited concentration of extracts (Cohen et al., 2002, Abrahamsen et al., 2003).

We employed a novel TaqMan® PreAmp technique which we found to be a practical solution to decrease C_T values, and in particular suitable in our hands to generate real-time PCR results from limited amounts of input RNA, such as extracted from laser captured microdissected material (Denning et al., 2007).

The TaqMan® PreAmp technique addresses the challenge faced by researchers working with rare or precious samples, which only limited RNA could be extracted from, to perform gene expression analyses using real-time QRT-PCR. The simple process enables the user to perform uniform amplification from as little as one nanogram of cDNA (which was used in this study) or alternatively conduct up to 200 real-time PCR reactions per pre-amplification reaction without compromising the available sample material. Our results demonstrated that TaqMan® PreAmp overcame the difficulties usually caused by low yields of RNA extraction from FFPE.

4.5.4 Influence of TaqMan® Master Mix and amplicon length

This study demonstrated that the sensitivity of TaqMan® detection was influenced by choice of Master Mix and amplicon length in assay design. We evaluated UPMM and GEMM which showed similar sensitivity for short amplicons (less than 90bp), while GEMM displayed better sensitivity for longer amplicons (over 100bp) compared with UPMM in parallel snap frozen and FFPE extracts (Figure 4.9). This effect was dissipated when UPMM was used after pre-amplification, possibly because of the increased copy number of template available or because of the composition of the PreAmp MasterMix which is closer in components to GEMM than UPMM. Reagents can have a significant effect on assay reproducibility (Burgos et al., 2002) due to some parameters such as different polymerases sensitivity (Bustin and Mueller, 2005), primer binding efficiency and the concentration of Mg^{2+} (Karrer et al., 1995). Karrer et al. described the Monte Carlo effect using plant material suggesting that the PCR reproducibility could be limited when the number of available templates is low. Increased concentrations of Mg^{2+} reduced PCR variation possibly by allowing a higher proportion of annealed primers extended by the more active polymerase (Karrer et al., 1995).

Our data corroborated the observation that amplicon size is crucial in designing assays to analyze gene expression levels not only using FFPE extracts but also using RNAs with high integrity (Godfrey et al., 2000, Abrahamsen et al., 2003). Many researchers have found that short amplicons generated lower C_Ts than longer amplicons on analysis of the same gene in FFPE (Lehmann and Kreipe, 2001, Antonov et al., 2005). Data generated in this study evaluating snap frozen samples using two sizes of

GAPDH (Figure 4.7) demonstrated GAPDH-67 generated a reduction in C_T by 2 -3 cycles over GAPDH-122 in both GEMM and PreAmp experiments, demonstrating that smaller amplicons give more consistent results (Fleige et al., 2006).

In addition, we found C_Ts between FFPE and snap frozen were closer for small amplicons than that for large amplicons (Figure 4.11). For example, the analysis of GAPDH using a target amplicon of 67bp displayed C_Ts 1 – 2.5 cycles closer between FFPE and snap frozen than the same experiment using the longer amplicon size of 122bp. We further measured the amplification efficiency associated with these two sizes of GAPDH assays using a broad dilution range, five Log_{10}s, which showed closed efficiencies with 99.98% for GAPDH-67 and 99.92% for GAPDH-122 (Figure 4.12). This measurement eliminates non-specific amplification that could contribute to decreased amplification efficiency of the true target. Therefore, it seems reasonable to conclude that the shift of efficiency detected from frozen to fixed material (Figure 4.11) is due to degradation of RNA in FFPE, and logical to extrapolate that the longer an amplicon is, the more likely its template will be degraded in extracted RNA. As a general rule, house-keeping genes or normalising assays should have amplicon sizes that match the size of the target whose expression is to be measured (Cronin et al., 2004) and amplicons less than 100bp should be employed in gene expression studies using FFPE materials.

4.6 Conclusion

We evaluated the effect of modifying recommended extraction protocols to reproducibly produce RNA that may be successfully amplified using QRT-PCR. We have found the TaqMan® PreAmp system to be a robust and practical solution to limited quantities of RNA and have demonstrated comparable results in matched FFPE and snap frozen preparations providing proof of principle that this method may reliably be utilised in the context of multiple expression analyses from individual FFPE samples.

4.7 References

ABRAHAMSEN, H. N., STEINICHE, T., NEXO, E., HAMILTON-DUTOIT, S. J. & SORENSEN, B. S. (2003) Towards quantitative mRNA analysis in paraffin-embedded tissues using real-time reverse transcriptase-polymerase chain reaction: a methodological study on lymph nodes from melanoma patients. *J Mol Diagn,* 5, 34-41.

AFONINA, I., ZIVARTS, M., KUTYAVIN, I., LUKHTANOV, E., GAMPER, H. & MEYER, R. B. (1997) Efficient priming of PCR with short oligonucleotides conjugated to a minor groove binder. *Nucleic Acids Res,* 25, 2657-60.

ANTONOV, J., GOLDSTEIN, D. R., OBERLI, A., BALTZER, A., PIROTTA, M., FLEISCHMANN, A., ALTERMATT, H. J. & JAGGI, R. (2005) Reliable gene expression measurements from degraded RNA by quantitative real-time PCR depend on short amplicons and a proper normalization. *Lab Invest,* 85, 1040-50.

BARTLETT, J. M. & STIRLING, D. (2003) A short history of the polymerase chain reaction. *Methods Mol Biol,* 226, 3-6.

BURGOS, J. S., RAMIREZ, C., TENORIO, R., SASTRE, I. & BULLIDO, M. J. (2002) Influence of reagents formulation on real-time PCR parameters. *Mol Cell Probes,* 16, 257-60.

BUSTIN, S. A. & MUELLER, R. (2005) Real-time reverse transcription PCR (qRT-PCR) and its potential use in clinical diagnosis. *Clin Sci (Lond),* 109, 365-79.

CAHILL, S., SMYTH, P., FINN, S. P., DENNING, K., FLAVIN, R., O'REGAN, E. M., LI, J., POTRATZ, A., GUENTHER, S. M., HENFREY, R., O'LEARY, J. J. & SHEILS, O. (2006) Effect of ret/PTC 1 rearrangement on transcription and post-transcriptional regulation in a papillary thyroid carcinoma model. *Mol Cancer,* 5, 70.

CHAW, Y. F., CRANE, L. E., LANGE, P. & SHAPIRO, R. (1980) Isolation and identification of cross-links from formaldehyde-treated nucleic acids. *Biochemistry,* 19, 5525-31.

COHEN, C. D., GRONE, H. J., GRONE, E. F., NELSON, P. J., SCHLONDORFF, D. & KRETZLER, M. (2002) Laser microdissection and gene expression analysis on formaldehyde-fixed archival tissue. *Kidney Int,* 61, 125-32.

CRONIN, M., PHO, M., DUTTA, D., STEPHANS, J. C., SHAK, S., KIEFER, M. C., ESTEBAN, J. M. & BAKER, J. B. (2004) Measurement of gene expression in archival paraffin-embedded tissues: development and performance of a 92-gene reverse transcriptase-polymerase chain reaction assay. *Am J Pathol,* 164, 35-42.

DENNING, K. M., SMYTH, P. C., CAHILL, S. F., FINN, S. P., CONLON, E., LI, J., FLAVIN, R. J., AHERNE, S. T., GUENTHER, S. M., FERLINZ, A., O'LEARY J, J. & SHEILS, O. M. (2007) A molecular expression signature distinguishing follicular lesions in thyroid carcinoma using preamplification RT-PCR in archival samples. *Mod Pathol,* 20, 1095-102.

FLEIGE, S. & PFAFFL, M. W. (2006) RNA integrity and the effect on the real-time qRT-PCR performance. *Mol Aspects Med,* 27, 126-39.

FLEIGE, S., WALF, V., HUCH, S., PRGOMET, C., SEHM, J. & PFAFFL, M. W. (2006) Comparison of relative mRNA quantification models and the impact of RNA integrity in quantitative real-time RT-PCR. *Biotechnol Lett,* 28, 1601-13.

FÖRSTER, V. (1948) Zwischenmolekulare Energiewanderung und Fluoreszenz. . *Annals of Physics*, 55-75.

GIBSON, U. E., HEID, C. A. & WILLIAMS, P. M. (1996) A novel method for real time quantitative RT-PCR. *Genome Res,* 6, 995-1001.

GODFREY, T. E., KIM, S. H., CHAVIRA, M., RUFF, D. W., WARREN, R. S., GRAY, J. W. & JENSEN, R. H. (2000) Quantitative mRNA expression analysis from formalin-fixed, paraffin-embedded tissues using 5' nuclease quantitative reverse transcription-polymerase chain reaction. *J Mol Diagn,* 2, 84-91.

GOLDSWORTHY, S. M., STOCKTON, P. S., TREMPUS, C. S., FOLEY, J. F. & MARONPOT, R. R. (1999) Effects of fixation on RNA extraction and amplification from laser capture microdissected tissue. *Mol Carcinog,* 25, 86-91.

GROVE, D. (1999) Quantitative real-time polymerase chain reaction for the core facility using TaqMan and the Perkin-Elmer/Applied Biosystems Division 7700 Sequence Detector. *J Biomol Tech.* , 10, 11-16.

HAMATANI, K., EGUCHI, H., TAKAHASHI, K., KOYAMA, K., MUKAI, M., ITO, R., TAGA, M., YASUI, W. & NAKACHI, K. (2006) Improved RT-PCR amplification for molecular analyses with long-term preserved formalin-fixed, paraffin-embedded tissue specimens. *J Histochem Cytochem,* 54, 773-80.

HASELKORN, R. & DOTY, P. (1961) The reaction of formaldehyde with polynucleotides. *J Biol Chem,* 236, 2738-45.

HEID, C. A., STEVENS, J., LIVAK, K. J. & WILLIAMS, P. M. (1996) Real time quantitative PCR. *Genome Res,* 6, 986-94.

HIGUCHI, R., DOLLINGER, G., WALSH, P. S. & GRIFFITH, R. (1992) Simultaneous amplification and detection of specific DNA sequences. *Biotechnology (N Y),* 10, 413-7.

KARRER, E. E., LINCOLN, J. E., HOGENHOUT, S., BENNETT, A. B., BOSTOCK, R. M., MARTINEAU, B., LUCAS, W. J., GILCHRIST, D. G. & ALEXANDER, D. (1995) In situ isolation of mRNA from individual plant cells: creation of cell-specific cDNA libraries. *Proc Natl Acad Sci U S A,* 92, 3814-8.

KOCH, I., SLOTTA-HUSPENINA, J., HOLLWECK, R., ANASTASOV, N., HOFLER, H., QUINTANILLA-MARTINEZ, L. & FEND, F. (2006) Real-time quantitative RT-PCR shows variable, assay-dependent sensitivity to formalin fixation: implications for direct comparison of transcript levels in paraffin-embedded tissues. *Diagn Mol Pathol,* 15, 149-56.

KUBISTA, M., ANDRADE, J. M., BENGTSSON, M., FOROOTAN, A., JONAK, J., LIND, K., SINDELKA, R., SJOBACK, R., SJOGREEN, B., STROMBOM, L., STAHLBERG, A. & ZORIC, N. (2006) The real-time polymerase chain reaction. *Mol Aspects Med,* 27, 95-125.

KUTYAVIN, I. V., LUKHTANOV, E. A., GAMPER, H. B. & MEYER, R. B. (1997) Oligonucleotides with conjugated dihydropyrroloindole tripeptides: base composition and backbone effects on hybridization. *Nucleic Acids Res,* 25, 3718-23.

LAKOWICZ, J. (1983) Energy Transfer. *Principles of Fluorescence Spectroscopy,* 303-339.

LEHMANN, U. & KREIPE, H. (2001) Real-time PCR analysis of DNA and RNA extracted from formalin-fixed and paraffin-embedded biopsies. *Methods,* 25, 409-18.

LEWIS, F., MAUGHAN, N. J., SMITH, V., HILLAN, K. & QUIRKE, P. (2001) Unlocking the archive--gene expression in paraffin-embedded tissue. *J Pathol,* 195, 66-71.

LI, J., SMYTH, P., FLAVIN, R., CAHILL, S., DENNING, K., AHERNE, S., GUENTHER, S. M., O'LEARY J, J. & SHEILS, O. (2007) Comparison of miRNA expression patterns using total RNA extracted from matched samples of formalin-fixed paraffin-embedded (FFPE) cells and snap frozen cells. *BMC Biotechnol,* 7, 36.

MACABEO-ONG, M., GINZINGER, D. G., DEKKER, N., MCMILLAN, A., REGEZI, J. A., WONG, D. T. & JORDAN, R. C. (2002) Effect of duration of fixation on quantitative reverse transcription polymerase chain reaction analyses. *Mod Pathol,* 15, 979-87.

MASUDA, N., OHNISHI, T., KAWAMOTO, S., MONDEN, M. & OKUBO, K. (1999) Analysis of chemical modification of RNA from formalin-fixed samples and optimization of molecular biology applications for such samples. *Nucleic Acids Res,* 27, 4436-43.

MOCELLIN, S., ROSSI, C. R., PILATI, P., NITTI, D. & MARINCOLA, F. M. (2003) Quantitative real-time PCR: a powerful ally in cancer research. *Trends Mol Med,* 9, 189-95.

RAIT, V. K., ZHANG, Q., FABRIS, D., MASON, J. T. & O'LEARY, T. J. (2006) Conversions of formaldehyde-modified 2'-deoxyadenosine 5'-monophosphate in conditions modeling formalin-fixed tissue dehydration. *J Histochem Cytochem,* 54, 301-10.

SAIKI, R. K., GELFAND, D. H., STOFFEL, S., SCHARF, S. J., HIGUCHI, R., HORN, G. T., MULLIS, K. B. & ERLICH, H. A. (1988) Primer-directed enzymatic amplification of DNA with a thermostable DNA polymerase. *Science,* 239, 487-91.

SAIKI, R. K., SCHARF, S., FALOONA, F., MULLIS, K. B., HORN, G. T., ERLICH, H. A. & ARNHEIM, N. (1985) Enzymatic amplification of beta-globin genomic sequences and restriction site analysis for diagnosis of sickle cell anemia. *Science,* 230, 1350-4.

SCICCHITANO, M. S., DALMAS, D. A., BERTIAUX, M. A., ANDERSON, S. M., TURNER, L. R., THOMAS, R. A., MIRABLE, R. & BOYCE, R. W. (2006) Preliminary comparison of quantity, quality, and microarray performance of RNA extracted from formalin-fixed, paraffin-embedded, and unfixed frozen tissue samples. *J Histochem Cytochem,* 54, 1229-37.

SHEILS, O. M., O'LEARY, J. J. & SWEENEY, E. C. (2000) Assessment of ret/PTC-1 rearrangements in neoplastic thyroid tissue using TaqMan RT-PCR. *J Pathol,* 192, 32-6.

SHEILS, O. M. & SWEENEY, E. C. (1999) TSH receptor status of thyroid neoplasms--TaqMan RT-PCR analysis of archival material. *J Pathol,* 188, 87-92.

VAN DEERLIN, V. M., GILL, L. H. & NELSON, P. T. (2002) Optimizing gene expression analysis in archival brain tissue. *Neurochem Res,* 27, 993-1003.

CHAPTER FIVE

COMPARISON OF MICRORNA EXPRESSION PATTERNS USING TOTAL RNA EXTRACTED FROM MATCHED SAMPLES OF FORMALIN-FIXED PARAFFIN-EMBEDDED (FFPE) CELLS AND SNAP FROZEN CELLS

5.1 Summary

MicroRNAs are a class of small RNAs and appear to play important roles in gene regulation, while their survivability and expression level in FFPE blocks are largely unknown. This study analyzed 160 miRNAs in paired snap frozen and FFPE cells to investigate if miRNAs may be successfully detected in archival specimens. The results show that miRNA extracted from FFPE blocks was successfully amplified using Q-RT-PCR. The levels of expression of miRNA detected in total RNA extracted from FFPE were higher than that extracted from snap frozen cells when the quantity of total RNA was identical. This phenomenon is most likely explained by the fact that larger numbers of FFPE cells were required to generate equivalent quantities of total RNA than their snap frozen counterparts. We hypothesise that methylol cross-links between RNA and protein which occur during tissue processing inhibit the yield of total RNA. However, small RNA molecules appear to be less affected by this process and are recovered more easily in the extraction process. In general miRNAs demonstrated reliable expression levels in FFPE compared with snap frozen paired samples, suggesting these molecules might prove to be robust targets amenable to detection in archival material in the molecular pathology setting.

5.2 Introduction

MicroRNAs (miRNAs) are small, non-coding, single stranded RNAs of approximately 20 to 22 nucleotides in length, which down regulate gene expression. microRNAs were first discovered in *C-elegans* (Lee et al., 1993) and then found in many species. They are encoded by genes but not translated into protein, instead they are processed from

primary transcripts to short stemloop structure and finally to functional mature microRNA. microRNAs molecules are partially complementary to one or more messenger RNA molecules and play important roles in the regulation of target genes by binding to these messenger transcripts to repress their translation or regulate degradation (Griffiths-Jones et al., 2006). This regulation appears to be involved in many fundamental cellular processes, including development, differentiation, proliferation, apoptosis, stress response, fat metabolism and insulin secretion (Wijnhoven et al., 2007).

5.2.1 microRNA discovery

microRNAs were first described in the early 1990s by Lee and colleagues while studying developmental timing in the nematode *Caenohabditis elegans* (Feinbaum and Ambros, 1999, Lee et al., 1993). They found that lin-4 gene does not code for a protein but instead produces a pair of small non-coding RNAs, which negatively regulated the translation of lin-14 by directly base pairing to complementary sites within its 3' untranslated region (3' UTR) (Wightman et al., 1993). Several years later, let-7 was identified as an additional regulator of developmental timing in *C-elegans* (Reinhart et al., 2000), together with lin-4, function for a cascade of gene expression that regulates developmental events by post-transcriptional gene silencing. The importance of this class of tiny regulatory RNAs, called microRNAs or miRNAs, became apparent in 2001 when many of them were identified and cloned from several organisms including human (Lagos-Quintana et al., 2001, Lau et al., 2001, Lee and Ambros, 2001, Bartel, 2004).

The total number of different miRNA sequences in human genome might approach 1000 based on the computational algorithms (Berezikov et al., 2005). The most recent release, at the time of writing, of the miRBase Registry (http://microrna.sanger.ac.uk/) (12.0, released on September 2008) lists 8619 entries representing hairpin precursor miRNAs, expressing 8273 mature miRNA products identified in primates, rodents, birds, fish, worms, flies, plants and viruses, and 701 human miRNAs (Griffiths-Jones et al., 2008).

5.2.2 microRNA classification and location

miRNAs can be grouped into families on the basis of sequence homology which is found primarily at the 5' end of the mature miRNA but whether members of the same miRNA family control similar biological events remains to be seen. Mammalian microRNA genes have been distinguished by using the prefix hsa-miR followed by a unique identifying number (Ambros et al., 2003). The prefix Lin and Let refer to microRNAs originally identified in *C. elegans*.

In humans, miRNA genes are located in all chromosomes, with the exception of the Y chromosome (Kim and Nam, 2006). About 50% of identified miRNAs are found in clusters and transcribed as polycistronic primary transcripts. The microRNAs in a given cluster are often related to each other. The majority of mammalian microRNA genes are located in intergenic regions, introns of protein-coding genes or introns of non-coding RNA genes displaying an anti-sense orientation with respect to the protein-coding gene (Negrini et al., 2007). Less often they reside in exons of non-coding

transcription units, for example miR-155 locates in the third exon of non-coding gene, *BIC* (Kim and Nam, 2006).

5.2.3 microRNA biogenesis

Many reports have described the process of miRNA biogenesis and mode of action (Figure 5.1). In the nucleus, miRNAs are generally transcribed by RNA polymerase II to form large RNA precursors called pri-miRNAs (Esquela-Kerscher and Slack, 2006, Lee et al., 2003) that contain a 5' CAP structure and a poly (A) tail at their 3' end. Pri-miRNAs are cleaved by Drosha/DGCR8 complex to produce stem loop structured precursor molecules of 70 nucleotides in length called pre-miRNAs (Han et al., 2006). Drosha is a RNase III endonuclease, which cleaves both strands at sites near the base of the primary stem loop to produce an end with 5' phosphate and about 2nt 3' overhang (Bartel, 2004), and requires its cofactor, DGCR8/Pasha, the double-stranded RNA-binding protein to function. DGCR8 is believed to assist Drosha to recognize the substrate because it contains two double-stranded RNA-binding domains (Kim and Nam, 2006, Han et al., 2006).

The pre-miRNAs are then exported into the cytoplasm by the RAN GTP-dependent transporter Exportin-5 and undergo an additional processing step. Pre-miRNAs are processed by Dicer into miRNA:miRNA* duplex. Dicer is a cytoplasmic RNase III endonuclease, which first recognizes the double-stranded portion of the pre-miRNA, and then cleaves both strands of the duplex at about two helical turns away from the base of the stem loop to generate the other end with same character, 5' phosphate and about 2nt 3' overhang (Bartel, 2004). In miRNA:miRNA* duplex, one strand remains

stably and is incorporated into a large protein complex known as the RNA-induced silencing complex or RISC (Tang, 2005). This strand is called the mature miRNA which negatively regulates its targets, the opposite strand known as passenger strand or miRNA* is disposed of during RISC assembly. The mature miRNA guides the RISC to target mRNAs that, depending on the level of complementarity between the miRNA and target sequence, are either translationally repressed or directly cleavaged (Tang, 2005).

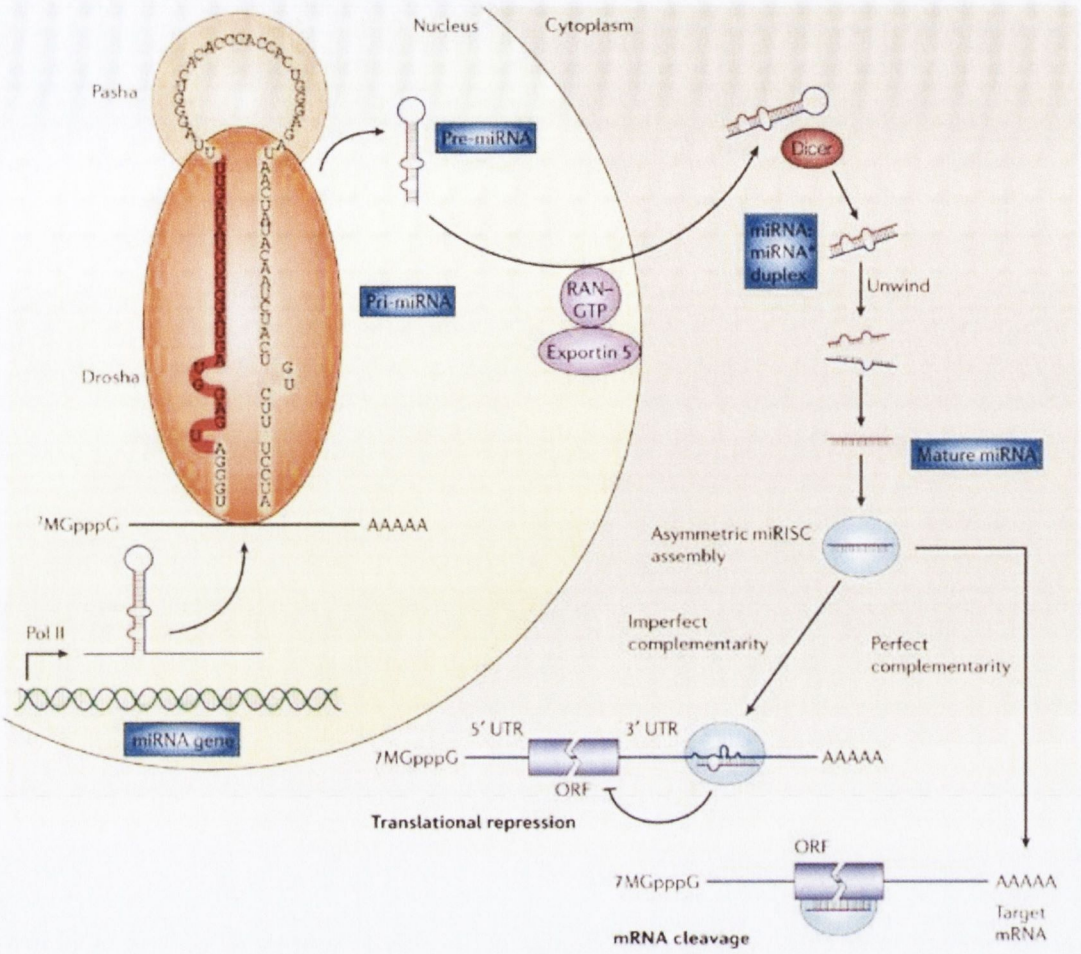

Figure 5.1 Overview of microRNA biogenesis

miRNAs are transcribed by RNA polymerase II in the nucleus as pri-miRNAs that contain a 5' CAP and a 3' poly (A) tail. Pri-miRNAs are cleaved by Drosha/DGCR8 complex to produce stem loop structured pre-miRNAs. The pre-miRNAs are then exported in to the cytoplasm by the transporter Exportin-5 and cleaved by Dicer into miRNA:miRNA* duplex. One strand of this duplex remains stably incorporated into RISC as mature miRNA. The mature miRNA guides the RISC to target mRNAs that, depending on the level of complementarity between the miRNA and target sequence, are either translationally repressed or directly cleavaged (Esquela-Kerscher and Slack, 2006).

5.2.4 microRNA biological function

It is believed that miRNAs are responsible for fine tuning gene expression and regulation of approximately 30% of the human genome (Hwang and Mendell, 2006). Comprising 1-4% of all expressed human genes, this makes miRNAs one of the largest classes of gene regulators. In recent years, studies on the regulatory roles of miRNAs in several organisms suggest that they are involved in a variety of cellular processes, such as in processes of development and metabolism (Wiemer, 2007, Negrini et al., 2007), including cell proliferation, cell differentiation, stress response, immunity, fat metabolism, apoptosis, insulin secretion, stem cell maintenance, neuronal patterning, and transcriptional regulation (Wiemer, 2007, Cowland et al., 2007). Disruptions of many of these pathways are also hall marks of cancer.

To date, many microRNAs have been suggested to play key roles as control switches in development and cell differentiation (Negrini et al., 2007, Esquela-Kerscher and Slack, 2006). For example, miRNAs that are encoded by lin-4 and let-7 control the timing of cell differentiation and proliferation in *C. elegans*. The mammalian homologues of lin-4 and let-7 have been shown to control cell proliferation in human cell lines. Other characterised miRNAs have essential functions during development and direct the proper differentiation of cells into various tissues. Examples include mir-273 and the miRNA encoded by lys-6 which are involved in patterning the *C. elegans* nervous system, mir-430 in *Danio rerio* brain development; mir-181 in differentiation of mammalian haematopoietic cells; mir-375 in mammalian pancreatic islet-cell development and the regulation of insulin secretion; mir-143 in mammalian adipocyte

differentiation; mir-196 in mammalian limb patterning and the mir-1 genes during mammalian heart development (Esquela-Kerscher and Slack, 2006).

Following the initial report demonstrating changes it has become increasingly evident that deregulation of miRNAs is involved in many different types of cancer as summarized in Table 5.1. microRNAs can function as tumor suppressors, in which the reduction or deletion of a microRNA leads to tumor formation, and oncogenes, in which the amplification or overexpression of a microRNA would also result in tumor formation (Esquela-Kerscher and Slack, 2006). Expression of some miRNAs, such as let-7 (Takamizawa et al., 2004), the mir-15a/mir-16-1 cluster (Calin et al., 2002, Bottoni et al., 2005) and neighboring mir-143/145 (Slaby et al., 2007, Michael et al., 2003), have been reported to be reduced in the malignancies, suggesting their potential tumor suppressor activities. In contrast, some other miRNAs, such as the mir-21 (Si et al., 2007), mir-17-92 cluster and mir-155bic, are known to be overexpressed, suggesting their oncogenic potentials. In addition, some miRNAs with altered expression levels appear to be associated with certain genetic alterations, such as deletion, amplification and mutation (Osada and Takahashi, 2007).

Table 5.1 Oncogenic and tumor suppressor miRNAs and their targets

NA= not analyzed (targets only predicted in databases not shown). microRNAs have been described in recent reviews (Cowland et al., 2007, Osada and Takahashi, 2007, Wiemer, 2007, Cho, 2007) and their chromosomal location are based on database http://microrna.sanger.ac.uk/sequences/search.shtml.

miRNA no.	Chromosomal localization	Target	Type of cancer
Let-7 family	Multiple loci	Ras, PRDM1	Lung, Colon
9	1q22	PRDM1	Hodgkin disease
10b	2q31.1	NA	Breast
15a	13q14.3	BCL-2	B-cell chronic lymphocytic leukemia, Pituitary adenomas
16–1	13q14.3	BCL-2	B-cell chronic lymphocytic leukaemia, Pituitary adenomas
17–92 cluster	13q31.3	Tsp1, CTGF	Lymphoma, Colon, Chronic myeloid leukemia
17–5p	13q31.3	AIB1, E2F1	Breast
20a	13q31.3	E2F1	Breast
21	17q22	BCL-2	Glioblastoma, Breast, Cholangio-carcinoma, Pancreatic
29b	1q32.2/7q32.3	MCL-1, TCL-1	Acute myeloid leukaemia, Aggressive CLL, 11qdel
31	9p21.3	NA	Colorectal
34a	1p36.23	E2F3	Pancreas
96	7q32.2	NA	Colorectal
98	Xp11.22	HMGA2	Head and neck
107	10q23.31	NA	Leukaemia, Pancreas
106a	Xq26.2	RB-1	Colon, Pancreas, Prostate

124a	8p23.1	CDK6	Colon, Breast, Lung, Leukemia, Lymphoma
125b	11q24.1/21q21.1	NA	Breast cancer
127	14q32.31	BCL-6	Bladder, Burkitt lymphoma
133b	6p12.2	NA	Colorectal
135b	1q32.1	NA	Colorectal
141	12p13.31	CLOCK	Cholangiocarcinoma
142	17	NA	Aggressive B-cell lymphoma
143	5q32–33	NA	Colon
145	5q32–33	NA	Colon, breast
146b	10q24.32	Kit	Thyroid carcinoma
155-bic	21q21	NA	Hodgkin, Diffuse large B-cell lymphoma, Primary mediastinal Lymphoma, Breast
181b	1q31.3	Tcl-1	Aggressive CLL, 11qdel
183	7q32.2	NA	Colorectal
184	15q25.1	NA	Neuroblastoma
191	3p21.31	NA	Colon, lung, pancreas, prostate, stomach
200b	1p36.33	PTPN12	Cholangio-carcinoma
221	Xp11.3	Kit	Glioblastoma, Leukemia, Thyroid
222	Xp11.3	Kit	Leukemia, Thyroid
223	Xq12	NFIA	Leukaemia
372	19q13.41	LATS2	Testicular
373	19q13.41	LATS2	Testicular

5.2.5 Techniques and strategies of microRNA study

All known miRNAs are registered in a public web-based registry, the 'miRBase' database which provides up-to-date information on all identified miRNAs (Griffiths-Jones et al., 2008). Computationally, microRNA genes can be discovered by bioinformatics approaches searching for evolutionary conserved stem-loop structures in the genome (Berezikov et al., 2006) or degree of hybridization between the microRNA and messenger RNA molecules (Watanabe et al., 2007). Experimentally, microRNAs are discovered by cloning all small RNAs from a certain tissue type or developmental stage and subsequent sequencing to identify the subgroup of microRNAs (Sassen et al., 2008). However, it has been significantly difficult to validate all the predicted microRNAs in actual tissues.

Technically, microRNAs can not be analyzed using most of the conventional messenger RNA detection methods due to their small sizes, the relative low expression levels and low comparative power of the current methods used for the large RNA detection. Many technical methods have been modified and developed specifically to detect microRNA expression, most notably LNA-probe northern blot analysis (Valoczi et al., 2004), membrane arrays using radioactive detection methods, oligonucleotide microarray for microRNA technology (Liu et al., 2008), bead based flow cytometric analysis, a modified invader assay and a new single molecule technique. Each of these methods has distinct advantages and disadvantages. Real-time PCR however, has unparalleled sensitivity and specificity, which is the preferred method in recent publications (Schmittgen et al., 2008). The TaqMan® MicroRNA assays are looped-primer RT-PCR (Chen et al., 2005), a new real time quantification method to

accurately detect mature miRNAs. The stem-loop structure, which is specific to the 3' end of the mature miRNA, creates steric hindrance to prevent priming of the precursor miRNA. The stem-loop also extends the very short mature miRNA molecule and adds a universal 3' priming site for real-time PCR.

Strategically, although the total number of different miRNA sequences predicted in humans might approach a thousand, only a few hundreds of them have been verified on fresh or snap-frozen samples to date. To discover the full regulatory impact of miRNA species and to understand individual biological functions within disease settings, larger scale analysis needs to be performed in a robust and reliable manner. Formalin–Fixed, Paraffin–Embedded (FFPE) tissue samples are the most readily available archival material and generally may be retrieved with documented clinico-pathological histories. Thus FFPE tissues represent an invaluable source for the study of microRNA in human disease. Our previous study in Chapter 4 show that messenger RNA molecules can be successfully detected using extracts of FFPE materials, and amplicons with small size generate consistent detection results. Therefore, microRNAs are likely to be detectable in FFPE extracts. It is potentially meaningful to discover microRNA survivability and expression level in FFPE blocks compared with fresh samples.

5.2.6 Aims

This study aimed to examine the reliability of microRNA detection in FFPE materials. In this chapter, we compared 160 microRNA assays in paired RNA extracts from snap-frozen and FFPE samples using a cell line model. We first extracted total RNA using the optimal protocols of Ambion RecoverAll™ Total Nucleic Acid Isolation Kit for FFPE cell pellets and Ambion *mir*Vana™ miRNA Isolation Kit for snap-frozen cell pellets. We further performed 160 microRNA assays using TaqMan® Early Access Human miRNA Panel with the identical quantity of total RNA extracts in each reaction. Statistical analysis was finally carried out using software MINITAB® 14 on C_Ts and ΔC_Ts.

5.3 Materials and Methods

5.3.1 Cell culture and formalin fixation

Nthy-ori 3-1 (ECACC, Wiltshire, UK) is a normal thyroid follicular epithelial cell line derived from adult thyroid tissue that has been transfected with a plasmid encoding for the SV40 large T gene (Cahill et al., 2006). This cell line was grown to confluence in a humidified atmosphere containing 5% CO_2 at 37°C as described in Chapter 2.2. Approximately $1x10^5$ suspended cells were aliquot and were pelleted (a) snap frozen and (b) formalin fixed and paraffin embedded into a cell block as described in Chapter 2.3.1.

5.3.2 RNA extraction

RNA was extracted from fresh cells using *mir*Vana™ miRNA Isolation kit (Ambion Ltd., Cambridgeshire, UK) and from FFPE cells using RecoverAll™ Total Nucleic Acid Isolation kit (Ambion Ltd., Cambridgeshire, UK) following the manufacturer's protocol as described in Chapter 2.5.8 and 2.5.2. For snap-frozen extraction, one extraction was performed using approximately $4x10^5$ cells. For FFPE extraction, 4 extractions were performed in parallel with one pellet ($1x10^6$ cells) in each extraction. The entire pellet was dissected from each block and was finely minced using a scalpel. These preparations were then deparaffinized, followed by proteinase K digestion for 3 hours at 50°C, on column DNase digestion and elution as described in the protocol. At that point all 4 FFPE extracts were combined into one tube designated the FFPE sample. The concentrations of these two samples were measured using a NanoDrop®

ND-1000 Spectrophotometer (Wilmington, USA) as described in Chapter 2.6 and extracts were diluted to 10ng/µl. RNA quality was measured using the RNA 6000 Pico LabChip® Kit on an Agilent 2100 Bioanalyser (Agilent technologies, Waldbronn, Germany) as described in Chapter 2.7.

5.3.3 TaqMan® miRNA assays

Applied Biosystems TaqMan® microRNA (miRNA) assays (designed for mature miRNA quantification using Applied Biosystems real time PCR instruments) were utilised in this study as described in Chapter 2.8.5. The human panel early access kit (P/N: 4365381, Applied Biosystems) used in this study contained 160 individual assays and comprised two steps: Reverse Transcription (RT) and real time PCR. The stem-loop RT primer specifically hybridizes to a miRNA molecule and is reverse transcribed with a MultiScribe reverse transcriptase (Chen et al., 2005). The RT products are then quantified using real-time TaqMan® PCR.

Applied Biosystems High-Capacity cDNA Archive Kit (P/N: 4322171, Applied Biosystems, CA, USA) was used following manufacturer's protocol for reverse transcription. Each RT reaction contained 50ng of extracted total RNA, 50nM stem-looped RT primer, 1x RT buffer, 0.25mM each of dNTPs, 3.33U/µl Multiscribe reverse transcriptase and 0.25U/µl RNase Inhibitor. The 15µl reactions were incubated in an Applied Biosystems Thermocycler in a 96-well plate for 30 minutes at 16°C, 30 minutes at 42°C, 5 minutes at 85°C and then held at 4°C.

For the Real-time PCR step, amplification was carried out using sequence specific primers on the Applied Biosystems 7900HT Real-Time PCR system. The 20μl reaction included 1.33μl RT product, 1x TaqMan® Universal PCR Master Mix with no UNG (P/N: 4324018, Applied Biosystems) and 1x TaqMan® MicroRNA assays. The reactions were incubated in a 96-well optical plate at 95°C for 10 minutes, following by 40 cycles of 95°C for 15 seconds and 60°C for 1 minute. The real-time PCRs for each miRNA were run in triplicate. hsa-let-7a was included as an endogenous control and cel-lin-4 was incorporated as a negative control.

5.3.4 Statistical analysis

Replicates were omitted if C_T standard deviation was greater than 1.5. All 160 miRNAs were detectable with the exception of c-lin-4 in FFPE and c-lin-4, mir-104, mir-122a, mir-144, mir-302b and mir-325 in snap frozen sample. The data was collected using Microsoft Excel and was statistical analyzed using MINITAB® 14 on ΔC_Ts with the formulas below:

$\Delta C_T = C_T\_Mean(FFPE) - C_T\_Mean(Snap\ frozen)$

$\Delta\Delta C_T = \Delta C_T - \Delta C_T\_Mean$

Expression level = $2^{-\Delta\Delta CT}$

5.4 Results

5.4.1 RNA extraction

To achieve 50ng of total RNA for each RT reaction, 10,000ng of total RNA (for 200 assays) was extracted from approximately 2x 10^6 of FFPE cells and from approximately 1.7x 10^5 snap frozen cells. Analysis using an Agilent 2100 Bioanalyser showed that the RNA Integrity Number (RIN Number) was 9.1 for the snap frozen cell preparations and 6.4 for the corresponding FFPE preparation.

5.4.2 miRNA expression

There was a good correlation of miRNA expression pattern between FFPE and snap frozen cells, with $R^2 > 0.95$ (Figure 5.2). The mean of ΔC_Ts was -1.04107 (Figure 5.3). The median of ΔC_Ts was -1.152, (126 below 0 and 28 above 0) with $P < 0.0001$. The sign test of median showed that miRNA exhibited approximately two fold higher expression with the total RNA extracted from the FFPE cells than that extracted from the snap frozen cells.

65.58% of $\Delta\Delta C_T$s (101 out of 154 determined assays), were between +1 and -1 (Figure 5.3). Furthermore the abundance of some individual miRNAs changed in FFPE cells with a total of 23 miRNAs displaying increased expression and 30 miRNAs decreased expression (Table 5.2 and Figure 5.4).

Table 5.2 Sorted expression levels of 160 miRNA using $\Delta\Delta C_T$s

65.58% of $\Delta\Delta C_T$s (101 out of 154 determined assays), were between +1 and -1.

Decreased expression	Increased expression	$\Delta\Delta C_T$s between +/-1				Undetermined
mir-30b	mir-302b*	mir-9	mir-133b	mir-200a	mir-370	c-lin-4
mir-130a	mir-302a	mir-10a	mir-134	mir-200b	mir-371	mir-104
mir-218	let-7b	mir-15a	mir-137	mir-200c	mir-372	mir-122a
mir-30e	mir-184	mir-17-3p	mir-138	mir-203	mir-373	mir-144
mir-34a	mir-183	mir-17-5p	mir-140	mir-204	let-7d	mir-302b
mir-135a	mir-211	mir-23a	mir-142-5p	mir-210	let-7e	mir-325
mir-20	mir-128b	mir-23b	mir-145	mir-213	mir-2	
mir-15b	mir-189	mir-25	mir-147	mir-214	let-7g	
mir-135b	mir-128a	mir-26b	mir-148a	mir-215	let-7i	
mir-31	mir-154	mir-27a	mir-149	mir-216	let-7a	
mir-9*	mir-198	mir-27b	mir-150	mir-219	mir-16	
mir-338	mir-139	mir-28	mir-151	mir-221		
mir-190	mir-373*	mir-30a-3p	mir-152	mir-222		
mir-133a	mir-100	mir-30c	mir-154*	mir-223		
mir-29a	mir-323	mir-30d	mir-155	mir-224		
mir-142-3p	mir-125b	mir-34b	mir-181a	mir-296		
mir-141	mir-105	mir-34c	mir-181b	mir-299		
mir-335	mir-182*	mir-92	mir-181c	mir-302c		
mir-29c	mir-129	mir-96	mir-182	mir-302c*		
mir-26a	mir-159a	mir-98	mir-185	mir-320		
mir-220	mir-199a	mir-99a	mir-186	mir-324-5p		
mir-374	mir-367	mir-103	mir-187	mir-326		
mir-95	mir-107	mir-106a	mir-191	mir-328		
mir-21		mir-124a	mir-193	mir-330		
mir-302d		mir-124b	mir-194	mir-331		
mir-29b		mir-125a	mir-195	mir-337		
mir-301		mir-126	mir-197	mir-339		
mir-205		mir-127	mir-199a*	mir-340		
mir-19a		mir-130b	mir-199b	mir-342		
mir-146		mir-132	mir-199-s	mir-368		

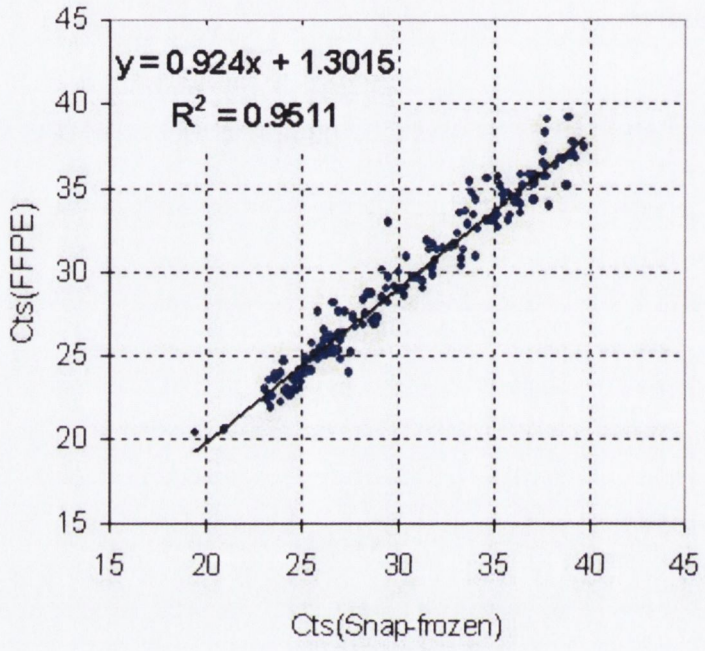

Figure 5.2 Comparison of C_T values from paired FFPE and Snap-frozen cell lines

Identical amount of total RNA was employed in each assay. Total 154 miRNA assays were detected in both samples. R^2 was over 95% between two cell lines indicating a good correlation between two samples.

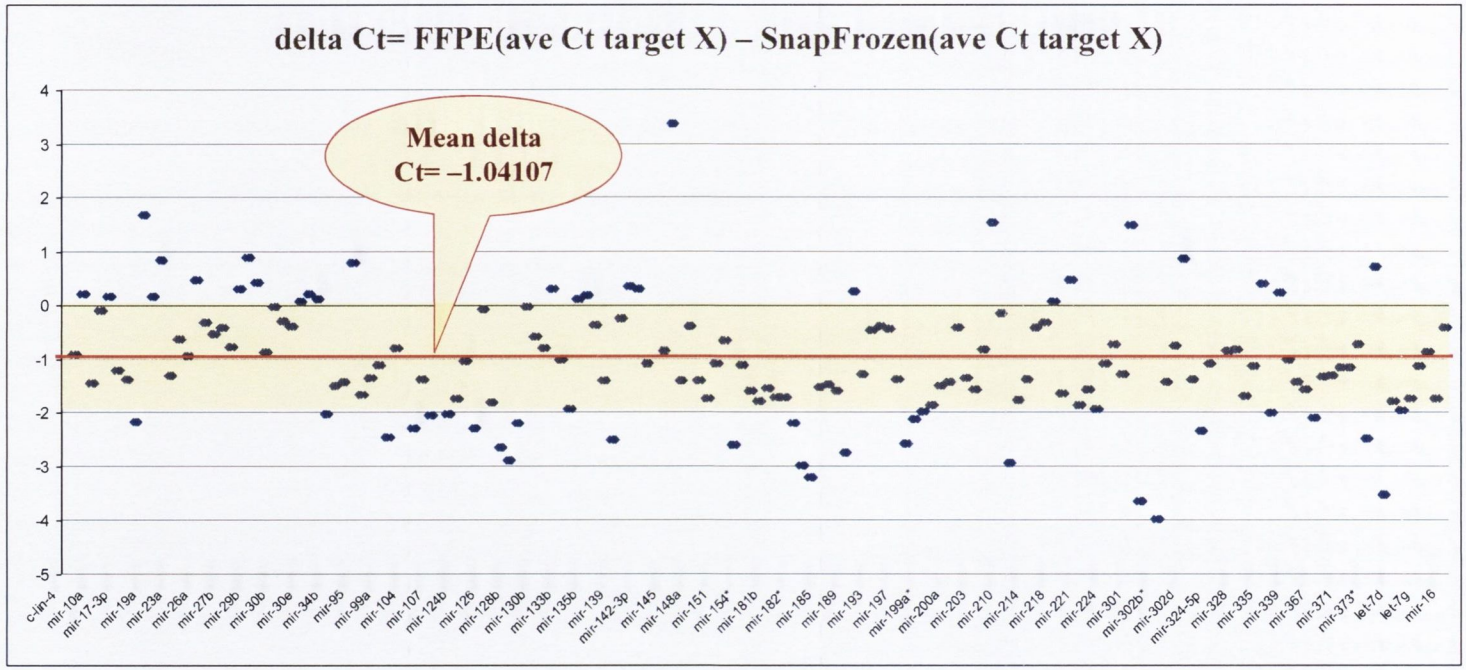

Figure 5.3 ΔC_T analysis of 154 miRNA assays from paired FFPE and Snap-frozen cell lines

The mean of ΔC_Ts was -1.04107 indicating that miRNA exhibited approximately two fold higher expression with the total RNA extracted from the FFPE cells than that extracted from the snap frozen cells. 65.58% of ΔC_Ts, 101 out of 154 determined assays, were in between ΔC_Ts_mean +1 and -1.

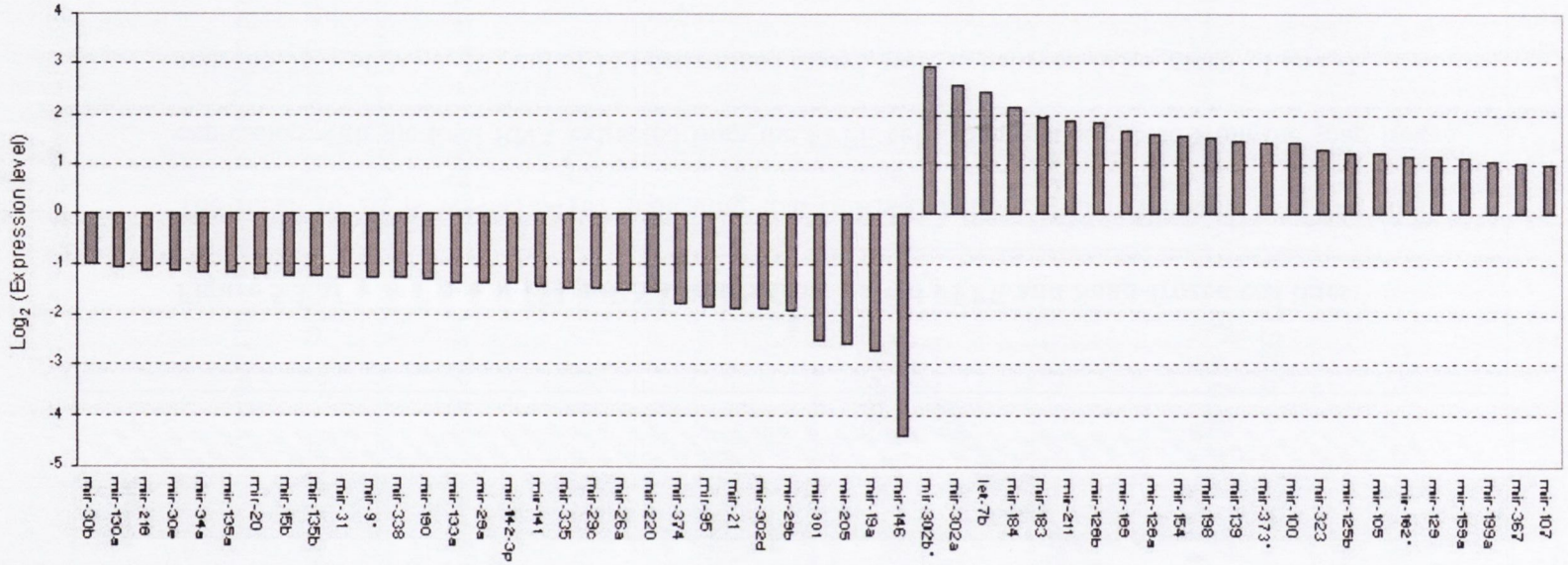

Figure 5.4 Sorted Log_2(Expression level) of assays in outside of ΔC_Ts_mean +1 and -1

The majority of the assays are close to ΔC_Ts_mean +1 and -1. 30 miRNAs show decreased expression and 23 show increased expression in FFPE compared to that in snap-frozen. The most significantly altered expression was seen in mir-146 with decreased expression and mir-302b* with increased expression.

5.5 Discussion

Since their discovery, miRNA analysis has generally been performed on snap-frozen or fresh samples, using variable techniques including microarray, northern blot analysis and PCR (Wijnhoven et al., 2007). FFPE tissues, as a readily available source, could be invaluable in performing miRNA expression analysis if their expression were maintained following processing. In this study we compared miRNA profiling performed on fresh samples and FFPE using stem-loop RT-PCR quantification techniques in a cell line model. We found that miRNA profiling could be performed on routinely fixed FFPE blocks.

5.5.1 miRNA abundance in FFPE

Some laboratories have examined mRNA gene expression profiles using real-time RT-PCR in paired snap-frozen and FFPE tissue samples (Godfrey et al., 2000, Specht et al., 2001, Abrahamsen et al., 2003, Koch et al., 2006). The general consensus is that mRNA detection from archival material is limited due to the labile nature of mRNA and the deleterious effects of enzymatic fragmentation during long periods of storage and RNA modification induced by formalin fixation. Subsequently, it has been suggested that small amplicons (Antonov et al., 2005), shorter than ~130 (Godfrey et al., 2000, Abrahamsen et al., 2003) nucleotides, could have utility as robust markers in gene expression studies using FFPE tissues. Indeed, our own experiments confirmed this phenomenon using mRNA targets over a range of amplicon sizes in this cell line model (Chapter 4). For example, FFPE extracts produced C_Ts 4 to 10 cycles higher than their snap frozen counterparts depending on the amplicon sizes used (62 to 164bp)

(Chapter 4.4, Figure 4.7). C_Ts between FFPE and snap frozen were closer for small amplicons than that for large amplicons. For example analysis of GAPDH using a target amplicon of 67bp displayed a mean difference of 4.28 cycles, whereas an assay designed for the same gene (GAPDH) using a target amplicon size of 122bp displayed a mean difference of 6.51 C_Ts between FFPE and snap frozen material (Chapter 4.4.4).

miRNAs have the advantage of small size, being only approximately 20 to 22 nucleotides long. In addition, they are protein protected by the RISC complex. Consequently they may not be as susceptible to RNA degradation as mRNA in FFPE tissues. Our results showed that the amount of miRNA in total RNA extracted from FFPE was greater than that extracted from snap frozen cells when the input amounts of total RNA were identical. The average quantity of miRNAs derived from total RNA extracted from FFPE was double (one C_T lower) that in snap frozen cells which is most likely a consequence of methylol cross-links between RNA and protein introduced during processing.

We extracted identical quantities of total RNA (10,000ng) for analysis. In practical terms this required input of almost ten times the number of FFPE cells (2x 10^6 cells) compared to snap frozen (1.7x 10^5 cells). This difference in extracted yields was consistent with previous reports. This suggests the amount of RNA that can be extracted from FFPE tissue represents only a fraction of that which is obtainable from fresh-frozen tissue (Abrahamsen et al., 2003). The residual cross-links in every RNA molecule that have not been removed by proteinase K digestion prevent this RNA being extracted (Figure 5.5). The longer an RNA molecule is, the greater the likelihood that a cross-link still exists after the proteinase K digestion procedure. Therefore, small

RNA molecules are more amenable to extraction than larger mRNA molecules resulting to a higher expression of miRNA in FFPE compared to that in snap frozen.

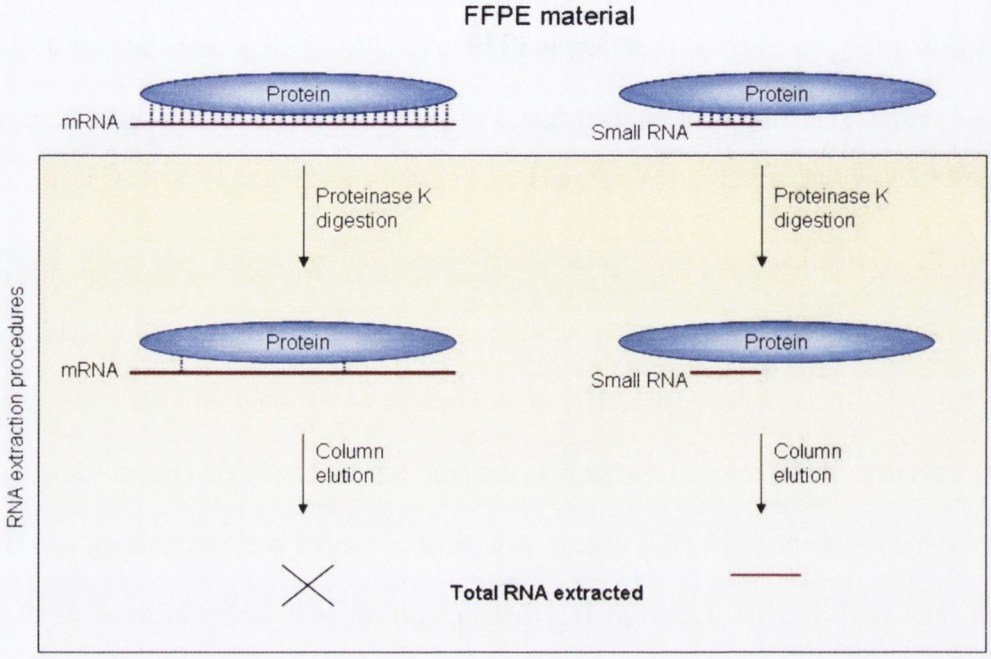

Figure 5.5 A schematic representation of the impact of cross-links on RNA extraction

In FFPE materials, RNA has been chemically modified by methylol groups to form cross-links with protein. Digestion with proteinase K (Masuda et al., 1999) followed by column elution is the common method used to extract RNA from FFPE. However, a fraction of RNA remains impervious to extraction because of un-removed cross-links. The longer an RNA molecule is, the more likely cross-links will remain after the digestion procedure. Therefore, it is easier to extract small RNA molecules than larger ones from archival material.

5.5.2 Reliability of miRNA in FFPE

It is plausible to anticipate that miRNA species are less susceptible to RNA degradation associated with tissue processing than occurs with mRNA, and this formed the hypothesis to be tested in this study. We found a good correlation of miRNA expression levels between FFPE and snap frozen cells with $R^2 > 0.95$. Our data is in agreement with a recent study (Xi et al., 2007) and demonstrated that, for majority of miRNAs, the expression in FFPE is comparable with snap frozen cells. 65.58% of miRNAs displayed $\Delta\Delta C_T$s in a range between +/-1 indicating that these normalized profiles were essentially identical between the two samples.

However, there was some outlying data where there was poor correlation between expression profiles for the paired snap-frozen and FFPE samples. The most significant of these was mir-146 with decreased expression and mir-302b* with increased expression. These changes could possibly occur during formalin fixation procedure or could also be caused by post fixation handling. mir-146 overexpression has been found in PTC tissues (He et al., 2005) and was also suggested to be involved in cellular stress (Marsit et al., 2006) and innate immune responses (Taganov et al., 2006). Interestingly, we found it was decreased in FFPE extracted Nthy-ori cells. For those overexpressed miRNAs, it is possible that precursors of miRNA might have been cleaved by RNase to produce positive signals because FFPE blocks are often stored at room temperature in the absence of an RNase free environment. Alternatively, increased cellular stress following harvesting and during the fixation process may have contributed to the altered expression patterns in specific miRNAs. In these cases, the FFPE material

could still be used to compare relative miRNA expression patterns if a series of known blocks were fixed and handled simultaneously or in the same manner.

5.6 Conclusion

We analyzed 160 miRNAs expression levels in freshly fixed FFPE by comparing to snap frozen in a cell line model. Although the RNA extracted from FFPE blocks is often compromised, we demonstrated the robustness of miRNA profiles in FFPE material which could provide a source of study material for large scale or retrospective studies. This study has confirmed the proof of principle that miRNA species may be successfully extracted and analysed from archival sources. Further work may be required to determine precise effects of FFPE on miRNA expression profiles across different tissue samples.

5.7 References

ABRAHAMSEN, H. N., STEINICHE, T., NEXO, E., HAMILTON-DUTOIT, S. J. & SORENSEN, B. S. (2003) Towards quantitative mRNA analysis in paraffin-embedded tissues using real-time reverse transcriptase-polymerase chain reaction: a methodological study on lymph nodes from melanoma patients. *J Mol Diagn,* 5, 34-41.

AMBROS, V., BARTEL, B., BARTEL, D. P., BURGE, C. B., CARRINGTON, J. C., CHEN, X., DREYFUSS, G., EDDY, S. R., GRIFFITHS-JONES, S., MARSHALL, M., MATZKE, M., RUVKUN, G. & TUSCHL, T. (2003) A uniform system for microRNA annotation. *Rna,* 9, 277-9.

ANTONOV, J., GOLDSTEIN, D. R., OBERLI, A., BALTZER, A., PIROTTA, M., FLEISCHMANN, A., ALTERMATT, H. J. & JAGGI, R. (2005) Reliable gene expression measurements from degraded RNA by quantitative real-time PCR depend on short amplicons and a proper normalization. *Lab Invest,* 85, 1040-50.

BARTEL, D. P. (2004) MicroRNAs: genomics, biogenesis, mechanism, and function. *Cell,* 116, 281-97.

BEREZIKOV, E., CUPPEN, E. & PLASTERK, R. H. (2006) Approaches to microRNA discovery. *Nat Genet,* 38 Suppl, S2-7.

BEREZIKOV, E., GURYEV, V., VAN DE BELT, J., WIENHOLDS, E., PLASTERK, R. H. & CUPPEN, E. (2005) Phylogenetic shadowing and computational identification of human microRNA genes. *Cell,* 120, 21-4.

BOTTONI, A., PICCIN, D., TAGLIATI, F., LUCHIN, A., ZATELLI, M. C. & DEGLI UBERTI, E. C. (2005) miR-15a and miR-16-1 down-regulation in pituitary adenomas. *J Cell Physiol,* 204, 280-5.

CAHILL, S., SMYTH, P., FINN, S. P., DENNING, K., FLAVIN, R., O'REGAN, E. M., LI, J., POTRATZ, A., GUENTHER, S. M., HENFREY, R., O'LEARY, J. J. & SHEILS, O. (2006) Effect of ret/PTC 1 rearrangement on transcription and post-transcriptional regulation in a papillary thyroid carcinoma model. *Mol Cancer,* 5, 70.

CALIN, G. A., DUMITRU, C. D., SHIMIZU, M., BICHI, R., ZUPO, S., NOCH, E., ALDLER, H., RATTAN, S., KEATING, M., RAI, K., RASSENTI, L., KIPPS, T., NEGRINI, M., BULLRICH, F. & CROCE, C. M. (2002) Frequent deletions and down-regulation of micro- RNA genes miR15 and miR16 at 13q14 in chronic lymphocytic leukemia. *Proc Natl Acad Sci U S A,* 99, 15524-9.

CHEN, C., RIDZON, D., BROOMER, A., ZHOU, Z., LEE, D., NGUYEN, J., BARBISIN, M., XU, N., MAHUVAKAR, V., ANDERSEN, M., LAO, K., LIVAK, K. & GUEGLER, K. (2005) Real-time quantification of microRNAs by stem-loop RT-PCR. *Nucleic Acids Res,* 33, e179.

CHO, W. C. (2007) OncomiRs: the discovery and progress of microRNAs in cancers. *Mol Cancer,* 6, 60.

COWLAND, J. B., HOTHER, C. & GRONBAEK, K. (2007) MicroRNAs and cancer. *Apmis,* 115, 1090-106.

ESQUELA-KERSCHER, A. & SLACK, F. J. (2006) Oncomirs - microRNAs with a role in cancer. *Nat Rev Cancer,* 6, 259-69.

FEINBAUM, R. & AMBROS, V. (1999) The timing of lin-4 RNA accumulation controls the timing of postembryonic developmental events in Caenorhabditis elegans. *Dev Biol,* 210, 87-95.

GODFREY, T. E., KIM, S. H., CHAVIRA, M., RUFF, D. W., WARREN, R. S., GRAY, J. W. & JENSEN, R. H. (2000) Quantitative mRNA expression analysis from formalin-fixed, paraffin-embedded tissues using 5' nuclease quantitative reverse transcription-polymerase chain reaction. *J Mol Diagn,* 2, 84-91.

GRIFFITHS-JONES, S., GROCOCK, R. J., VAN DONGEN, S., BATEMAN, A. & ENRIGHT, A. J. (2006) miRBase: microRNA sequences, targets and gene nomenclature. *Nucleic Acids Res,* 34, D140-4.

GRIFFITHS-JONES, S., SAINI, H. K., VAN DONGEN, S. & ENRIGHT, A. J. (2008) miRBase: tools for microRNA genomics. *Nucleic Acids Res,* 36, D154-8.

HAN, J., LEE, Y., YEOM, K. H., NAM, J. W., HEO, I., RHEE, J. K., SOHN, S. Y., CHO, Y., ZHANG, B. T. & KIM, V. N. (2006) Molecular basis for the recognition of primary microRNAs by the Drosha-DGCR8 complex. *Cell,* 125, 887-901.

HE, H., JAZDZEWSKI, K., LI, W., LIYANARACHCHI, S., NAGY, R., VOLINIA, S., CALIN, G. A., LIU, C. G., FRANSSILA, K., SUSTER, S., KLOOS, R. T., CROCE, C. M. & DE LA CHAPELLE, A. (2005) The role of microRNA genes in papillary thyroid carcinoma. *Proc Natl Acad Sci U S A,* 102, 19075-80.

HWANG, H. W. & MENDELL, J. T. (2006) MicroRNAs in cell proliferation, cell death, and tumorigenesis. *Br J Cancer,* 94, 776-80.

KIM, V. N. & NAM, J. W. (2006) Genomics of microRNA. *Trends Genet,* 22, 165-73.

KOCH, I., SLOTTA-HUSPENINA, J., HOLLWECK, R., ANASTASOV, N., HOFLER, H., QUINTANILLA-MARTINEZ, L. & FEND, F. (2006) Real-time quantitative RT-PCR shows variable, assay-dependent sensitivity to formalin fixation: implications for direct comparison of transcript levels in paraffin-embedded tissues. *Diagn Mol Pathol,* 15, 149-56.

LAGOS-QUINTANA, M., RAUHUT, R., LENDECKEL, W. & TUSCHL, T. (2001) Identification of novel genes coding for small expressed RNAs. *Science,* 294, 853-8.

LAU, N. C., LIM, L. P., WEINSTEIN, E. G. & BARTEL, D. P. (2001) An abundant class of tiny RNAs with probable regulatory roles in Caenorhabditis elegans. *Science,* 294, 858-62.

LEE, R. C. & AMBROS, V. (2001) An extensive class of small RNAs in Caenorhabditis elegans. *Science,* 294, 862-4.

LEE, R. C., FEINBAUM, R. L. & AMBROS, V. (1993) The C. elegans heterochronic gene lin-4 encodes small RNAs with antisense complementarity to lin-14. *Cell,* 75, 843-854.

LEE, Y., AHN, C., HAN, J., CHOI, H., KIM, J., YIM, J., LEE, J., PROVOST, P., RADMARK, O., KIM, S. & KIM, V. N. (2003) The nuclear RNase III Drosha initiates microRNA processing. *Nature,* 425, 415-9.

LIU, C. G., CALIN, G. A., VOLINIA, S. & CROCE, C. M. (2008) MicroRNA expression profiling using microarrays. *Nat Protoc,* 3, 563-78.

MARSIT, C. J., EDDY, K. & KELSEY, K. T. (2006) MicroRNA responses to cellular stress. *Cancer Res,* 66, 10843-8.

MASUDA, N., OHNISHI, T., KAWAMOTO, S., MONDEN, M. & OKUBO, K. (1999) Analysis of chemical modification of RNA from formalin-fixed samples and optimization of molecular biology applications for such samples. *Nucleic Acids Res,* 27, 4436-43.

MICHAEL, M. Z., SM, O. C., VAN HOLST PELLEKAAN, N. G., YOUNG, G. P. & JAMES, R. J. (2003) Reduced accumulation of specific microRNAs in colorectal neoplasia. *Mol Cancer Res,* 1, 882-91.

NEGRINI, M., FERRACIN, M., SABBIONI, S. & CROCE, C. M. (2007) MicroRNAs in human cancer: from research to therapy. *J Cell Sci,* 120, 1833-40.

OSADA, H. & TAKAHASHI, T. (2007) MicroRNAs in biological processes and carcinogenesis. *Carcinogenesis,* 28, 2-12.

REINHART, B. J., SLACK, F. J., BASSON, M., PASQUINELLI, A. E., BETTINGER, J. C., ROUGVIE, A. E., HORVITZ, H. R. & RUVKUN, G. (2000) The 21-nucleotide let-7 RNA regulates developmental timing in Caenorhabditis elegans. *Nature,* 403, 901-6.

SASSEN, S., MISKA, E. A. & CALDAS, C. (2008) MicroRNA: implications for cancer. *Virchows Arch,* 452, 1-10.

SCHMITTGEN, T. D., LEE, E. J., JIANG, J., SARKAR, A., YANG, L., ELTON, T. S. & CHEN, C. (2008) Real-time PCR quantification of precursor and mature microRNA. *Methods,* 44, 31-8.

SI, M. L., ZHU, S., WU, H., LU, Z., WU, F. & MO, Y. Y. (2007) miR-21-mediated tumor growth. *Oncogene,* 26, 2799-803.

SLABY, O., SVOBODA, M., FABIAN, P., SMERDOVA, T., KNOFLICKOVA, D., BEDNARIKOVA, M., NENUTIL, R. & VYZULA, R. (2007) Altered expression of miR-21, miR-31, miR-143 and miR-145 is related to clinicopathologic features of colorectal cancer. *Oncology,* 72, 397-402.

SPECHT, K., RICHTER, T., MULLER, U., WALCH, A., WERNER, M. & HOFLER, H. (2001) Quantitative gene expression analysis in microdissected archival formalin-fixed and paraffin-embedded tumor tissue. *Am J Pathol,* 158, 419-29.

TAGANOV, K. D., BOLDIN, M. P., CHANG, K. J. & BALTIMORE, D. (2006) NF-kappaB-dependent induction of microRNA miR-146, an inhibitor targeted to signaling proteins of innate immune responses. *Proc Natl Acad Sci U S A,* 103, 12481-6.

TAKAMIZAWA, J., KONISHI, H., YANAGISAWA, K., TOMIDA, S., OSADA, H., ENDOH, H., HARANO, T., YATABE, Y., NAGINO, M., NIMURA, Y., MITSUDOMI, T. & TAKAHASHI, T. (2004) Reduced expression of the let-7 microRNAs in human lung cancers in association with shortened postoperative survival. *Cancer Res,* 64, 3753-6.

TANG, G. (2005) siRNA and miRNA: an insight into RISCs. *Trends Biochem Sci,* 30, 106-14.

VALOCZI, A., HORNYIK, C., VARGA, N., BURGYAN, J., KAUPPINEN, S. & HAVELDA, Z. (2004) Sensitive and specific detection of microRNAs by northern blot analysis using LNA-modified oligonucleotide probes. *Nucleic Acids Res,* 32, e175.

WATANABE, Y., TOMITA, M. & KANAI, A. (2007) Computational methods for microRNA target prediction. *Methods Enzymol,* 427, 65-86.

WIEMER, E. A. (2007) The role of microRNAs in cancer: no small matter. *Eur J Cancer,* 43, 1529-44.

WIGHTMAN, B., HA, I. & RUVKUN, G. (1993) Posttranscriptional regulation of the heterochronic gene lin-14 by lin-4 mediates temporal pattern formation in C. elegans. *Cell,* 75, 855-62.

WIJNHOVEN, B. P., MICHAEL, M. Z. & WATSON, D. I. (2007) MicroRNAs and cancer. *Br J Surg,* 94, 23-30.

XI, Y., NAKAJIMA, G., GAVIN, E., MORRIS, C. G., KUDO, K., HAYASHI, K. & JU, J. (2007) Systematic analysis of microRNA expression of RNA extracted from fresh frozen and formalin-fixed paraffin-embedded samples. *Rna,* 13, 1668-74.

CHAPTER SIX

ANALYSIS OF MICRORNA LET-7A AND MIR-140 EXPRESSION LEVELS USING LASER CAPTURE MICRODISSECTION (LCM) ON FORMALIN-FIXED PARAFFIN-EMBEDDED (FFPE) THYROID ARCHIVE TISSUES

6.1 Summary

Thyroid cancer incidence has increased significantly during the past decades and has become one of the leading cancer types in females. The objective of this chapter was to examine microRNA (miRNA) expression levels in thyroid disease. We used laser capture microdissection on 182 samples of thyroid FFPE tissues representing different variants of thyroid disease. Using TaqMan® real-time PCR specifically designed for microRNA, we analyzed let-7a and mir-140 expression levels in total RNA extracted from each of these samples. We found let-7a has a higher expression level in PTC versus Hashmoto thyroiditis or non-autoimmune thyroiditis and mir-140 has a higher expression level in neoplastic and malignant tissues compared with non-neoplastic or hyperplastic, suggesting that these microRNAs may be regulatory factors playing important roles in thyroid disease.

6.2 Introduction

The normal adult thyroid gland is composed of two lobes joined by the isthmus, which lies across the trachea anteriorly, below the level of the cricoid cartilage. It is made up of round or oval follicles that vary in size with an average diameter of 2cm (Rosai, 2004). Follicles are lined with cuboidal-to-low columnar epithelium which is filled with thyroglobulin-containing colloid (Figure 6.1). The thyrocytes are highly polarised with a basal nucleus and are surrounded by basement membrane. Groups of calcitonin-producing, neuroendocrine parafollicular cells (C cells) may be observed among the follicular cells, particularly in the upper zones of the gland, or in the confines of the basement membrane. C cells however make up less than 0.1% of the total thyroid

cellular mass. Thyroid disease represents the most common endocrine disease. Various thyroid diseases and some of the common and clinically significant types of diseases are discussed below.

6.2.1 Thyroid disease

The thyroid is one of the most responsive organs in the human body and can respond to many stimuli. During puberty, pregnancy or bouts of hyperactivity, the gland increases in size and becomes more active, resulting in transient hyperplasia. In response to trophic agents from the hypothalamus, thyroid stimulating hormone (TSH) is released by thyrotrophin in the anterior pituitary into the blood. The TSH causes the thyrocytes to pinocytose colloid and converts thyroglobulin to thyroxine (T_4) and triiodothyronine (T_3), which results in shrinkage of the colloid and the thyrocytes can become tall and columnar, sometimes forming infolded buds or papillae. T_4 and T_3 are subsequently released into the systemic circulation and are bound to plasma proteins such as thyroxine-binding globulin (TBG) for transport to peripheral tissues (Ekins et al., 1994). TBG is one of three proteins, along with transthyretin and albumin, responsible for carrying the thyroid hormones T_4 and T_3 in the bloodstream. Of these three proteins, TBG has the highest affinity for T_4 and T_3, but is present in the lowest concentration. When the thyroid hormones are released at the ultimate destinations, they enter cells and interact with nuclear receptors. These receptors alter gene expression profiles in catabolic pathways and ultimately increase the basal metabolic rate (Kohrle et al., 1987).

Thyroid diseases may be either non-neoplastic or neoplastic. Non-neoplastic thyroid diseases include thyroiditis and hyperplasia. Neoplastic tumours include benign adenomas and malignant lesions, which can be derived from the thyroid follicular epithelial cells or C-cells. Thyroid carcinomas are the most common malignancy of the endocrine system and incidence rates have steadily increased over recent decades. More than 95% of thyroid carcinomas are derived from follicular cells and a minority of 3% of tumours are of C-cell origin (Sheils, 2005, Kondo et al., 2006).

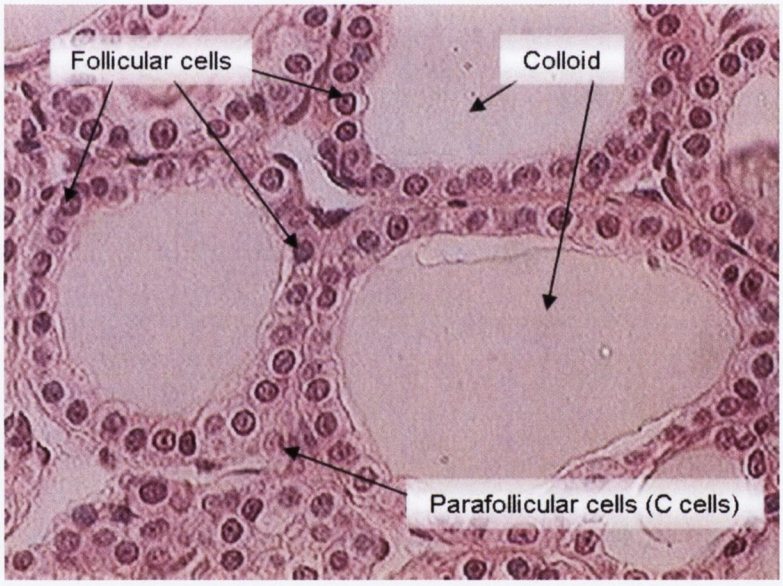

Figure 6.1 Normal microscopic histology of the thyroid

Each follicle appears as a ring of cells surrounding one thyroglobulin colloid. Follicular cells remove iodide from the blood and use it to form T_3 and T_4 thyroid hormones. In the process, each follicle also stores large amounts of T_3/T_4 precursor in the form of thyroglobulin. Parafollicular cells (C cells) lie just outside of the follicle cells and produce calcitonin.

6.2.2 Non-neoplastic diseases

Thyroiditis is an inflammation of the thyroid gland may be caused by infection, radiation, or trauma, or caused by autoimmune conditions, medications or an idiopathic fibrotic process (Bindra and Braunstein, 2006). The most common type is Hashimoto disease. Other types include subacute granulomatous thyroiditis, postpartum thyroiditis, subacute lymphocytic thyroiditis, and drug-induced thyroiditis. Hashimoto disease is a chronic autoimmune condition presenting as diffuse firm thyroid enlargement, which is characterized by the infiltration of the thyroid by lymphocytes and the formation of Askanazy cells. It occurs 7 times more commonly in women than man, with the peak incidence occurring between 40 and 60 years of age (Dayan and Daniels, 1996). In Hashimoto thyroiditis, a genetic association with human leucocyte antigen (HLA)-DR family genes has been found, and associations with many other autoimmune diseases are suggested (Takami et al., 2008).

Thyroid hyperplasia is an enlargement of the thyroid glands due to abnormal proliferation of the epithelial cells lining the follicles. Based on their presumed mechanism of production, morphologic features, and clinical manifestations, hyperplastic disorders of the thyroid have been classified into three major forms including dyshormonogenetic goiter, Graves' disease and nodular hyperplasia (Rosai, 2004). Nodular hyperplasia is the most common case, which can be largely prevented by the addition of iodine to common salt. The deficiency in thyroid hormone production induced by the iodine deficiency leads to an increase in TSH secretion, which results initially in a hyperactive thyroid with tall follicular epithelium and small

amounts of colloid and later in follicular atrophy with massive storage of colloid (Rosai, 2004).

6.2.3 Neoplastic tumours

Thyroid cell malignancies account for >95% of all thyroid carcinomas and include papillary thyroid carcinoma (PTC), follicular thyroid carcinoma (FTC), the Hurthle cell variant of FTC, insular thyroid carcinoma, anaplastic thyroid carcinoma (ATC), and medullary thyroid carcinoma. PTC is the most frequent and well studied of tumour malignancies, and is discussed below. Follicular adenoma is the only benign epithelial tumour of thyroid gland, which occurs mostly in adults aged from 20 to 50 years and is more common in women. The characteristic features that distinguish a follicular carcinoma from a follicular adenoma is the presence of vascular or capsular invasion (Liska et al., 2005).

6.2.4 Papillary thyroid carcinomas

Papillary thyroid cancer (PTC) is the most common histological type of thyroid cancer accounting for approximately 70-80% of all thyroid cancers, which affects females more frequently than males, with a ratio of 3:1 and can be present in any age group, the mean age at the time of initial diagnosis being ~ 40 years. Most thyroid malignancies in children are of this type. PTC is defined as a malignant epithelial tumour showing evidence of follicular cell differentiation, typically with papillary and follicular structures as well as characteristic nuclear changes (Liska et al., 2005). Microscopically, classic PTC has very distinctive features of numerous true papillae

that separate it from other thyroid carcinomas. The papillae are usually complex, branching, and randomly oriented, with a central fibrovascular core and a single or stratified lining of cuboidal cells. These papillae are nearly always associated with the formation of follicles which tend to be irregularly shaped, often tubular and branching.

6.2.5 Other thyroid carcinomas

Accounting for ~15% of thyroid malignancies, Follicular thyroid carcinoma (FTC) is associated with iodine deficiency. Like PTC, it also predominantly affects females however it occurs on average in older patients. FTC is defined as a malignant thyroid tumour displaying evidence of follicular cell differentiation (Rosai, 2004). Grossly, FTC is grey-tan-pink, fleshy and is sometimes semi-translucent when large colloid-filled follicles are present. Microscopically FTC lacks the nuclear features that define papillary carcinoma. Its appearance is variable, ranging from well-formed follicles, cribriform areas, or trabecular formations may be present. Focal or extensive cytoplasmic clear changes can occur. Psammoma bodies are absent and metaplasia is rare. Cytologically, the cells are usually uniform, and form small follicles with colloid(Oertel and Oertel, 2000).

Anaplastic thyroid cancer (ATC) (or undifferentiated) has a very poor prognosis due to its aggressive behaviour and resistance to cancer treatments. It is relatively rare with a mean age of 65 years at presentation. Such tumours are made up mainly of undifferentiated cells without structural follicular cell differentiation. There are three main morphological patterns, squamoid, pleomorphic giant cell and spindle cell (Rosai, 2004).

Medullary thyroid carcinoma (MTC) is a thyroid malignancy originating from the calcitonin secreting C-cells of the thyroid gland (Massoll and Mazzaferri, 2004). Two forms of MTC exist: sporadic and familial. The sporadic form affects adults with a mean age of 45 years comprising about 80% of all cases. The familial form, comprising 20% of cases, becomes clinically apparent in a younger age group with a mean age of 35 years.

6.2.6 Thyroid cancer genes and the signaling network

Carcinogenesis is a multi-step process that essentially arises from accumulation of mutations or activation of oncogenes. The progression of a tumour from normal cells to cancer is the result of the clonal expansion of cells that have acquired a selective growth advantage (Blagosklonny, 2005) which is led by the changes in genes that control cellular proliferation and cell death. These changes are caused by activation of oncogenes that promote cellular proliferation or differentiation and inhibit cell death or alternatively by deactivation of tumour suppressor genes (TSG) or DNA repair genes. Many genes relevant to thyroid carcinogenesis are normally engaged in proliferation and/or survival pathways. These pathways are integrated and cross linked as the thyrocyte signalling network leading to carcinogeneses (Garcia-Jimenez and Santisteban, 2007, Riesco-Eizaguirre and Santisteban, 2007b, Riesco-Eizaguirre and Santisteban, 2007a) (Figure 6.2).

The most studied pathway involved in thyroid tumourigenesis is the RET/RAS/BRAF/MAP kinase pathway, which is believed to be essential for the

development of PTC (Sheils, 2005). Mutations in these genes are found in over 70% of PTC and they rarely overlap in the same tumour (Nikiforova and Nikiforov, 2008). In this pathway, growth factors induce receptor-tyrosine kinase such as RET dimerization, resulting in activation of Ras which activates the kinase activity of BRAF and its downstream signalling cascade. BRAF phosphorylates the mitogen-activated protein kinase (MAPK) kinase (MEK), which phosphorylates and activates extracellular-signal-regulated kinase (ERK). Activated ERK migrates to the nucleus where it phosphorylates and activates various transcription factors that are involved in cell proliferation and differentiation (Kondo et al., 2006).

Thyrocyte growth occurs mainly through the TSH receptor mediated cAMP-dependent protein kinase (PKA) pathway (Garcia-Jimenez and Santisteban, 2007). Activating mutations of the TSH receptor increasing Adenylyl Cyclase activity have been identified in benign follicular adenomas and less commonly in carcinomas of the thyroid. In this pathway, TSH stimulated TSH receptor dissociates the G protein at the cell surface of follicular cells, and increases cAMP production. cAMP stimulates PKA, which in turn phosphorylates target proteins including membrane receptors, signalling molecules and transcription factors to promote growth and differentiation. The variety of targets will further amplify and diversify the final outcome of this pathway. One PKA substrate is the nuclear transcription factor CREB, which activates the transcription of cAMP-responsive genes after being phosphorylated by PKA.

TSH receptor-PLC-PKC is an overlapped pathway suggested to be involved in thyroid cancer (Garcia-Jimenez and Santisteban, 2007). TSH receptor in human thyrocytes stimulates phospholipase C (PLCb) leading to the yield of di-acyl-glycerol (DAG) and

inositol tri phosphate (IP3). DAG directly stimulates PKC. IP3 increases cytosolic Ca^{+2} levels, which act through a number of effectors including PKC. PKC stimulation is the major effector of tumour promoters, which activation leads to proliferation and de-differentiation in FRTL-5 and PC CL3 thyrocytes.

The phosphatidylinositol 3-kinase (PI3K)/Akt pathway alterations have been reported to be downstream of many growth factor receptors involved in cell survival, proliferation and cancer (Riesco-Eizaguirre and Santisteban, 2007b, Garcia-Jimenez and Santisteban, 2007). Silencing its upstream suppressor PTEN is frequently associated with thyroid carcinoma. PI3K/Akt is also suggested to be regulated by Ras and G protein forming the cross talk with other pathways (Garcia-Jimenez and Santisteban, 2007).

Other genes involved in thyroid cancer including p53, Wnt and the PAX8/PPAR rearrangement (DeLellis, 2006, Patel and Singh, 2006). Inactivating point mutations of the p53 tumour suppressor gene are highly prevalent in anaplastic and poorly differentiated thyroid tumours, implying p53 inactivation as an important step in late stage progression of thyroid cancer (Patel and Singh, 2006). The Wnt pathway plays a pivotal role in development and in epithelial renewal, which components such as b-catenin, APC and E-cadherin are often mutated in thyroid cancer. PAX8/PPAR rearrangement has been identified in a significant proportion of FTC, FA, PTC or Hurthle cell carcinoma (Riesco-Eizaguirre and Santisteban, 2007b).

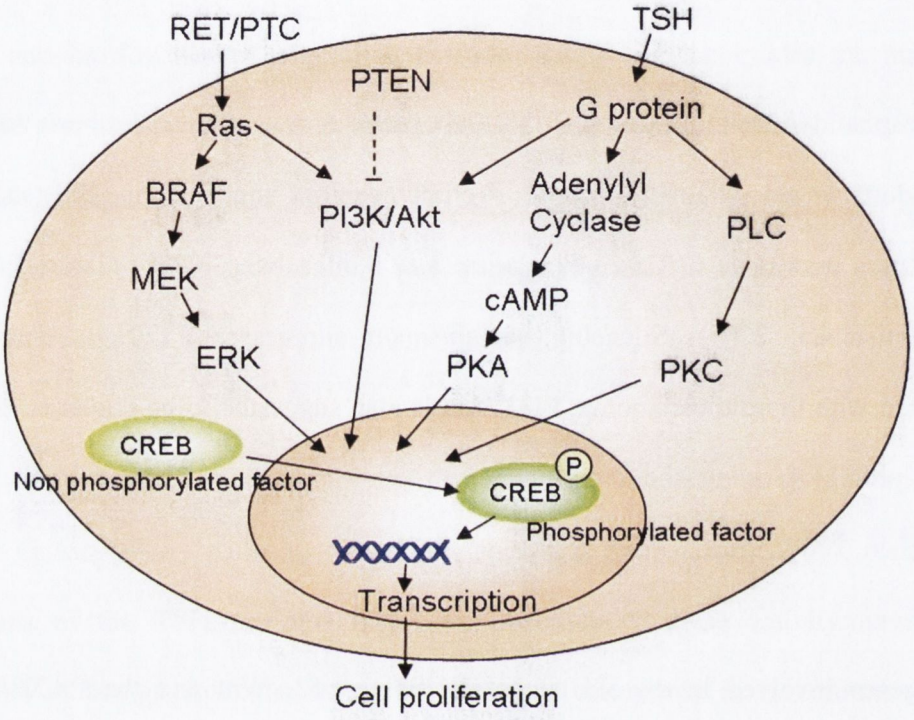

Figure 6.2 Thyroid cancer genes and the signalling network

Two major pathways are RET/RAS/BRAF/MAP kinase pathway and the TSH receptor/cAMP/PKA pathway. They are cross talked with PI3K/Akt pathway and PLC/PKC pathways to form signalling network in the thyroid follicular cell to regulate cell proliferation and differentiation.

6.2.7 Aims

The objective of this study was to examine microRNA expression across a spectrum of thyroid disease including benign, malignant, inflammatory, and hyperplastic. In this chapter, we specifically examined expression of let-7a and mir-140 across 182 of FFPE blocks. Employing laser captured microdissection (LCM) technique, homogenous cell populations were obtained. Total RNA was extracted from these limited amounts of LCM preparation. Then, the expression levels of let-7a and mir-140 were detected using TaqMan® real-time PCR technology with RNU6B as an endogenous control.

6.3 Materials and Methods

6.3.1 Archival formalin fixed paraffin embedded (FFPE) tissue samples

A total of 182 samples (Table 6.1), including malignant, benign, normal and hyperplasia (HP), accessioned from archives dating between 2000 and 2005 in St. James's Hospital, Dublin were employed in this experiment. Haematoxylin and eosin (H&E) stained sections were reviewed by a histopathologist and classified according to a recognised system (Rosai et al., 1992).

Table 6.1 Numbers of cases included in each group for a total of 182 samples

Groups (Total numbers of cases)		Types of thyroid	Numbers of cases
Neoplastic (79)	Benign (18)	Follicular adenomas	18
	Malignant (61)	Papillary thyroid carcinoma (PTC)	43
		Hurthle cell carcinoma	7
		Follicular thyroid carcinoma	9
		Medullary thyroid carcinoma	1
		Anaplastic thyroid carcinoma	1
Non-Neoplastic (103)	Normal & Inflammatory (53)	No evidence Malignant	14
		Goitre	30
		Hashimoto's thyroiditis (HT)	5
		Lymphocytic thyroiditis	4
	HP (50)	Hyperthyroidism	1
		Hyperplasia NOS	44
		Graves' disease	5

6.3.2 Laser capture microdissection

One to three of seven micrometer thick sections were cut using a microtome (Microm HM 325, Medical Supply Co. Ltd, Ireland) from each FFPE tissue block, mounted on a slide, deparaffined and H&E stained (Tissue-Tek DRS 2000 Autostainer, Sakura, CA, USA). Pure populations of thyrocytes were obtained from each section by laser capture microdissection using the PixCell II System (Acturus Engineering Inc., CA, USA) (Denning et al., 2007), which procedures have been described in Chapter 2.4. Cells were captured using one to three of Capsures (Capsuret Macro LCM caps, LCM 0201, Techno-Path Ltd, Ireland) for each sample to achieve sufficient amount of cells for subsequent analysis. The capsures containing the microdissected cells were then placed in sterile microcentrifuge tubes ready for RNA extraction.

6.3.3 RNA extraction

RNA was extracted using RecoverAll™ Total Nucleic Acid Isolation kit (Ambion Ltd., Cambridgeshire, UK) following the manufacturer's protocol described in Chapter 2.5.2, with the exception of the tissue deparaffinization step as the sections had been deparaffinised during H&E staining. The extraction started with proteinase K digestion for 3 hours at 50°C in a total volume of 404µl, followed by on column DNase digestion and elution as described in the protocol. When three Capsures were used to microdissect one sample, the proteinase K digestion reaction was split into a maximum of three tubes which were then combined into one single tube after digestion to complete the extraction. The concentration of samples was measured using a

NanoDrop® ND-1000 Spectrophotometer (Wilmington, USA) as described in Chapter 2.6.

6.3.4 miRNA assays and TaqMan® Gene Expression

Applied Biosystems TaqMan® microRNA (miRNA) assays, described in Chapter 2.8.5, were utilised in this study, including two human targets, let-7a and mir-140 (P/N: 4373169 and 4373138, Applied Biosystems). RNU6B (P/N: 4373381, Applied Biosystems) is a constantly expressed small RNA and was selected as an endogenous control. The analysis comprised two steps: Reverse Transcription (RT) and real time PCR. The stem-loop RT primer specifically hybridizes to a miRNA molecule and is reverse transcribed with a MultiScribe reverse transcriptase (Chen et al., 2005). The RT products are then quantified using real-time TaqMan® PCR.

Applied Biosystems High-Capacity cDNA Archive Kit (P/N: 4322171, Applied Biosystems, CA, USA) was used. Each 15µl RT reaction contained approximately 5ng of extracted total RNA, 50nM stem-looped RT primer, 1x RT buffer, 0.25mM each of dNTPs, 3.33U/µl Multiscribe reverse transcriptase and 0.25U/µl RNase Inhibitor.

For the Real-time PCR step, amplification was carried out using sequence specific primers on the Applied Biosystems 7900HT Real-Time PCR system. The 20µl reaction included 1.33µl RT product, 1x TaqMan® Universal PCR Master Mix with no UNG (P/N: 4324018, Applied Biosystems) and 1x TaqMan® MicroRNA assays (Table 6.2). The real-time PCRs for each miRNA were run in triplicate with non-template control included in each plate.

Table 6.2 Sequences of microRNA

Gene Name	Sequence
RNU6B (PN: 4373381)	CGCAAGGAUGACACGCAAAUUCGUGAAGCGUUCCAU AUUUUU
hsa-Let-7a (PN: 4373169)	UGAGGUAGUAGGUUGUAUAGUU
hsa- Mir-140 (PN:4373138)	AGUGGUUUUACCCUAUGGUAG

6.3.5 Statistical analysis

Replicates were omitted if C_T standard deviation was greater than 1.5. The relative quantification (RQ) value, generated automatically according to the $2^{-\Delta\Delta CT}$ method (Livak and Schmittgen, 2001) with the RNU6B as the endogenous control and one FA sample as the calibrator (see the formulas below), was collected using Microsoft Excel. Nonparametric Mann–Whitney statistical analysis was performed on RQ values using Analyse-it® statistical software for Microsoft® Excel®.

RQ value was generated according to the $2^{-\Delta\Delta CT}$ method with the formulas below:

$\Delta C_T = C_T\_Mean(microRNA) - C_T\_Mean(RNU6B)$

$\Delta\Delta C_T = \Delta C_T\_Sample - \Delta C_T\_FA$

$RQ = 2^{-\Delta\Delta CT}$

6.4 Results

The total yields of RNA generated from laser capture microdissected FFPE samples were in the range of 90 to 1200ng, which were low yet sufficient for the TaqMan® analysis of a few microRNA targets. Statistically analysis among different diseases in Table 6.1 was performed using relative quantification (RQ) values. Significant groups are graphically represented as box plots. microRNA let-7a was found to be overexpressed in the papillary thyroid carcinoma (PTC) group in contrast to the thyroiditis (P=0.0048) or Hashimoto thyroiditis (HT) (P=0.0004) (Figure 6.3). microRNA mir-140 was found to be upregulated in the neoplastic group compared to hyperplasia (HP) (P=0.0233) or Non-Neoplastic group (P=0.0168) (Figure 6.4), and was also found to be overexpressed in the malignant group in contrast to the HP (P=0.0233) or Non-Neoplastic group (P=0.0076) (Figure 6.5).

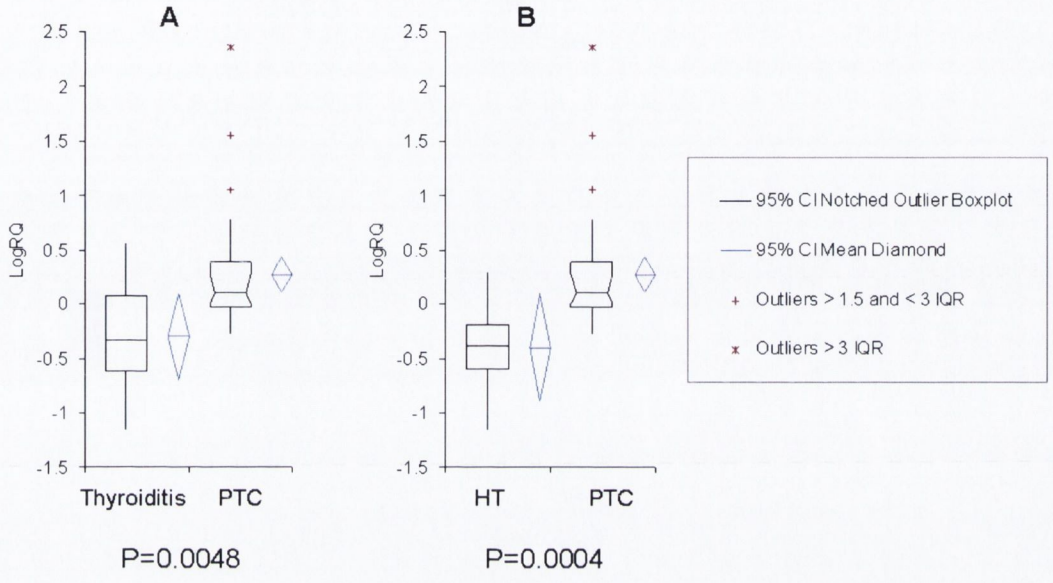

Figure 6.3 miRNA let-7a expression in samples of PTC versus Thyroiditis or HT

A represents upregulation of microRNA let-7a in the PTC group in contrast to the thyroiditis with P=0.0048. B represents upregulation of microRNA let-7a in the PTC group in contrast to the HT with P=0.0004.

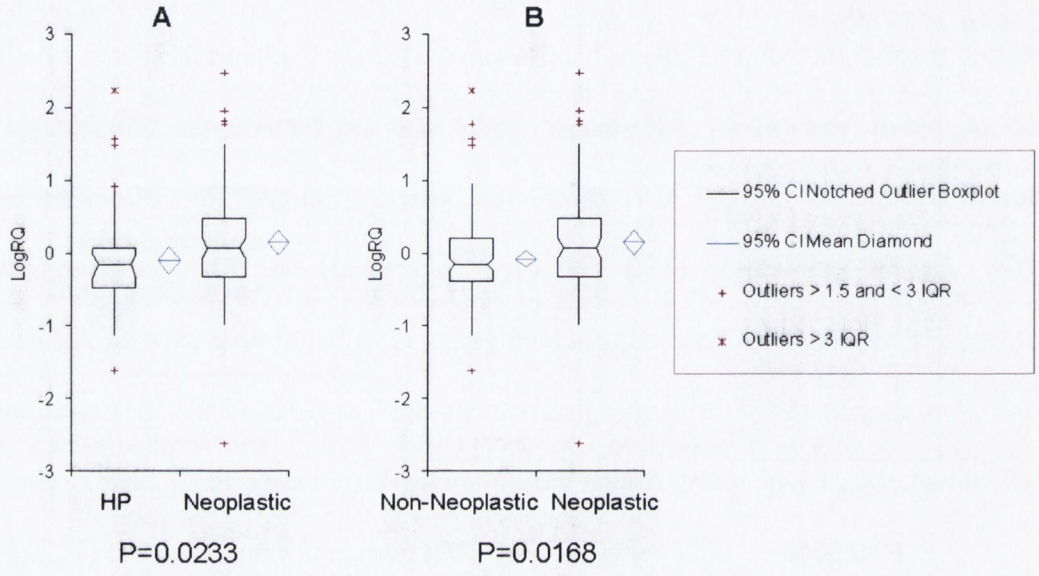

Figure 6.4 miRNA mir-140 expression in samples of Neoplastic versus HP or Non-Neoplastic

A represents upregulation of microRNA mir-140 in the Neoplastic group in contrast to the HP with P=0.0233. B represents upregulation of microRNA mir-140 in the Neoplastic group in contrast to the Non-Neoplastic group with P=0.0168.

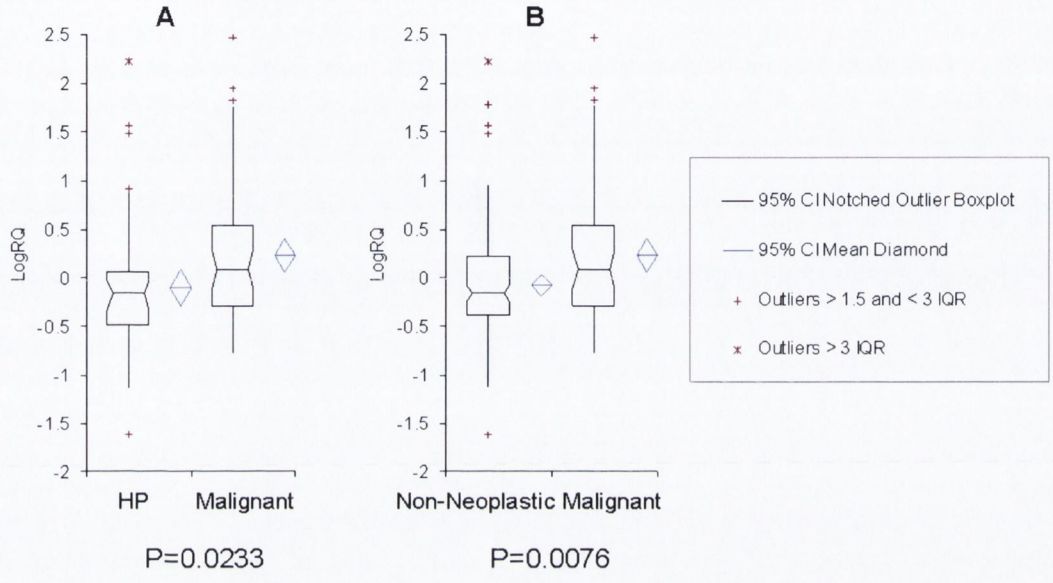

Figure 6.5 miRNA mir-140 expression in samples of Malignant versus HP or Non-Neoplastic

A represents upregulation of microRNA mir-140 in the Malignant group in contrast to the HP with P=0.0233. B represents upregulation of microRNA mir-140 in the Malignant group in contrast to the Non-Neoplastic group with P=0.0076.

6.5 Discussion

miRNAs present several challenges that make them more difficult to analyze than messenger RNA. For example, the short length of mature miRNAs provides very little sequence length to work with for the design of complementary probes (Wark et al., 2008); the amount of miRNA present in the tissue or in the total RNA sample is very low leading to the difficulty of consistent detection. However, TaqMan® stem-loop RT-PCR quantification technique was specially designed for mature miRNA detection (Chen et al., 2005). Although gene profiling generally requires high quality of nucleic acid, our (Chapter 5) and other recent studies (Siebolts et al., 2008, Doleshal et al., 2008) showed that miRNA species can be successfully detected in archival FFPE sources. In this study, we analyzed two miRNA targets in 182 of thyroid tissue samples and found let-7a overexpressed in PTC and mir-140 overexpressed in neoplastic and malignant groups.

6.5.1 microRNA techniques

There are several common used techniques to detect and quantify miRNA in tissue samples, including direct detection such as in situ hybridization and extraction based detection such as northern blotting, PCR-based techniques and microarray. In situ hybridization is the least commonly used among these techniques possibly due to the detection efficiencies. Very recently, using FFPE materials, Nuovo described improved protocols for detection of miRNAs in situ using both RT in situ PCR and in situ hybridization with locked nucleic acid (LNA) modified probes (Nuovo, 2008). Northern blot was used to detect these small RNAs when first miRNAs were described

(Lee et al., 1993). Although various modifications, including using verified gels or locked nucleic acid (LNA)-modified oligonucleiotide probes (Valoczi et al., 2004, Varallyay et al., 2007), optimized the technique to allow sensitive and highly specific detection of mature miRNAs, northern blotting is not practical in large clinical studies to detect the expression of hundreds of miRNAs and it also requires large amounts of total RNA from each sample. Microarray is an efficient profiling technique allowing over one thousand of miRNA targets to be studied on one chip (Liu et al., 2008). It is particular useful in screening microRNA targets expressed abnormally in disease samples by comparison to normal samples (Liu et al., 2004).

The TaqMan® real-time PCR is one of the popular techniques, which is highly sensitive and specific to detect low copy number of miRNAs on both the precursor and the mature form (Schmittgen et al., 2008). It is comparably cheap and can be used extensively for clinical samples with limited amounts of available RNA. Compared to microarray, TaqMan® real-time PCR not only allows the profiling of large numbers of miRNA on a few samples, but also allows individual miRNA studies using a large number of samples simultaneously. Our previous work studied the miRNA expression patterns in FFPE samples (Li et al., 2007) and found a good detection level in extracted total RNA demonstrating small RNA molecules are amenable to extraction and can be analysed in FFPE samples. This is in agreement with several other reports (Doleshal et al., 2008, Wang et al., 2007, Xi et al., 2007) indicating a higher stability of miRNAs compared to mRNA in samples obtained from FFPE tissues.

6.5.2 microRNAs involved in thyroid disease

Although over 400 microRNAs have been discovered on variable samples, not every individual regulatory of microRNA has been illustrated. There are several microRNAs found to function within different thyroid diseases to date, such as in PTC, ATC and FTC. Most of them have been demonstrated to contribute to PTC development. For example, microRNAs mir-221, mir-222 and mir-146 were found to be upregulated in PTC tumours compared to normal thyroid tissue using snap-frozen samples (He et al., 2005). Upregulation of these microRNA induced a decrease of *KIT* transcript and the expression of its protein (He et al., 2005). The overexpression of these three microRNAs were confirmed by Chen et al (Chen et al., 2008) using FFPE and fine-needle aspirate specimens indicating that reliable microRNA results can be generated using FFPE tissues. Furthermore, these three and another four targets including mir-187, mir-155, mir-224 and mir-197 were screened to be overexpressed microRNAs in thyroid tumors versus hyperplastic nodules in a recent study using TaqMan® real-time PCR (Nikiforova et al., 2008). In addition, mir-181b (Pallante et al., 2006) and mir-21 (Tetzlaff et al., 2007) was also reported in separate studies to increase in PTC compared to normal thyroid tissue and benign proliferative multinodular goiter, respectively. In follicular thyroid carcinoma (FTC), mir-192, mir-197, mir-328 and mir-346 were identified by Weber et al. to be overexpressed compared with FAs (Weber et al., 2006). There are microRNA targets found to significantly decrease in anaplastic thyroid carcinomas (ATC), such as mir-30d, mir-125b, mir-26a and mir-30a-5p detected in comparison to normal thyroid tissue (Visone et al., 2007). Mir-138 downregulates in ATC cell lines and associates with increase expression of protein hTERT (Mitomo et al., 2008). These previous reports, taken together, indicate

microRNA alterations associated with thyroid tumours and suggest microRNA deregulation as an important event in thyroid cell transformation.

6.5.3 microRNA let-7a in PTC

microRNA let-7 family was first identified in *Caenorhabditis elegans* to regulate developmental timing (Reinhart et al., 2000). Similarly in human, the expression of let-7 is in a very low level in embryonic stages while increases after differentiation (Lee et al., 2005). Recent studies have shown that let-7 negatively regulate some proteins, such as HMGA2 and RAS, playing down-regulation roles in cancers including lung cancer (Johnson et al., 2005), head and neck cancers, uterine leiomyomas and gastric cancer (Motoyama et al., 2008). However, some research groups show that let-7a also targets tumor suppressor genes or apoptosis genes to up-regulate in cancer. A detailed study by Meng et al. demonstrated that let-7a directly targeted a tumor suppressor gene *NF2* and increased Stat-3 phosphorylation leading to an overexpression of the inflammation-associated cytokine interleukin-6 (*IL-6*) (Meng et al., 2007). Increased expression of *IL-6* occurs in several human cancers including multiple myeloma, prostate cancer and cholangiocarcinoma. Moreover, let-7a shares complimentary sequence with and possibly targets tumour suppressor gene *BAG2* based on the computational prediction (MirGen). Bcl-2-associated athanogene (BAG) family proteins are characterized by their property of interaction with a variety of partners involved in modulating the proliferation or death balance including Bcl-2. cDNA microarray profiles showed tumour suppressor gene *BCL2* down-regulated in PTC (Kondo et al., 2006). Wang at el. suggested that BAG2 is a novel molecule exhibiting a pro-apoptotic property in death of thyroid cancer cells induced by

proteasome inhibition (Wang et al., 2008). These studies suggest that let-7a is involved and possibly is an important effector in tumorigenesis.

Hashimoto thyroiditis (HT) is the most common inflammatory thyroid disease and the most common cause of hypothyroidism. It has been highly debated for many years that HT relates to PTC with the evidence to date of 11% to 36% of patients with both diseases coexistent (Repplinger et al., 2007). Although RET/PTC chromosomal rearrangement, resulting from the fusion of the tyrosine kinase domain of RET to the 5' portion of different genes (Nikiforov, 2002), is believed to be an specific oncogenic marker for PTC, several research groups described expression of the RET/PTC oncogene in HT tissue samples (Wirtschafter et al., 1997, Rhoden et al., 2006, Arif et al., 2002, Sheils et al., 2000) and supported that HT and PTC are associated diseases. In addition, Prasad et al. demonstrated PTC associated proteins, GAL3, CITED1, CK19, HBME1 and FN1, to be focally expressed in HT of thyrocytes with PTC-like nuclear changes, while quantitatively different being diffuse in PTC, suggesting shared as well as different molecular, genetic and morphological features (Prasad et al., 2004).

The degree of molecular relation and discrimination between these two diseases remains unclear. Our result shows that let-7a has a higher expression level in PTC compared to HT or thyroiditis with P value less then 0.05 suggesting that these diseases are possibly regulated by different microRNA mechanisms. Although there has not been any direct experimental evidence linking microRNA let-7a to any of the identified marker genes in thyroid signalling pathways, it is likely that specific microRNAs play important roles in degradation of tumour suppressor genes resulting in progressive growth of PTC compared to HT or thyroiditis.

6.5.4 microRNA mir-140 in thyroid

To date, there are only a few studies investigating the molecular role of mir-140 in biological functions. Wienholds et al. reported that mir-140 was specifically expressed in the cartilage of the jaw, head, and fins during zabrafish embryonic development, and its presence was entirely restricted to those regions (Wienholds et al., 2005). Tuddenham et al. later demonstrated a specific expression in cartilage tissues of mouse embryos during both long and flat bone development and suggested that *HDAC4* being a target of mir-140 (Tuddenham et al., 2006).

Our results show that mir-140 has a higher expression level in neoplastic compared to non-neoplastic or hyperplastic, and has a higher expression level in malignant in contrast to non-neoplastic or hyperplastic tissues with P values less than 0.05, suggesting that mir-140 possibly regulates mRNA targets involved in molecular mechanisms behind thyroid carcinogenesis. Mir-140 shares complementary sequence with the genes that were identified to be underexpressed in thyroid malignancy including *ANK2*, *LMAN1* and *POLI* in a microarray study (Finn et al., 2007). Decreased expression of ankyrin-B in mice or human mutations in the ankyrin-B gene (*ANK2*) results in potentially fatal cardiac arrhythmias. It is suggested that ANK2 is subject to complex transcriptional regulation that likely results in differential ankyrin-B polypeptide function (Cunha et al., 2008). Lectin, mannose-binding 1 (LMAN1), with MCFD2 (multiple coagulation factor deficiency protein 2), forms the best known mammalian cargo receptor protein complex. LMAN1 and MCFD2 have been proposed to function in concert to facilitate transport of factors V and VIII (F5F8D) in the early

secretory pathway in mammals (Baines and Zhang, 2007). DNA polymerase iota (POL I) functions in transcription elongation in the analogous POL II transcription system and transcribes genes encoding the 18S, 5.8S, and 25–28S rRNAs that form the catalytic core of ribosomes (Haag and Pikaard, 2007). Besides these genes above, like let-7a, mir-140 also potentially targets apoptosis gene *BAG2* indicating its potential role in thyroid malignancy. It would be interesting to further investigate the biological roles of these genes in thyroid malignancy and to experimentally identify the relations between these genes and microRNA mir-140 in thyroid diseases.

6.6 Conclusions

We successfully analyzed miRNAs let-7a and mir-140 expression levels in 182 thyroid samples of laser captured microdissected FFPE tissue using TaqMan® real time PCR. We found microRNA let-7a has a higher expression level in PTC versus HT or thyroiditis, and mir-140 has a higher expression level in groups of malignancy and neoplastic compared to non-neoplastic and hyperplastic. These over expressions of microRNA possibly result in the deregulation of tumour suppressor genes and the genes involved in thyroid signalling pathways, thus leading to the unbalance between cellular proliferation and cell death. To understand the precise roles of these microRNAs in thyroid and to identify actual messenger RNA targets, further work might be required to investigate expression levels of some tumour repressor genes or apoptosis related targets in malignant samples.

6.7 References

ARIF, S., BLANES, A. & DIAZ-CANO, S. J. (2002) Hashimoto's thyroiditis shares features with early papillary thyroid carcinoma. *Histopathology,* 41, 357-62.

BAINES, A. C. & ZHANG, B. (2007) Receptor-mediated protein transport in the early secretory pathway. *Trends Biochem Sci,* 32, 381-8.

BINDRA, A. & BRAUNSTEIN, G. D. (2006) Thyroiditis. *Am Fam Physician,* 73, 1769-76.

BLAGOSKLONNY, M. V. (2005) Molecular theory of cancer. *Cancer Biol Ther,* 4, 621-7.

CHEN, C., RIDZON, D., BROOMER, A., ZHOU, Z., LEE, D., NGUYEN, J., BARBISIN, M., XU, N., MAHUVAKAR, V., ANDERSEN, M., LAO, K., LIVAK, K. & GUEGLER, K. (2005) Real-time quantification of microRNAs by stem-loop RT-PCR. *Nucleic Acids Res,* 33, e179.

CHEN, Y. T., KITABAYASHI, N., ZHOU, X. K., FAHEY, T. J., 3RD & SCOGNAMIGLIO, T. (2008) MicroRNA analysis as a potential diagnostic tool for papillary thyroid carcinoma. *Mod Pathol.*

CUNHA, S. R., LE SCOUARNEC, S., SCHOTT, J. J. & MOHLER, P. J. (2008) Exon organization and novel alternative splicing of the human ANK2 gene: Implications for cardiac function and human cardiac disease. *J Mol Cell Cardiol.*

DAYAN, C. M. & DANIELS, G. H. (1996) Chronic autoimmune thyroiditis. *N Engl J Med,* 335, 99-107.

DELELLIS, R. A. (2006) Pathology and genetics of thyroid carcinoma. *J Surg Oncol,* 94, 662-9.

DENNING, K. M., SMYTH, P. C., CAHILL, S. F., FINN, S. P., CONLON, E., LI, J., FLAVIN, R. J., AHERNE, S. T., GUENTHER, S. M., FERLINZ, A., O'LEARY J, J. & SHEILS, O. M. (2007) A molecular expression signature distinguishing follicular lesions in thyroid carcinoma using preamplification RT-PCR in archival samples. *Mod Pathol,* 20, 1095-102.

DOLESHAL, M., MAGOTRA, A. A., CHOUDHURY, B., CANNON, B. D., LABOURIER, E. & SZAFRANSKA, A. E. (2008) Evaluation and validation of total RNA extraction methods for microRNA expression analyses in formalin-fixed, paraffin-embedded tissues. *J Mol Diagn,* 10, 203-11.

EKINS, R. P., SINHA, A. K., PICKARD, M. R., EVANS, I. M. & AL YATAMA, F. (1994) Transport of thyroid hormones to target tissues. *Acta Med Austriaca,* 21, 26-34.

FINN, S. P., SMYTH, P., CAHILL, S., STRECK, C., O'REGAN, E. M., FLAVIN, R., SHERLOCK, J., HOWELLS, D., HENFREY, R., CULLEN, M., TONER, M., TIMON, C., O'LEARY, J. J. & SHEILS, O. M. (2007) Expression microarray analysis of papillary thyroid carcinoma and benign thyroid tissue: emphasis on the follicular variant and potential markers of malignancy. *Virchows Arch,* 450, 249-60.

GARCIA-JIMENEZ, C. & SANTISTEBAN, P. (2007) TSH signalling and cancer. *Arq Bras Endocrinol Metabol,* 51, 654-71.

HAAG, J. R. & PIKAARD, C. S. (2007) RNA polymerase I: a multifunctional molecular machine. *Cell,* 131, 1224-5.

HE, H., JAZDZEWSKI, K., LI, W., LIYANARACHCHI, S., NAGY, R., VOLINIA, S., CALIN, G. A., LIU, C. G., FRANSSILA, K., SUSTER, S., KLOOS, R. T., CROCE, C. M. & DE LA CHAPELLE, A. (2005) The role of microRNA genes in papillary thyroid carcinoma. *Proc Natl Acad Sci U S A,* 102, 19075-80.

JOHNSON, S. M., GROSSHANS, H., SHINGARA, J., BYROM, M., JARVIS, R., CHENG, A., LABOURIER, E., REINERT, K. L., BROWN, D. & SLACK, F. J. (2005) RAS is regulated by the let-7 microRNA family. *Cell,* 120, 635-47.

KOHRLE, J., BRABANT, G. & HESCH, R. D. (1987) Metabolism of the thyroid hormones. *Horm Res,* 26, 58-78.

KONDO, T., EZZAT, S. & ASA, S. L. (2006) Pathogenetic mechanisms in thyroid follicular-cell neoplasia. *Nat Rev Cancer,* 6, 292-306.

LEE, R. C., FEINBAUM, R. L. & AMBROS, V. (1993) The C. elegans heterochronic gene lin-4 encodes small RNAs with antisense complementarity to lin-14. *Cell,* 75, 843-854.

LEE, Y. S., KIM, H. K., CHUNG, S., KIM, K. S. & DUTTA, A. (2005) Depletion of human micro-RNA miR-125b reveals that it is critical for the proliferation of differentiated cells but not for the down-regulation of putative targets during differentiation. *J Biol Chem,* 280, 16635-41.

LI, J., SMYTH, P., FLAVIN, R., CAHILL, S., DENNING, K., AHERNE, S., GUENTHER, S. M., O'LEARY J, J. & SHEILS, O. (2007) Comparison of miRNA expression patterns using total RNA extracted from matched samples of formalin-fixed paraffin-embedded (FFPE) cells and snap frozen cells. *BMC Biotechnol,* 7, 36.

LISKA, J., ALTANEROVA, V., GALBAVY, S., STVRTINA, S. & BRTKO, J. (2005) Thyroid tumors: histological classification and genetic factors involved in the development of thyroid cancer. *Endocr Regul,* 39, 73-83.

LIU, C. G., CALIN, G. A., MELOON, B., GAMLIEL, N., SEVIGNANI, C., FERRACIN, M., DUMITRU, C. D., SHIMIZU, M., ZUPO, S., DONO, M., ALDER, H., BULLRICH, F., NEGRINI, M. & CROCE, C. M. (2004) An oligonucleotide microchip for genome-wide microRNA profiling in human and mouse tissues. *Proc Natl Acad Sci U S A,* 101, 9740-4.

LIU, C. G., CALIN, G. A., VOLINIA, S. & CROCE, C. M. (2008) MicroRNA expression profiling using microarrays. *Nat Protoc,* 3, 563-78.

LIVAK, K. & SCHMITTGEN, T. (2001) Analysis of relative gene expression data using real-time quantitative PCR and the 2(-Delta Delta C(T)) Method. *Methods* 25, 402-8.

MASSOLL, N. & MAZZAFERRI, E. L. (2004) Diagnosis and management of medullary thyroid carcinoma. *Clin Lab Med,* 24, 49-83.

MENG, F., HENSON, R., WEHBE-JANEK, H., SMITH, H., UENO, Y. & PATEL, T. (2007) The MicroRNA let-7a modulates interleukin-6-dependent STAT-3 survival signaling in malignant human cholangiocytes. *J Biol Chem,* 282, 8256-64.

MITOMO, S., MAESAWA, C., OGASAWARA, S., IWAYA, T., SHIBAZAKI, M., YASHIMA-ABO, A., KOTANI, K., OIKAWA, H., SAKURAI, E., IZUTSU, N., KATO, K., KOMATSU, H., IKEDA, K., WAKABAYASHI, G. & MASUDA, T. (2008) Downregulation of miR-138 is associated with overexpression of human telomerase reverse transcriptase protein in human anaplastic thyroid carcinoma cell lines. *Cancer Sci,* 99, 280-6.

MOTOYAMA, K., INOUE, H., NAKAMURA, Y., UETAKE, H., SUGIHARA, K. & MORI, M. (2008) Clinical significance of high mobility group A2 in human gastric cancer and its relationship to let-7 microRNA family. *Clin Cancer Res,* 14, 2334-40.

NIKIFOROV, Y. E. (2002) RET/PTC rearrangement in thyroid tumors. *Endocr Pathol,* 13, 3-16.

NIKIFOROVA, M. N. & NIKIFOROV, Y. E. (2008) Molecular genetics of thyroid cancer: implications for diagnosis, treatment and prognosis. *Expert Rev Mol Diagn,* 8, 83-95.

NIKIFOROVA, M. N., TSENG, G. C., STEWARD, D., DIORIO, D. & NIKIFOROV, Y. E. (2008) MicroRNA expression profiling of thyroid tumors: biological significance and diagnostic utility. *J Clin Endocrinol Metab,* 93, 1600-8.

NUOVO, G. J. (2008) In situ detection of precursor and mature microRNAs in paraffin embedded, formalin fixed tissues and cell preparations. *Methods,* 44, 39-46.

OERTEL, Y. C. & OERTEL, J. E. (2000) Thyroid cytology and histology. *Baillieres Best Pract Res Clin Endocrinol Metab,* 14, 541-57.

PALLANTE, P., VISONE, R., FERRACIN, M., FERRARO, A., BERLINGIERI, M. T., TRONCONE, G., CHIAPPETTA, G., LIU, C. G., SANTORO, M., NEGRINI, M., CROCE, C. M. & FUSCO, A. (2006) MicroRNA deregulation in human thyroid papillary carcinomas. *Endocr Relat Cancer,* 13, 497-508.

PATEL, K. N. & SINGH, B. (2006) Genetic considerations in thyroid cancer. *Cancer Control,* 13, 111-8.

PRASAD, M. L., HUANG, Y., PELLEGATA, N. S., DE LA CHAPELLE, A. & KLOOS, R. T. (2004) Hashimoto's thyroiditis with papillary thyroid carcinoma (PTC)-like nuclear alterations express molecular markers of PTC. *Histopathology,* 45, 39-46.

REINHART, B. J., SLACK, F. J., BASSON, M., PASQUINELLI, A. E., BETTINGER, J. C., ROUGVIE, A. E., HORVITZ, H. R. & RUVKUN, G. (2000) The 21-nucleotide let-7 RNA regulates developmental timing in Caenorhabditis elegans. *Nature,* 403, 901-6.

REPPLINGER, D., BARGREN, A., ZHANG, Y. W., ADLER, J. T., HAYMART, M. & CHEN, H. (2007) Is Hashimoto's Thyroiditis a Risk Factor for Papillary Thyroid Cancer? *J Surg Res.*

RHODEN, K. J., UNGER, K., SALVATORE, G., YILMAZ, Y., VOVK, V., CHIAPPETTA, G., QUMSIYEH, M. B., ROTHSTEIN, J. L., FUSCO, A., SANTORO, M., ZITZELSBERGER, H. & TALLINI, G. (2006) RET/papillary thyroid cancer rearrangement in nonneoplastic thyrocytes: follicular cells of Hashimoto's thyroiditis share low-level recombination events with a subset of papillary carcinoma. *J Clin Endocrinol Metab,* 91, 2414-23.

RIESCO-EIZAGUIRRE, G. & SANTISTEBAN, P. (2007a) Molecular biology of thyroid cancer initiation. *Clin Transl Oncol,* 9, 686-93.

RIESCO-EIZAGUIRRE, G. & SANTISTEBAN, P. (2007b) New insights in thyroid follicular cell biology and its impact in thyroid cancer therapy. *Endocr Relat Cancer,* 14, 957-77.

ROSAI, J. (2004) *Rosai and Ackerman's surgical pathology* St. Louis, Mo. ; London : Mosby.

ROSAI, J., CARCANGIU, M. & DELELLIS, R. (1992) *Atlas of Tumour Pathology – Tumours of the Thyroid Gland,* Washington DC, USA, AFIP.

SCHMITTGEN, T. D., LEE, E. J., JIANG, J., SARKAR, A., YANG, L., ELTON, T. S. & CHEN, C. (2008) Real-time PCR quantification of precursor and mature microRNA. *Methods,* 44, 31-8.

SHEILS, O. (2005) Molecular classification and biomarker discovery in papillary thyroid carcinoma. *Expert Rev Mol Diagn,* 5, 927-46.

SHEILS, O. M., O'EARY J, J., UHLMANN, V., LATTICH, K. & SWEENEY, E. C. (2000) ret/PTC-1 Activation in Hashimoto Thyroiditis. *Int J Surg Pathol,* 8, 185-189.

SIEBOLTS, U., VARNHOLT, H., DREBBER, U., DIENES, H. P., WICKENHAUSER, C. & ODENTHAL, M. (2008) Tissues from routine pathology archives are suitable for microRNA analyses by quantitative PCR. *J Clin Pathol.*

TAKAMI, H. E., MIYABE, R. & KAMEYAMA, K. (2008) Hashimoto's thyroiditis. *World J Surg,* 32, 688-92.

TETZLAFF, M. T., LIU, A., XU, X., MASTER, S. R., BALDWIN, D. A., TOBIAS, J. W., LIVOLSI, V. A. & BALOCH, Z. W. (2007) Differential expression of miRNAs in papillary thyroid carcinoma compared to multinodular goiter using formalin fixed paraffin embedded tissues. *Endocr Pathol,* 18, 163-73.

TUDDENHAM, L., WHEELER, G., NTOUNIA-FOUSARA, S., WATERS, J., HAJIHOSSEINI, M. K., CLARK, I. & DALMAY, T. (2006) The cartilage specific microRNA-140 targets histone deacetylase 4 in mouse cells. *FEBS Lett,* 580, 4214-7.

VALOCZI, A., HORNYIK, C., VARGA, N., BURGYAN, J., KAUPPINEN, S. & HAVELDA, Z. (2004) Sensitive and specific detection of microRNAs by northern blot analysis using LNA-modified oligonucleotide probes. *Nucleic Acids Res,* 32, e175.

VARALLYAY, E., BURGYAN, J. & HAVELDA, Z. (2007) Detection of microRNAs by Northern blot analyses using LNA probes. *Methods,* 43, 140-5.

VISONE, R., PALLANTE, P., VECCHIONE, A., CIROMBELLA, R., FERRACIN, M., FERRARO, A., VOLINIA, S., COLUZZI, S., LEONE, V., BORBONE, E., LIU, C. G., PETROCCA, F., TRONCONE, G., CALIN, G. A., SCARPA, A., COLATO, C., TALLINI, G., SANTORO, M., CROCE, C. M. & FUSCO, A. (2007) Specific microRNAs are downregulated in human thyroid anaplastic carcinomas. *Oncogene,* 26, 7590-5.

WANG, H., ACH, R. A. & CURRY, B. (2007) Direct and sensitive miRNA profiling from low-input total RNA. *Rna,* 13, 151-9.

WANG, H. Q., ZHANG, H. Y., HAO, F. J., MENG, X., GUAN, Y. & DU, Z. X. (2008) Induction of BAG2 protein during proteasome inhibitor-induced apoptosis in thyroid carcinoma cells. *Br J Pharmacol.*

WARK, A. W., LEE, H. J. & CORN, R. M. (2008) Multiplexed detection methods for profiling microRNA expression in biological samples. *Angew Chem Int Ed Engl,* 47, 644-52.

WEBER, F., TERESI, R. E., BROELSCH, C. E., FRILLING, A. & ENG, C. (2006) A limited set of human MicroRNA is deregulated in follicular thyroid carcinoma. *J Clin Endocrinol Metab,* 91, 3584-91.

WIENHOLDS, E., KLOOSTERMAN, W. P., MISKA, E., ALVAREZ-SAAVEDRA, E., BEREZIKOV, E., DE BRUIJN, E., HORVITZ, H. R., KAUPPINEN, S. & PLASTERK, R. H. (2005) MicroRNA expression in zebrafish embryonic development. *Science,* 309**,** 310-1.

WIRTSCHAFTER, A., SCHMIDT, R., ROSEN, D., KUNDU, N., SANTORO, M., FUSCO, A., MULTHAUPT, H., ATKINS, J. P., ROSEN, M. R., KEANE, W. M. & ROTHSTEIN, J. L. (1997) Expression of the RET/PTC fusion gene as a marker for papillary carcinoma in Hashimoto's thyroiditis. *Laryngoscope,* 107**,** 95-100.

XI, Y., NAKAJIMA, G., GAVIN, E., MORRIS, C. G., KUDO, K., HAYASHI, K. & JU, J. (2007) Systematic analysis of microRNA expression of RNA extracted from fresh frozen and formalin-fixed paraffin-embedded samples. *Rna,* 13**,** 1668-74.

CHAPTER SEVEN

GENERAL DISCUSSION, CONCLUSIONS AND FUTURE WORK

7.1 Introduction

Archival Formalin–Fixed, Paraffin–Embedded (FFPE) tissue samples are the most abundant material and represent a robust and invaluable source for the study of human disease. Compared to fresh and snap frozen tissue, FFPE tissue has an inherent advantage in that retrospective patient data, including survival history and treatment response etc, is readily available, allowing immediate comparison with clinical pathological parameters. Data generated can potentially highlight biomarkers useful in disease classification, diagnosis and prognosis, and potentially elucidate novel therapeutic targets (Lewis et al., 2001, Srinivasan et al., 2002).

FFPE tissue is the standard processing methodology practiced in pathology laboratories the world over. These samples are highly stable at room temperature, are easily stored and, most importantly, make up a vast archive of pathologically well characterized and well annotated clinical samples from randomized trials. Some essential biomedical subjects including histology, cytology and pathology are largely based on FFPE tissues. Subsequent technologies are developed to perform scientific studies including biological staining, immunohistochemistry, laser capture microdissection, tissue microarray and in situ hybridization, etc., some of which become important tools used in clinical diagnostic. In molecular biology, however, these tissues have not been widely used due to the poor quality of RNA extracted from FFPE blocks (Srinivasan et al., 2002) which is degraded to fewer than 300 bases in length (Cronin et al., 2004) and also chemically modified by methylol groups during formalin fixation (Masuda et al., 1999). Thus, the value of FFPE materials in

molecular setting has been shadowed by the technical difficulties limiting extensive analysis of gene expression.

The main focus of this thesis was centred on the establishment of an analysis system to study RNA expression efficiently using FFPE material. In this project, archival FFPE thyroid tissue blocks and a cell line model, created especially for the comparison purpose, were employed in the experiments. With the facilitation of modern molecular techniques of Nano-Drop Spectrophotometer and Agilent Bioanalyzer, Applied Biosystems real-time TaqMan® RT-PCR was utilized as the core technology to analyze and quantify messenger RNA and microRNA expression levels in the extracts of FFPE. Stratagene Absolutely RNA® FFPE Kit and Ambion RecoverAll™ Total Nucleic Acid Isolation Kit were identified as suitable protocols for FFPE materials, which were further modified by introducing a heating step to improve messenger RNA detection as indicated with higher quantity, larger fragments and lower TaqMan® C_T values. A novel TaqMan® PreAmp system was demonstrated to consistently decrease C_Ts without bias as a robust and practical solution to limited quantities of RNA, which may reliably be utilised in the context of multiple messenger RNA expression analyses from individual FFPE samples. For microRNA analysis, TaqMan® stem-loop RT primer microRNA assays have generated comparable results in matched FFPE and snap frozen preparations. This method was finally used in actual thyroid disease settings to investigate individual microRNA expression levels in total RNA extracted from a large number of laser captured microdissected FFPE tissue blocks, providing proof of principle that microRNA can be successfully extracted and analysed from archival sources.

7.2 Formalin modification of RNA

To further develop the extraction technique and the subsequent detection of gene expression from FFPE tissue, it is essential to understand the mechanisms of formalin fixation and modification of RNA. Formalin has been suggested to chemically fix tissues depending on cross-links formed between proteins, protein and nucleic acids, and between nucleic acids. In formalin solution, methylene glycol ($H_2C(OH)_2$) is present by addition of a molecule of water to one of formaldehyde (CH_2O). In the fixative solution, methylene glycol reacts with the nitrogen atoms to bind the amino acids to fix protein (Ramos-Vara, 2005). The fixation reaction has been suggested to involve two steps: the addition of the methylol groups ($–CH_2OH$) to the uncharged reactive amino groups (–NH or NH_2); and the formation of a methylene bridge ($–CH_2–$) between two amino groups.

The methylol cross-links formed during fixation cause the problems of analysing protein and nucleic acids in FFPE tissue. Protein studies have been widely carried out using immunohistochemistry technology with the facilitation of antigen retrieval. The principle of antigen retrieval is suggested to reverse or cleave the methylol cross-links formed among proteins, by protease treatment (Huang et al., 1976) or high-temperature treatment (Shi et al., 1991). The macromolecules in the tissue sections are then 'unmasked' or 'unlocked' exposing to the penetrated antibodies, therefore, resulting in greatly intensified immunoreaction (Yamashita, 2007, Taylor et al., 2002).

Although the chemical reaction of methylene glycol with RNA is not fully understood yet, Masuda and colleagues (Masuda et al., 1999) suggested that the similar reactions

involving formaldehyde reacting with RNA forming an N-methylol followed by an electrophilic attack to form a methylol bridge between amino groups. They demonstrated these two reaction using oligo RNA and showed that the reactivity of the bases are of the order A/C>>G>U, suggesting that the tertiary amino group is the primary target for formalin attack (Masuda et al., 1999). Taking together with the chemical structure of the methylol cross-links suggested previously by Chaw group (Chaw et al., 1980), it is reasonable to conclude that methylene glycol modifies the amino group where hydrogen band will form at the same position during reverse transcription (Figure 7.1), resulting in the problems of cDNA extension and subsequent PCR detection due to insufficient cDNA templates.

Moreover, the mechanism of high temperature heating reversing cross-links formed among RNAs could be very similar with the principle of antigen retrieval in protein analysis. In the comparison cell line model (Chapter 4), with the degradation parameter eliminated, intact RNA molecules were extracted from FFPE cells, including a large approximately 5kb band, a 4kb band which is slightly larger than 28s, and a 2kb band which is slightly larger than 18s (Chapter 4, Figure 4.8). Interestingly, incubation at high temperature removed the 5kb band and made the other two bands smaller and closer to 28s and 18s in size respectively, suggesting these large bands are cross-linked RNAs and high temperature reverses or breaks up the cross-links among RNA molecules. In addition, our real-time PCR results show that the extracts generated using the heating included protocols have a better detection rate compared to the extracts using normal protocols, as indicated by lower C_Ts in the former. This evidence supports our hypothesis that heating can remove the methylol groups or cross-links at

the hydrogen band forming position during reverse transcription, leading to an improved quantity of cDNA templates and an increased real-time PCR detection rate.

In conclusion, the methylol cross-links formed between RNA and protein prevent this RNA molecule being extracted, and among RNA molecules prevent this RNA being detected. The high temperature heating introduced into extraction protocols can reverse, at least in part, methylene modification resulting in the extracts with improved quantity and quality of RNAs. Apart from the normal RNA molecules obtained, we suggest that modified RNA molecules present in the FFPE extracts could have several forms (Figure 7.1): first, single RNA fragments with the addition of many methylol groups ($-CH_2OH$); second, a few RNA fragments cross-linking together forming a big multi RNA molecule; and third, two RNA fragments cross-linking to each other forming a double stranded RNA. Because efficient extraction processing can generally reverse modifications by removing cross-links between RNA and protein, between RNA and DNA, and between RNA and RNA, majority of modified RNAs are likely present in extracts as the single RNA fragments. Minority of RNA molecules cross-linked together in the tissue are possibly extracted as big multi RNA molecules. Very few of the RNA molecules cross-linked to each other present as double stranded RNA.

To further confirm the structure of modified RNA, biochemistry work is required and might be focused on the purified extracts of FFPE containing modified intact RNA molecules. Without the effects of RNA degradation, the chemical structure of formalin modified RNA could be revealed.

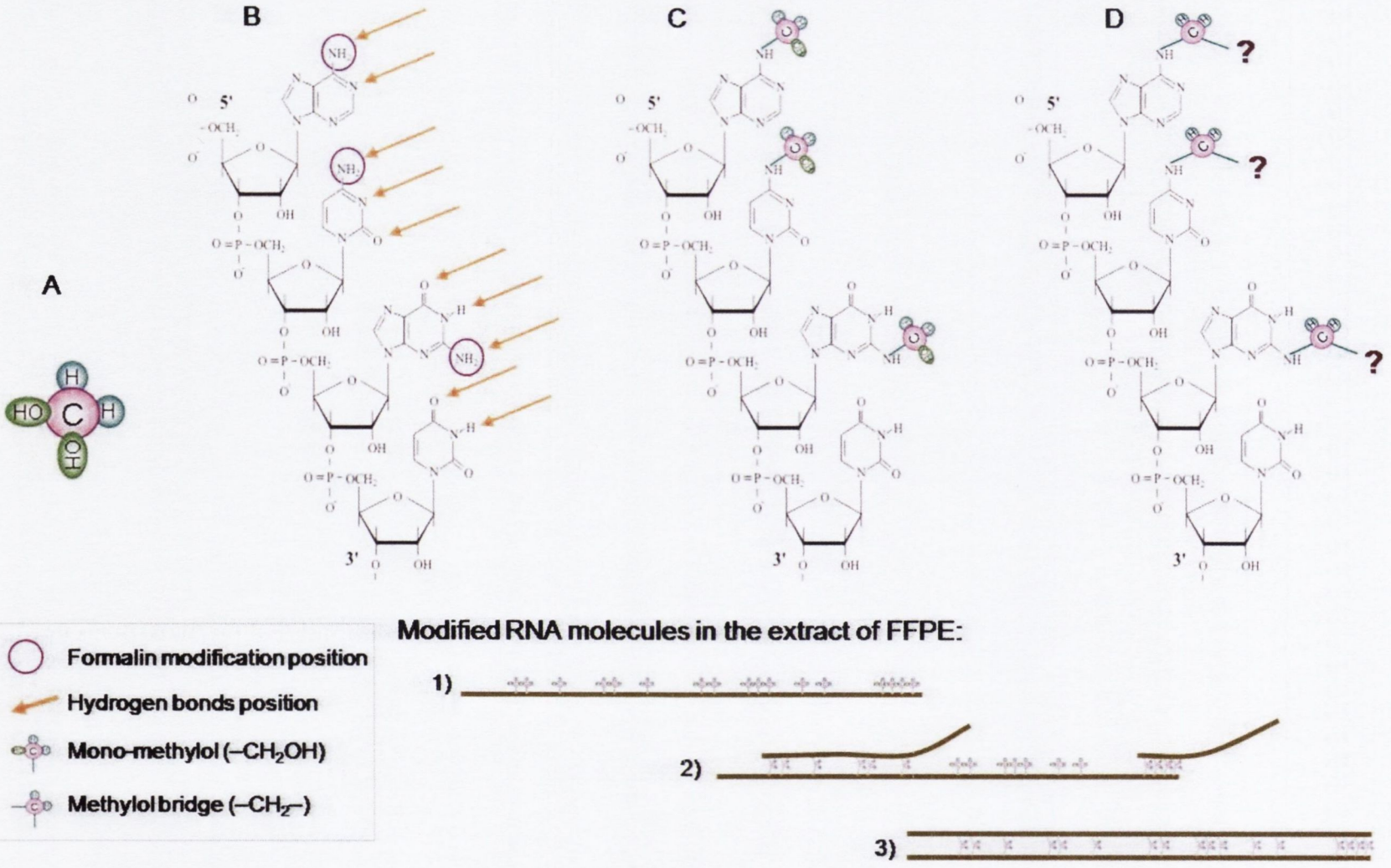
A
B
C
D
5'
3'
OH
?
Formalin modification position
Hydrogen bonds position
Mono-methylol (–CH2OH)
Methylol bridge (–CH2–)
Modified RNA molecules in the extract of FFPE:
1)
2)
3)

Figure 7.1 Formalin modification of RNA and hypothesis of modified structures

A, Structure of methylene glycol ($H_2C(OH)_2$). Methylene glycol ($H_2C(OH)_2$) is present by addition of a molecule of water to one of formaldehyde (CH_2O) in aqueous solution. B, Positions of methylene modification on RNA. Methylene glycol modifies the amino groups where hydrogen band will form at the same positions during reverse transcription. C, Modified RNA with additional methylol groups (–CH_2OH). The first step of modification is to add the mono-methylol groups to uncharged reactive amino groups (–NH or NH_2) on RNA. D, Methylol bridge (–CH_2–) cross-linking RNA with other molecules. Methylene bridges are formed between two amino groups after mono-methylol reacting with RNA, and cross-link this RNA with other molecules, possibly including protein, DNA and RNA. We therefore hypothesis three types of modified RNA molecules present in the extract of FFPE: 1), single RNA fragments with the addition of many methylol groups (–CH_2OH) as the major type; 2), a few RNA fragments cross-linking together forming a big multi RNA molecule as the minor type; and 3), two RNA fragments cross-linking to each other forming a double stranded RNA as the rare type.

7.3 Messenger RNA studies

For messenger RNA studies, general techniques include extraction-based detection or quantification, such as northern blotting, microarray and real-time PCR, and no extraction required detection such as in situ hybridization. Real-time TaqMan® RT PCR has become the standard and the most suitable method to perform gene expression using FFPE extracts for its many advantages including sensitivity, accuracy and reliability. Most importantly, it requires only very little amount of RNA extracts and can work on short sizes of amplicons such as degraded RNA in FFPE. Using FFPE materials, a successful gene expression study requires careful consideration of several issues including optimal extractions, RT random primers, short amplicons, and a suitable TaqMan® method.

Firstly, an optimal RNA extraction method is critical in producing a good quality of extract, which is a prerequisite for subsequent valid quantitative data (Bustin and Mueller, 2005). Our study shows that detectable RNAs can not be extracted from FFPE using the simple protocols developed for snap-frozen materials, and some essential procedures must be included in the extraction of FFPE, including deparaffinization, proteinase K digestion, buffer washing and column elution. A high temperature incubation step, after proteinase K digestion, is highly recommended adding into the suitable protocols in order to produce improved quantity and quality of RNA for subsequent detection. The incubation at 70°C for 20 minutes, introduced into commercial protocols of Ambion and Stratagene, is demonstrated to disrupt cross-links while not compromising RNA integrity comparing with other tested conditions. Recently, Oberli et al. demonstrated the importance of cross-link reversing process in

their own extraction protocol (Oberli et al., 2008), which is in agreement with our founding and suggested an optimal extraction protocol is crucial for downstream TaqMan® analysis.

Secondly, primer selection of the reverse transcription is important since it affects the sensitivity of the RT-PCR assays (Bustin and Nolan, 2004). Three types of primer are commonly used in RT step, including oligo (dT), gene specific primer and random primer. For FFPE tissues, random primer is recommended for yielding reliable and reproducible results with the least bias compared to the other two. It has been suggested that oligo (dT) is not able to anneal to the poly (A) tail and does not extend cDNA synthesis during reverse transcription using FFPE extracts. Because adenine is the most susceptible for the methylene modification, it is likely that the poly (A) tail of formalin fixed messenger RNA is heavily modified (Srinivasan et al., 2002). Moreover, the RNA extracted from FFPE tissues may not contain the poly (A) tail due to possibly being cleaved by RNase in the first step of degradation process. For gene specific primer, it can synthesize the most specific cDNA, however, requiring separate priming reactions for each target. Thus, it is labour intensive and wasteful if only limited amounts of extracts are available (Bustin and Nolan, 2004).

Thirdly, the length of amplicon size is especially critical because RNA is generally degraded into small sizes in the extracts of FFPE (Cronin et al., 2004). Theoretically, RNA fragmentation affects PCR results as every break in the RNA that occurs between two primers inevitably separates the two ends of the amplicon into two different cDNA molecules and is therefore lost as template for subsequent PCR (Antonov et al., 2005). Our results in Chapter 4 show that short amplicons generate consistent reliable C_Ts in

the comparison of FFPE and snap-frozen materials, which is likely due to the reason that the longer an amplicon is, the more likely its template will be degraded in extracted RNA. Therefore, the amplicon sizes of target genes and endogenous control genes are necessarily designed to be in the similar short length, less than 100bp.

Finally, reproducible detection methods, including appropriate reagents and suitable protocols, are required to produce reliable expression profile. Our results in Chapter 4 show that TaqMan® Gene Expression Master Mix generate consistent sensitivity for both short and long amplicons, while TaqMan® Universal PCR Master Mix does not, indicating that assay reproducibility is effected by different reagents with various polymerases activity and primer binding efficiency (Burgos et al., 2002). Moreover, TaqMan® PreAmp technique is found to decrease C_Ts efficiently and to generate real-time PCR results from limited amounts of FFPE extracts. Our results show that it is feasible to uniformly amplify cDNA templates without introducing bias, thus facilitating subsequent PCR amplification. It is particularly useful in the context of multiple expression analyses from individual FFPE samples, and might be an ideal solution to profile gene expression on rare or precious samples.

In conclusion, real-time TaqMan® RT PCR is an extremely powerful technique and can be used to produce biological meaningful results on FFPE materials. It is vital to carefully design experiment and consider each stage of the experimental protocol, proceeding through RNA extraction, RT and the real-time PCR step. Only if every one of these stages is properly validated and appropriate controls are included is it possible to obtain reliable quantitative data from archival FFPE blocks.

7.4 microRNA studies

Over the past few decades, a plethora of studies have concentrated largely on protein coding messenger RNAs in a quest to identify variety diseases associated genes. The recent discovery that in fact a large group of non-coding microRNAs potentially play a very important regulatory role helping to coordinate multicellular life has led to a proliferation of research in the literature of late (Boyd, 2008, Esquela-Kerscher and Slack, 2006, Negrini et al., 2007). However, because it is generally believed that RNA is compromised to be detected using archive materials, in addition, microRNAs are even more difficult to be analysed compared to messenger RNA due to their small sizes and low expression levels in tissues, there were little microRNA work carried out using FFPE before our study.

In Chapter 5, we compared 160 microRNA expression levels using total RNA extracted from matched samples of FFPE and snap-frozen cells, and utilizing real-time TaqMan® human microRNA assays with stem-loop RT primers for which has been favourably employing by researchers among many developed technical methods. We found that microRNAs can be analysed in FFPE extracts and they have reliable expression levels in FFPE compared with snap-frozen paired samples. It is reasonable to conclude that they have the advantage to be small and appear to be less affected by methylene modification and enzyme degradation during fixation process, therefore, are easily to be extracted and detected. In Chapter 6, we then studied two microRNA targets, let-7a and mir-140, using limited extracts of laser captured microdissected samples of a large number of FFPE blocks representing different thyroid diseases, which demonstrate an experimental example that these molecules might be robust

targets amenable to detection in archival material in the molecular studies. Thus, pathways and processes involved can potentially be elucidated, which help understanding of molecular mechanism of signalling network controlling each disease.

To date, larger scale analysis needs to be performed in a robust manner to illustrate the full regulatory impact of microRNA and to correlate individual biological functions to disease settings. An immediate obstacle facing research groups at present is the lack of accurate confirmation of microRNA gene targets, although multiple approaches have been suggested from bioinformatics including many prediction algorithms. Each microRNA found to be significantly deregulated in a certain type of cell line or tissue can be inputted into the microRNA databases, such as miRBase, miRGen, PicTar and TargetScan, to search for potential miRNA:mRNA target pairings. FFPE tissue samples, as the most readily available archival material, can then be used to valid gene target or discover functions of microRNA relating to protein expression data due to their well documentation of protein information. Furthermore, FFPE tissue samples, could be the solution of the source shortage of fresh or snap-frozen clinical tissues allowing immediate profiling across large number of samples, and thus opening an invaluable source for the study of microRNA in human disease settings. It is noteworthy that standard FFPE tissue preserves microRNAs in a reasonably intact and extractable state. Once these tools are clinically validated more extensively, they should enable microRNA measurements to become a part of the pathologist's diagnostic armamentarium.

7.5 From techniques to application

Molecular analysis of nucleic acids extracted from FFPE had been problematic for many decades. Using the advanced technologies of Nano-Drop Spectrophotometer, Agilent Bioanalyzer and real-time TaqMan® PCR, we have successfully identified methods to utilize FFPE in expression profiling of messenger RNA and microRNA.

The histopathology archive represents a vast, well-characterized source of specimens covering almost every disease and is available for molecular biological investigation. It provides a valuable source of material form with expressed genes can be studied at virtually every stage of development of a disease. Its importance cannot be underestimated since the prospective collection of specimens can take a considerable length of time, particularly for rarer diseases. With appropriate consent, these specimens are available for investigation as new technologies develop for their elucidation and diagnosis. This archive has already proved invaluable for the development of many immunohistochemical assays now utilized in routine diagnostic procedures. As better techniques evolve for the extraction and quantitation of RNA from formalin-fixed, paraffin-embedded tissue, the value of the archive will grow even stronger.

The ultimate task of many molecular research projects is to be able to identify biomarkers that can be used in a clinical setting to rapidly characterize a patient's disease type, to develop a greater understanding of the changes that occur in gene function during the progression of a disease, and use that information to apply the most appropriate treatment strategy. This study has produced optimised protocols for

extraction and detection of nucleic acids for molecular pathology applications. It demonstrated RNA reliable expression levels in FFPE, which not only has evaluated mRNA and microRNA analysis that have been performed on FFPE, but also could provide a source of study material for large scale and prospective studies on archival blocks. On one hand, real-time TaqMan® PCR, the most preferred gene expression technique, is firmly established as a mainstream research technology, which will hopefully yield fruitful results in discovery of effective diagnostic and prognostic biomarkers using FFPE to contribute clinical treatment. On the other hand, our understanding of the formalin modification will facilitate the development of other detection and profiling techniques to promote the research of translational medicine.

Clearly, the ability to discover and validate biomarkers on large FFPE sample sets is what allowed molecular research to go forward and move into the clinic. This technology is just beginning to be applied to cancer research and as its use becomes widespread it has the potential to have an important impact on research of any other diseases. FFPE tumour tissue samples are, therefore, the most important and abundant source of material available from randomized clinical trials that will allow for well controlled hypothesis testing to be conducted.

7.6 References

ANTONOV, J., GOLDSTEIN, D. R., OBERLI, A., BALTZER, A., PIROTTA, M., FLEISCHMANN, A., ALTERMATT, H. J. & JAGGI, R. (2005) Reliable gene expression measurements from degraded RNA by quantitative real-time PCR depend on short amplicons and a proper normalization. *Lab Invest,* 85, 1040-50.

BOYD, S. D. (2008) Everything you wanted to know about small RNA but were afraid to ask. *Lab Invest,* 88, 569-78.

BURGOS, J. S., RAMIREZ, C., TENORIO, R., SASTRE, I. & BULLIDO, M. J. (2002) Influence of reagents formulation on real-time PCR parameters. *Mol Cell Probes,* 16, 257-60.

BUSTIN, S. A. & MUELLER, R. (2005) Real-time reverse transcription PCR (qRT-PCR) and its potential use in clinical diagnosis. *Clin Sci (Lond),* 109, 365-79.

BUSTIN, S. A. & NOLAN, T. (2004) Pitfalls of quantitative real-time reverse-transcription polymerase chain reaction. *J Biomol Tech,* 15, 155-66.

CHAW, Y. F., CRANE, L. E., LANGE, P. & SHAPIRO, R. (1980) Isolation and identification of cross-links from formaldehyde-treated nucleic acids. *Biochemistry,* 19, 5525-31.

CRONIN, M., PHO, M., DUTTA, D., STEPHANS, J. C., SHAK, S., KIEFER, M. C., ESTEBAN, J. M. & BAKER, J. B. (2004) Measurement of gene expression in archival paraffin-embedded tissues: development and performance of a 92-gene reverse transcriptase-polymerase chain reaction assay. *Am J Pathol,* 164, 35-42.

ESQUELA-KERSCHER, A. & SLACK, F. J. (2006) Oncomirs - microRNAs with a role in cancer. *Nat Rev Cancer,* 6, 259-69.

HUANG, S. N., MINASSIAN, H. & MORE, J. D. (1976) Application of immunofluorescent staining on paraffin sections improved by trypsin digestion. *Lab Invest,* 35, 383-90.

LEWIS, F., MAUGHAN, N. J., SMITH, V., HILLAN, K. & QUIRKE, P. (2001) Unlocking the archive--gene expression in paraffin-embedded tissue. *J Pathol,* 195, 66-71.

MASUDA, N., OHNISHI, T., KAWAMOTO, S., MONDEN, M. & OKUBO, K. (1999) Analysis of chemical modification of RNA from formalin-fixed samples and optimization of molecular biology applications for such samples. *Nucleic Acids Res,* 27, 4436-43.

NEGRINI, M., FERRACIN, M., SABBIONI, S. & CROCE, C. M. (2007) MicroRNAs in human cancer: from research to therapy. *J Cell Sci,* 120, 1833-40.

OBERLI, A., POPOVICI, V., DELORENZI, M., BALTZER, A., ANTONOV, J., MATTHEY, S., AEBI, S., ALTERMATT, H. J. & JAGGI, R. (2008) Expression profiling with RNA from formalin-fixed, paraffin-embedded material. *BMC Med Genomics,* 1, 9.

RAMOS-VARA, J. A. (2005) Technical aspects of immunohistochemistry. *Vet Pathol,* 42, 405-26.

SHI, S. R., KEY, M. E. & KALRA, K. L. (1991) Antigen retrieval in formalin-fixed, paraffin-embedded tissues: an enhancement method for immunohistochemical staining based on microwave oven heating of tissue sections. *J Histochem Cytochem,* 39, 741-8.

SRINIVASAN, M., SEDMAK, D. & JEWELL, S. (2002) Effect of fixatives and tissue processing on the content and integrity of nucleic acids. *Am J Pathol,* 161, 1961-71.

TAYLOR, C., SHI, S.-R., BARR, N. & WU, N. (2002) Techniques of immunohistochemistry: principles, pitfalls, and standardization. *Diagnostic Immunohistochemistry.* ed. Dabbs DJ, ed. New York, Churchill Livingstone.

YAMASHITA, S. (2007) Heat-induced antigen retrieval: mechanisms and application to histochemistry. *Prog Histochem Cytochem,* 41, 141-200.